# CANADIAN THESES

# THÈSES CANADIENNES

## NOTICE

The quality of this microfiche is heavily dependent upon the quality of the original thesis submitted for microfilming. Every effort has been made to ensure the highest quality of reproduction possible.

If pages are missing, contact the university which granted the degree.

Some pages may have indistinct print especially if the original pages were typed with a poor typewriter ribbon or if the university sent us an inferior photocopy.

Previously copyrighted materials (journal articles, published tests, etc.) are not filmed.

Reproduction in full or in part of this film is governed by the Canadian Copyright Act, R.S.C. 1970, c. C-30.

## AVIS

La qualité de cette microfiche dépend grandement de la qualité de la thèse soumise au microfilmage. Nous avons tout fait pour assurer une qualité supérieure de reproduction.

S'il manque des pages, veuillez communiquer avec l'université qui a conféré le grade.

La qualité d'impression de certaines pages peut laisser à désirer, surtout si les pages originales ont été dactylographiées à l'aide d'un ruban usé ou si l'université nous a fait parvenir une photocopie de qualité inférieure.

Les documents qui font déjà l'objet d'un droit d'auteur (articles de revue, examens publiés, etc.) ne sont pas microfilmés.

La reproduction, même partielle, de ce microfilm est soumise à la Loi canadienne sur le droit d'auteur, SRC 1970, c. C-30.

## THIS DISSERTATION HAS BEEN MICROFILMED EXACTLY AS RECEIVED

## LA THÈSE A ÉTÉ MICROFILMÉE TELLE QUE NOUS L'AVONS REÇUE

ISBN 0-315-36527-7

UNIVERSITÉ D'OTTAWA
UNIVERSITY OF OTTAWA

TABLE OF CONTENTS

(Table of Contents continued ....)

(Table of Contents continued ....)

## Acknowledgements

I am indebted to Professors David M. Bishop and Robert C. Smith for smoothing the way when I came to the University of Ottawa in 1978 as an undergraduate.

I am thankful to my friend and colleague, Carl Tripp, for the challenging discussions related to my work and for the equally challenging tennis matches we have played. I also wish to thank Carl and his wife Carol for "invitations" to several enjoyable barbecues.

I am grateful to Egon Krastoff, our superb glassblower, for his patience and in particular for making and repairing the Raman cell.

Thanks are due to Andrew J. McFarlan for proof-reading this thesis and to his friend Jo-Anne for comic relief.

My thanks to D.F.T. for being there.

Finally, I wish to thank my research supervisor, Professor Barry A. Morrow, for his patience and understanding throughout my sojourn at the University of Ottawa. It has been a pleasure.

Richard A. McFarlane
Ottawa
22nd August, 1986

*" Inconspicuous molehill sometimes more important than conspicuous mountain "*

*Charlie Chan*

## ABSTRACT

Infrared and Raman spectroscopies have been utilized to study the adsorption of $TiCl_4$, $[(CH_3)_3Si]_2NH$, $CH_3OH$, $B(C_2H_5)_3$, $B_2H_6$ and $Ga(CH_3)_3$ on silica and of $B_2H_6$ and $Ga(CH_3)_3$ on $\gamma$-alumina. Raman spectroscopy has also been used to investigate the adsorption of $CH_3OH$, $C_2H_4$, $C_6H_6$, $NO_2$, $SO_2$ and $H_2S$ on $H^+$-exchanged zeolite ZSM-5.

Techniques have been developed to prepare thin silica films which are infrared transparent over the region 4000-500cm$^{-1}$. This has allowed the acquisition of vibrational information formerly unobtainable by transmission infrared spectroscopy because of the lack of transparency of self-supporting silica discs below about 1300cm$^{-1}$. Thus, the important adsorbant-adsorbate stretching vibrations and skeletal vibrations of adsorbates which occur below 1300cm$^{-1}$ and which are crucial to the assignment of the surface species have been observed for the above molecules on silica. Furthermore, the problem of the intense fluorescence background in the Raman spectrum of silica and alumina, which overwhelms and masks the weaker adsorbate peaks, has been overcome. Consequently, Raman spectroscopic data in the 4000-100cm$^{-1}$ region complimentary to that given by infrared spectroscopy may be obtained.

Titanium tetrachloride reacts in two ways with silica as evidenced by the observation of two distinct types of $\equiv$Si-O-Ti vibrations. On moderately dehydroxylated surfaces the sole reaction is

(1) $\equiv SiOH + TiCl_4 \longrightarrow \equiv Si\text{-}O\text{-}TiCl_3 + HCl\uparrow$

whereas on highly hydroxylated surfaces the additional reaction:

(2) 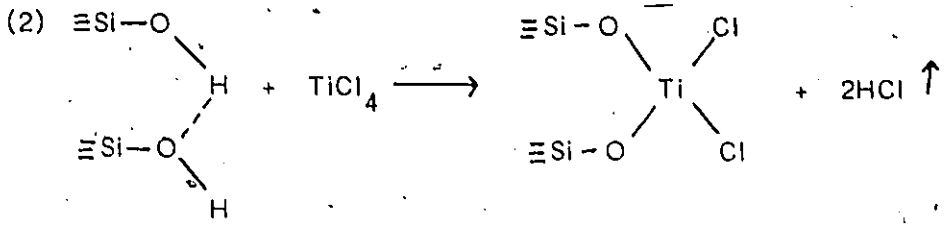

occurs. As expected, $[(CH_3)_3Si]_2NH$ and $CH_3OH$ only react with individual surface silanols (whether or not they are hydrogen-bonded) to yield $\equiv$Si-O-Si$(CH_3)_3$ and $\equiv$Si-O$CH_3$ respectively and the corresponding $\equiv$ Si-O-Si and $\equiv$ Si-OC vibrations have been observed.

The infrared spectrum of silica which contained both paired and isolated hydroxyls and which was treated with $B(C_2H_5)_3$ show that only one product, $\equiv$Si-O-$B(C_2H_5)_2$, is produced. However, a time resolved study using infrared spectroscopy shows that the isolated hydroxyl groups with a sharp band at 3748cm$^{-1}$ react fastest while hydroxyl groups with a pair of bands at 3717 and 3525cm$^{-1}$ react slower. This pair of bands has been assigned to two hydrogen-bonded hydroxyl groups.

Diborane ($B_2H_6$) at pressures of 10-20 torr does not react with hydroxyl groups on silica at 25°C. However, at slightly elevated temperatures (such as that due to the heat from the infrared source in a dispersive spectrometer) there is some reaction and at 100°C all hydroxyl groups react rapidly. Regardless of the extent of reaction, three distinct species, designated A, B and C, are produced. Species A, $\equiv SiOB_2H_5$, is formed from the reaction with isolated hydroxyl groups or with reactive siloxane bridges produced on highly dehydroxylated silica and is stable in the presence of gaseous diborane. Upon evacuation, species A converts to B, $\equiv SiOBH_2$, but can be restored by the readdition of diborane. Species C, $(\equiv SiO)_2BH$, is produced by the reaction of

diborane with paired hydroxyl groups and is more abundant when the initial surface hydroxyl density is greater. Diborane also reacts with the reactive siloxane sites which are created as a result of high temperature dehydroxylation to yield species A (or B after evacuation) and ≡SiH. The reactions between diborane and silica are:

(3) $\equiv SiOH + B_2H_6 \longrightarrow$ 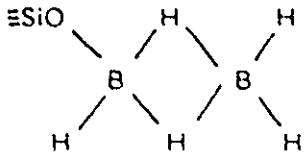 $+ H_2\uparrow$

A

(4) 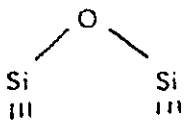 $+ B_2H_6 \longrightarrow \equiv Si\text{-}O\text{-}B_2H_5 + \equiv SiH$

A

(5) 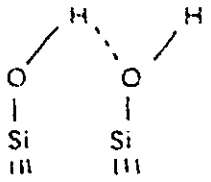 $+ \frac{1}{3}B_2H_6 \rightarrow$ 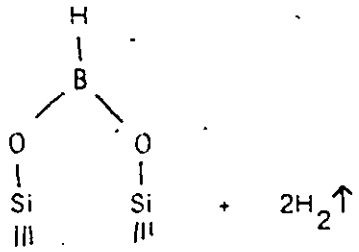 $+ 2H_2\uparrow$

C

(6) $\equiv SiOB_2H_5 \longrightarrow \equiv Si\text{-}O\text{-}B(H)H + \frac{1}{3}B_2H_6\uparrow$

A B

Diborane reacts with the more basic hydroxyl groups on γ-alumina at 25°C.

The Raman and infrared bands observed for the surface species are broad but have been assigned to $\equiv AlOBH_2$(I) and $(\equiv AlO)_2BH$(II). A reaction also occurs with neighbouring Lewis acid and base sites to produce species I and a borohydride species, $\equiv AlBH_4$(III). None of these species changes with the addition and evacuation of gaseous diborane. The least basic hydroxyl groups react with diborane at 100°C to produce species I and III. Alumina which had been treated with diborane at 25 or 100°C catalyzes the polymerization of acetylene to give the intensely coloured trans-polyacetylene polymer.

Regardless of the temperature used to activate the silica under vacuum the major reaction of $Ga(CH_3)_3$ is with the surface hydroxyl groups.

(7) $\equiv SiOH + Ga(CH_3)_3 \longrightarrow \underset{(I)}{\equiv SiOGa(CH_3)_2} + CH_4\uparrow$

For silica activated at greater than 400°C, reactive siloxane bridges also react to yield species I and $\equiv Si(CH_3)$ (II). Almost all vibrational modes of species I have been observed. At 25°C, $MH_3$(M=N, P, As) coordinate to the gallium of I and there is also a small degree of decomposition of this complex since traces of $\equiv SiOH$ and $CH_4$ are observed. With increasing temperature this decomposition is accelerated until, near 500°C (M=N) or 250°C (M=P, As) GaM is formed. Species I reacts within one minute at 25°C with gaseous HCl to eliminate one methyl group as $CH_4$, and over the next 24 hrs the second methyl group is also converted to $CH_4$. The mechanism of the reaction is complex since $\equiv SiOH$ groups are also created, thus indicating that HCl can cleave the Si-O-Ga bond and spectroscopic evidence shows that monomeric $GaCl_3$ and $\equiv SiOGaCl_2$ may constitute the final product.

Two types of reactions of trimethylgallium with alumina are observed and

their relative proportion depends on the activation temperature of the alumina during evacuation. On a highly hydroxylated alumina the major reaction is with hydroxyl groups to produce $\equiv AlOGa(CH_3)_2$ and $CH_4$. On a dehydroxylated alumina a reaction also occurs with Lewis sites to yield $\equiv AlOGa(CH_3)_2$ and $\equiv AlCH_3$. These two reactions constitute a simple method to determine the relative amounts of hydroxyl sites and Lewis acid sites.

Raman spectroscopy shows that methanol, ethylene, benzene and nitrogen dioxide are physisorbed on $H^+$-ZSM-5. Prolonged exposure or heating of the sample in $CH_3OH$, $C_2H_4$ or $C_6H_6$ causes an intense fluorescence background to appear. In the case of $NO_2$ however, the spectrum remained unchanged. Sulphur dioxide is also physisorbed on $H^+$-ZSM-5 but evacuation of the excess gaseous $SO_2$ and the addition of $H_2S$ leads to the formation of sulphur and this suggests that this zeolite might be an effective Claus catalyst.

# CHAPTER 1

## INTRODUCTION

The realization in the past forty years of the importance of surfaces in physical and chemical processes has resulted in extensive studies of interfaces using various techniques, and the blossoming of the new field of surface science.

The nature of a surface at the molecular level is critical to understanding its behaviour. However, studies aimed at obtaining such information are limited to the gas-solid interface because the majority of the newer electron spectroscopic techniques available (see below) only operate under high or ultra-high vacuum conditions. This therefore precludes studies of the solid-liquid interface (except when conventional techniques such as Raman, Infrared and nuclear magnetic resonance spectroscopies are used) which is important in biological and electrochemical processes and of the solid-solid interface which is important for understanding mechanical properties. A study of the solid-gas interface does, however, provide some information which is helpful in the studies, albeit at the macroscopic level, of the other interfaces.

Many surface sensitive techniques such as low energy electron diffraction (LEED), ultraviolet and x-ray photoelectron spectroscopies (UPS and XPS), Auger electron spectroscopy (AES), nuclear magnetic resonance (NMR) and secondary ionization mass spectrometry (SIMS) give information about the electronic and structural properties of the surface and its chemical composition. A complete study of surfaces requires vibrational information which would give, in addition to structural data of the surface itself,

information regarding the structure of adsorbates and of their interactions with the surface.

Vibrational data of surfaces and its adsorbates can be obtained from techniques involving electron scattering, neutron and Raman scattering and infrared absorption spectroscopies. High-resolution electron energy loss spectroscopy (HREELS) is capable of giving vibrational data for smooth metal surfaces (clean or adsorbate covered) in ultra-high vacuum. Neutron inelastic scattering (NIS) can give vibrational data for metallic or non-metallic surfaces without requiring ultra-high vacuum but does require a nuclear reactor. Infrared and Raman spectroscopies are useful for studying any type of solid surface in the presence or absence of a gas or liquid.

Studies of surface properties of macroscopic solids are hampered by the fact that only a small percentage of the atoms are at the surface. Probes involving electrons (e.g. LEED, HREELS, AES, UPS, XPS and SIMS) which have small penetration depths in solids, are inherently surface sensitive. However, probes such as NIS, infrared and Raman spectroscopies which use neutrons or electromagnetic radiation may have relatively long penetration depths, resulting in bulk effects which may effectively mask or overwhelm the surface effects.

One way of overcoming bulk effects in Raman and infrared spectroscopies is to use highly dispersed (high surface area) materials, i.e., materials which have very small particle size and hence relatively more surface atoms to bulk atoms when compared to those with larger particle sizes. Many vibrational studies of surfaces have been done with highly dispersed oxides such as $SiO_2$, $Al_2O_3$, and $TiO_2$ and dispersed metals supported on these oxides. (Dispersed metals require oxide supports because

of their tendency, by themselves, to form aggregates.) Of course, the vibrational spectra of these high surface area materials will still contain features due to the bulk properties but surface effects can now compete with those of the bulk.

Silica is widely used as a relatively inert high surface area support for dispersed metal catalysts. It is also extensively used in modified forms for chromatographic columns. As a result of this, silica has been extensively studied by infrared spectroscopy and to a smaller extent by Raman spectroscopy. Two of the first successful infrared spectroscopic studies were carried out using high surface area porous glass[1] and silica gel[2].

Alumina is extensively used as a catalyst and also a chromatographic support. Like silica, it has received extensive study by infrared spectroscopy but very little study by Raman spectroscopy.

The zeolite called ZSM-5 which is a crystalline alumino-silicate has recently emerged as the pre-eminent oxide catalyst and is receiving great attention. However, few infrared and practically no Raman studies of this material have been carried out.

This thesis is concerned with the use of infrared and Raman spectroscopies to study silica, alumina and ZSM-5. In particular, these studies seek to refine the infrared and Raman techniques so that more information can be obtained from them without complex or difficult experimental adaptations. Further, new probe molecules are employed to give new information about the surface properties of these oxides. To aid in the comprehension of the work to be presented in this thesis a brief review of some of the known relevant surface properties of silica and alumina is given here. A separate introduction to the properties of the zeolite ZSM-5 is

given in Chapter 9.

Part A

Silica

Several excellent reviews concerning the nature, concentration and reactions of the surface groups on silica have been published[3-5]. In the interpretation of studies with silica a distinction between silica as a gel and an aerosil must be made.

Silica gels are generally produced by the acid hydrolysis of sodium silicate, silicon tetrachloride or tetraethoxysilane.

(1) $Na_2SiO_3 + 2H^+ \longrightarrow SiO_2 + H_2O + 2Na^+$

(2) a) $SiCl_4 + 4H_2O \longrightarrow Si(OH)_4 + 4HCl$

b) $Si(OH)_4 \longrightarrow SiO_2 + 2H_2O$

(3) a) $Si(C_2H_5O)_4 + 4H_2O \xrightarrow{H+} Si(OH)_4 + 4\ C_2H_5OH$

b) $Si(OH_4)_4 \longrightarrow SiO_2 + 2H_2O$

These gels have similar properties in that the surfaces of newly formed gels are highly hydroxylated with 4-8 surface hydroxyls per $nm^2$, whereas aerosils have 1-4 per $nm^2$. As shown by electron microscopy[6], the individual gel particles are non-uniform in shape and are honeycombed with micropores which are accessible to various molecules including water. The properties of gels have been reported to depend on the sizes of these micropores and on the types of hydroxyl groups on the surface and in these pores[7-11].

Aerosils are prepared by the flame hydrolysis of silicon tetrachloride in a stream of hydrogen and air at about 1000°C and the ratio of the three components in the flame controls the particle size and surface characteristics[12]. Electron

microscopy[13] has shown that aerosil particles are usually spherical in shape and lack micropores. Aerosils, because they are formed under relatively dry conditions do not generally contain as many surface hydroxyl groups as does silica gel. Furthermore, whereas silica gel can have very high surface areas (as high as $800m^2g^{-1}$) due to the presence of micropores, aerosils have a somewhat lower maximum area ( $400m^2g^{-1}$). It is important to realize that aerosils and gels are amorphous materials. It is generally accepted that these silicas consist of $SiO_4$ units connected together by bridging oxygens in a continuous random network[14]. X-ray diffraction studies[15] show that long range order is destroyed by Si-O-Si bond angle variations which can be quite large.

The silica used in the investigations reported in this thesis was an aerosil. The following discussion therefore deals mainly with the properties of aerosils and gels will only be mentioned for comparative purposes.

The Infrared Spectrum of Silica

Figure 1-1 shows the infrared spectrum of a self-supporting disc of aerosil before and after degassing at $150^oC$ for 1hr to remove water. The totally absorbing bands centered around 1108 and $815cm^{-1}$ have been assigned[16] to antisymmetric and symmetric Si-O-Si stretching modes, respectively. The band at $1640cm^{-1}$ has been assigned as an overtone of that at $815cm^{-1}$ while those at 1875 and $2000cm^{-1}$ are combination bands. The bands from 3750-$3300cm^{-1}$ have been assigned to O-H stretches of various hydroxyls.

Figure 1-2 shows the infrared spectrum of an aerosil in the O-H stretching region after degassing at various temperatures. It has been well established that the sharp band at $3748cm^{-1}$ is due to isolated hydroxyl groups on the silica

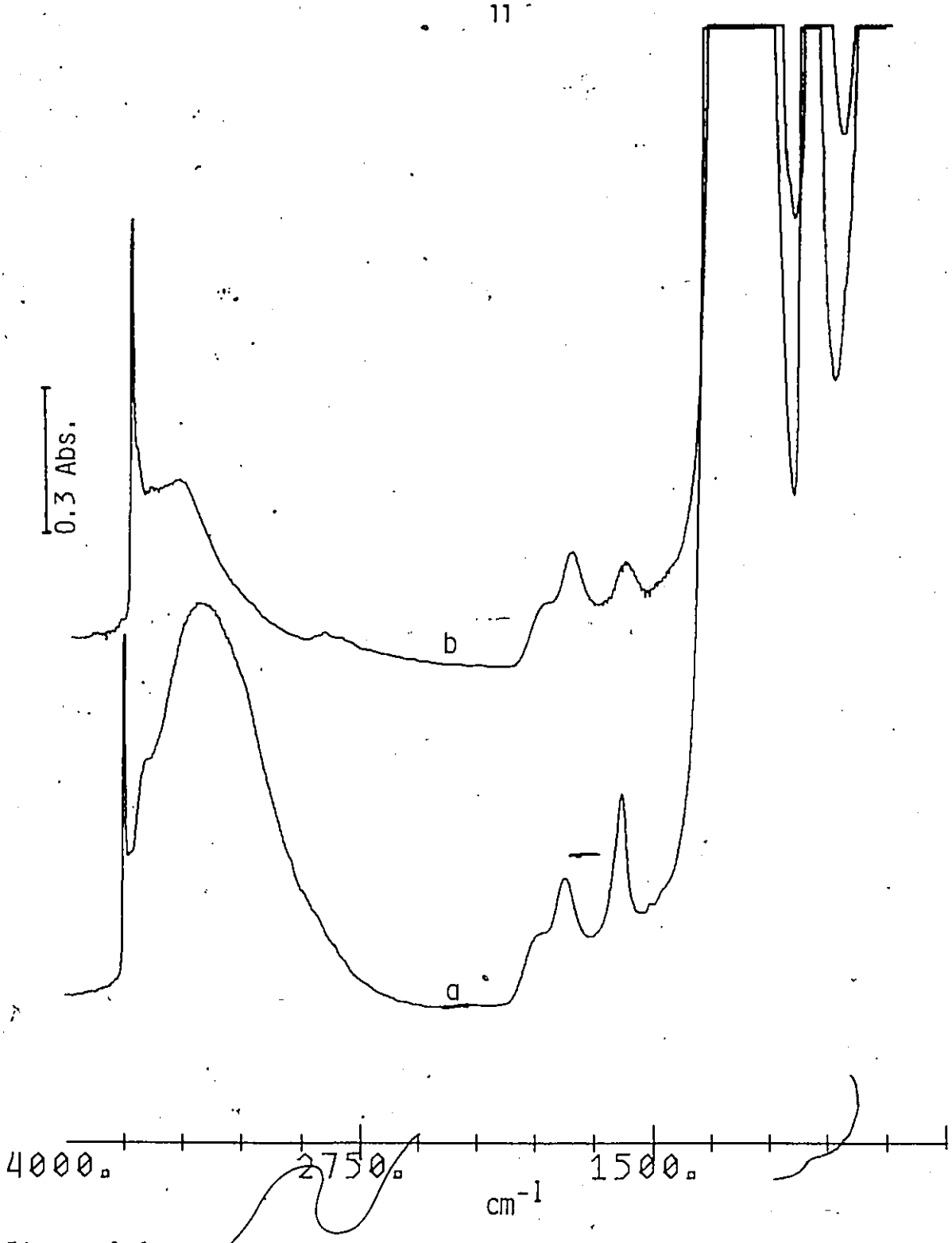


Figure 1-1
The infrared spectra of aerosil (10mg/cm$^2$)
a) as received aerosil before degassing
b) after degassing at 150°C for 1 hr.

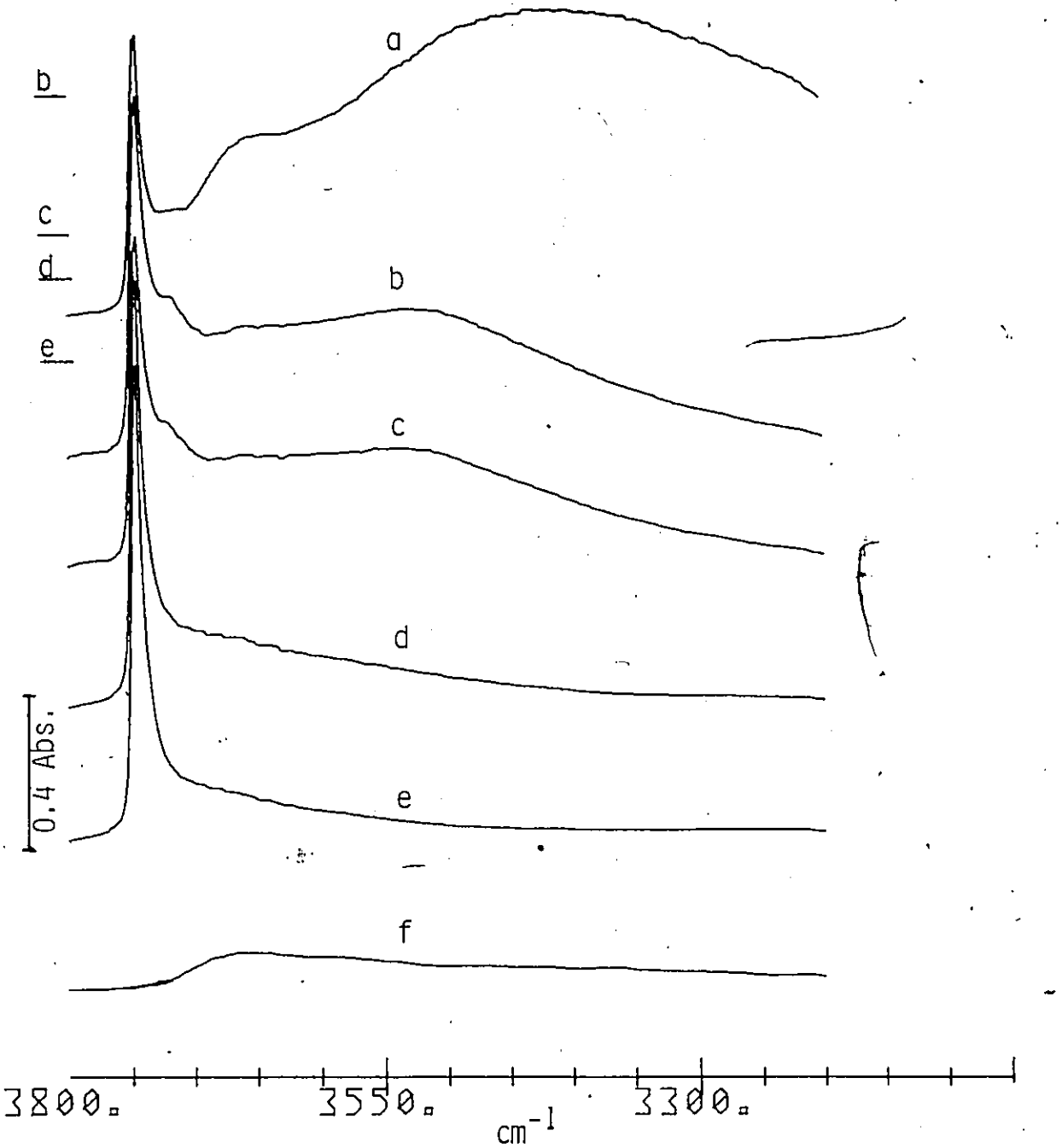


Figure 1-2
Infrared spectra of aerosil (10mg/cm$^2$) in the OH stretching region
a) before degassing and after degassing for 1 hr at b) 25°C;
c) 150°C; d) 300°C and e) 450°C.
f) spectrum of a sample similar to c) after exchange with $D_2O$ at 150°C and evacuation at this temperature for 1 hr.
(from Morrow et al. ref. 51)

surface which are not perturbed by neighbouring hydroxyls[11]. Peri[17] has calculated that the Si-O-H bond angle in isolated hydroxyls (I) on silica gel was 113° and a similar value is expected for this on aerosil. This bond angle implies that the SiOH bond has a high degree of covalency.

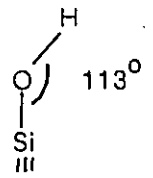


(I)

The bands observed at 3720, 3650 and 3550cm$^{-1}$ have been variously attributed to different types of hydroxyl groups or adsorbed water by several authors and some of these assignments are discussed below.

The broad band centered near 3550cm$^{-1}$ in Figure 1-2 persists until degassing above 400°C and has been assigned to either adsorbed water or hydrogen-bonded hydroxyl groups. Galkin et al.[18] have reported that aerosils previously degassed at temperatures between 200 and 800°C and then exposed to water retained water upon degassing at 200°C but that this was removed at 400°C. Fripiat et al.[19, 20] concluded from their investigations that silica gel also retained water, even up to 300°C. Conversely, Demarquay and Frissard[21] using nuclear magnetic resonance spectrosocpy (NMR), have shown that water was removed from silica gel at 100°C. Ghiotti et al.[22] have shown from infrared studies with aerosil that there was no further change in the spectrum at 1627cm$^{-1}$ ($H_2O$ deformation) after degassing at 25°C for 8 hrs and that therefore all adsorbed water could be removed at this temperature. This result has also been supported by the work of Hockey and Pethica,[23] Bermudez [24] and others[25-27] and has been verified for the

aerosil used in the investigations reported in this thesis.

Two possible assignments of the 3550cm$^{-1}$ band were considered by Hambelton et al.[28] . The silica surface was first exchanged with $D_2O$ to produce Si-OD groups in order to avoid interference by bands due to atmospheric water during their infrared studies. This exchange produced bands at 2760 and 2620cm$^{-1}$ corresponding to those initially at 3748 and 3550cm$^{-1}$, respectively. They observed that upon the addition of $D_2O$ new bands appeared at 2550 and 2690cm$^{-1}$ assignable to adsorbed $D_2O$ and perturbed isolated $\equiv$SiOD. If the band at 2620cm$^{-1}$ were due to $\equiv$SiOD groups perturbed by $D_2O$ then this band should have diminished as $\equiv$SiOD groups were removed by degassing at high temperatures. However it was found that the 2620cm$^{-1}$ could be completely removed at lower degassing temperatures than the bands at 2690cm$^{-1}$ and 2550cm$^{-1}$ which still appeared upon the addition of $D_2O$. Hence the band at 2620cm$^{-1}$ cannot be due to a species perturbed by $D_2O$. Conversely, if the 2620cm$^{-1}$ band were due to $D_2O$ bound to the surface then there should be a broad band at lower frequency which mimics its behaviour. Such a band was not observed. Therefore Hambelton et al. concluded that the band at 2620cm$^{-1}$ in the OD spectrum (or 3550cm$^{-1}$ in the OH spectrum) was due to two closely neighbouring hydroxyl groups hydrogen-bonded to each other. The broadness of the band for this species was attributed to variations in the strength of this interaction because of differing distances between any two such hydroxyls.

Subsequent work by van Roosmalen and Mol[29] with silica gel which also had infrared bands at 3748, 3720, 3650 and 3550cm$^{-1}$, showed that the band at 3720cm$^{-1}$ followed the behaviour of the band at 3550cm$^{-1}$ during degassing. After evacuation at 67$^{o}$C no further change was observed in the water

deformation region of the infrared spectrum for silica gel and difference spectra obtained after subsequent evacuations clearly showed that bands at 3720 and 3550cm$^{-1}$ continued to disappear during degassing up to 600°C. By comparing these difference spectra with the infrared spectra of phenol and methanol dimers and certain 1:1 water-base complexes van Roosmalen and Mol assigned the band at 3720cm$^{-1}$ to vibrations of free-OHa and that at 3550cm$^{-1}$ to hydrogen-bonded -OHb in species (II)

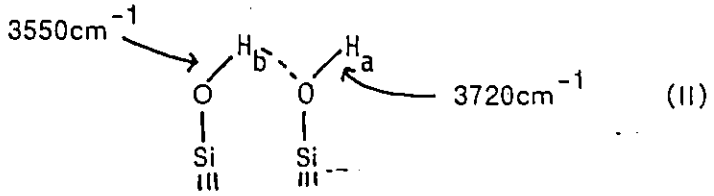


(II)

Ghiotti et al.[22a] have also assigned two IR bands observed with an aerosil at 3720 and 3520cm$^{-1}$ to a pair of hydrogen-bonded hydroxyl as above. Their assignment was made by analogy with the bands produced by the reaction of $H_2O$ with the siloxanes on a highly dehydroxylated silica as reported by Morrow and Cody[30, 31] and Morrow et al.[32] (to be discussed later).

Galkin et al.[33] have observed that the amount of water adsorbed on silica depended on the pretreatment temperature. It was reported that more water was adsorbed on a silica which had been previously degassed at 400°C than on one which has been degassed at only 200°C. Young[12] had reported in earlier work that the greater portion of the silica surface was hydrophobic based on the much lower surface area obtained using water as an adsorbent compared to nitrogen in a B.E.T. surface area measurement (Brunauer-Emmett-Teller[34]). Young[12] and others[18, 33, 35-43] have found that the amount of adsorbed water depended on the concentration of surface hydroxyl groups. Recently, Hobza et al.[44] using semi-empirical molecular orbital calculations

have shown that water adsorption takes place on the silanol groups which act as proton donors to the adsorbed water. They have also shown that lattice siloxane sites ( ≡Si-O-Si≡ ) have very little ability to form hydrogen-bonds with water. Their calculations also suggest that water adsorption first takes place on isolated or hydrogen-bonded pairs of hydroxyls. At higher coverages the tendency of water to self-associate dominates and water cluster formation prevents monolayer formation. Hobza et al. also conclude that a substantial fraction of water will be adsorbed where two hydrogen-bonds can be formed, i.e., with two ≡SiOH groups, whereas only a small portion will be adsorbed via one hydrogen-bond with an isolated hydroxyl group.

Silica degassed at 200°C is known to have more surface hydroxyls than one degassed at 400°C but the observations of Galkin et al.[33] would seem to be at odds with this. However, Young[12] and others [23, 36] have pointed out that degassing silica above 75°C results in the evolution of water from the collapse of the hydrogen bonded-hydroxyl groups to form siloxane groups. (reaction 4)

(4) 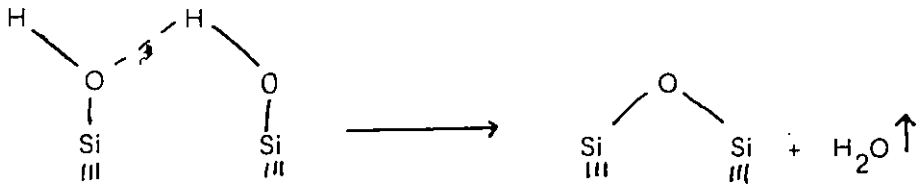

Young reports that provided, the silica is not degassed above 400°C, reaction (4) was reversible. If the degassing temperature exceeds 400°C, rehydration does not regenerate all the hydroxyl sites and the 3550cm$^{-1}$ band does not return to its original intensity.

The 3650cm$^{-1}$ band observed with aerosils is relatively weak compared to that observed with gels. This band observed with gels is generally believed to be due to hydroxyl groups which are perturbed as a result of interparticle contact. As the pressure at which the silica disc is pressed increases, i.e., as the particles approach each other more closely, the intensity of the 3650cm$^{-1}$ band increases. The 3650cm$^{-1}$ band in aerosils also appears to increase with pressure[28b, 45] but is still relatively weak. These hydroxyl groups are usually termed inaccessible because they do not react with molecules which readily react with the isolated and hydrogen-bonded hydroxyls and they do not completely exchange with $D_2O$, as is illustrated in Figure 1-2. These hydroxyls are irreversibly removed with the elimination of water by degassing above 500°C and, according to Hockey[28a], this corresponds to an annealing process whereby the relatively weak hydrogen bond between these hydroxyls are replaced by stable siloxane bridges.

As previously mentioned, gels are generally more hydroxylated than aerosils. Gels have been reported to have about 4.6 hydroxyl groups per nm$^2$ [7, 46-49] while aerosils have about half as much or less[50, 51]. Using the value of 4.6 OH/nm$^2$ several workers[46, 52] have attempted to model the silica gel surface to that of the faces of the polymorphs of crystalline silica (i.e. $\alpha$-, $\beta$- quartz, cristobalite and tridymite). In addition to isolated and hydrogen-bonded pairs of hydroxyl groups two other types called vicinal (III) and geminal (IV) hydroxyl groups have been postulated (the hydroxyls of species (III) would not be hydrogen-bonded like those of

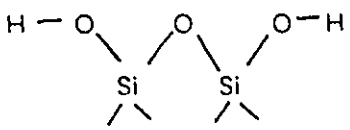


(III)

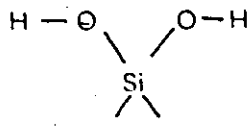


(IV)

species (II) and would be much like isolated hydroxyls). However, as Armistead et al.[53] correctly pointed out, any attempt to find one crystal plane to represent highly dispersed silica gel must be incorrect because in a finely powdered crystalline silica, all possible crystalline faces with their differing hydroxyl surface density would be exposed. Further, as was previously mentioned, silica gel is in fact amorphous and has very small particles of about 10 nm diameter.

Hair and Hertl[54] and van Cauwelaert et al.[55] have reported that for an aerosil there are distinct shoulders at high and low frequency to the peak due to isolated hydroxyl groups. These shoulders at 3751 and 3741cm$^{-1}$ have been assigned by these authors to the coupled vibrational modes of geminal hydroxyl groups. Their assignment has been refuted by Hockey[56] and Morrow and Cody[57]. Hockey[56] and Morrow and Cody[57] showed that the spectra of Hair and van Cauwelaert could be reproduced by an improper compensation of atmospheric water by their infrared spectrometers. Hockey also showed that for $D_2O$ exchanged silica, where there would be no interference due to atmospheric water, no shoulders about the isolated ≡SiOD band were observed. Later van Cauwelaert replied to Hockey's criticism by stating that their spectra were obtained under complete compensation. Furthermore, they claimed that the shoulders shifted with temperature, which would not be the case if they were due to atmospheric water.

However, it is well known as illustrated by Morrow and Cody[57] and Ryason[45], that the frequency of the $\equiv$SiOH stretch shifts with the temperature of the sample. Such a shift of the $\equiv$SiOH stretch would result in an apparent shift of the shoulders since the bands due to atmospheric water would not shift with the temperature of the sample. That no shoulders were observed with the $D_2O$ exchanged sample was explained by van Cauwelaert by (sic) "a loss in identity of the middle and high frequency components."

Although there is no evidence for the presence of geminal hydroxyls on aerosil, van Rossmalen and Mol[58] have reported infrared evidence for geminal hydroxyl groups on silica gel. Their finding was based upon the observation of two bands at 3742 and 3734cm$^{-1}$ in addition to that at 3749cm$^{-1}$ assigned to isolated hydroxyls. The occurrence of two bands which they assigned to geminal hydroxyls was accounted for by a slight hydrogen-bonding between the two hydroxyls in a geminal group. That no corresponding bands were observed for the $D_2O$ exchanged gel was explained by the formation of a weaker hydrogen-bond between $\equiv$SiOD groups than between $\equiv$SiOH groups. This weaker interaction van Roosmalen and Mol contend would resuit in a smaller frequency difference between geminal and isolated hydroxyls such that only one band would be observed for both species.

Using cross-polarization magic angle spinning (CP-MAS)$^{29}$Si NMR to study silica gel, Maciel and Sindorf[59] have assigned three peaks with similar chemical shifts to $\equiv$SiOH, $=$Si(OH)$_2$ and Si$^{*}$(OSi$\equiv$)$_4$ (* indicates silicon atom corresponding to a peak in the spectrum). This assignment was based partly on the $^{29}$Si NMR studies by Marsmann[60] of silicate-water glass solutions and the observed chemical shifts for Si$^{*}$(OSi$\equiv$), HOSi$^{*}$(OSi$\equiv$) and (HO)$_2$ Si$^{*}$(OSi$\equiv$)$_2$. Their assignments also correlated well with the spin relaxation times for silicon

atoms connected to zero, one or two hydroxyl groups. That the species studied by NMR are indeed surface or near surface species was assured by the use of cross polarization since only those silicon nuclei near protons, i.e., those nuclei at or near the surface are detected. An excellent introduction to the use of CP-MAS NMR in the study of silicates is given by Fyfe[61].

Recently, Sauer and Schroder[62] have reported the results of semi-empirical Self-Consistent Field Molecular Orbital (SCF-MO) calculations for geminal silanols. From their calculations they concluded that the O-H vibrational frequencies were the same for geminal and isolated hydroxyls and that the coupling constant for the two OH vibrations for the geminal species was zero within the error of their calculation. There is only one O-H vibrational frequency so there would be no hydrogen-bonding between the two hydroxyls of the geminal species and they found that the most stable conformation would be that shown below.

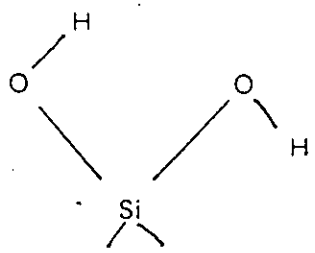


(V)

It would therefore appear from the calculations of Sauer and Schroder that it is impossible to differentiate by infrared spectroscopy between geminal and isolated hydroxyl groups. The arguments for geminal hydroxyl groups are quite strong but for the above reasons the presence of these groups on aerosils or gels cannot be ruled out. The NMR evidence appears to support the presence of geminal hydroxyls, at least on gels. However, it is noted that while the presence of hydrogen-bonded hydroxyls are well established on aerosils and gels

no such species were detected in the NMR of gels.

Dehydroxylation and Hydration of Silica

As was mentioned previously, adsorbed water on aerosils can be removed by degassing at 25°C and for degassing up to 400°C the dehydroxylation of hydrogen-bonded hydroxyl pairs is reversible. The dehydroxylation process below and above 400° C will now be examined in more detail. For convenience, in the following discussion isolated and hydrogen-bonded paired hydroxyls are called A- and B- types respectively. Siloxane sites produced by the collapse of B- types hydroxyls are termed B- type siloxanes while those produced by the dehydroxylation of a surface with A- type hydroxyls are termed A- type siloxanes.

In Figure 1-3 the variation in the number of hydroxyl groups on silica gel surface and the ability of the dehydroxylated surface to rehydrate are shown. The ability of B- type siloxane to rehydrate decreases beyond 400°C until rehydration becomes very difficult after degassing at 850°C. Further, after heating above 450°C the number of A- type hydroxyls decreases and new highly strained A- type siloxanes were produced[5, 63-65]. This observation might indicate that a kind of annealing of the surface was taking place.

Morrow et al.[51] have recently reinvestigated the dehydration of aerosil up to 450°C. It was observed that the intensity of the infrared band at 3748cm$^{-1}$ increased with degassing temperatures up to 400° but beyond this temperature it begins to decrease (Figure 1-2). The total numbers of accessible hydroxyl groups at 150 and 450°C were determined gravimetrically by $D_2O$ exchange and were found to be 2.4 and 1.2 hydroxyls per nm$^2$, respectively. Many previous determinations of hydroxyl content relied upon reactions of the hydroxyl groups with various

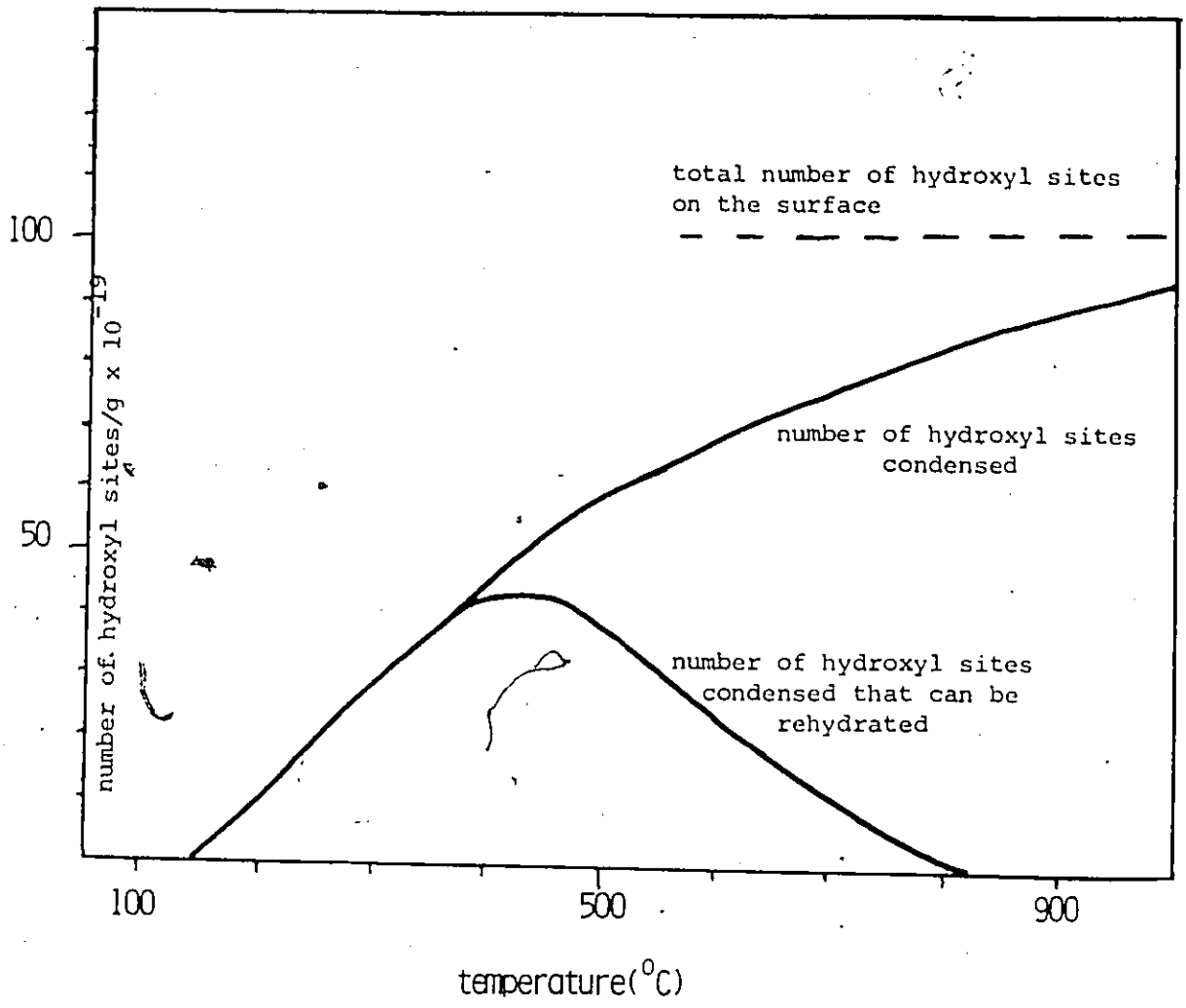


Figure 1-3
Change in surface silanol sites with heat treatment of the sample (from G.J. Young ref. 12).

reagents or by the amount of water lost at various temperatures. The first of these methods yields uncertain results because reactions of likely but really unknown stoichiometries were used. The water loss methods lead to erroneous results because, as pointed out previously, inaccessible hydroxyls will condense and eliminate water upon degassing of silica. Davydov et al.[66] have shown in an earlier work that $D_2O$ exchange would give the best measure of surface hydroxyl concentration, so the results of Morrow et al. must be deemed reliable.

Morrow et al.[51] were able to show that the increase in isolated hydroxyl groups might be due to three hydrogen-bonded hydroxyls (VI) which would condense to form one molecule of water and one B- type siloxane and one A- type hydroxyl (Reaction 5).

(5) 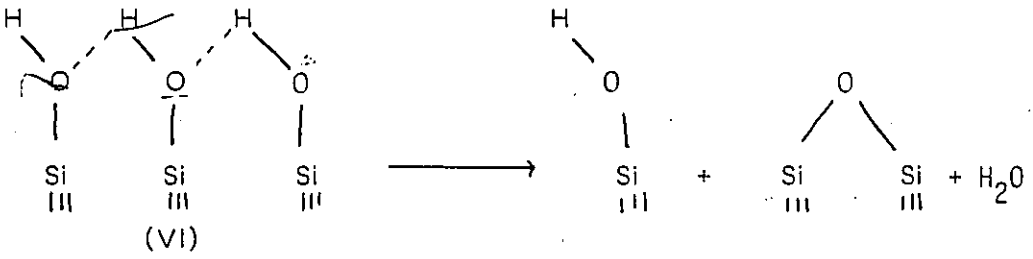


The OH vibrational frequencies of these hydrogen-bonded and terminal hydroxyls would be expected to be similar to those for an hydrogen-bonded pair. The siloxane produced upon dehydroxylation would also be expected to behave like a B- type siloxane.

Morrow et al.[31, 65] have reported that upon degassing an aerosil above 400°C the concentration of A- type hydroxyls diminished and a weak pair of bands appeared at 908 and 888$cm^{-1}$. These bands were assigned to a highly strained siloxane (A- type) formed by the collapse of A- type hydroxyls. The formation of such siloxanes from isolated hydroxyls which are at least 10Å apart

(1.2 OH/100$\mathring{A}^2$ at 400°C) must involve migration of surface cations and/or anions $Si^{4+}$, $H^+$, $OH^-$, $O^{2-}$. There is evidence from NMR spectroscopy that the hydrogen of the surface hydroxyls on silica gel has considerable mobility at high temperatures [67].

Whereas the siloxanes from B- type hydroxyls are not easily rehydrated at 25°C after heat treatment above 850°C, the highly strained A- type siloxanes can be rehydrated even after heating the silica at 1100°C, as reported by Morrow et al.[31, 32]. These siloxanes were highly reactive and reactions with $H_2O$, $NH_3$ and $CH_3OH$ at 25°C were reported (Reaction (6) ).

(6)

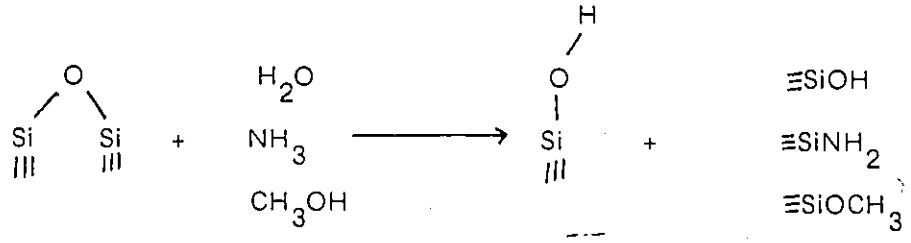


The B- type siloxanes are not known to undergo the above reactions under the same conditions.

Interestingly, Morrow et al.[32] report that the two hydroxyl groups formed by the reaction of $H_2O$ with A- type siloxanes have a single band at 3741$cm^{-1}$ so that they are apparently not hydrogen-bonded. However, this band was considerably broader than the ≡SiOH band at the same frequency formed by the reaction of $NH_3$ or $CH_3OH$. Morrow et al. postulated that the two hydroxyl groups formed with water are not equivalent but that the frequency separation of their IR bands was much smaller than the band widths so only one broad band was observed. They supposed that the reason for this was that the siloxane site was not symmetrical and support for this was given by the adsorption on these siloxanes of pyridine and trimethylamine which reportedly did not affect the intensities of bands at

908 and 888cm$^{-1}$ equally. Furthermore, Cody[68] notes that it is difficult to assign a siloxane type species to two bands at 908 and 888cm$^{-1}$ as this would indicate an Si-O-Si band angle of nearly 90°. The assignment becomes even more dubious as Cody also notes that an additional weak band was present at 930cm$^{-1}$ when the aerosil was degassed at 1200°C.

Morrow et al.[32] have also reported that on a silica with A- type siloxanes, in addition to the band at 3741cm$^{-1}$ that appeared upon the addition of sufficient water to remove the bands at 908 and 888cm$^{-1}$, a pair of new bands appeared at 3720 and 3520cm$^{-1}$ when larger quantities of water were added. Strong evidence was presented which supported the assignment of these bands at 3720 and 3520cm$^{-1}$ to a pair of hydrogen-bonded silanols which were formed by the reaction of water with another type of siloxane which may be similar to the B- type in reaction (4). Volkov et al.[43] had proposed that excess water adsorbed on a highly dehydroxylated silica formed species (VII).

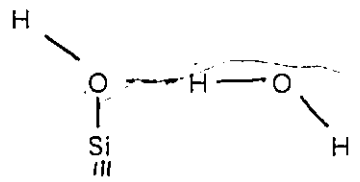

VII

Based on the infrared frequencies found for the water dimer[69, 70], Kiselev proposed that the $OH_a$ and $OH_b$ vibrations occured at 3520 and 3720cm$^{-1}$, respectively. However, the results of Morrow et al.[32] for the adsorption of $H_2{}^{18}O$ showed that Kiselev's model was incorrect. As would be expected, the reaction of $H_2{}^{18}O$ with $\equiv Si^{16}O\text{-}Si\equiv$ produced two bands at 3720 and 3710cm$^{-1}$ corresponding to the $\equiv Si^{16}OH$ and $\equiv Si^{18}OH$ stretch of terminal OH and the band at 3520cm$^{-1}$ showed no measurable isotopic shift due to its large half-width. Using $D_2O$, Morrow et al. observed two bands at 2740 and 2610cm$^{-1}$ which corresponded to those at 3720 and 3520cm$^{-1}$ with

$H_2O$. Furthermore, the species responsible for the bands at 3720 and 3520cm$^{-1}$ could only be removed by degassing above 250°C whereas hydrogen-bonded water on aerosil, as previously mentioned, can be removed at 25°C. Kliel et al.[71] investigated the near infrared spectrum of water adsorbed on silica. They concluded that silanol groups act as proton donors to water. Hobza et al.[44] also concluded from semi-empirical molecular orbital calculations that silanols were the proton donors when hydrogen-bonded to water, so that species VII proposed by Kiselev is extremely unlikely to occur.

The Raman Spectrum of Silica

The Raman spectrum of aerosil silica is shown in Figure 1-4. Laughlin and Joannopoulos[72] have assigned the peaks observed at 450, and 800cm$^{-1}$ as well as a very weak one at 1050cm$^{-1}$ to the rocking, bending and stretching vibrations respectively of an $Si_2O$ bond in the $Si_2O_7$ unit shown below.

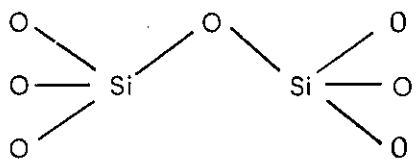


The major cause of the broadening of these bands has been attributed by Laughlin and Joannopoulous[72] and Gaskell and Johnson[73] to the Si-O-Si bond angle variations. X-ray diffraction studies[15] have shown that this bond angle variation may be as large as 20° from the average angle of 144°. The band at 3740cm$^{-1}$ in Figure 1-4 has been assigned to the O-H stretch of surface $\equiv$SiOH[74-77] and associated with this band is one at 980cm$^{-1}$ and its assignment as the Si-O stretch of $\equiv$SiOH is well established[77, 78]. Murray and Greytak[77] have assigned a weak broad band at 380cm$^{-1}$, which is not obvious in Figure 1-4, to the

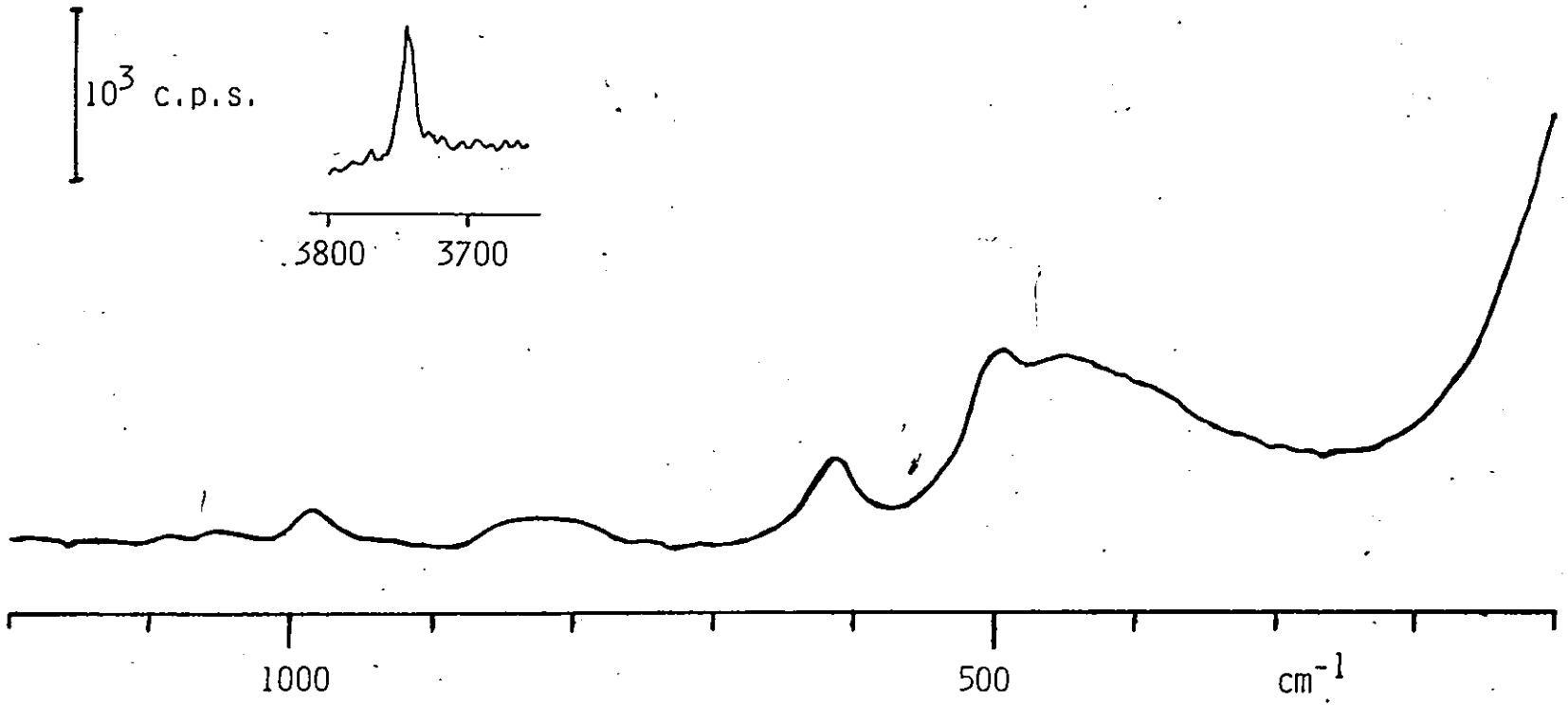


Figure 1-4
The Raman spectrum of aerosil which had been degassed at 480°C.

wagging vibration of ≡SiOH.

The assignments of the bands at 490 and 606cm$^{-1}$ have been the subject of some controversy. These bands have been assigned to defects in the silica network because their intensities relative to the bands assigned to bulk features increased with neutron bombardment[79] or with fictive (glass transition) temperature[80, 81]. It was also found that in fused silica (heated at 500-1500°C) additional utraviolet absorption[82] and paramagnetic optically active centers[83, 84] are observed which are associated with the creation of these defects.

It has been suggested by Bates et al.[85] that the band at 606cm$^{-1}$ was related to a dangling silicon bond in the network, possibly as the associated complex ≡Si• •OSi≡ . Galeener et al.[86] proposed that this band was in fact due to the non-bridging oxygen of the above complex. Calculations by Laughlin and Joannopoulos[87] showed that both $O_3Si$• and •$OSiO_3$ had vibrations near 600cm$^{-1}$ but that this vibration was Raman active only for the latter species. Later work by Laughlin and Joannopoulos[87, 88] suggests that the band at 606cm$^{-1}$ was due to a Si-Si stretching vibration which would be Raman active. However Galeener et al.[86] have disputed this assignment because the analogous band in the Raman spectrum of $GeO_2$ did not increase in intensity for germanium rich samples, i.e., $Ge_xO_2$ when x was greater than 1.

Recently, Mikkelsen and Galeener[89] have reported the Raman spectra of vitreous silica equilibrated at various fictive temperatures and then quenched in water. They found that the band at 606cm$^{-1}$ increased exponentially with increasing fictive temperature. They also reported that the activation energy for the formation of the defect was one order of magnitude less than the energy barrier for viscosity which is associated with Si-O bond breaking. For this

reason they suggested that the defect was not associated with broken Si-O bonds. Mikkelsen and Galeener have also determined that the 606cm$^{-1}$ band was independent of the presence of hydroxyl groups, which is contrary to the reports of Murray and Greytak[77] and Stolen and Walrafen[80]. Finally, all the above Raman studies did note that the 490cm$^{-1}$ band increased with the 600cm$^{-1}$ band but the relative changes in this band were difficult to determine because of the sharply sloping background at 500cm$^{-1}$.

In a recent publication, Silin et al.[90] postulate that the defect band at 606cm$^{-1}$ was due to a peroxy linkage in the silica network, i.e., ≡Si-O-O-Si≡ . This conclusion was based on calculations for a model of silica at the fictive temperature where 3- coordinate silicon atoms ( ≡Si•, a - type defect) and non-bridging oxygen atoms ( ≡Si-O•, b- type defect) were mobile with activation energies slightly less than the Si-O bond breaking energy. For such a system it was proposed that, in addition to recombination of the mobile defects to restore the original silica network (R), two 3- coordinate silicon atoms could combine to form a silicon-silicon bond ( ≡ Si-Si ≡ , A- type defect), and two non-bridging oxygen atoms could create a peroxy bond ( ≡ Si-O-O-Si≡ , B- type defect). From their calculations Silin et al. found a similar fictive temperature dependence of the 606cm$^{-1}$ band as did Mikkelsen and Galeener[89]. Further support for this assignment presented by Silin et al. was the Raman spectrum of [redacted]used silica enriched by 50% with oxygen-18. The simulated spectrum for this sample based upon $^{18}O$-$^{18}O$, $^{16}O$-$^{18}O$ and $^{16}O$-$^{16}O$ peroxy linkages with vibrational frequencies 575, 590 and 606cm$^{-1}$, respectively, and equal band widths agreed very well with the observed spectrum.

The assignment of the so called defect modes at 490 and 600cm$^{-1}$ remains controversial. There is some indication that peroxy linkages might be

responsible for these bands, however, an assignment based on broken ≡SiOSi≡ linkages with dangling bonds cannot be ruled out particularly since the defects can be produced by neutron bombardment at 25°C, which is well below the fictive temperature.

Finally, it is noted that there is no reported Raman spectrum for highly dehydroxylated silica, i.e., silica containing the highly strained siloxane bridges. It is very likely that bands due to such a siloxane bridge would be very weak in the Raman not only because of the low abundance of such species but also because all Si-O modes are generally only weakly Raman active.

Site Concentration and Reactions on Silica

There have been many attempts to determine the concentrations of A- and B-type hydroxyls and reactive siloxane sites via their respective reactions with so called hydrogen sequestering reagents such as $SiCl_xMe_{4-x}$, $GeCl_xMe_{4-x}$ (x=1-4, Me=$CH_3$), $Al_2Me_6$, $AlCl_3$, $BCl_3$, $TiCl_4$ and $(Me_3Si)_2NH$[8,17,24,28,47,48,53,54,91-97]. Earlier studies with reagents such as $AlCl_3$ and $BCl_3$ relied upon measurements of the amount of HCl evolved in the initial adsorption step and in the subsequent hydrolysis, or, upon elemental analysis of the treated silica. In any case, it was necessary to assume that these reagents, e.g., $BCl_3$, must have reacted with paired or isolated hydroxyls in the following manner.

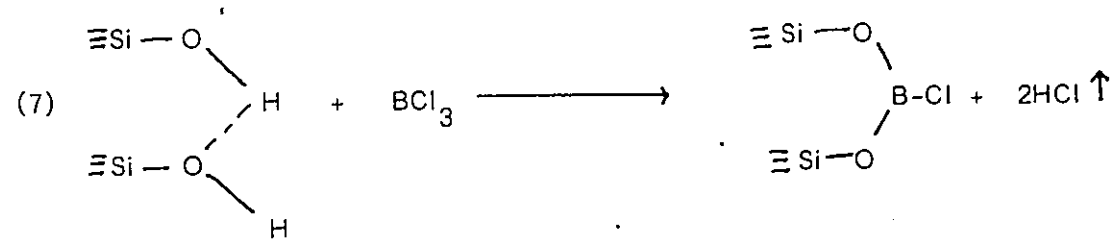

(7) ≡Si—O, ≡Si—O, H + $BCl_3$ ⟶ ≡Si—O, ≡Si—O, B-Cl + 2HCl↑

(8) ≡SiOH + $BCl_3$ ⟶ ≡Si-$OBCl_2$ + HCl↑

Hockey and Armistead[91] have reported that $BCl_3$, $MeCl_3Si$ or $SiCl_4$ reacted with both A- and B- type hydroxyls but that the latter type reacted more slowly. In contrast, they also reported that $Me_2Cl_2Si$ or $Me_3ClSi$ reacted only with A-type hydroxyls. These observations have been rationalized in terms of the stereochemistry of the reaction and is discussed in Chapter 4 of this thesis.

Peri[17] and more recently McDaniel[48] have reported the reactions of $SiCl_4$ with silica gel. McDaniel concluded that for silica gel dried at 200°C 70% of the reacting hydroxyls reacted as pairs, 40% at 400°C and none at 700°C. McDaniel also reported that siloxanes also react with $SiCl_4$ under more severe heating than was required for reactions with hydroxyl groups. The reactions postulated were:

(9) $\equiv SiOH + SiCl_4 \longrightarrow \equiv Si\text{-}OSiCl_3 + HCl\uparrow$

(10) $2\equiv SiOH + SiCl_4 \longrightarrow \equiv Si\text{-}O\text{-}SiCl_2\text{-}O\text{-}Si + 2HCl\uparrow$

(11) $\equiv S\text{-}O\text{-}Si\equiv + SiCl_4 \longrightarrow \equiv Si\text{-}O\text{-}OSiCl_3 + \equiv SiCl$

The types of studies to determine the concentration of hydroxyl species on silica mentioned above have the inherent flaw of having to assume that only reactions of certain stoichiometries can occur with isolated or hydrogen-bonded hydroxyl groups. There is no reason to assume, for example, that some pairs of hydroxyls could not conceivably react as singles. More fundamentally, there is even no reason to assume that pairs are the only type of hydrogen-bonded hydroxyls, i.e., that triplets and quartets of hydroxyl groups do not exist which might also react differently. Furthermore, the reactions employed could not distinguish between hydroxyl groups that were hydrogen-bonded or geminal pairs.

In order to use the above types of reactions to determine the concentrations of hydroxyl groups, the reactions that occur with a given reagent

must first be unambiguously established. Subsequent chapters in this thesis deal with the determination of the stoichiometry of such reactions using vibrational spectroscopic techniques. In particular, new techniques (Infrared and Raman) have been developed in order to obtain low frequency spectra characteristic of the adsorbent-adsorbate stretching modes.

Part B

Alumina

In contrast to the silicas discussed in the previous section, aluminas, even high surface area ones, exist in various crystalline forms. The aluminas used in industrial processes and academic research are usually in the $\eta$ - or $\gamma$ - form. Aluminas are used mostly as catalyst supports[98] for metals and other oxides and are widely used in the petroleum industry. By itself, alumina is useful as catalysts for simple organic reactions such as the conversion of alcohols to alkenes and ethers, isomerizations of alkenes, ortho-para conversion of hydrogen and for the Claus process[99, 100].

Alumina is an important material in catalysis because of several factors. First, it is readily available in large quantities and in high purity. Aluminas are also quite thermally stable and have relatively high surface areas (100-300 $m^2/g$). They are microporous and the pore volume can be controlled during fabrication. Furthermore, aluminas are amphoteric materials and thus possess both acid and basic properties. This acidity and basicity is controlled by the surface groups or ions which terminate the micro-crystallites and can be modified by heat treatment or various additives. These properties are the fundamental reasons for the importance of alumina as a catalyst and as a catalyst support.

Two excellent reviews on the structure and properties of $\eta$- and $\gamma$ - alumina have been published by Knözinger[100] and Knözinger and Ratnasamy[99] and the following discussion is largely based on these reviews.

Structure of $\eta$- and $\gamma$ - alumina

Alumina in the $\gamma$ - form can be obtained by thermal dehydration of boehmite ( AlO(OH) ) at 450°C. In addition, $\gamma$ - alumina can undergo the following thermal transitions:

$$2AlO(OH) \xrightarrow[-H_2O]{450°C} \gamma\text{-}Al_2O_3 \xrightarrow{730°C} \delta\text{-}Al_2O_3 \xrightarrow{1000°C} \theta + \alpha\text{-}Al_2O_3 \xrightarrow{1200°C} \alpha\text{-}Al_2O_3$$

Similarly, - alumina can be obtained from mineral bayerite ( $Al(OH)_3$):

$$2Al(OH)_3 \xrightarrow[-H_2O]{230°C} \eta\text{-}Al_2O_3 \xrightarrow{850°C} \theta\text{-}Al_2O_3 \xrightarrow{1200°C} \alpha\text{-}Al_2O_3$$

Both $\eta$ - and $\gamma$ - alumina can be considered as defect spinel structures which are tetragonally distorted, this distortion being greatest for the $\gamma$ - form. The unit cell of spinel ($Al_2MgO_4$) consists of 32 oxygen atoms and 24 cations. Thus for alumina in the spinel structure with 32 oxygens, only 21 1/3 cation positions are occupied and so there are 2 2/3 vacant cation positions. The oxygen sub-lattice is built up of cubic close-packed stacking of oxygen layers. According to Lippens[101, 102] this stacking in $\gamma$ - alumina is regular (e.g.,ABCABCABC) but in $\eta$ - alumina deviations can occur (e.g., ABCACABABCBC). Leonard et al.[103], from radial electron distribution and fluorescence measurements, have shown that the oxygen sub-lattice is more densely packed for $\gamma$ - alumina than for $\eta$ - alumina since the Al-O bond lengths

calculated from these measurements were shorter for $\gamma$ - alumina. Their results also indicated that the octahedral sites (6-coordination) in the oxygen sub-lattice were preferentially occupied by $Al^{3+}$ compared to the tetrahedral sites (4 - coordination). Recently, John et al.[104] have measured the occupancies of these sites for $\eta$ - and $\gamma$ - alumina by using $^{27}Al$ MAS-NMR and found that a greater fraction (0.37) of tetrahedral sites were occupied for $\eta$ - alumina than for $\gamma$ - alumina (0.25). In addition, whereas the occupancy did not change with temperature for the $\gamma$ - form, for $\eta$ - alumina the tetrahedral occupancy decreased slightly with increasing temperature.

The above differences in $\eta$ - and $\gamma$ - alumina results in slightly different properties. The crystalline aluminas develop slightly different maximum surface areas with the $\eta$ - form having the higher value. This is probably due to the lower packing density for $\eta$ - alumina. Ammonia adsorption[99, 242] shows that $\eta$ - and $\gamma$ - aluminas have similar numbers of acid sites but that these were significantly stronger for the $\eta$ - form. The catalytic activity of $\eta$ - alumina is also higher.

Several workers have attempted to model the surface of alumina by considering certain preferentially exposed crystal faces in the micro-crystallites. Lippens[101, 102] considered that the densely packed (111) face of $\eta$ - alumina could account for its surface chemistry while for $\gamma$ - alumina the exposed faces were the less densely packed (110) or (100) faces. Peri[105] and Butt et al.[106, 107] in their models of the $\gamma$ - alumina surface considered only the (100) face.

Energy considerations dictate that anion layers will terminate a crystallite and Knözinger and Ratnasamy[99] have shown that for the alumina surface this layer will consist of hydroxyl groups. They have shown that for the (111)

face of an alumina having the spinel structure five types of hydroxyl groups are possible while for the (110) face three types are possible and for the (100) face only one type is possible. Knözinger and Ratnasamy considered that the (111) plane had two types of layers parallel to it called A and B (following the designation of Lippens et al.[101, 102]) and that the (110) plane also had two layers, C and D, while the (100) plane gave only one layer. The layers parallel to the (111) and (110) planes are shown in Figures 1-5 and 1-6, respectively. The A layer has $Al^{3+}$ in 16 tetrahedral and 8 octahedral positions while the B layer has 24 cations in octahedral positions. The C layer contains equal numbers of cations in tetrahedral and octahedral sites while the D layer contains cations in only octahedral sites.

When the A-layer in the (111) plane is covered by a layer of hydroxyl anions two types of terminal hydroxyl groups are possible called, by Knözinger and Ratnasamy types Ia and IIa. The type Ia consists of a tetrahedrally coordinated $Al^{3+}$

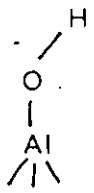


Ia

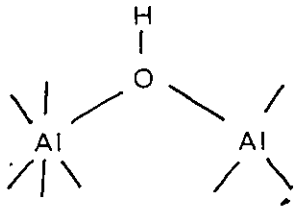


IIa

while the type IIa has an octahedral and a tetrahedral $Al^{3+}$ bridged by a hydroxyl group. Type IIa occurs three times more frequently than type Ia. The B layer of the (111) plane covered by hydroxyl anions has two types of hydroxyls called IIb and III shown below. There are three times as many type IIb as type III.

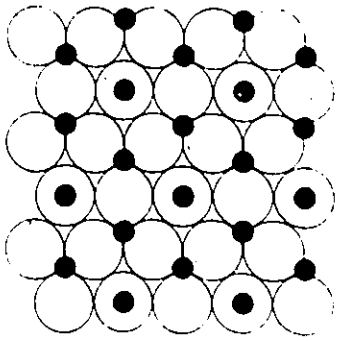

a

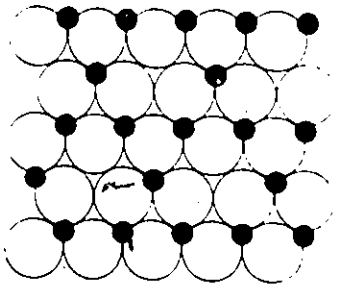

b

Figure 1-5
(111) face of the alumina spinel lattice
a) A-layer
b) B-layer

○ - oxygen atom ● - aluminum atom

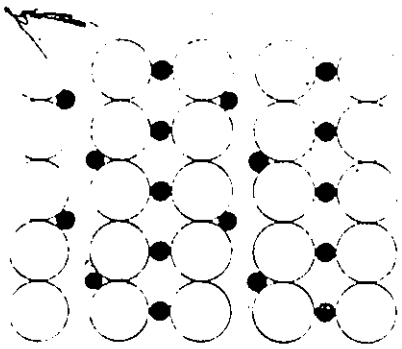

a

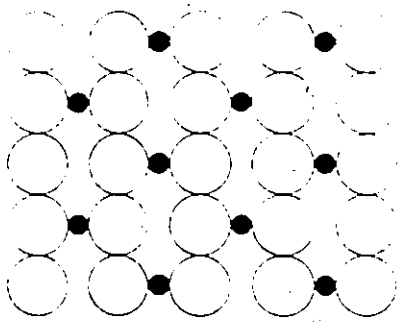

b

Figure 1-6
The (110) of the alumina spinel lattice
a) C-layer
b) D-layer

○ - oxygen atom ● - aluminum atom

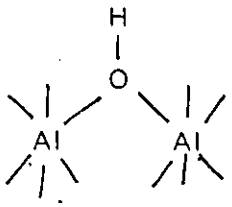


IIb

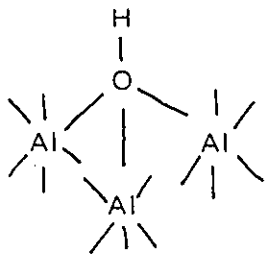


III

If possible cation vacancies are considered (2 2/3 per unit cell) then a fifth type of hydroxyl type Ib is possible if the tetrahedral cation is removed from type IIa or one of the octahedral ones from type IIb.

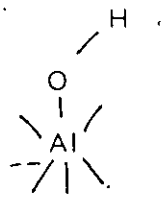


Ib

The two possible types for layer C parallel to the (110) plane are types Ia and IIb which occur to an equal extent, while for layer D and for the (100) face, only type Ib is possible. Thus the maximum number of hydroxyl types on an alumina surface is five and their relative concentrations will depend on the degree of exposure of the various crystal faces.

Knözinger and Ratnasamy have estimated the net charges at the hydroxyl group and at the oxygen atom of this group after removal of the proton. The order of increasing positive charge at the hydroxyl group (and hence decreasing negative charge at the remaining oxygen) is Ib < Ia < IIb < IIa < III. It is therefore expected that type III hydroxyls should have the greatest Bronsted acidity since the removal of a proton from this hydroxyl leaves the smallest

negative charge. Conversely type Ib would have the greatest basicity because removal of an hydroxyl group would leave the smallest positive charge at the anion vacancy.

The infrared spectrum of $\gamma$ - alumina from 4000-500cm$^{-1}$ is shown in Figure 1-7 and Figure 1-8 shows the region from 4000-3000cm$^{-1}$ on an expanded scale. Peri[105], who considered only the (100) face of alumina in his model for $\gamma$ - alumina, assigned the five infrared bands in the O-H stretching region to five distinct hydroxyl group (of the type Ib) in which the OH group had 0 - 4 nearest oxide neighbours. One weakness of this model, which Peri himself admits, is that only one crystal face was considered. Furthermore, as Knözinger and Ratnasamy point out, the assumption that the number of nearest oxide neighbour would be the determining factor for the OH stretching frequencies is questionable.

Jones[108] has reported the infrared spectrum of crystalline lithium hydroxide and assigned a band at 3839cm$^{-1}$ to the O-H$^-$ stretch. Jones compared this value with the stretches of OH and OH$^+$ at 3735 and 2955cm$^{-1}$, respectively, as reported by Herzberg[109] and concluded that the OH stretch in general increased with increasing negative charge. On this basis Knözinger and Ratnasamy assigned the five possible types of hydroxyl groups to the five infrared bands observed for $\eta$ - or $\gamma$ - alumina. Thus, the infrared bands in Figure 1-8 for $\gamma$ - alumina at 3790, 3772, 3747, 3727 and 3684cm$^{-1}$ (3795, 3780, 3737, 3733 and 3689cm$^{-1}$ for $\eta$ - alumina[99]) are assigned to types Ib, Ia, IIb, IIa and III respectively. The relative intensities of these bands will obviously depend on the concentrations of the respective surface hydroxyl group and these may differ for $\eta$ - and $\gamma$ - alumina.

The relative acidity and basicity of the hydroxyl groups on alumina would be expected to be a determining factor in the dehydroxylation process on alumina,

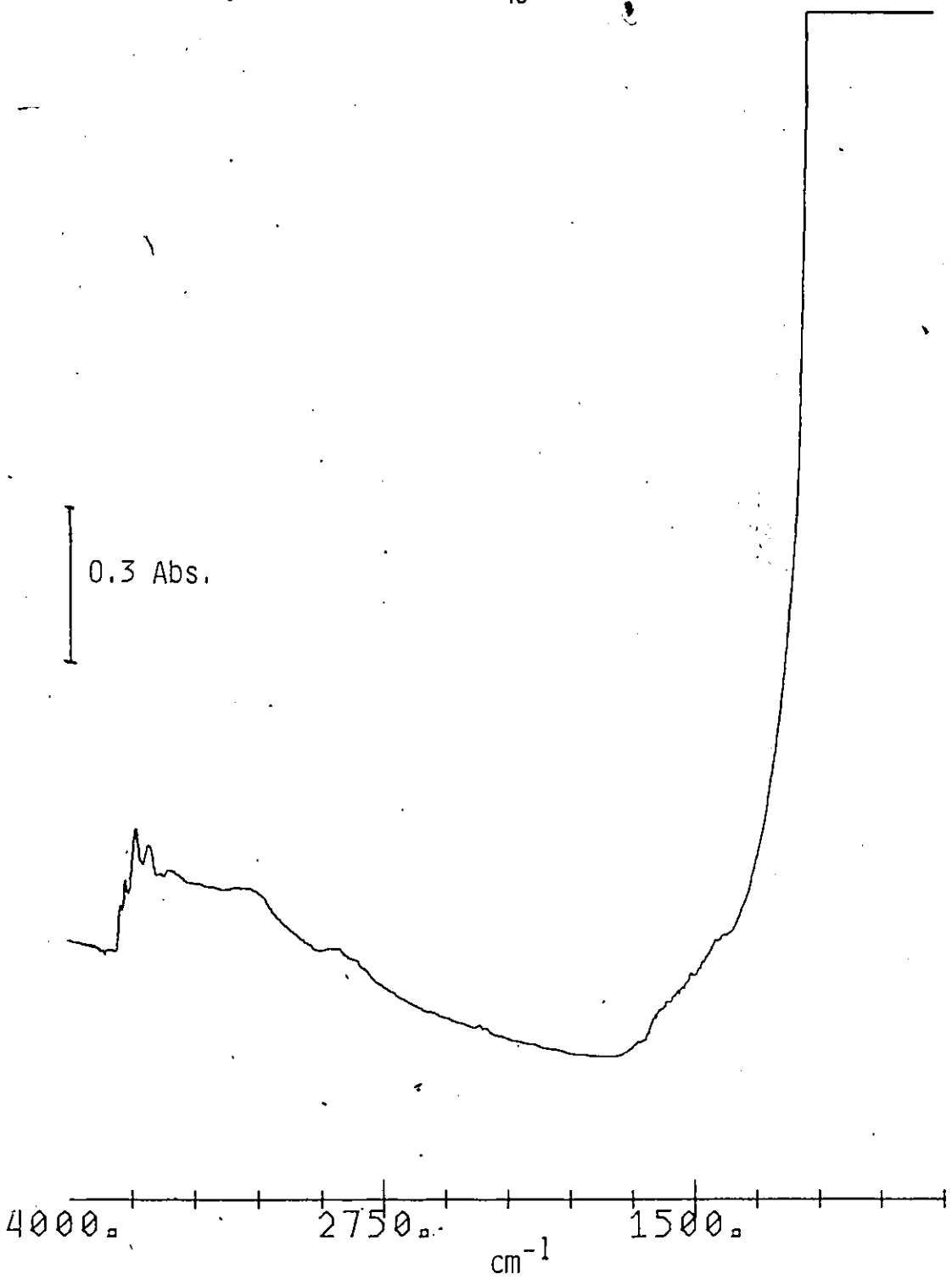


Figure 1-7
Infrared spectrum of $\gamma$ -alumina ($20mg/cm^2$) which had been degassed at 450°C for 1 hr.

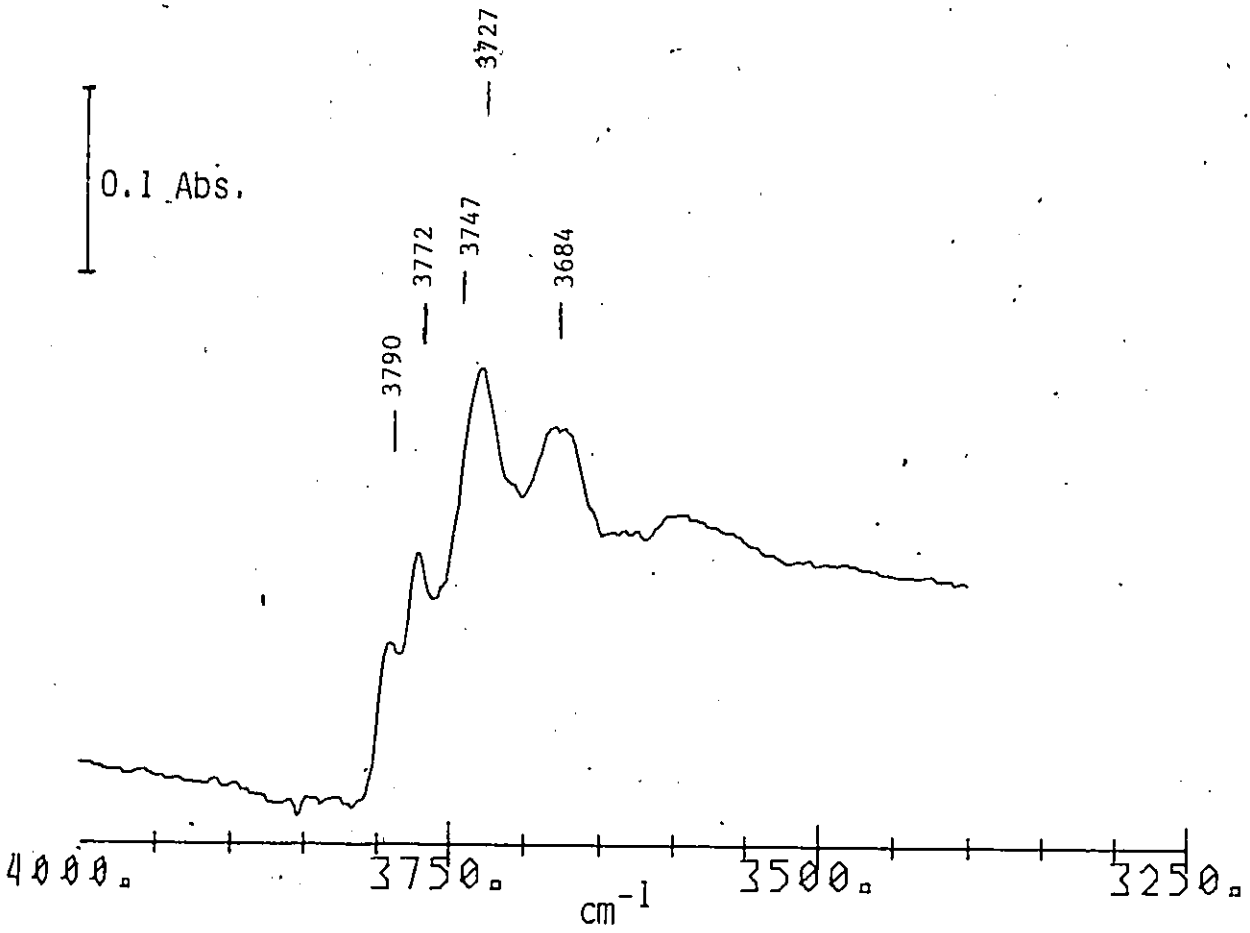


Figure 1-8
Infrared spectrum of the $\gamma$ -alumina sample in Figure 1-7 in the OH stretching region.

at least in the initial stages at low temperature when proton mobility would be low. It has been shown that type Ia and IIa hydroxyls occur in layer A of the (III) face and that type IIa occurs three times more than the type Ia and is the more acidic hydroxyl. In fact these two hydroxyl groups occur as neighbours. Thus, during dehydroxylation type IIa would lose $OH^-$ and type Ia $H^+$, evolve $H_2O$ and to create an anion vacancy (Lewis acid site) exposing a coordinatively unsaturated (cus) 3- coordinate $Al^{3+}$ with a neighbouring cus oxygen (Lewis base site) which bridges 4- and 6- coordinated $Al^{3+}$ cations.

(12)

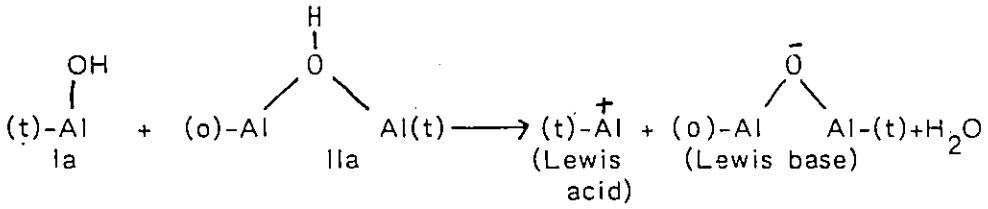


(t) - tetrahedral

(o) - octahedral

Similarly in layer B types IIb and III are nearest neighbours and type IIb is the more basic and occurs thrice as frequently. The dehydroxylation process would therefore be:

(13)

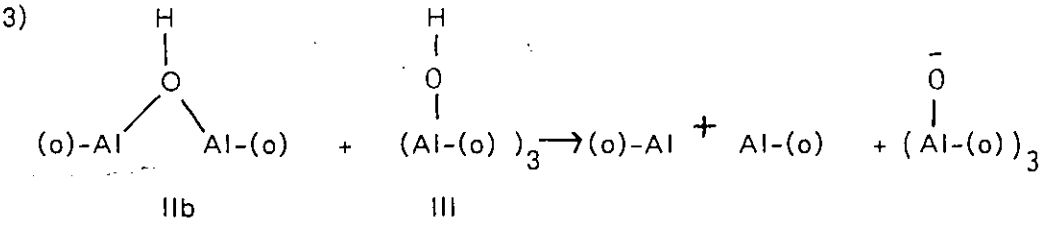


In the C-layer of the (110) plane types Ia and IIb are nearest neighbour and dehydroxylate according to the same principles to expose a cus 3- coordinate $Al^{3+}$ and a cus oxygen bridging two 6- coordinate $Al^{3+}$. In the D- layer of the

(110) face and on the (110) face only one kind of hydroxyl group occurs and so dehydroxylation to produce cus oxygens and aluminum atoms probably procedes in a statistical manner such as that proposed by Peri[105] in his model of the alumina surface.

The interaction between neighbouring hydroxyl groups via hydrogen-bonding would be expected to play a role in the dehydroxylation scheme outlined above. This interaction will depend on the coordination of the hydroxyl group because this determines the orientation of the O-H bond and of the oxygen lone pair electrons of this group with respect to the surface. This situation is examined for the (111) face of alumina. In the A- layer the type IIa hydroxyls are 2- coordinate and have a lone pair of electrons available for bonding but are held in fixed positions with the O-H bond pointing away from the surface so that hydrogen-bonding between type IIa hydroxyls is unfavourable. Conversely, the type Ia hydroxyls in the A- layer can rotate about their single bonds and can therefore have favourable orientations for hydrogen-bonding with neighbouring type IIa hydroxyls. The type IIa hydroxyls are the more acidic hydroxyls and will thus be the proton donors for the hydrogen-bonds and therefore the more perturbed ones (see Part A for hydrogen-bonded silanols). For the B- layer, type IIb hydroxyls have the same orientation as type IIa and therefore would not likely interact with each other. Type III hydroxyls are 3- coordinate and therefore rigid, with O-H bonds pointing away from the surface. Also, they do not have any lone pair of electrons or free orbitals suitable for any further bonding.

The above consideration means that type III hydroxyls with an infrared band at 3684cm$^{-1}$ for $\chi$ - alumina should remain unperturbed at high surface hydroxyl densities whereas the bands at 3772, 3747 and 3727cm$^{-1}$ for types Ia, IIb and IIa respectively should be perturbed to some extent. The dehydroxylation

reaction for type III hydroxyls is not as simple as shown in reaction (13) because the transfer of the proton from this hydroxyl group would not be facilitated by any interaction with the type IIb. This probably therefore involves some proton mobility for the type III hydroxyls during dehydroxylation.

If dehydroxylation proceedes as outlined above a situation would soon be reached for the A- and B- layers of the (111) plane where only the more abundant hydroxyls of type IIa and IIb respectively are left. The degree of dehydroxylation at this point would be 50% since type IIa and IIb are initially three times more abundant than their neighbours. This picture of dehydroxylation is overly simplified and the regular dehydroxylation may be disrupted by a number of possible occurences. Such occurences might be, for example, less favourable dehydroxylation of neighbouring groups IIa or IIb hydroxyls on the (111) or (110) faces. Another occurence could be the formation of type Ib hydroxyls from type IIB hydroxyls in the B- or C- layers or from type IIa in the A- layer.

If regular dehydroxylation proceeds as outlined above then it would be expected that initially the infrared bands at 3727 and 3747$cm^{-1}$ corresponding to types IIa and IIb would be the most intense if the (111)-face were preferentially exposed since these hydroxyl types are three times more abundant than the Ia and III hydroxyls. Once dehydroxylation commences the two infrared bands for Ia and III hydroxyls should be decreased to a greater extent than those for types IIa and IIb. This behaviour has in fact been observed for $\eta$ - alumina by Knözinger and Ratsanamy[99] and Borello et al.[110]. For $\gamma$ - alumina Peri and Hannan[111] and Peri[112] have reported a more ready removal of the infrared band due to type IIb than the bands for the other types and this may be due to a greater proportion of the C- layer of the (110) face for which types Ia and IIb exist in equal proportions. It has also been observed[99] that, as expected, the type III

hydroxyls are the least perturbed at high hydroxyl densities and that types Ia, IIa and IIb are considerably perturbed.

The scheme proposed for the regular dehydroxylation of alumina is one where the more basic hydroxyls sites combine with the more acid hydroxyls to eliminate water thus leaving cus-oxygen and cus-aluminum atoms with the smallest possible charge. This means that the neighbouring Lewis acid and base sites thus formed are weak. For both $\eta$ - and $\gamma$ - aluminas catalytic activity was observed only for a dehydroxylated surface. Knözinger[113] has reported that for regular dehydroxylation (up to 50%) as discussed above, there were 100 times more Lewis sites created than there were catalytic sites for e.g., $CH_4$ exchange with $D_2$ as determined by $CO_2$ poisoning experiments. Knözinger and Ratnasamy have pointed out that catalytic activity only appears after dehydroxylation above 300-400°C although $3.7 \times 10^{14} cm^{-2}$ of cus-oxygen and cus-aluminum atoms are already present. It was therefore concluded that these Lewis acid and base sites created by regular dehydroxylation could hardly be involved in catalytic activity. They considered that during dehydroxylation above 300°C special site configurations of low probability began to develop which have the structural and energetic properties required for an active site for catalysis and this site was identified with defects in the dehydroxylated surface.

In developing their model for the creation of these defect sites, Knözinger and Ratnasamy considered the case of the (111) face when 50% dehydroxylation has been achieved. At this stage, all types Ia and III hydroxyls have been condensed with neighbouring types IIa and IIb which are in threefold excess in the A- and B- layers, respectively. Thus, rows of types IIa and IIb remain in these A- and B- layers. Further dehydroxylation results in the condensation of equivalent hydroxyl groups which leads to the creation of defects in the form of a row with three cus-oxygens associated with three cus $Al^{3+}$.

However, Knözinger and Ratsanamy, acknowledging that some types III, Ia, and Ib hydroxyls still remained on alumina even after dehydroxylation at 300°C, concluded that irregular dehydroxylation must occur. Thus they state that at increasing temperatures the mobilities of both surface hydrogen and lattice cations can promote the restoration of hydroxyl configurations which have been eliminated at lower temperatures, particularly those configurations involving cations in tetrahedral sites. Thus, defect sites of low probability can be created.

The adsorption of carbon monoxide (CO) on $\eta$- and $\gamma$- alumina at 36°C has been used by Della Gatta et al.[114] to obtain information about the nature of these defect sites. No CO was adsorbed on either $\eta$- or $\gamma$- alumina degassed below 400°C. However, after dehydroxylation above 400°C, CO characterized by an infrared band at 2203-2215$cm^{-1}$ was adsorbed and the amount of adsorbed CO increased with dehydroxylation up to 600°C. Upon dehydroxylation above 500°C a new adsorbed CO species with an IR band at 2244$cm^{-1}$ was observed and, in addition the type Ia hydroxyl IR band was perturbed. This latter CO species was the more strongly adsorbed one with a heat of adsorption of 58.5kJ $mole^{-1}$ compared to 8.4kJ $mole^{-1}$ for the other species. Both species, however, can be described as CO linked to a cus-surface $Al^{3+}$ via $\sigma$- dative bonding. The site density for the strongly adsorbed CO species was determined to be $2\times10^{13}cm^{-2}$ and $6\times10^{12}cm^{-2}$ on $\eta$- and $\gamma$- alumina, respectively. Other molecules such as carbon dioxide[115-118], nitriles[119, 120], ketones[120], pyridines[120] and olefins[99] have been found to perturb the Ia hydroxyls under the same conditions as did CO and, because the concentrations of these compounds on the surface required for the pertubation of this hydroxyl were the same order of magnitude as in the case of CO, the same site was probably responsible. Fink[115] has designated these as X- sites.

No conclusion can be reached about the detailed nature of the stronger adsorption site for CO although it must be a type of defect site because it is observed only after dehydroxylation above 400°C. The second site (X - site) must also be a defect site and must also involve a neighbouring type Ia hydroxyl. This hydroxyl group must be in an environment where hydrogen-bonding was not possible with, for example, neighbouring cus-oxygens or other hydroxyls since a sharp IR band was observed for this hydroxyl group before CO adsorption. Conversley, this hydroxyl group must be close enough to be perturbed by CO adsorbed on a neighbouring anion vacancy.

In summary, η - and γ - alumina both have five types of surface hydroxyl groups which can be modelled very well by the (111), (110) and (100) faces of alumina with a defect spinel structure. The so called regular dehydroxylation below 400°C produces weak Lewis acid and base sites which are coordinately unsaturated aluminum cations and oxygen atoms, respectively. These Lewis sites are weak and are not responsible for all the observed catalytic activity of these aluminas. Dehydroxylation above 400°C, which can be described as irregular, produces the very strong Lewis acid site which is responsible for catalytic activity and has a neighbouring hydroxyl group which can interact with species adsorbed on this Lewis acid site. The acidity of η - alumina is slightly greater than γ - alumina. The greater catalytic activity of η - alumina compared to γ - alumina is probably due to the greater concentration of catalytic sites produced on η - alumina.

Objectives of the Present Study

We have shown that the surface of silica has different types of hydroxyl groups and siloxane bridges. The silanol groups are either isolated or hydrogen bonded, the latter being favored on highly hydroxylated samples. Dehydroxylation below 400°C brings about the conversion of the hydrogen-bonded silanols to

siloxane bridges which can be completely reformed when water is subsequently re-added. However, dehydration above 400°C leads to the elimination of the isolated hydroxyls with the formation of very reactive strained siloxane bridges and the normal siloxane bridges become increasingly resistant to rehydration. Previous attempts aimed at determining the numbers of various types of siloxane and silanol sites on silica have given ambiguous results because the structures of the chemisorbed probe molecules used were unknown.

The surface of fully hydrated $\gamma$-alumina has five different types of isolated hydroxyl groups. Dehydroxylation below 400°C is orderly and produces pairs of weak Lewis acid and base sites. Dehydroxylation above 400°C is not orderly and involves the creation and migration of surface defects. This latter process produces strong Lewis acid and base sites which are responsible for the catalytic activity exhibited by $\gamma$-alumina. Quantitative determination of the numbers of the various types of sites present as a function of activation temperature is, as with silica, difficult because most probe molecules react in a similar way with these sites and their structures are unknown.

The present investigation had two objectives. Firstly to develop new tchniques, using infrared and Raman spectroscopies, in order to obtain a complete vibrational spectrum from 4000 to 100 $cm^{-1}$. Secondly, to use these techniques in order to determine the numbers and types of the various types of active surface sites discussed above, on alumina and silica, as a function of the temperature of activation.

# CHAPTER 2

# GENERAL EXPERIMENTAL

## The Infrared Spectrometers

Infrared spectra in these studies were obtained using either a Perkin-Elmer 283 dispersive spectrometer or a BomemDA3-02 Fourier Transform Infrared (FTIR) spectrometer. With the Perkin-Elmer 283 spectrometer spectra were usually recorded using a scan speed of 150 $cm^{-1}$ $min^{-1}$ with a resolution of 3-5 $cm^{-1}$. The instrument was normally used in the double beam mode and spectra were recorded in % transmittance. The spectrometer had a post-sample chopper and this resulted in the unmodulated radiation from the source impinging on the sample which caused considerable heating. This heating effect is discussed in a later chapter of this thesis.

The Bomen FTIR spectrometer had two sample compartments, one equipped with a liquid nitrogen cooled mercury cadmium telluride (MCT) detector and the other with an ambient temperature tri-glycene sulphate (TGS) detector. Both detectors allowed the recording of infrared spectra between 4000-400 $cm^{-1}$ but the MCT detector had a higher sensitivity and was used exclusively in these studies. The spectrum was obtained by recording 100-400 coadded interferograms over a period of 40-160 seconds and then performing a Fourier transform. The spectral resolution employed was 4 $cm^{-1}$ although resolutions of 0.02 $cm^{-1}$ could be obtained if required.

## The Raman Spectrometer

The Raman spectra obtained in these studies were acquired from a Jobin-Yvon HG - 2 Raman spectrometer. The laser used was an argon ion laser

from either Control Laser Corporation or from Spectra Physics Inc. Usually the 514.5 nm laser line was used to irradiate the sample with 50-1000 mw of power. Plasma emission lines which would create sharp spikes in the spectrum were excluded by the use of an Anaspec Laser Filter Monochrometer. Spectra were usually recorded between 4000-100cm$^{-1}$ at a resolution of about 6cm$^{-1}$ with a scan time of 39 minutes.

The Vacuum Line

A standard pyrex vacuum line of about 1000 cm$^3$ volume was used in the preparation of degassed samples and to manipulate gases from various containers to the sample cells. Pumping was achieved by an oil or mercury diffusion pump backed by a mechanical pump with pumping speeds of 27 and 1 litre/s of air respectively. A liquid nitrogen trap separated the manifold from the two pumps. When using a mercury diffusion pump a second trap separated it from the oil pump. The manifold was equipped with a mercury manometer for measuring pressures greater than 1 torr, a McLeod gauge for pressures between 1 - .005 torr and a thermocouple gauge for quick rough pressure estimations. The manifold had several outlets equipped with high vacuum teflon stopcocks and ground glass connectors. The ultimate pressure achievable with such a vacuum system was $10^{-6}$-$10^{-7}$ torr. With the evacuated manifold isolated from the pumps the pressure rose to $10^{-4}$ torr in about 5 minutes. The sample cell and containers of gases and volatile liquids were connected to the vacuum line via ground glass joints greased with Apiezon N high vacuum grease.

Sample Cells

a) For Infrared Studies

Two types of infrared sample cells were used in these studies. The

first type shown in Figure 2-1 is the same as that described previously by Morrow and Ramamurthy[121]. The lower part of the cell with the furnace and infrared windows (either NaCl, KCl or $CaF_2$) was made of either pyrex or quartz. The sample holders were also invariably made from quartz while the cell tops were of pyrex. The ground glass joints of the cell top and bottom were greased with Apiezon H. The sample could be raised into the furnace region by means of a magnet applied to the holder's enclosed iron tip. The furnaces consisted of asbestos paper surrounding the cell around which was wound Kanthal wire at a density of 4 turns/cm. This was insulated by two layers of a ceramic paper tied securely with asbestos cord. A chromel-alumel thermocouple enclosed in a quartz tube was inserted between the insulation and the heating wire. Temperatures of 500°C could be achieved with the pyrex cells and 1200°C with the quartz cells.

Figure 2-2 shows the second type of infrared cell used. This cell and sample holder were made from quartz and equipped with a standard furnace described above. The infrared windows were of NaCl. One window was permanently cemented with epoxy resin directly to the quartz tube while the other was cemented to a Cajon Ultra-Torr vacuum adapter which fitted over the other end of the tube where the sample was inserted. The O-ring in the Cajon adapter was lightly coated with Apiezon H high-vacuum grease. This cell was used primarily when *in situ* heating of the sample positioned in the IR spectrometer was required.

b) Raman Cells

The Raman cell used is shown in Figure 2-3a. The cell was made from pyrex and the windows were of optical quartz. Two types of sample holder were employed and are shown in Figures 2-3b and 2-3c and d. The conventional sample holder in in Figure 2-3b was made from pyrex and was used with 12 mm sample discs. The

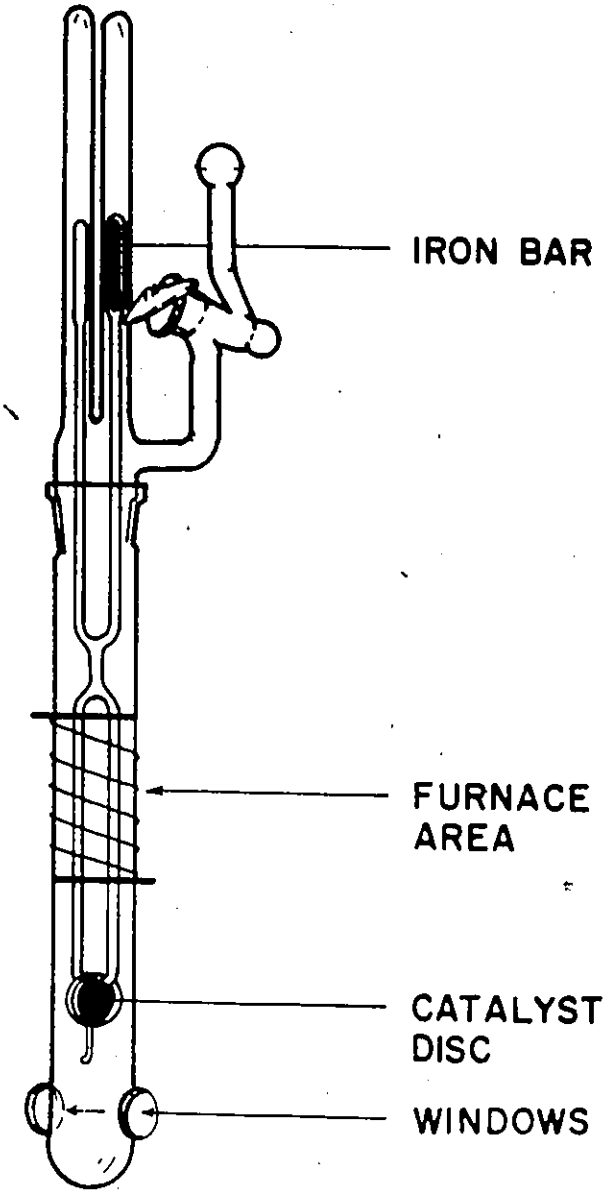


Figure 2-1
The standard infrared cell

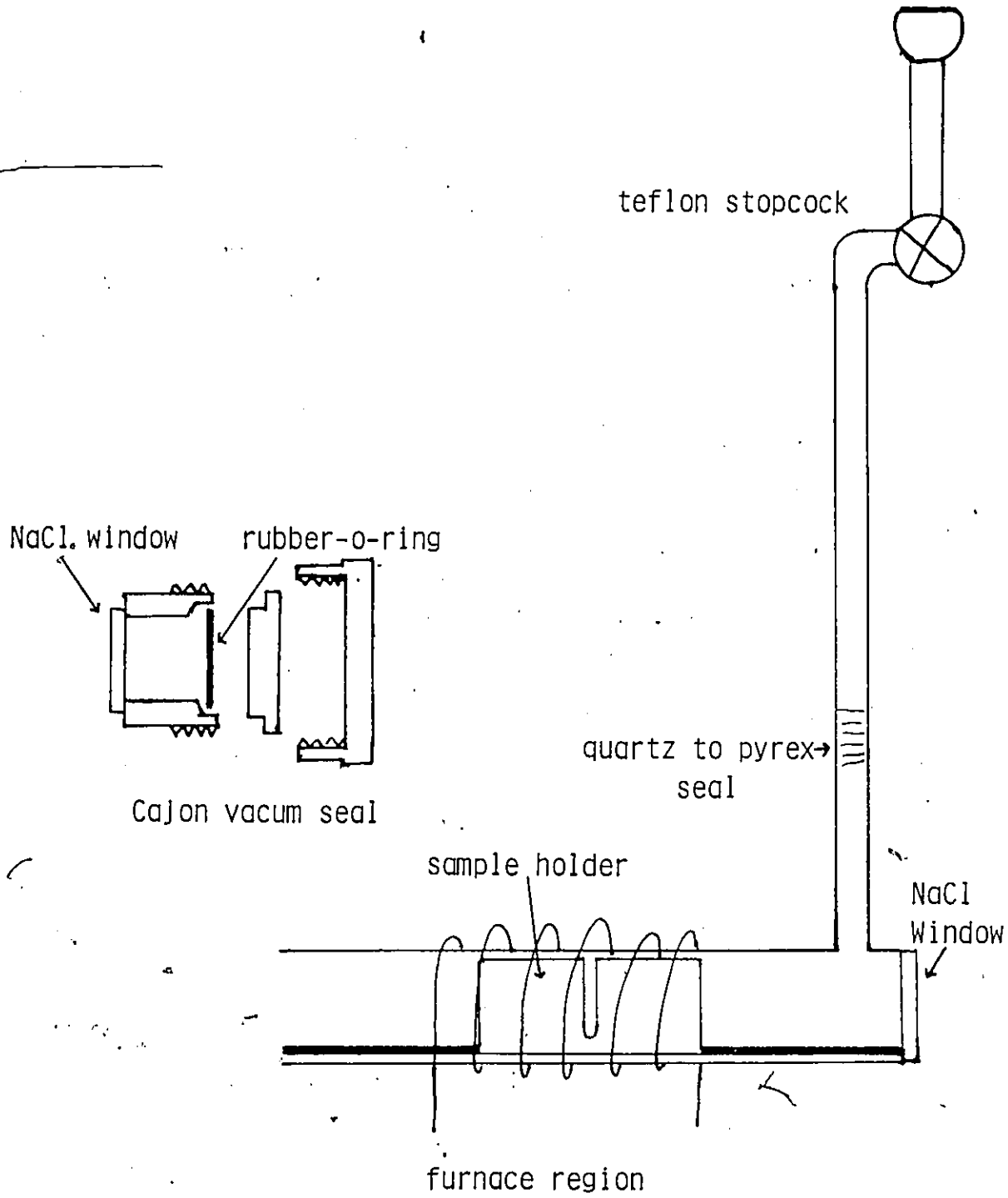


Figure 2-2
Infrared cell used for in situ studies

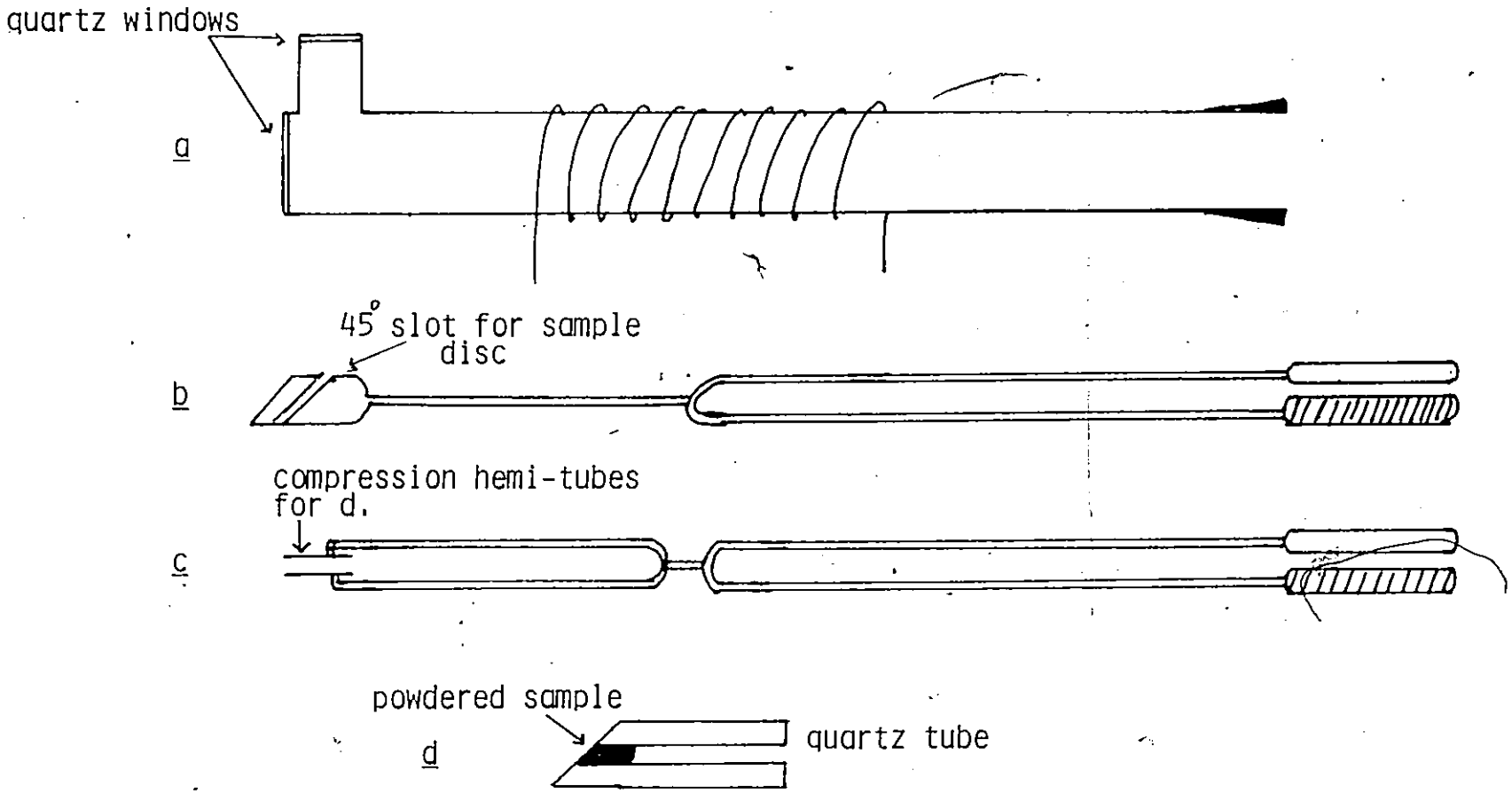


Figure 2-3
a) Bottom part of the Raman cell. The cell top is the same as that show in Figure 2-1
b) Conventional sample holder for Raman studies
c) Modified Raman sample holder for small quantities of a powdered sample
d) Sample tube from c).

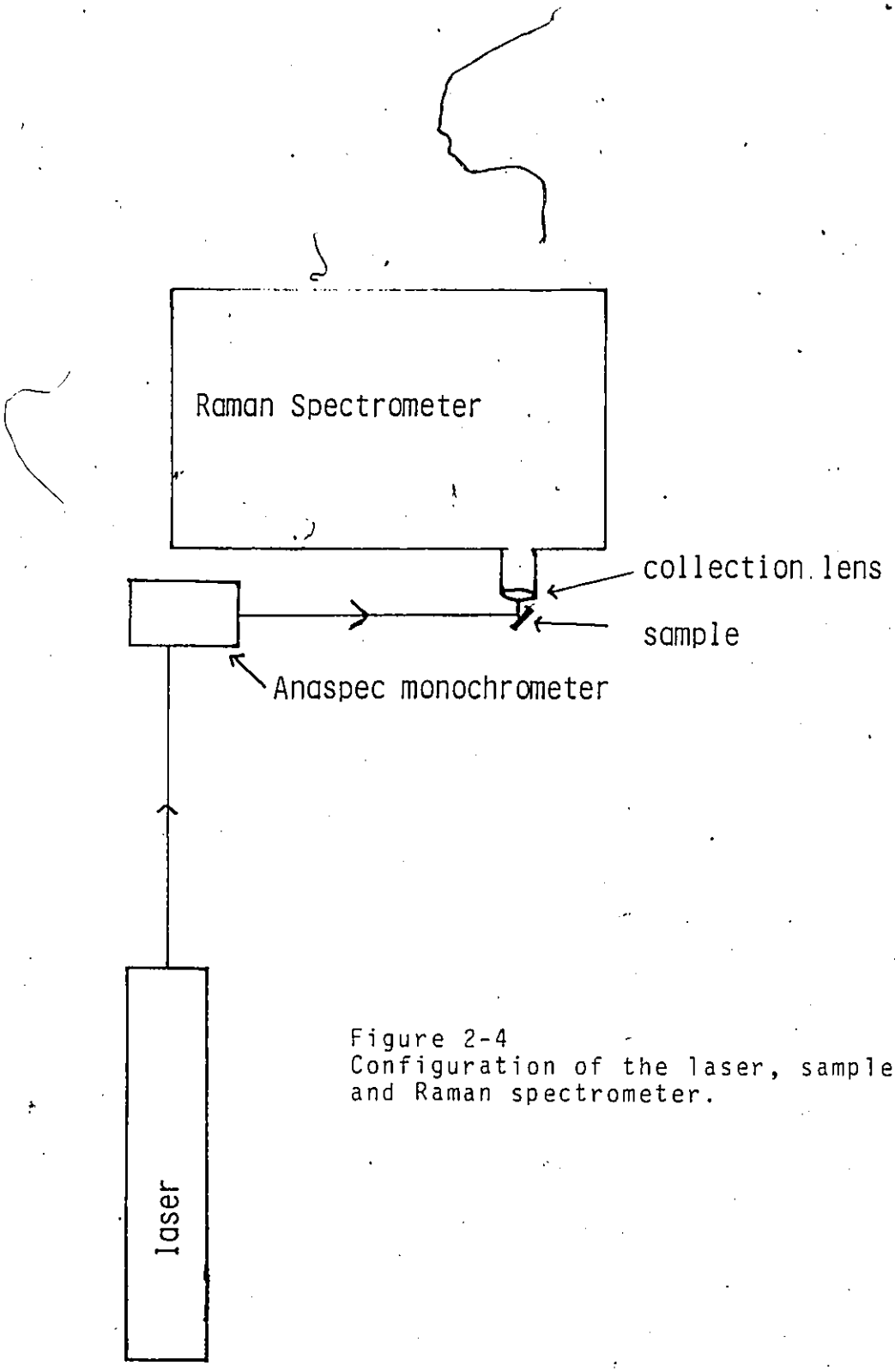


Figure 2-4
Configuration of the laser, sample and Raman spectrometer.

holder in Figure 2-3c and d which was in two parts was made from quartz and was used when only a few milligrams of sample was available and, in these studies, only for the zeolite ZSM-5.

This cell design was found to be the optimum one for the efficient collection of the Raman scattered light. Figure 2-4 shows the configuration of the laser, cell and spectrometer employed in this work. The $90^{o}$ scattering geometry was found to be the best one when compared with scattering geometries in which the angle of the incidence of the laser beam with the sample was varied from $22\frac{1}{2}^{o}$ to near $90^{o}$, i.e., $45^{o}$-$180^{o}$ scattering geometries. No difference was found in the intensity of the Raman spectrum whether the sample was run in the cell or not when using the optimum geometry.

## Materials

### Silica

The silica used was Cab-O-Sil HS-5 obtained from Cabot Inc. of Tuscola, Illinois, U.S.A. The oxide had a B.E.T. ($N_2$) surface area of 330 $m^2/g$. It was used either in the as received form or was calcined at $550^{o}C$ for several days before use in order to remove organic impurities.

Sample discs of silica for infrared studies were prepared by placing a preweighed amount of silica, 20 - 200 mg, in a 2.5 cm stainless steel die which was then compacted at a pressure of $10^7$ Pa. This sample could then be placed in the IR cells shown in Figures 2-1 and 2-2.

Thin silica films with .5 - 5 mg of silica on a 2.5 cm ZnS or ZnSe infrared window could be prepared in one of two ways. For thick films, .4-1.0 $mg/cm^2$, a preweighed amount of silica was placed on the face of the stainless steel die and was spread out in a thin layer. The IR window was laid on top and

twirled gently so that the silica was now spread in a thin relatively even layer between the die face and window. A slight pressure was then applied to the centre of the window and the window was raised vertically from the die. A relatively stable film of silica then adhered to the window and its weight could be determined accurately if neccessary. Silica films with less than 0.4 mg/cm$^2$ of material could be prepared by carefully spreading the silica on the IR window with a stainless steel spatula using firm smooth strokes. For most work the silica film was usually prepared so that the absorbance at 1108cm$^{-1}$ was 1.2-1.8 absorbance.

Alumina

The alumina used was Degussa Aluminum Oxid C from Degussa A.G. Frankfurt. It had a B.E.T. ($N_2$) surface area of 105 m$^2$/g. It was usually calcined in air at 550$^o$C for several days before use to remove organic contaminants and adsorbed $CO_2$.

Alumina often adhered to the surface of the stainless steel die during pellet pressing. In order to overcome this, wafers of lens paper were placed between the die faces and the alumina powder during pressing. This paper could easily be removed from the alumina disc afterwards. The minimum sample thickness obtainable by this method was 20 mg/cm$^2$. The lens paper was impregnated with alumina by pressing several alumina pellets before making the one actually used in an experiment.

Preparation of Raman Samples

The following sample preparation procedures were employed in all Raman experiments in this work unless otherwise specified. Initially the furnace region of the cell, and the sample holder were heated in air at 480$^o$C for 6 hrs.

The sample disc to be used in the experiment was calcined in air at 500°C for at least 2 hrs. This disc was then transferred to the cell within 10 minutes of removal from the oven and was evacuated at 25°C for about 10 minutes. Approximately 600 torr of $O_2$ was added to the cell which was then heated at 480°C for 30 min. followed by evacuation for 10 minutes. The addition and evacuation of $O_2$ was repeated three more times and the sample was cooled in 600 torr of $O_2$ to 25°C. Finally, the oxygen was evacuated and the sample was ready for the recording of the Raman spectrum. The above outlined prcedure was found to produce samples which were almost invariably fluorescence free.

## Chemicals

Natural isotopic abundance(n) diborane ($^nB_2H_6$) was prepared by the reaction of iodine with $NaBH_4$ in diglyme and was purified by triple distillation at -70°C over a dry ice/acetone bath. The purity was confirmed by infrared and mass spectrometry. Deuterated natural isotopic abundance diborane($^nB_2D_6$) was prepared in a similar manner using $NaBD_4$. Boron-10 labelled diborane was prepared by decomposing the $CaF_2$:$^{10}BF_3$ complex (96% $^{10}B$, from Oak Ridge National Laboratories) to yield $^{10}BF_3$ and then reducing the $^{10}BF_3$-ether solution with $LiAlH_4$.

Phosphine was prepared by thermally decomposing commercial $PH_4I$ and was purified by distillation.

Borane carbonyl was produced by the reaction of carbon monoxide with diborane in monoglyme over a dry ice/acetone bath at -20°C and the product was distilled at -78°C over another dry ice/acetone bath.

Arsine was produced by the reduction of $AsCl_3$ with $LiAlH_4$ in ether. Distillation removed most of the ether and the last traces could be removed by

passage over silica which had been degassed at 450°C.

HCN was made by the reaction of concentrated sulphuric acid on KCN. The HCN was dried over $P_2O_5$ and purified by distillation.

Trimethylgallium with a purity of 99.999% was obtained from Alpha Ventron and was used without further treatment.

All other chemicals used were obtained from standard sources. Purity checks of these chemicals were made when necessary by infrared and mass spectrometry and they were distilled, dried and degassed as needed. Degassing involved freezing of the gas at liquid nitrogen temperature and evacuation at this temperature. A small "experimental" section has been included in the succeeding Chapters with details of specific procedures pertinent to those experiments.

# CHAPTER 3

## TECHNIQUES FOR A COMPLETE VIBRATIONAL ASSIGNMENT OF AN ADSORBATE ON SILICA

### Introduction

The low frequency vibrational spectrum of absorbates on metal oxides, wherein lie the adsorbent-adsorbate stretching modes, is not normally accessible because the self-supporting oxide discs are infrared transparent only to about 1000 $cm^{-1}$. This limitation has been overcome in the case of silica by using a thin film of the oxide supported on an infrared window which, in the present case, gave samples that where transparent to 500 $cm^{-1}$. Further, the complimentary low frequency vibrational information which can in principle be provided by Raman spectroscopy has usually not been attainable because of the high background fluorescence of the oxide. However, a technique has been developed in the present work which yields spectra of negligible fluorescence and high signal-to-noise ratio. These techniques have been used in the present work to give almost complete vibrational information regarding the adsorption of hexamethyldisilazane ( $[(CH_3)_3\ Si\ ]_2NH$,HMDS), methanol and titanium tetrachloride ($TiCl_4$) on silica.

Infrared spectra from 4000-1300 $cm^{-1}$ and Raman spectra from 4000-100 $cm^{-1}$ for HMDS and $TiCl_4$ adsorbed on silica have been reported by several workers[53, 94, 122-124]. It has been accepted that the reaction with HMDS procedes according to reaction (1)[125]. However, the antisymmetric $\equiv$Si-O-Si$\equiv$ stretch has not been observed since it would lie in the region of total absorption below 1300 $cm^{-1}$.

$$(1) \quad 2 \equiv Si\text{-}OH + (CH_3)_3\,Si\text{-}\underset{\underset{H}{|}}{N}\text{-}Si\,(CH_3)_3 \longrightarrow 2 \equiv SiO\text{-}Si\,(CH_3)_3 + NH_3\uparrow$$

Recently Kinney and Staley[126] have reported infrared photoacoustic spectra (PAS) from 4000-600 $cm^{-1}$ for $TiCl_4$ on silica and have assigned low frequency $\equiv$Si-O-Ti vibrations purported to be due to the species $\equiv SiO\text{-}TiCl_3$ and $(\equiv Si\text{-}O)_2\,TiCl_2$.

This study is concerned with a re-examination of the adsorption of HMDS and $TiCl_4$ on silica using infrared and Raman spectroscopies. In addition, a critical comparison of the thin film technique and infrared photoacoustic spectroscopy is made using the results obtained for $TiCl_4$ and methanol on silica.

Experimental

Except where specified all silica samples used were calcined at 500°C in air and degassed in vacuum at 500°C for infrared experiments and at 480°C for Raman studies. In cases where the silica was degassed at 150°C an uncalcined silica was used. The infrared experiments with $TiCl_4$ were carried out in the conventional IR cell and in a typical experiment the sample was exposed to the vapour pressure of $TiCl_4$ for 1 minute and then evacuated for 1 hour at 25°C. The reactions with HMDS for infrared studies were done in the small cell capable of in situ heating and in these experiments the vapour pressure of HMDS was added to the cell which was heated to 150°C for 30 minutes followed by evacuation and cooling to 25°C for 1 hour. In the Raman experiments, the reaction with HMDS was carried out at 75°C for ½hr in order to minimize the background fluorescence which increases with heating of the sample. The reaction of methanol with silica was done at 325°C using the in situ cell and the sample was exposed to the vapour pressure of methanol which was changed every 10 minutes in order to minimize the effects of leakage of the seals of the cell at this temperature. The cell was

then evacuated and cooled to 25°C for 1 hr.

Results

The infrared spectrum of a silica film before and after its reaction with $TiCl_4$ is shown in Figures 3-1 and 3-2 for samples which had been degassed at 500 and 150°C, respectively, while Figures 3-3a and 3-3b show the corresponding difference spectra. In Figures 3-4a and 3-4b are the Raman spectra which were observed before and after treatment with $TiCl_4$ of silica which had been degassed at 480°C and Figure 3-5 shows the spectrum after reaction with silica which had been degassed at 150°C. No background Raman spectrum was obtained for the 150°C degassed sample due to the high background fluorescence present before addition of $TiCl_4$. The frequencies of all the observed bands are listed in Table 3-1.

In Figures 3-6a and 3-6b are shown the IR spectra of a thin silica film prior to and after reaction with HMDS. Figure 3-7 shows the difference spectrum (6b-6a) for HMDS while Figure 3-8 displays the difference spectrum for deuterated HMDS-d18 ( $[(CD_3)_3Si]_2NH$ ). Figures 3-9 and 3-10 show portions of the Raman spectrum for HMDS for and HMDS-d18 treated silica. All infrared and Raman band frequencies are listed in Table 3-2.

Figures 3-11 and 3-12 show the infrared spectra observed after reacting methanol with silica. The new peaks for the adsorbate in Figures 3-11b and 3-12 are observed at 2996, 2957, 2856, 1114 and 853 $cm^{-1}$.

Discussion

Part A : Titanium tetrachloride

The addition of $TiCl_4$ to silica resulted in the appearance of new IR bands in the region 1100-700 $cm^{-1}$ and the disappearance of the peak at 3748 $cm^{-1}$ indicates that the new features are due to species formed by the reaction with

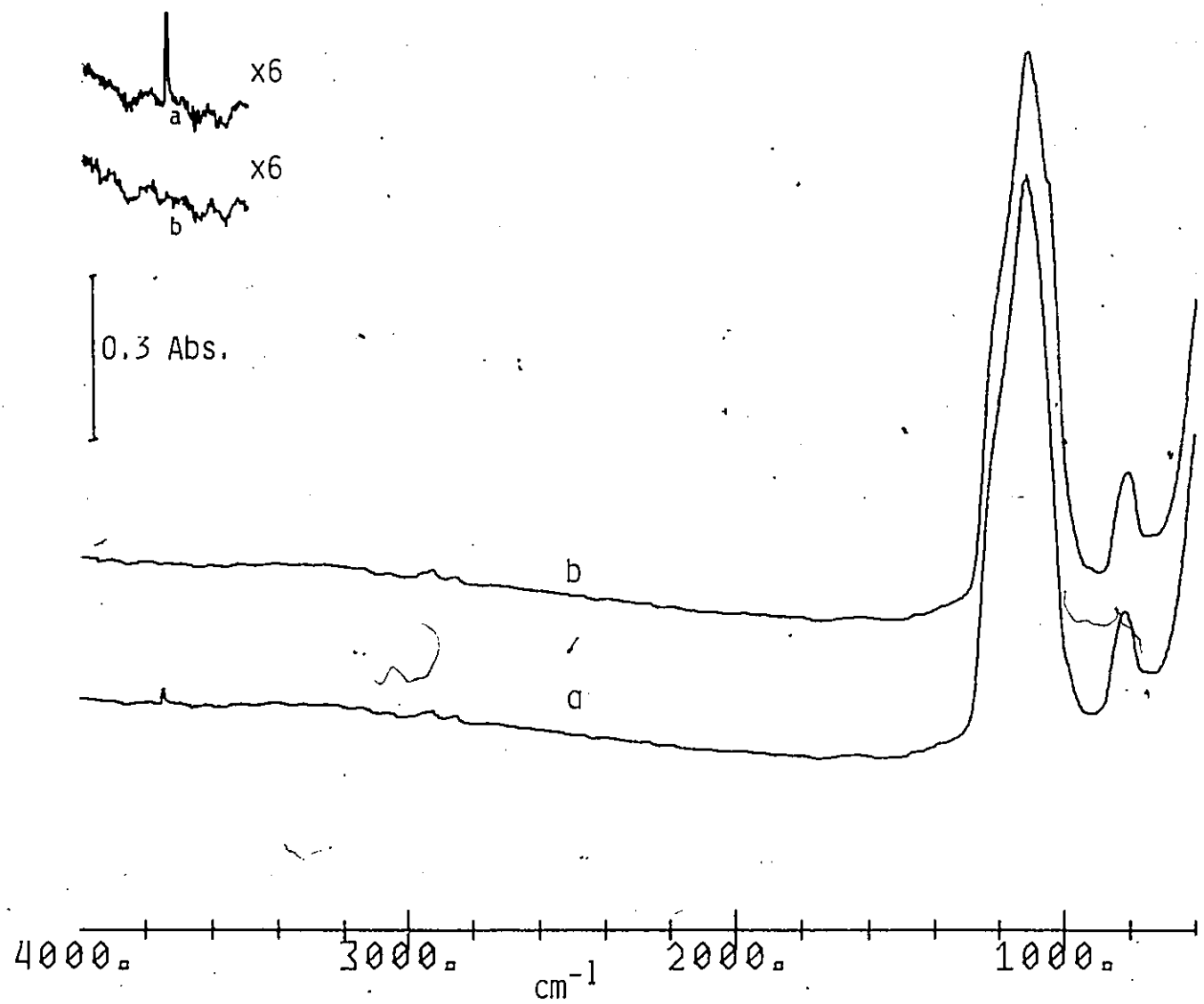


Figure 3-1
a) Infrared spectrum of a thin silica film degassed at 500°C for 1/2 hr.
b) After reaction of a) with $TiCl_4$ at 25°C followed by evacuation for 1 hr.
The region from 4000-3500 $cm^{-1}$ for curves a) and b) are shown on an expanded ordinate scale (inset).

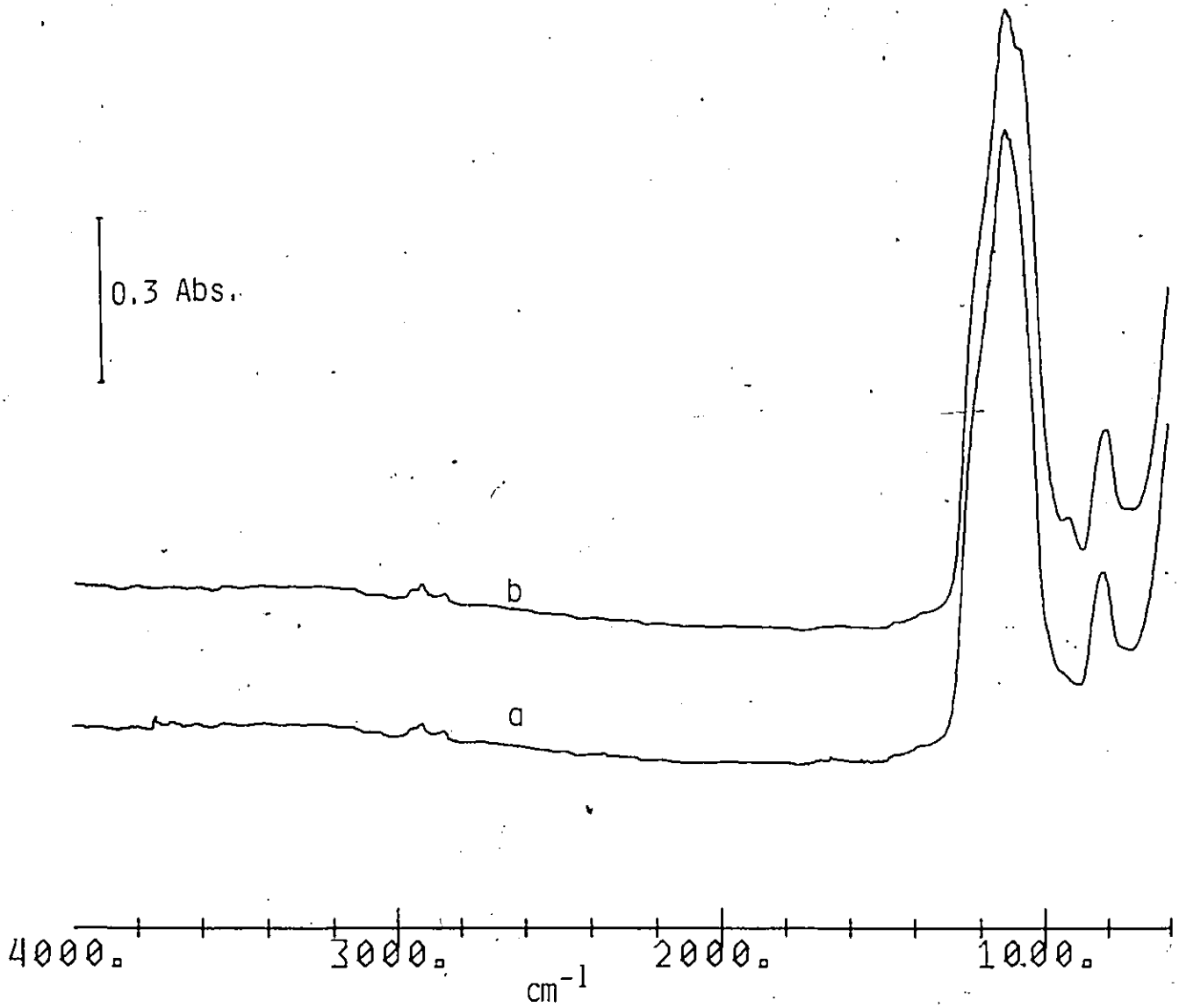


Figure 3-2
a) Infrared spectrum of a thin silica film degassed at 150°C for 1/2 hr.
b) After reaction of a) with $TiCl_4$ at 25°C and evacuation for 1 hr.

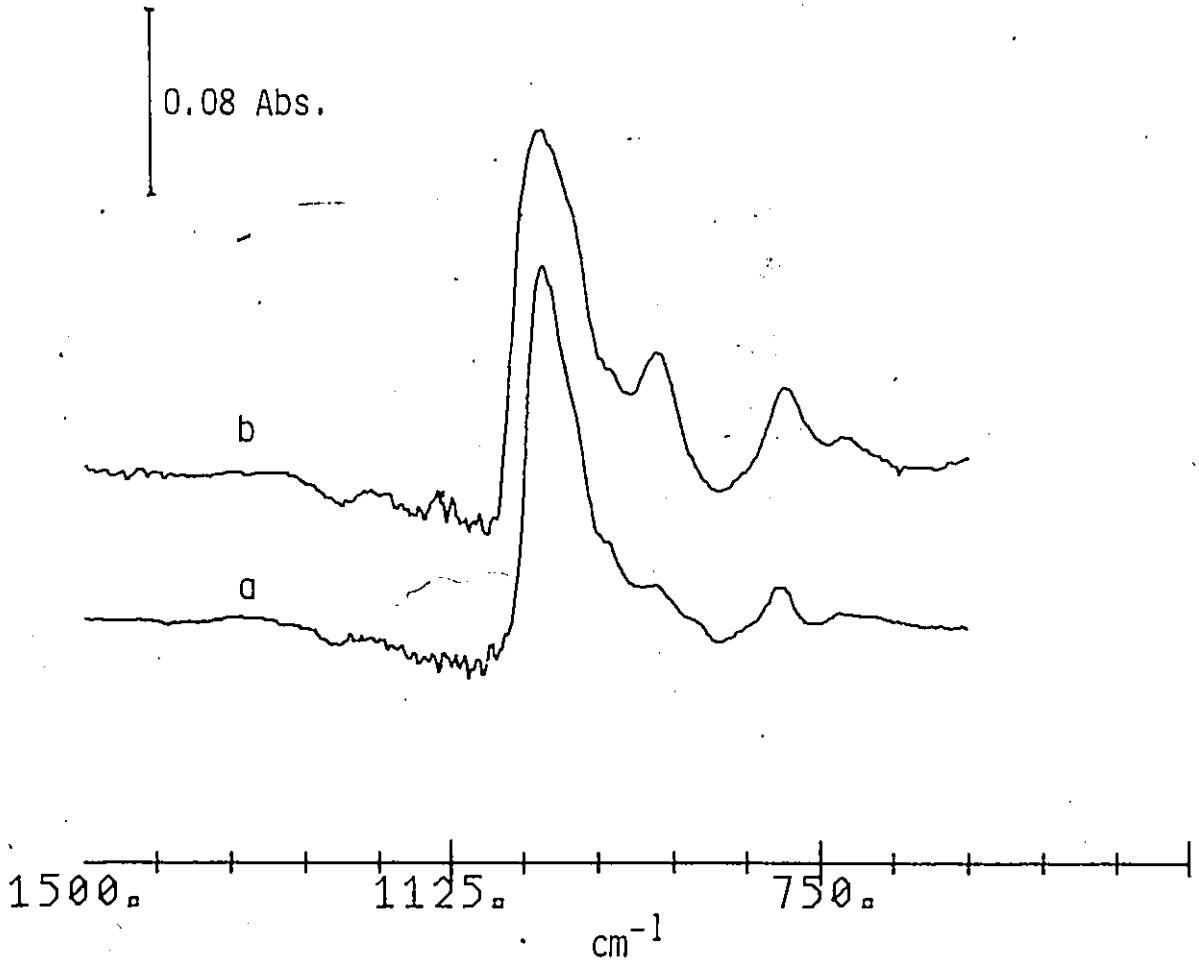


Figure 3-3
a) Difference spectrum Figure 3-1b minus Figure 3-1a for 500°C degassed silica reacted with $TiCl_4$.
b) Difference spectrum Figure 3-2b minus Figure 3-2a for 150°C degassed silica treated with $TiCl_4$.

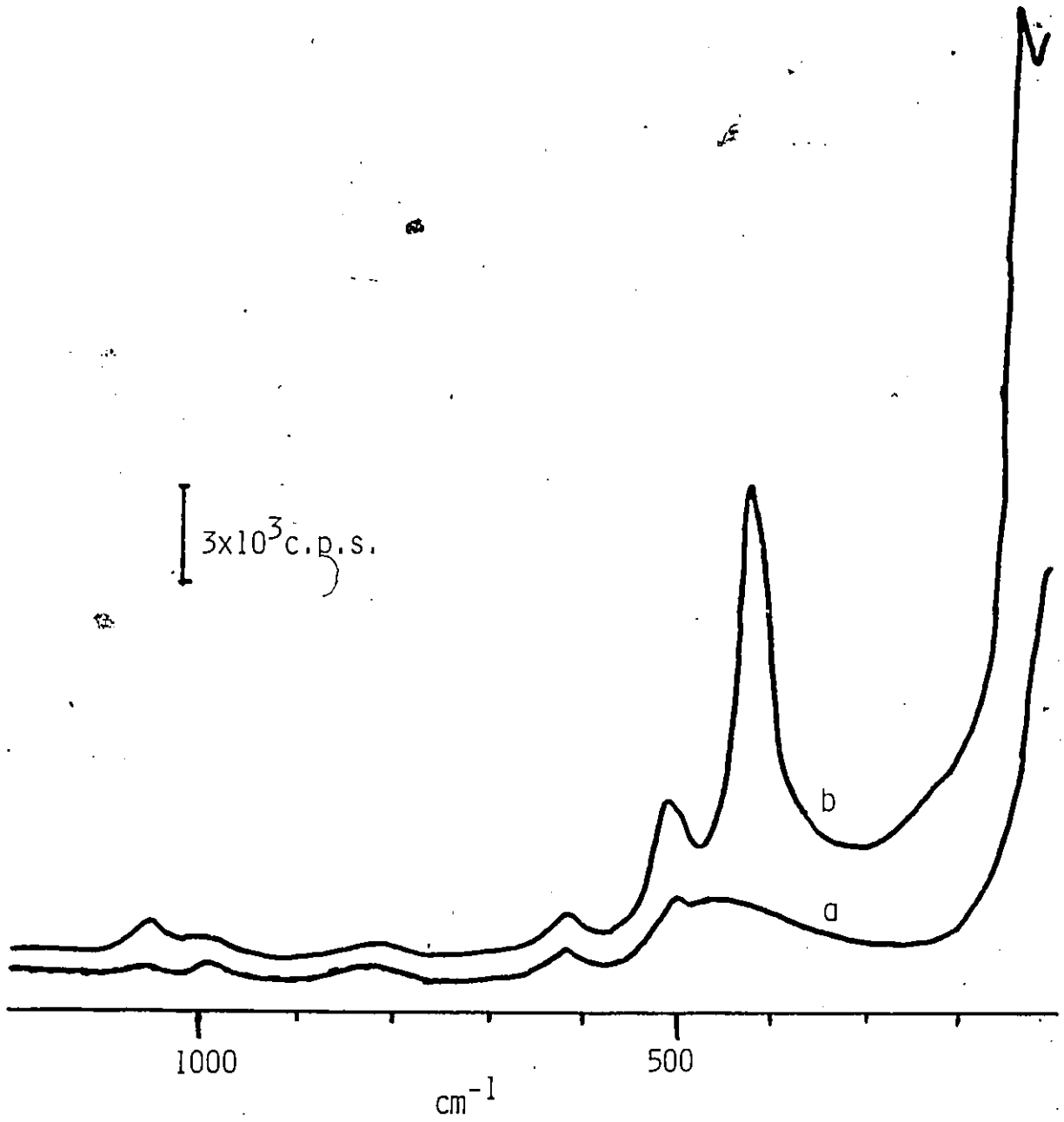


Figure 3-4
a) Raman spectrum of a silica degassed at 480°C for 1 hr.
b) Spectrum of a) after reaction with $TiCl_4$ and evacuation at 25°C for 1 hr.

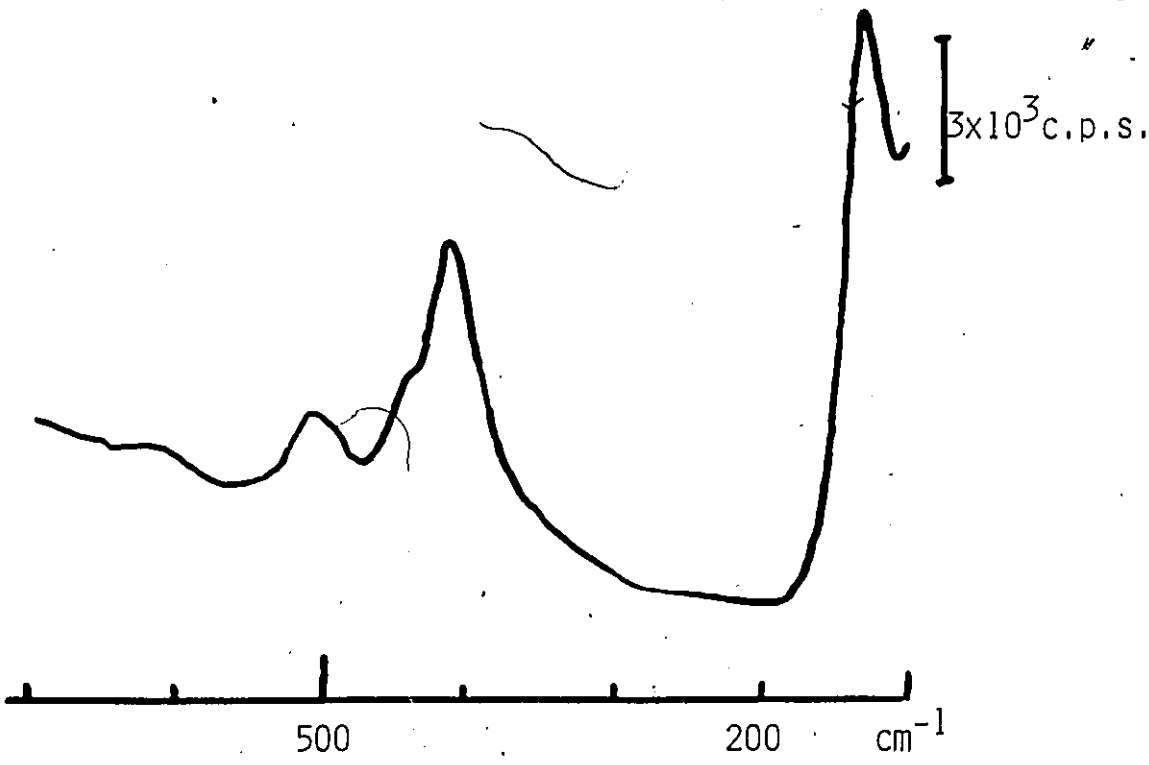


Figure 3-5
Raman spectrum of silica which had been degassed at 150°C for 1 hr., reacted with $TiCl_4$ at 25°C and evacuated for 1 hr.

Table 3-1

Frequencies of infrared and Raman bands for the reaction of titanium tetrachloride with silica.

| | Infrared/$cm^{-1}$ | Raman/$cm^{-1}$ |
|---|---|---|
| Silica degassed at 500°C | 1030 vs<br>922 w<br>790 m<br>730 vw | 1050 w<br>505 m<br>415 vs<br>127 s |
| Silica degassed at 150°C | 1035 vs<br>1010 sh<br>917 s<br>786 s<br>725 w | 1050 w<br>505 m<br>440 sh<br>415 vs<br>127 s |

vs- very strong
s - strong
m - medium
w - weak
vw- very weak
sh- shoulder

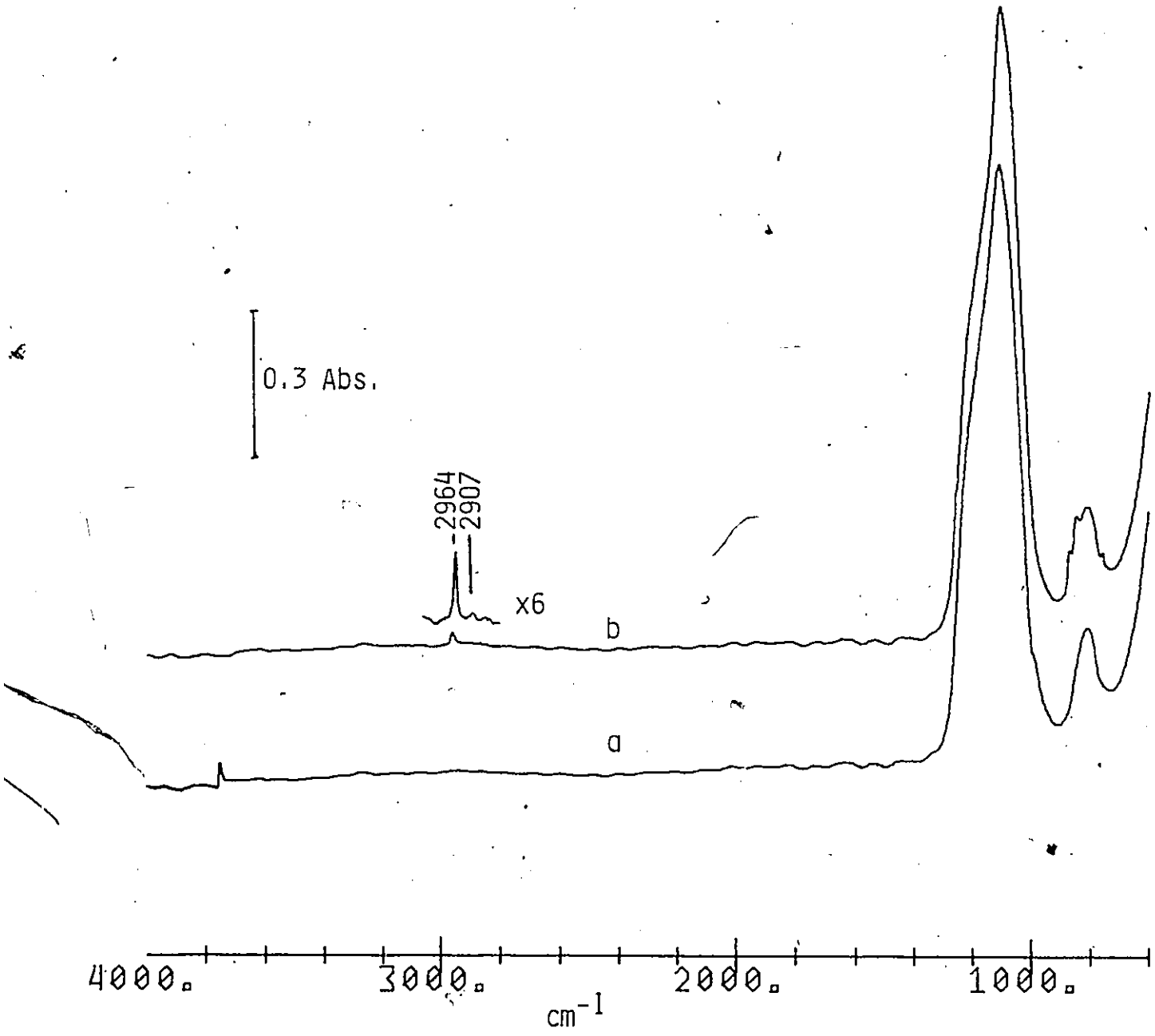


Figure 3-6
a) Infrared spectrum of a thin silica film degassed at 500°C for 1/2 hr.
b) After reaction of a) with HMDS at 75°C for 1/2 hr. and evacuation for 1 hr.
Inset shows ordinated expansion of the region from 3100-2700 $cm^{-1}$ of curve b).

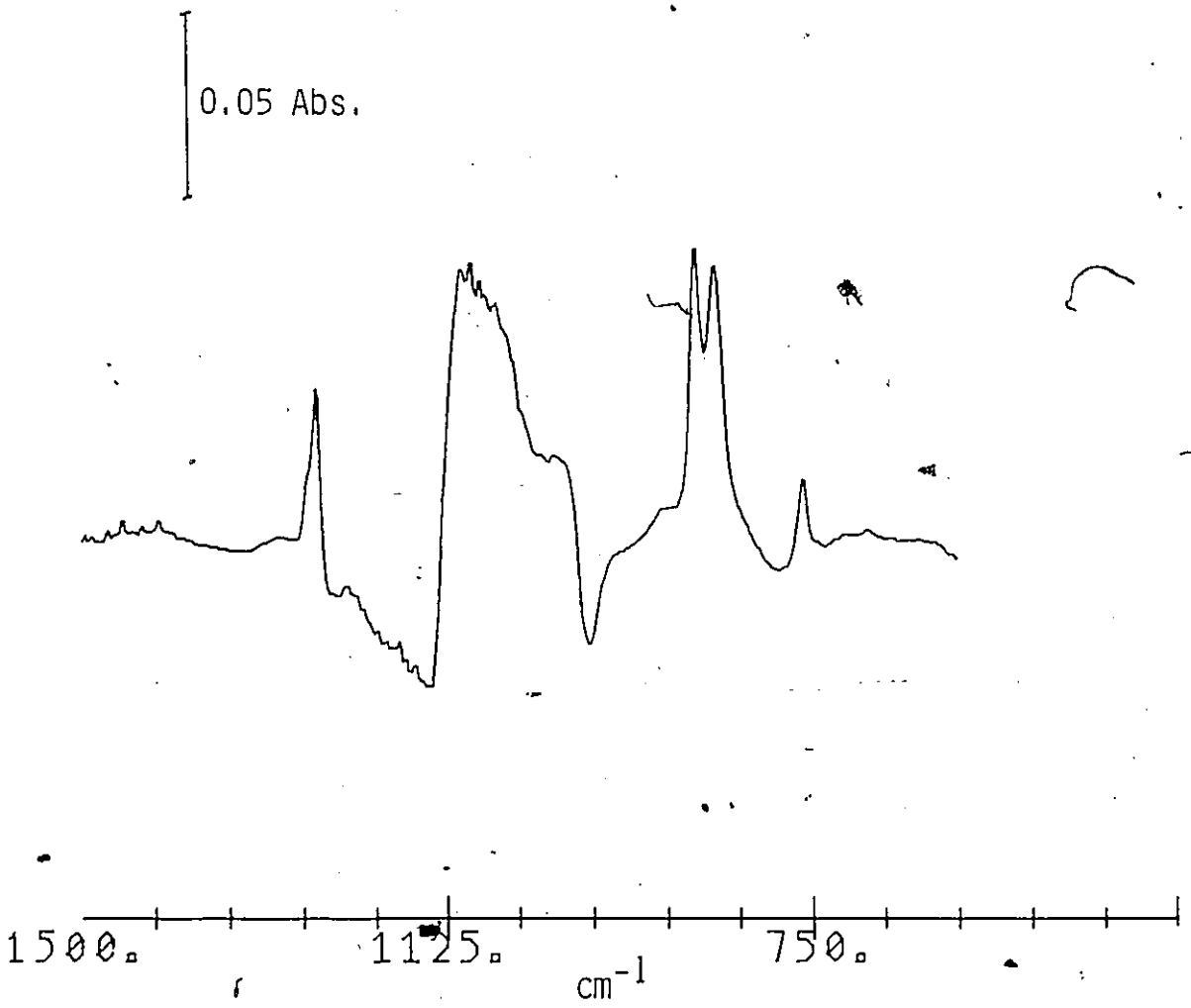


Figure 3-7
Difference spectrum Figure 3-6b minus Figure 3-6a, for the reaction of silica with HMDS.

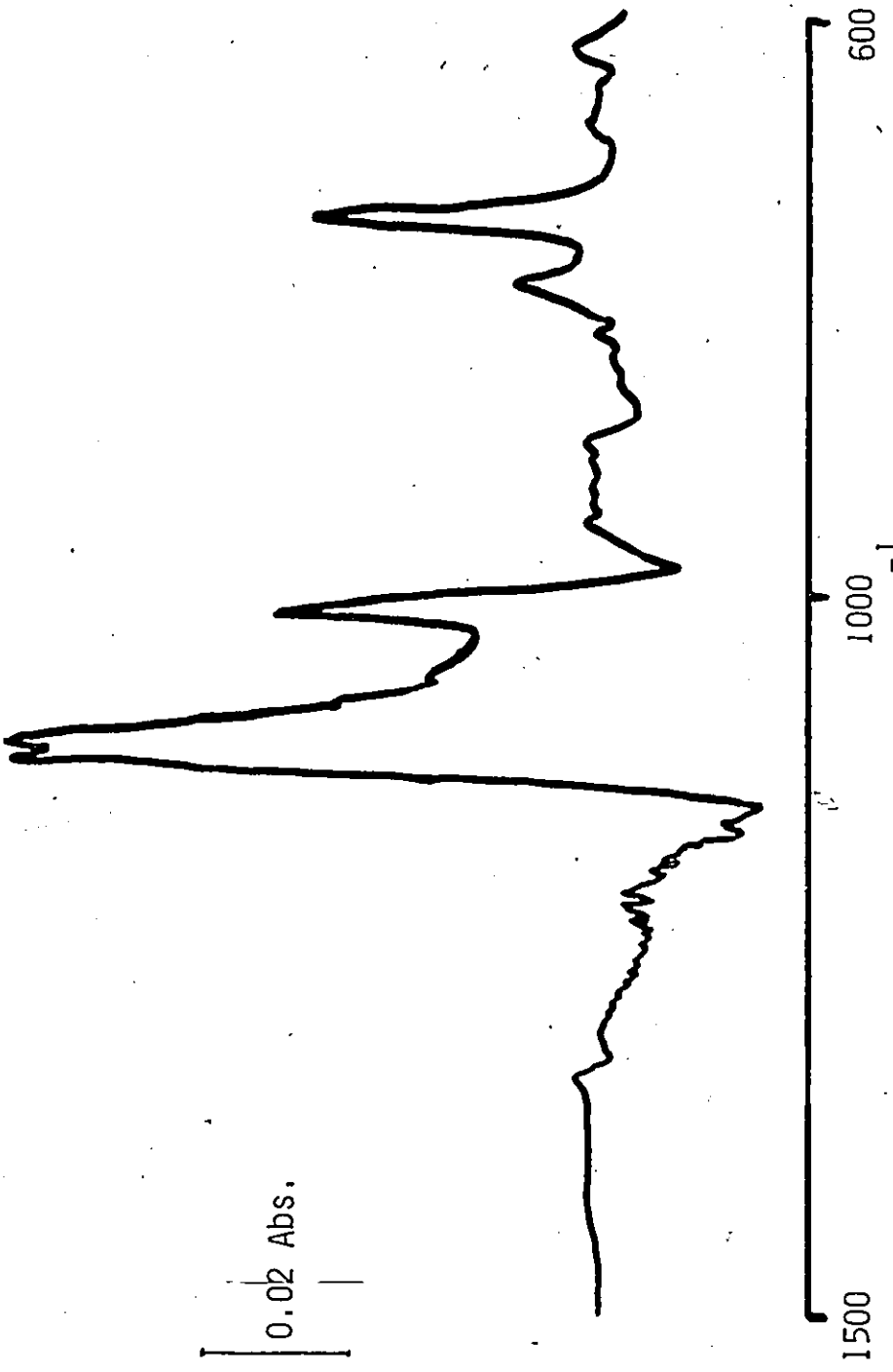


Figure 3-8
Difference spectrum for a silica degassed at 500°C which was reacted with HMDS-d18.

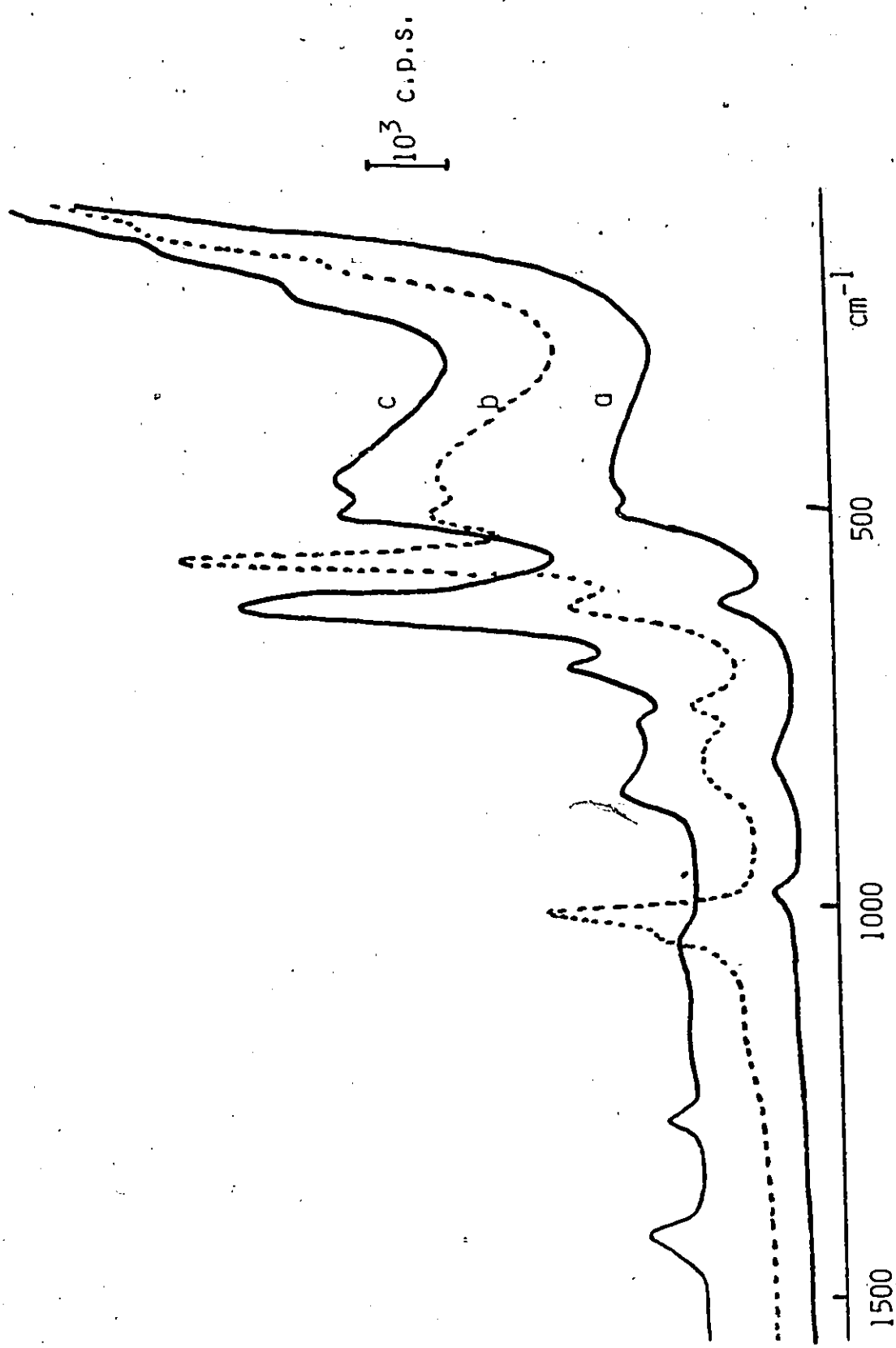


Figure 3-9
a) The Raman spectrum of a silica which had been degassed at 480°C for 1 hr.
b) After reaction of a) with HMDS-d18
c) After a similar reaction with HMDS.

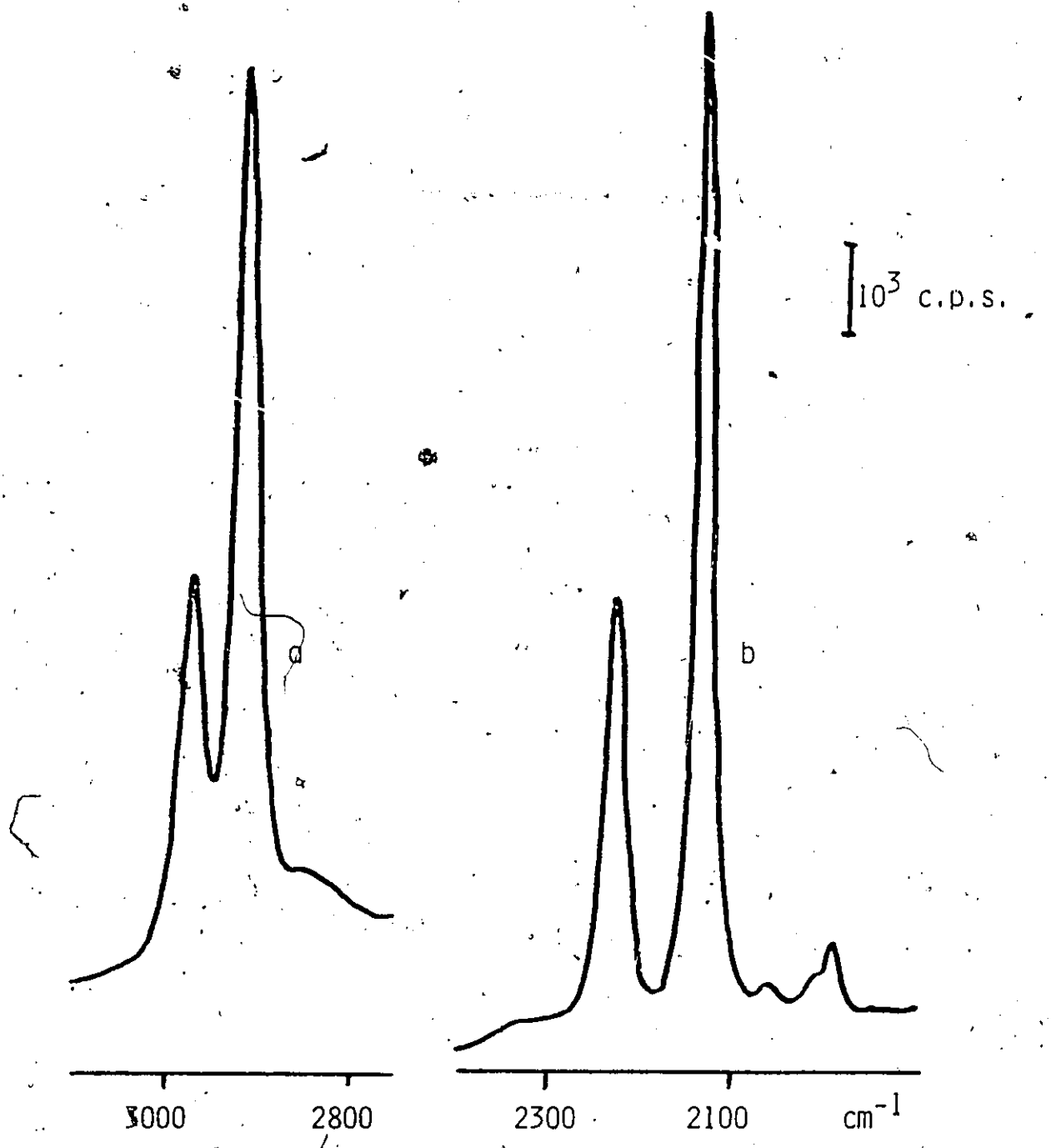


Figure 3-10
Raman spectra in the C-H and C-D stretching regions (a) and b) respectively) for the samples from Figures Figures 3-9b and 3-9c.

Table 3-2

Frequencies of infrared and Raman bands for silica reacted with hexamethyldisilazane(HMDS).

| HMDS | | HMDS-d18 | |
|---|---|---|---|
| Infrared/$cm^{-1}$ | Raman/$cm^{-1}$ | Infrared/$cm^{-1}$ | Raman/$cm^{-1}$ |
| 2964 vs | 2986 s | | 2222 s |
| 2907 s | 2910 vs | | 2124 vs |
| | 2850 w | | 2050,2010,1984 |
| | 1420 m | | 1080 sh |
| 1260 m | 1270 m | 1012 m | 1005 s |
| 1100 vs | 1050 vw | 1100 vs | |
| 870 s | | 784 w | |
| 850 s | 853 w | 740 s | 745 w |
| 758 m | 762 w | | |
| | 700 m | | 617 m |
| | 610 s | | 552 s |
| | 220 sh | | 180 sh |
| | 160 sh | | 120 sh |

vs- very strong
s - strong
m - medium
w - weak
vw- very weak
sh- shoulder

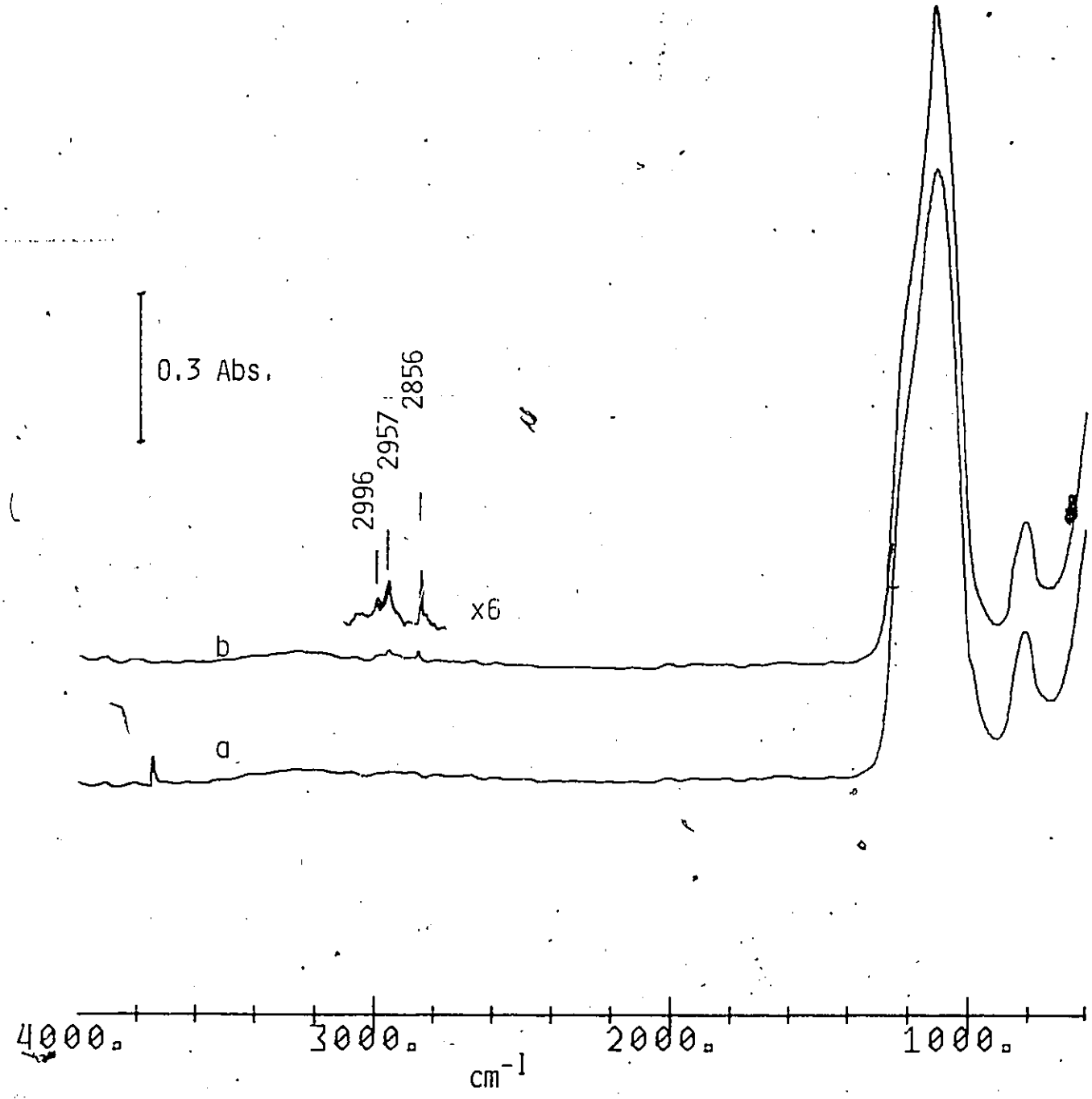


Figure 3-11
a) Infrared spectrum of a thin silica film degassed at 500°C for 1/2 hr.
b) After reaction of a) with methanol.
Inset shows an ordinate expansion of the region from 3100-2700cm$^{-1}$ of curve b).

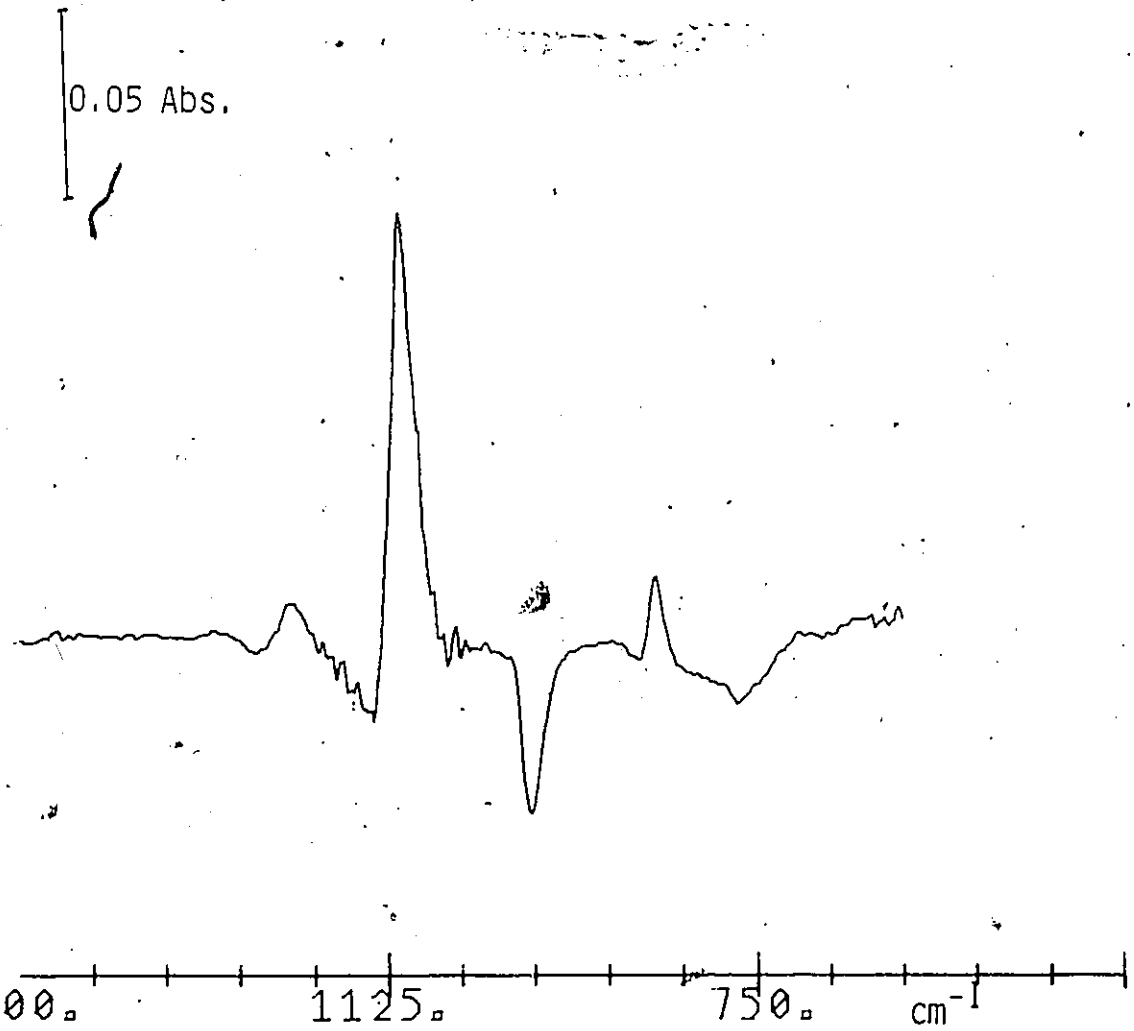


Figure 3-12
Difference spectrum Figure 3-11b minus Figure 3-11a for the reaction of silica with methanol.

the surface hydroxyl groups. Independent work has shown that using self-supporting silica discs the reaction with hydroxyl groups goes to completion in about 50 seconds[127]. The spectra shown in Figure 3-3 for silicas which have been degassed at 500 and 150°C prior to reaction are noticeably different, particularly with respect to the band at 920cm$^{-1}$. The silica degassed at 150°C has relatively more hydrogen bonded hydroxyl groups than one degassed at 500°C. The differing intensities of the band at 920 cm$^{-1}$ might indicate that $TiCl_4$ reacts in two ways with silica:

(2)

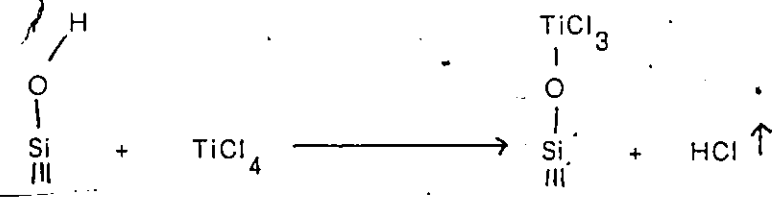


(3)

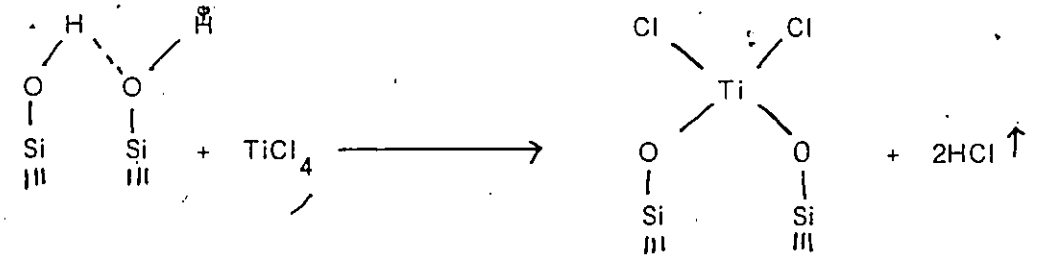


While the disappearance of the hydroxyl band and the evolution of HCl has been noted in earlier studies there has been no transmission infrared or Raman data which demonstrates that $TiCl_4$ might react in two ways with silica.

The infrared and Raman spectra of tetrakistrimethysiloxytitanium, $Ti[OSi(CH)_3]_4$, has been reported by Kriegsmann and Licht[128] and they assigned bands at 1060, 950 and 918 cm$^{-1}$ to Si-O(Ti) vibrations and that at 773 cm$^{-1}$ to an asymmetric Ti-O stretch. The species $\equiv SiO\text{-}TiCl_3$ from reaction (2) would be expected to be the predominant one for silica degassed at 500°C and the bands at

1030 and 790 $cm^{-1}$ may be assigned to the Si-O and Ti-O stretches respectively of this species. In Figure 3-3b, the bands at 1010, 917 $cm^{-1}$ and 786, 725 $cm^{-1}$ may be assigned to two asymmetric stretches of $\equiv$ Si-OTi and $\equiv$Ti-OSi, respectively, in $(\equiv SiO)_2\ TiCl_2$. A comparison of the spectra in Figures 3-3a and 3-3b shows that the intensities at 1010, 786 and 725$cm^{-1}$ increase with that at 917$cm^{-1}$ and that, therefore, the above assignment is probably correct, notwithstanding the overlap in the assignment of the band near 790 $cm^{-1}$.

The only significant difference in the Raman spectrum of the two silicas after reaction with $TiCl_4$ is the presence of a shoulder at 440 $cm^{-1}$ in the case of the sample degassed at 150°C. This band has not previously been observed and, in accord with the differences observed in the infrared spectra, this band may be assigned to the symmetric stretch for $>TiCl_2$ in $(\equiv SiO)_2TiCl_2$. The bands at 505 and 415 $cm^{-1}$ are assigned respectively to the antisymmetric and symmetric stretching modes of $-TiCl_3$ in $\equiv SiOTiCl_3$ whereas that at 127 $cm^{-1}$ can be assigned to a $-TiCl_3$ deformation mode. The antisymmetric and symmetric Ti-Cl stretching modes for $TiCl_4$ are reported[129] at 500 and 389 $cm^{-1}$, respectively, those for $BrTiCl_3$ at 508, 489 (doublet) and 439 $cm^{-1}$, while those for $Br_2TiCl_2$ are at 492 and 462 $cm^{-1}$. The TiCl deformation modes for these molecules all occur between 105 and 140 $cm^{-1}$. The above assignment for the bands at 505, 440, 415 and 127 $cm^{-1}$ are therefore quite reasonable. It is likely, given the weakness of the symmetric $>TiCl_2$ stretch, that the two other Raman bands for $(\equiv SiO)_2TiCl_2$ are obscured by those of $\equiv SiOTiCl_3$. The weak band at 1050 $cm^{-1}$ may be assigned to the $\equiv$Si-O stretch in $\equiv SiOTiCl_3$ since a strong band occurs near this frequency in the infrared spectrum of this species. However, a localized $\equiv$SiO-Si stretch in silica is known to occur here[77] and is further known to exhibit strong variation in its Raman scattering cross-section. In the present case this cross-

section may be increased by the presence of the new surface species.

Kinney and Staley[126] have studied the reaction of $TiCl_4$ with silica using photoacoustic spectroscopy and have reported that new peaks were observed at 990, 920, 790 and 730 $cm^{-1}$ with a shoulder at 1040 $cm^{-1}$. In their experiments Staley and Kinney added small doses of $TiCl_4$ to the silica and reported that a band at 980 $cm^{-1}$ in the background of silica disappeared with the appearance of the band at 920 $cm^{-1}$ and that, at this point, there was no change in the hydroxyl band at 3748$cm^{-1}$. They noted that only after further additions of $TiCl_4$ did the hydroxyl band disappear and a new band at 990 $cm^{-1}$ appear. On this basis they proposed the following reactions:

(4) 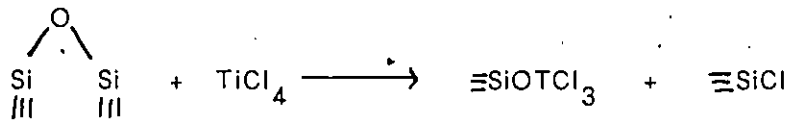

(5) 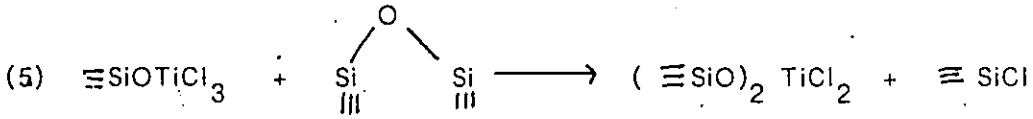

(6) 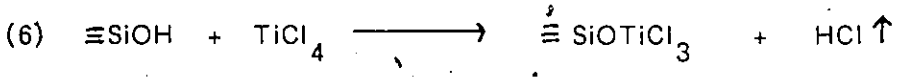

(7) 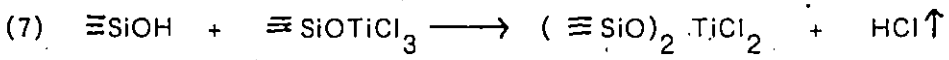

Kinney and Staley's spectra are displayed in Figure 3-13 and they show that the band at 920 $cm^{-1}$ is the dominant feature. The bands at 990 and 920 $cm^{-1}$ were assigned to the Si-O stretch of $\equiv SiOTiCl_3$ and $(\equiv SiO)_2TiCl_2$, respectively, while the bands at 790 and 730 $cm^{-1}$ were broadly assigned to Ti-O stretches. No assignment of the shoulder at 1040 $cm^{-1}$ was made. Kinney and Staley used a different kind of silica to that employed in this work and, while it was degassed under vacuum conditions, it was transfered to the photoacoustic cell in a dry box.

They also reported a drastic colour change of the silica when $TiCl_4$ was added but no such change was observed in this work or has been observed previously by others.

The assignment of the band at 980 $cm^{-1}$ to a siloxane bridge is questionable even though they contend that their siloxane bridge was different from that detected by Morrow et al.[30-32, 65] at 908 and 888 $cm^{-1}$ which was discussed in Chapter 1 of this thesis. Murray and Greytak[77] and Morrow et al.[130], among others[226, 131-133], have assigned a band at 980 $cm^{-1}$ to the ≡Si-O stretch of ≡SiOH. This band shifts upon deuteration and its assignment is well established.

The observation by Kinney and Staley that the 980 $cm^{-1}$ band disappeared and that the 920 $cm^{-1}$ band appeared before any change in the hydroxyl band is questionable in light of the information above regarding the assignment of this band. In the present study it was found that when small doses of $TiCl_4$ were added to silica a weak band first appeared at 1000 $cm^{-1}$ and at this point the hydroxyl band at 3748 $cm^{-1}$ had decreased. With further quantities of $TiCl_4$ the band at 1000 $cm^{-1}$ shifted to higher frequencies until the spectra in Figure 3-3 were obtained.

The spectra obtained in the current work and the changes observed as presented are quite different from those of Kinney and Staley. The difference in the type of silica used, the transference of the degassed silica to the photoacoustic cell and the drastic colour change on addition of $TiCl_4$ make further comparisons and discussion of their results difficult and perhaps unwarranted.

Part B : Hexamethyldisilazane

The reaction of HMDS with silica to produce ≡Si-O-Si$(CH_3)_3$ in reaction

(1) can be reconciled with the observed vibrational frequencies in Table 3-2. The assignment of the vibrations of this species is aided by referring to the vibrational data for hexamethyldisiloxane ($[(CH_3)_3\ Si]_2O$) shown in Table 3-3. The bands for the adsorbed species at 2964 and 2907 $cm^{-1}$ are the antisymmetric and symmetric $-CH_3$ stretches while those at 1420 and 1260$cm^{-1}$ are the corresponding deformation modes and those at 867, 850 and 762 $cm^{-1}$ are $CH_3$ rocking modes. The antisymmetric and symmetric $-SiC_3$ stretches are at 706 and 610 $cm^{-1}$ and the bands at 220 and 160 $cm^{-1}$ are SiOC deformation modes. The peak at 2850 $cm^{-1}$ in the Raman spectrum is probably an overtone of the $CH_3$ deformation at 1420 $cm^{-1}$. Deuteration shifts all the bands except for the intense infrared band at 1100 $cm^{-1}$ and it is therefore assigned to the antisymmetric Si-O-Si stretch. As was the case with $TiCl_4$, the band at 1050 $cm^{-1}$ in the Raman spectra with HMDS might be assigned to a $\equiv Si-O-Si\equiv$ stretch in the bulk silica or of the species $\equiv Si\text{-}O\text{-}Si(CH_3)_3$. The assignment for the bands observed with HMDS-d18 parallels that of HMDS as presented in Table 3-2.

Part C : Comparison of Techniques

The technique of photoacoustic spectroscopy (PAS), as discussed earlier, is capable of giving vibrational information of self-supported oxides which is not normally accessible with infrared transmission spectroscopy. It has been shown here, however, that low frequency vibrational data characteristic of an adsorbate bonded to silica surfaces may be obtained using thin silica films and conventional transmission infrared spectroscopy. The photoacoustic spectrum of $TiCl_4$ on silica obtained by Kinney and Staley and of methanol reacted with silica by Benziger *et al.*[135] are shown in Figure 3-13 and 3-14 respectively.

The obvious difference between the photoacoustic spectra and the cor-

## Table 3-3

## Infrared and Raman band frequencies for hexamethyldisiloxane[a,b]

| Mode | | H | | D | | H/D |
|---|---|---|---|---|---|---|
| | | IR | Raman | IR | Raman | |
| $\nu_s$ CH str. | | 2970 s | 2972 s | 2219 m | 2218 s | 1.338 |
| $\nu_s$ CH str. | | 2910 m | 2912 vsP | 2120 w | 2123 vsP | 1.373 |
| $\delta_s$ $CH_3$ | | 1412 m | 1414 w | 1037 s | 1032 w | 1.361 |
| | | 1400 w | 1270 wP | | 1008 vw | |
| $\delta_s$ $CH_3$ | | 1252 vs | 1260 vw | 1003 vs | 1000 sP | 1.25 |
| $\nu_s$ SiOSi | $B_1$ | 1052 vs | ... | 1059 s | ... | .99 |
| $\rho_r$ $CH_3$ | $A_1$ | 887 m | 897 wP | 780 w | 796 vw | 1.14 |
| | | ... | ... | 770 w | ... | |
| $\rho_r$ $CH_3$ | $A_1$ | 843 vs | 845 w | 738 vs | 728 w | 1.14 |
| $\rho_r$ $CH_3$ | $B_1$ | 824 s | ... | 738 | ... | 1.11 |
| $\rho_r$ $CH_3$ | | 760 s | 755 w | 682 | ... | 1.11 |
| $\nu_s$ $SiC_2$ | | 688 m | 690 wP | 613 | 618 w | 1.12 |
| $\nu_s$ $SiC_2$ | $A_1$ | ... | 668 sP | ... | 572 mP | 1.17 |
| $\nu_s$ $SiC_2$ | $B_1$ | 619 m | ... | 562 m | ... | 1.10 |
| $\nu_s$ SiOSi | $A_1$ | 522 w | 523 sP | 474 vw | 473 sP | 1.10 |
| $\delta_s$ $SiC_2$ | $A_1$ | 330 s | 338 wP | 297 m | 303 vwP | 1.11 |
| $\delta_s$ $SiC_2$ | $B_1$ | | 257 m | | 222 w | 1.16 |
| $\delta_s$ $SiC_2$ | $A_1$ | | | | | |
| $\delta_s$ $SiC_2$ | $B_1$ | | 220 m | | 182 w | 1.21 |
| $\rho$ $SiC_2$ | $B_1$, $B_2$ | | | | | |
| $\rho$ $SiC_2$ | $A_2$, $A_2$ | | 185 s | | 158 m | 1.17 |
| $\delta$ SiOSi | | | | | | |

[a] s = strong; m = medium; v = very; w = weak; P = polarized.

a) $((CH_3)_3Si-)_2O$

b) From Smith and Anderson ref. 134 .

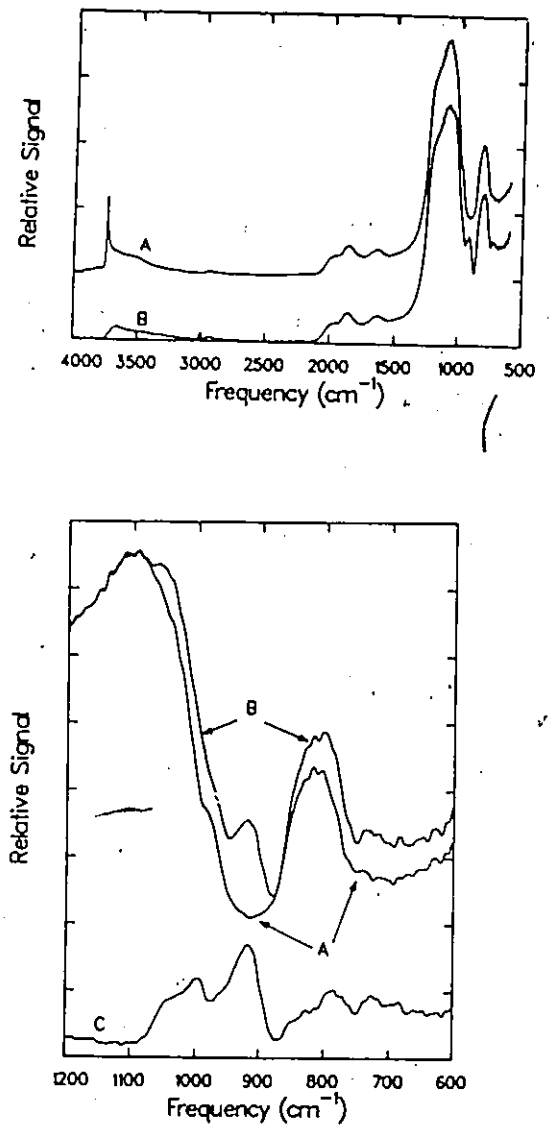


Figure 3-13
A. Infrared photoacoustic spectrum of silica degassed at 450°C.
B. After reaction of A with $TiCl_4$
C. Difference spectrum B-A.
(from Kinney and Staley ref. 126).

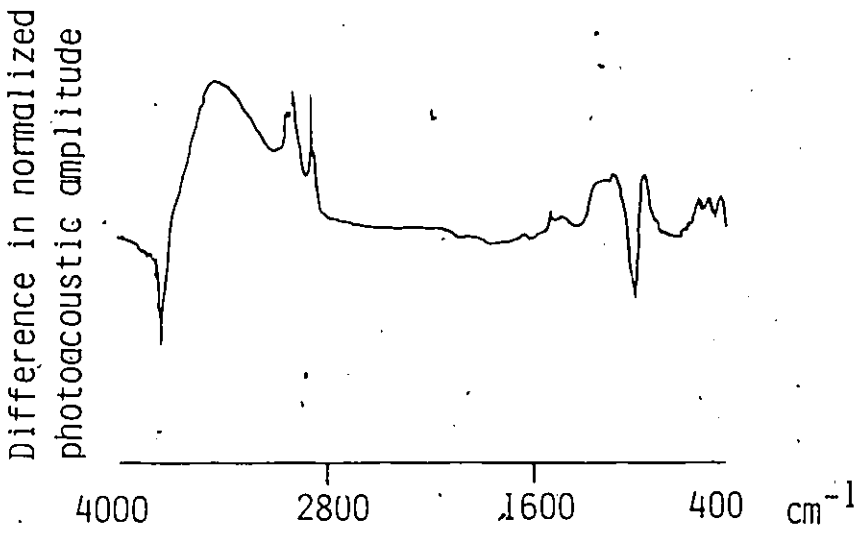


Figure 3-14
Photoacoustic infrared difference spectrum for a silica which had been degassed at 350°C and reacted with methanol at 400°C
(from Benziger et al. ref. 135).

responding infrared spectra is the signal-to-noise ratio which is significantly greater with the latter technique. Further, in the low frequency region the spectra are significantly different from those reported in this work. In both PAS experiments the type of silica used was identical but was different from that used in this research and may account for the differences compared to the spectra obtained here. The results of Kinney and Staley, which have been discussed, and the deficiencies in their assignment are obviously in part due to poor signal/noise ratio in addition to the other points mentioned.

Benziger observed bands at frequencies which are identical to those obtained here as well as bands at 1464 and 1404 $cm^{-1}$. Although these two bands were not observed with a thin film they have been observed by others using self-supporting discs[137, 138]. The band at 852 $cm^{-1}$ has been assigned by Benziger to the Si-O stretch and that at 1114 $cm^{-1}$ to the C-O stretch of $\equiv SiOCH_3$. However, the 852 $cm^{-1}$ band could be assigned to the $-CH_3$ rocking mode which would be expected to occur here and that at 1114 $cm^{-1}$ to the $\equiv$Si-O stretch which for $\equiv$Si-O $Si(CH_3)_3$ occurs at 1100 $cm^{-1}$. The assignment of the 852 $cm^{-1}$ band could be established by using deuterated methanol which would result in the band shifting by 80-100 $cm^{-1}$ to low frequency if it was a $-CH_3$ rocking mode. The assignment of the 1114 $cm^{-1}$ band is much more difficult since both C-O and Si-O stretches occur close to 1100 $cm^{-1}$. With the higher signal/noise ratio and the sharpness of the band using thin films it may be possible to use carbon -13 labelled methanol to help in the assignment because whereas a C-O stretch would be significantly shifted the Si-O stretch would not.

Sample preparation with PAS is simple since a bulk powder may be employed while some work is needed to prepare a thin film. However, degassing of a sample for PAS must be done in a separate vacuum cell and the sample must be transferred

under dry-box conditions to the photoacoustic cell. Furthermore, reactions with corrosive gases which would damage the photoacoustic cell, e.g., $TiCl_4$ must also be done in a separated vacuum cell and the sample then transferred as above. Thus an experiment with PAS might involve several transfers of the sample from reaction cell to the photoacoustic cells with the increasing risks of contamination due to oxygen and water from the atmosphere. The main advantage of the thin film technique is that all sample preparation and reactions including heating in the presence of corrosive gases may be carried out in the sample cell, i.e., sample handling is much easier than for PAS. Whereas the thin film technique can use any IR spectrometer with a computer for data handling in spectral subtractions, PAS requires special additional equipment such as an acoustic cell, microphone detector and a modulated light source. Because of the nature of PAS the spectra obtained are highly susceptible to airborne noise and building vibrations. Additionally, using the same Fourier Transform IR spectrometer, thin film spectra can be acquired in seconds while several minutes to hours are needed to get photoacoustic spectra with good signal/noise. The one important disadvantage of the thin film technique is that the sample must remain in a fixed position in the IR beam once the experiment has started which means that the instrument is not otherwise available for use, but its simplicity and excellent results compensate for this. As is the case with photoacoustic spectroscopy, the lowest frequency now attainable is determined by the IR source, the detector and the IR windows used for the cells and supporting the thin film. Thus, as far as studies with silica are concerned, the thin film technique appears to be superior to that of photoacoustic spectroscopy in terms of the speed of acquisition of spectra of high signal-to-noise ratio.

## Conclusions

Using thin films of silica, low frequency vibrational data for the adsorption of $TiCl_4$, $CH_3OH$ and HMDS have been obtained. Two adsorbed species are found after reaction of $TiCl_4$ with silica and Si-O-Ti vibrations at 1010, 920, 790 and 730 have been assigned to $(\equiv SiO)_2TiCl_2$ while those at 1030 and 790 have been assigned to $\equiv SiOTiCl_3$. For HMDS adsorbed on silica a band observed at 1100 $cm^{-1}$ has been assigned to the asymmetric Si-O-Si stretch of $\equiv Si\text{-}O\text{-}Si(CH_3)_3$. Raman spectra with high signal/noise have been obtained for the above species and show that with thin films and the use of conventional spectrometers total vibrational information leading to an unambiguous assignment of adsorbed species can be made.

# CHAPTER 4

## THE REACTION OF TRIETHYLBORANE WITH SILICA

### Introduction

It has been well established that the hydroxyl groups on aerosil surfaces are present in two main forms and that their relative proportions depend on the temperature at which the surface is degassed. These two forms are: 1) isolated hydroxyls having a sharp band at 3748 $cm^{-1}$ and 2) neighbouring hydrogen-bonded hydroxyl groups displaying a sharp band near 3720$cm^{-1}$ and a broader one around 3550 $cm^{-1}$. These bands may be modified by the presence of adsorbed water, but if the surface is degassed at 25°C, all adsorbed water can be removed[22-27]. In addition to the above types of hydroxyl groups, there exist perturbed interstitial hydroxyls whose concentration depends on the pressure at which the silica disc was made and on the temperature of degassing. These hydroxyls have a band at 3650 $cm^{-1}$ with a tail to 3400 $cm^{-1}$ and are inaccessible to most adsorbates and reactants at 25°C.

The hydrogen bonded and isolated hydroxyls have been reported to react with trichloromethylsilane and tetrachlorosilane at different rates at temperatures above 250°C whereas dimethylchlorosilane and trimethylchlorosilane react only with the isolated hydroxyls. Other reagents such as boron trichloride display no such selectivity in their reaction with these hydroxyl groups. The selectivity of the chlorosilanes and absence of such selectivity with boron trichloride has been explained[91] in terms of the transition state of the adsorbed molecules as shown below.

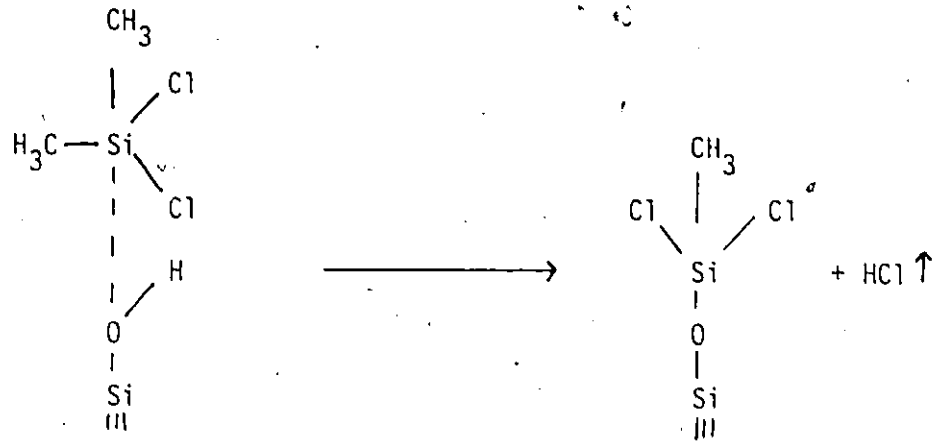

With isolated hydroxyls, because the silane is tetrahedral the more bulky $CH_3$ groups point away from the surface whereas the less bulky chlorines point towards it so that HCl elimination is facilitated. With hydrogen-bonded hydroxyls however, steric-hindrance due to the hydrogen-bond prevents such a transition state and the reaction is expected to be slower. The fact that boron trichloride is not selective was explained in terms of a tetrahedral transition state where all the chlorines point away from the surface so that all hydroxyls react at the same rate.

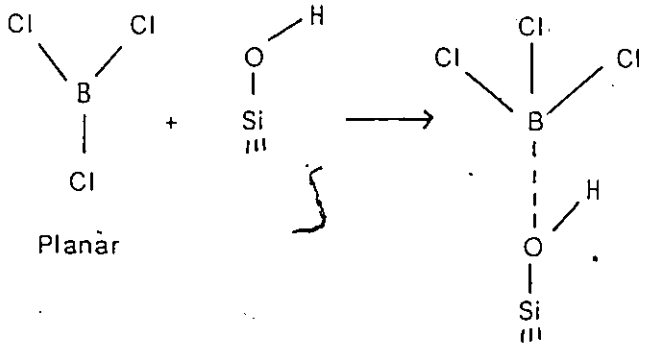


While the existence of isolated and hydrogen-bonded hydroxyl groups is known on aerosils the existence of geminal and vicinal hydroxyls has only been postulated. The presence of geminal hydroxyl groups on degassed aerosil which was postulated by Hair and Hertl[54] and Van Cauwelaert, Jacobs and Uytterhoeven[55]

has been convincingly refuted by Hockey[56] and by Morrow and Cody[57]. Although the presence of closely neighbouring non-hydrogen-bonded hydroxyls has been suggested to explain the reactions of chloromethylsilanes with highly degassed aerosils the existence of vicinal hydroxyl groups has not been proven spectroscopically. Geminal hydroxyl groups have subsequently been reported on silica gels by various researchers using infrared and nuclear magnetic resonance spectroscopies[58, 59].

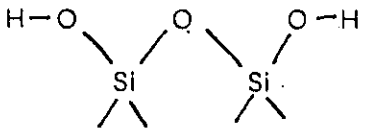


Vicinal Pair

$3720 cm^{-1}$

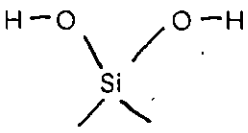


Geminal Pair

$3741 cm^{-1}$

The vicinal and geminal hydroxyl groups are not capable of intra-group hydrogen-bonding for steric reasons. Although the vibrations of the geminal hydroxyls groups could be coupled no such coupling has been observed for these groups on gels and the single infrared band reported at 3741 $cm^{-1}$ overlaps with that of the isolated hydroxyls at 3748 $cm^{-1}$.

The present study represents an attempt to resolve temporally the reactions between the hydroxyl groups on aerosil silica with triethylborane (TEB). Changes occuring during the reactions are clearly shown by the use of computer-aided spectral subtraction.

## Experimental

The silica used was either untreated before degassing or was calcined in air at 500°C. Self supporting discs containing either 10 or 20 mg $cm^{-2}$ of silica were pressed at $10^7$ Pa and then degassed at either 150 or 450°C for 1 hr. then cooled to room temperature prior to the addition of triethylborane

(TEB). Triethylborane, 99.99% was obtained from Aldrich and contained natural isotopic abundance boron - 10 and boron - 11. Before use the TEB was degassed during several freeze-thaw cycles using liquid nitrogen. Titanium tetrachloride from Aldrich was degassed in a similar manner. $D_2O$ (99.8%) from Merck, Sharpe and Dohme, degassed prior to use, was used to exchange the hydroxyl groups on silica by repeated exposure to the sample at 150°C. The water used in the hydrolysis of the TEB treated silica was triply distilled de-ionized water which had been degassed as above. Oxygen (99.8%) was obtained from Air Products. All spectra were recorded on the Bomen FTIR using the MCT detector and a resolution of 4 $cm^{-1}$.

Results

TEB did not react rapidly with surface silanols at 25°C and the initial spectra showed only the effects of physical adsorption. Figures 4-1 and 4-2 show the spectral changes in the hydroxyl stretching region after TEB was added at 25°C to silica which had been degassed at 450 and 150°C, respectively. In the former case, the peak at 3748 $cm^{-1}$ for isolated hydroxyls shifted to 3700$cm^{-1}$ whereas in the lattercase the shift was to 3696 $cm^{-1}$. In both cases the shifted peak was considerably broadened compared to the unperturbed hydroxyls and the shoulder initially present at 3720 $cm^{-1}$ in the 150°C degassed silica was no longer discernible in the shifted hydroxyl profile which could be restored by 5 minutes evacuation at room temperature in both cases.

Triethylborane reacted slowly over a period of 24 hrs to completely remove the peak due to the isolated hydroxyls. New strong peaks which were not removed by prolonged evacuation appeared at 2967, 2946, 2924, 2887, 1465, 1389, 1345 and 940 $cm^{-1}$. These peaks were at the same frequency regardless

of whether the sample had been degassed at 450, or 150°C except, in the latter case, they were more intense. Figure 4-3 shows spectra of a 50 mg silica disc before and after reaction with TEB while Figure 4-4 shows the corresponding difference spectrum between 3200 and 1300 $cm^{-1}$. Figure 4-5a shows the background spectrum of a thin silica film which had been degassed at 400°C for 30 minutes, Figure 4-5b shows the spectrum after reaction with TEB and Figure 4-6 the difference between these. Quite similar results were obtained for a thin silica film degassed at 150°C. The Raman spectrum of silica degassed at 480°C and reacted with TEB for 24 hrs showed only weak peaks at 2942 and 2895$cm^{-1}$.

Figure 4-7 shows the spectrum of the hydroxyl groups which had reacted on silica degassed at 450°C, i.e., Figure 4-3a has been subtracted from Figure 4-3b. Figure 4-8 shows the same presentation for silica which had been degassed at 150°C. There are two additional peaks at 3720 and 3550 $cm^{-1}$ in addition to that present at 3748 $cm^{-1}$ for the isolated hydroxyl. Figure 4-9 shows the further changes in the hydroxyl stretching region after reaction with titanium tetrachloride of a silica which had been degassed at 150°C and reacted with TEB. The broad peak is centered at 3480$cm^{-1}$ and has a shoulder at 3650$cm^{-1}$. No similar changes were discernable with a silica which had been degassed at 450°C.

Figure 4-10 shows the spectral changes with time after the addition of TEB to silica which had been degassed at 150°C. Every 2 hours the sample cell was evacuated for 4 minutes, the spectrum recorded and then subtracted from the previous recorded spectrum to yield the changes that occurred in the OH region in that 2 hr interval. After 10 hrs. reaction the TEB was left in the cell for 14 hrs. and then evacuated and the changes in this period are illustrated in Figure 4-11. Three distinct bands are observed at 3746, 3717, and 3525$cm^{1}$. The final overall change shown in Figure 4-12 is very similar to that shown in Figure 4-8.

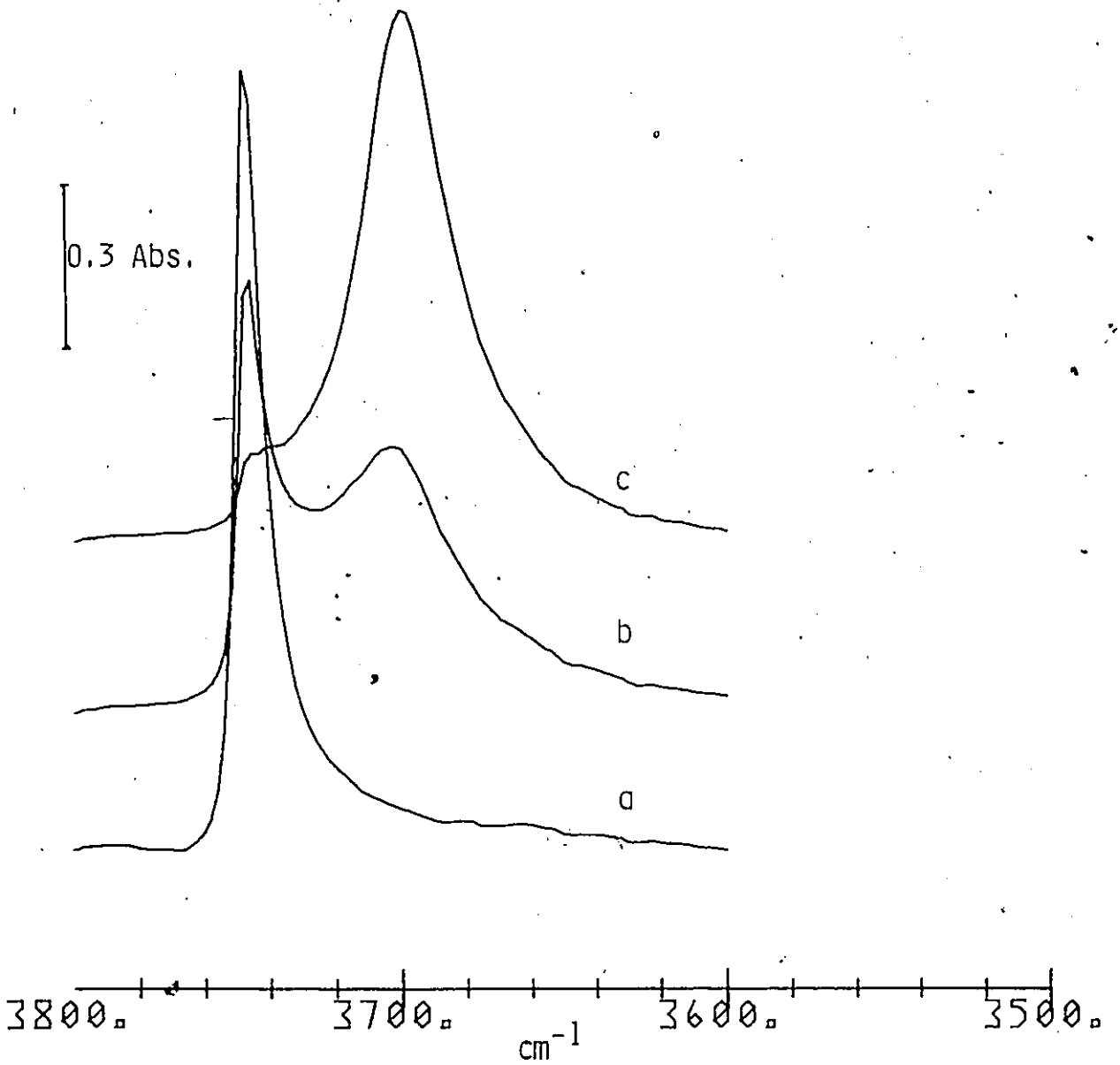


Figure 4-1
a) Infrared spectrum in the OH stretching region of silica (10mg/cm$^2$) degassed at 450°C for 1 hr.
b) After addition of 7 torr of triethylborane to a)
c) After addition of 34 torr of triethylborane.

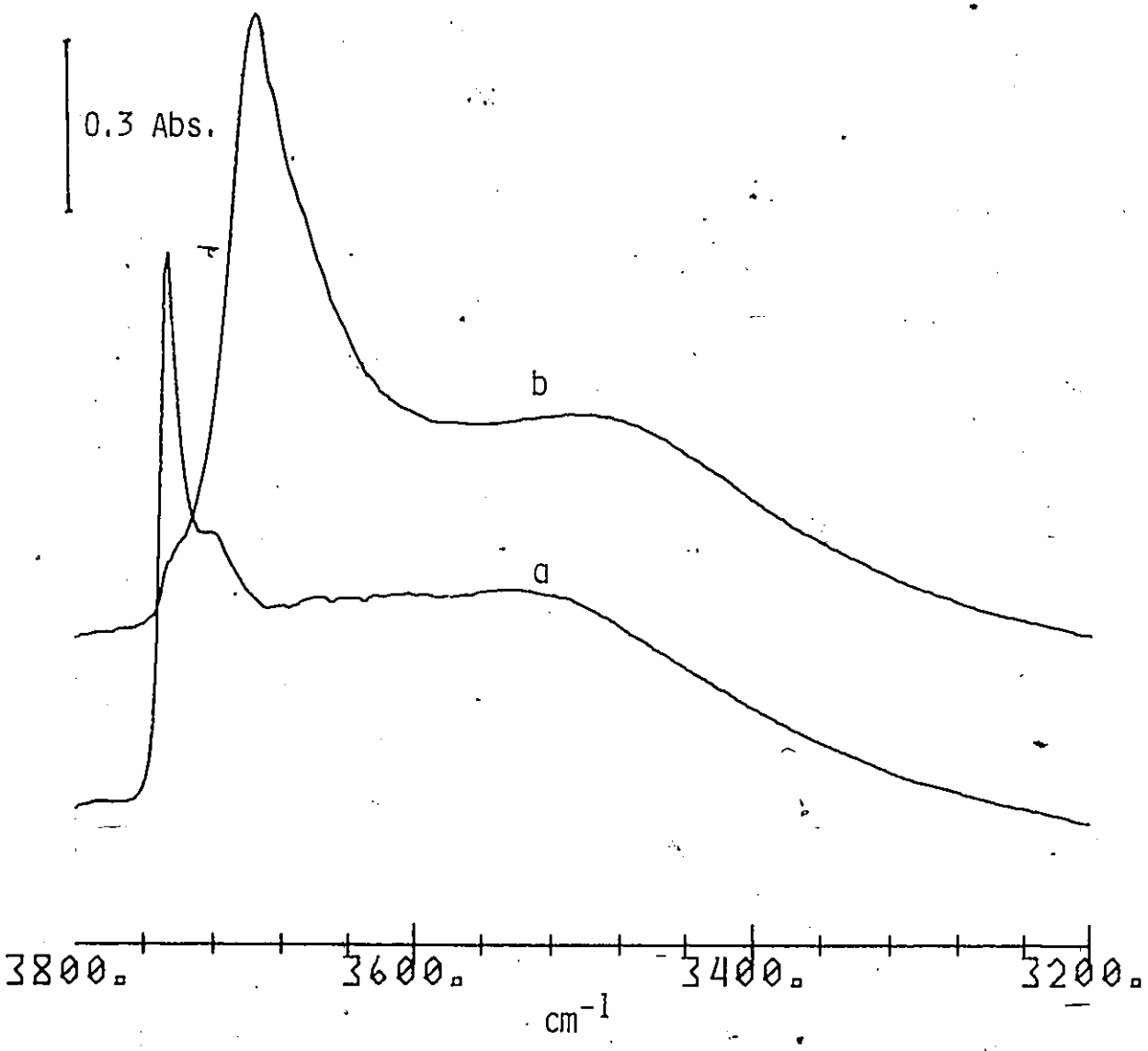


Figure 4-2
a) Infrared spectrum in the OH stretching region of silica ($10mg/cm^2$) degassed at 150°C for 1 hr.
b) After the addition of 34 torr of triethlborane to a).

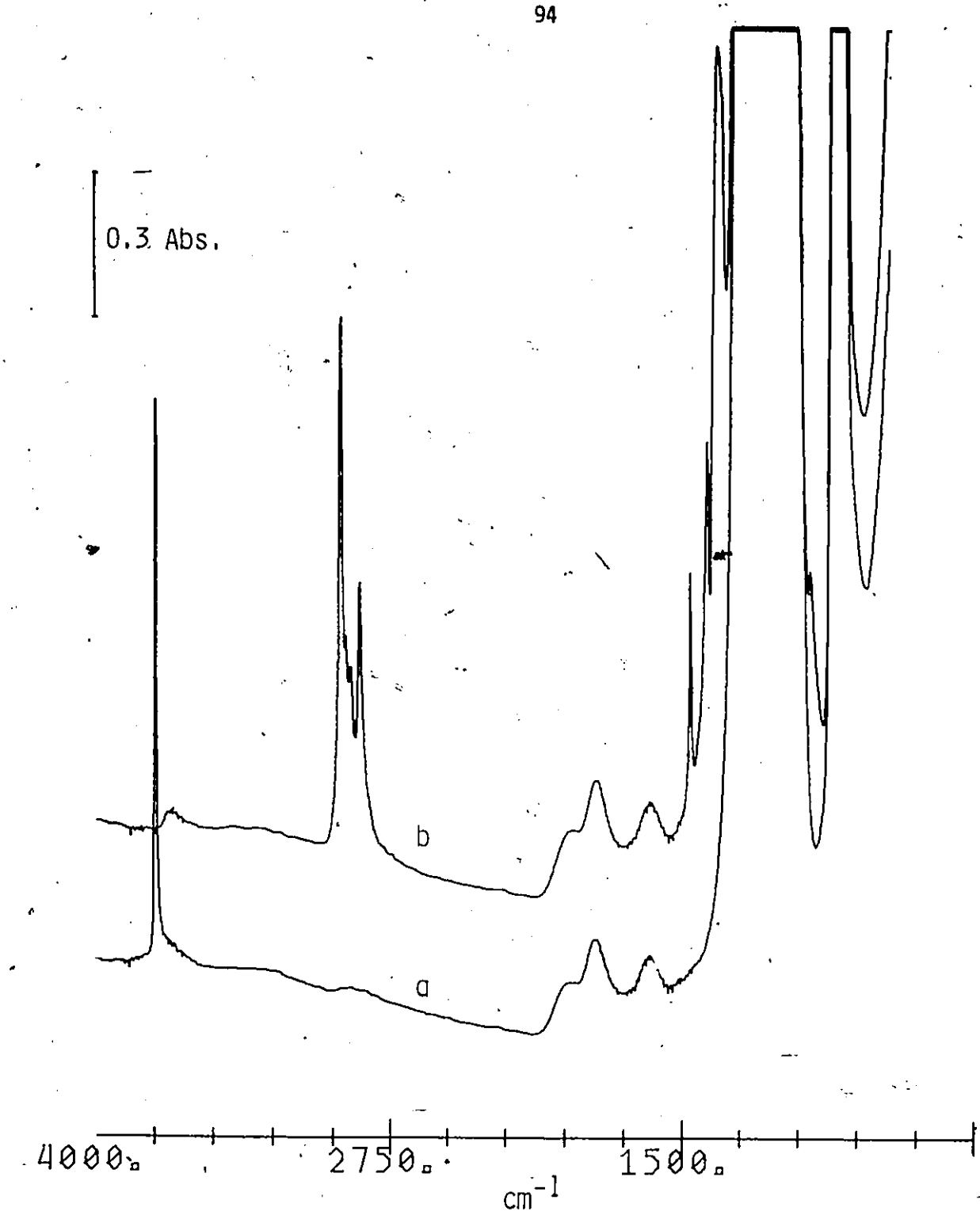


Figure 4-3
a) Intrared spectrum of silica (10mg/cm$^2$) degassed at 450°C for 1 hr.
b) After reaction of a) with 34 torr of triethylborane for 24 hrs. at 25°C followed by evacuation for 24 hrs.

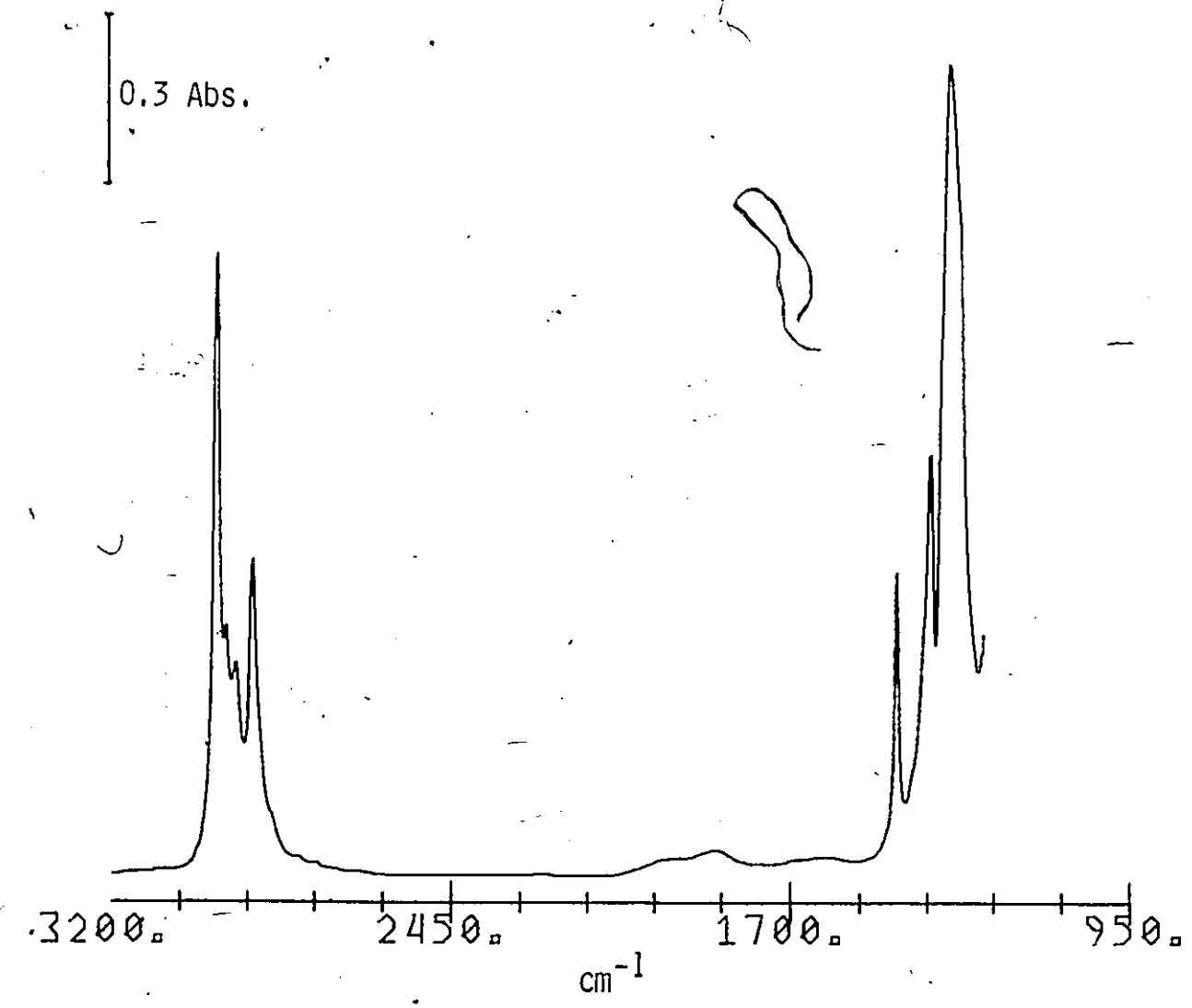


Figure 4-4.
Difference spectrum Figure 4-3b minus Figure 4-3a in the region 3200-1300cm$^{-1}$.

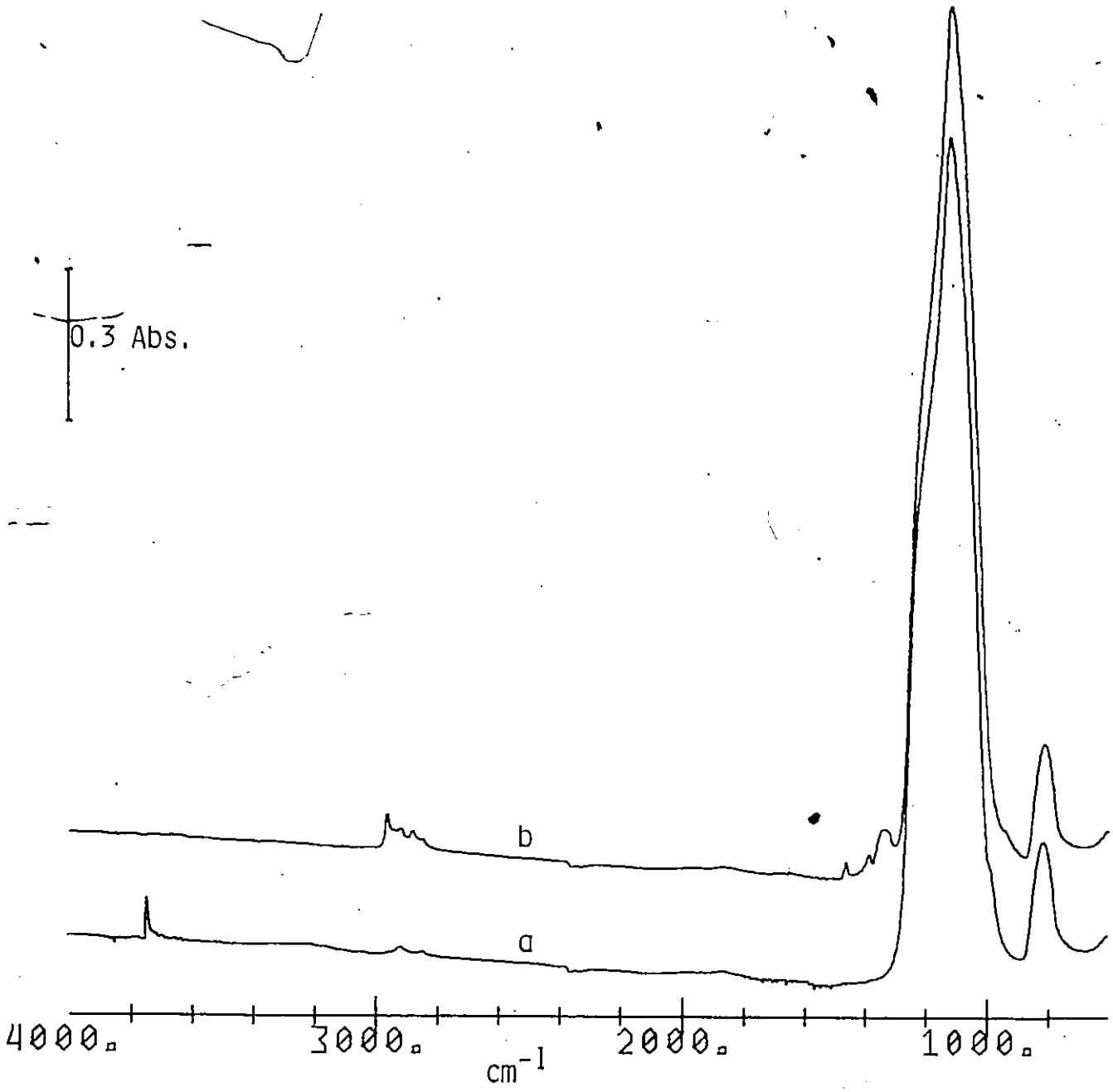


Figure 4-5
a) Infrared spectrum of a thin silica film degassed at 400°C for 1/2 hr.
b) After reaction of a) with triethylborane for 24 hrs and evacuation for 1 hr at 25°C.

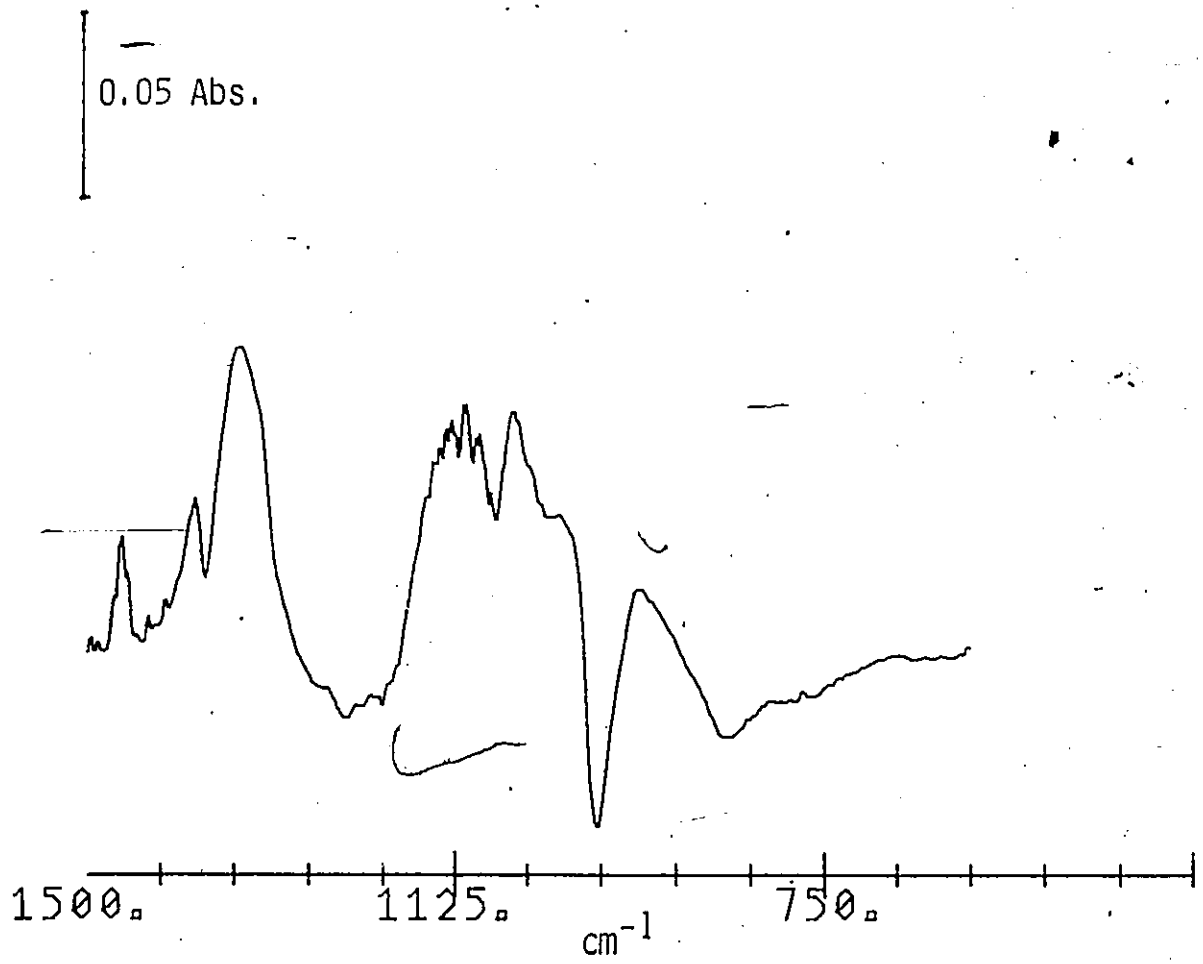


Figure 4-6
Difference spectrum Figure 4-5b minus Figure 4-5a in the region 1500-500cm$^{-1}$.

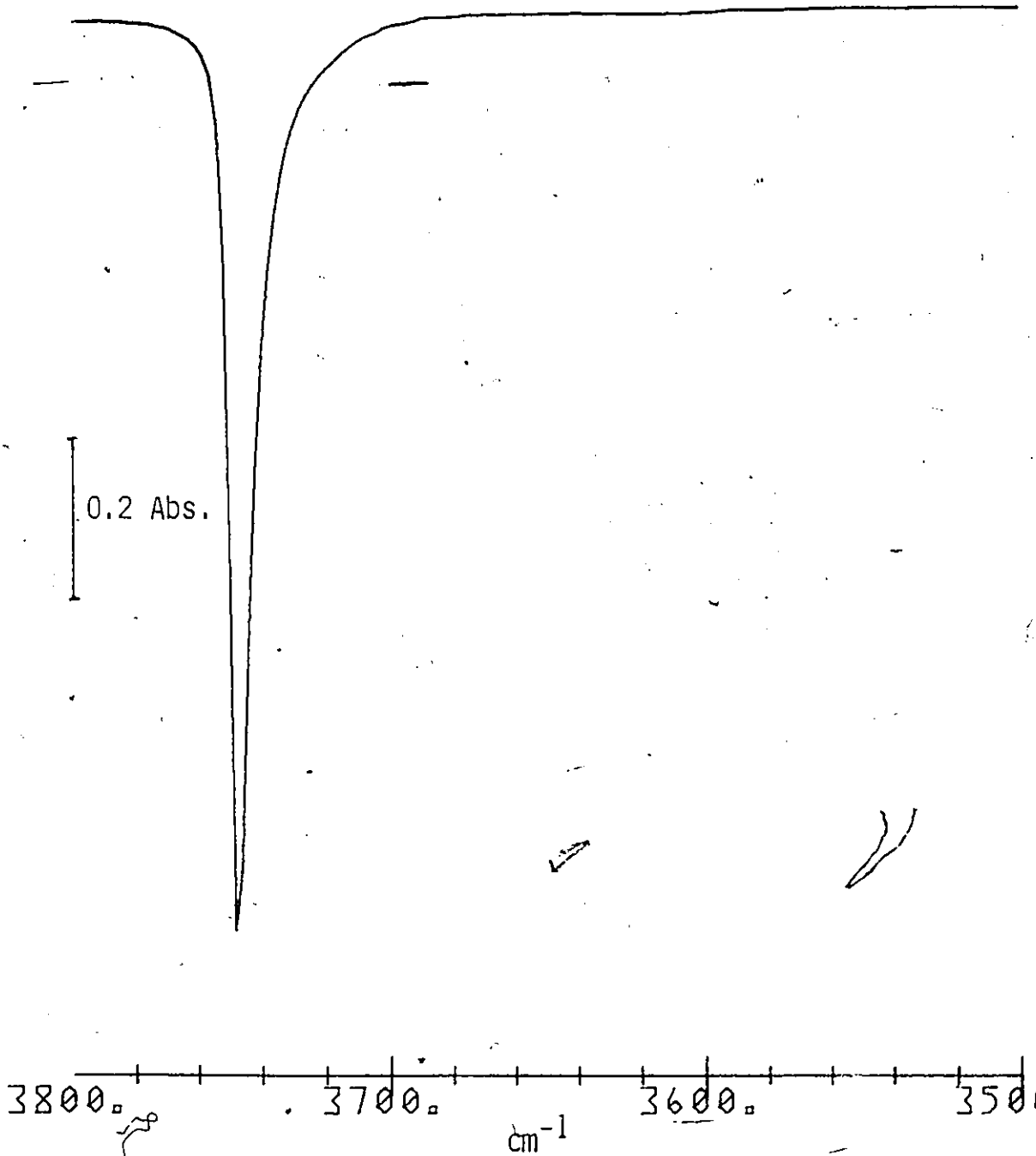


Figure 4-7
Difference spectrum in the OH stretching region for the 450°C degassed silica from Figure 4-3.

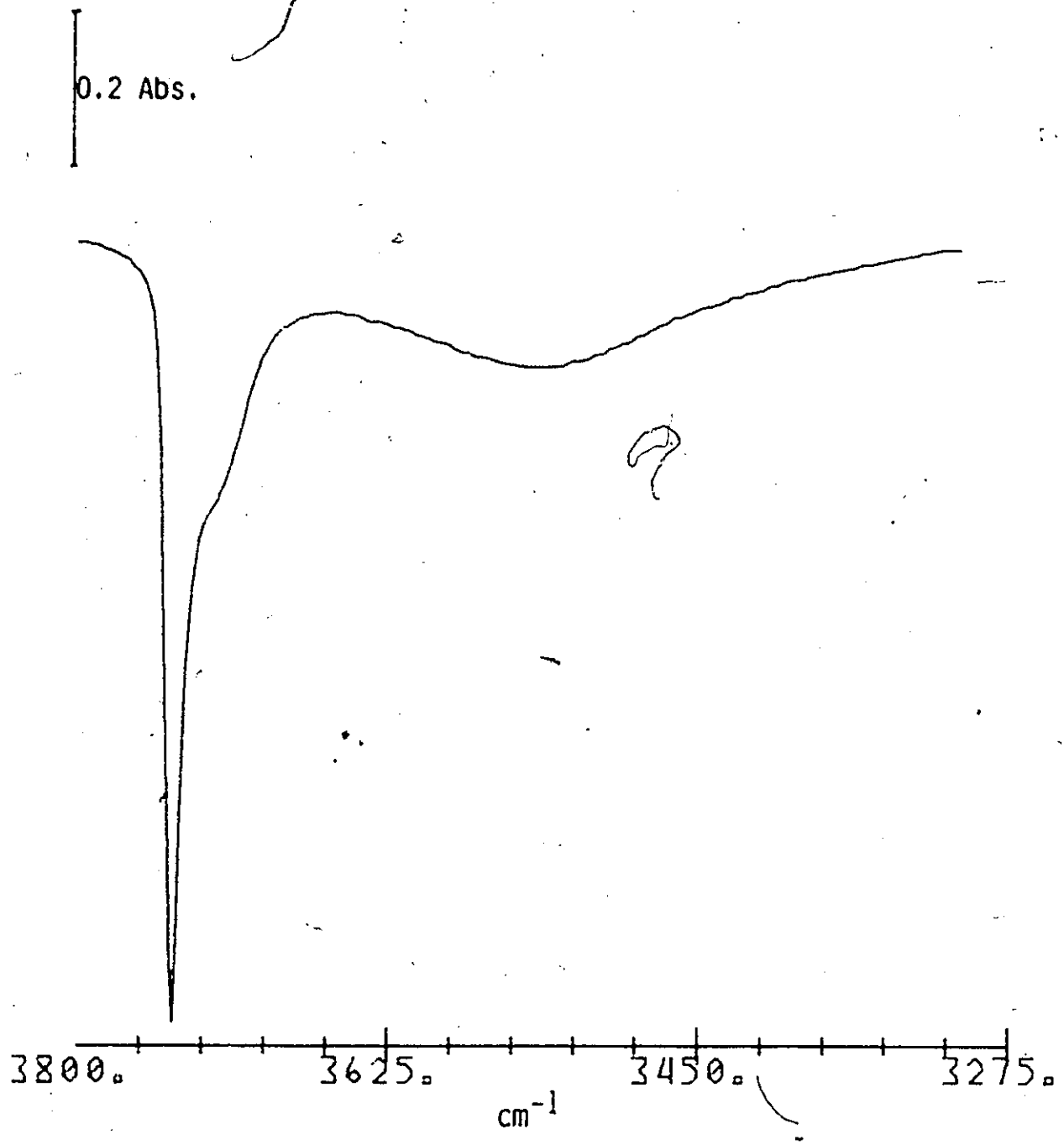


Figure 4-8
Difference spectrum in the OH stretching region for a silica (10mg/cm$^2$) which had been degassed at 150°C for 1 hr and then reacted with triethylborane for 24 hrs.

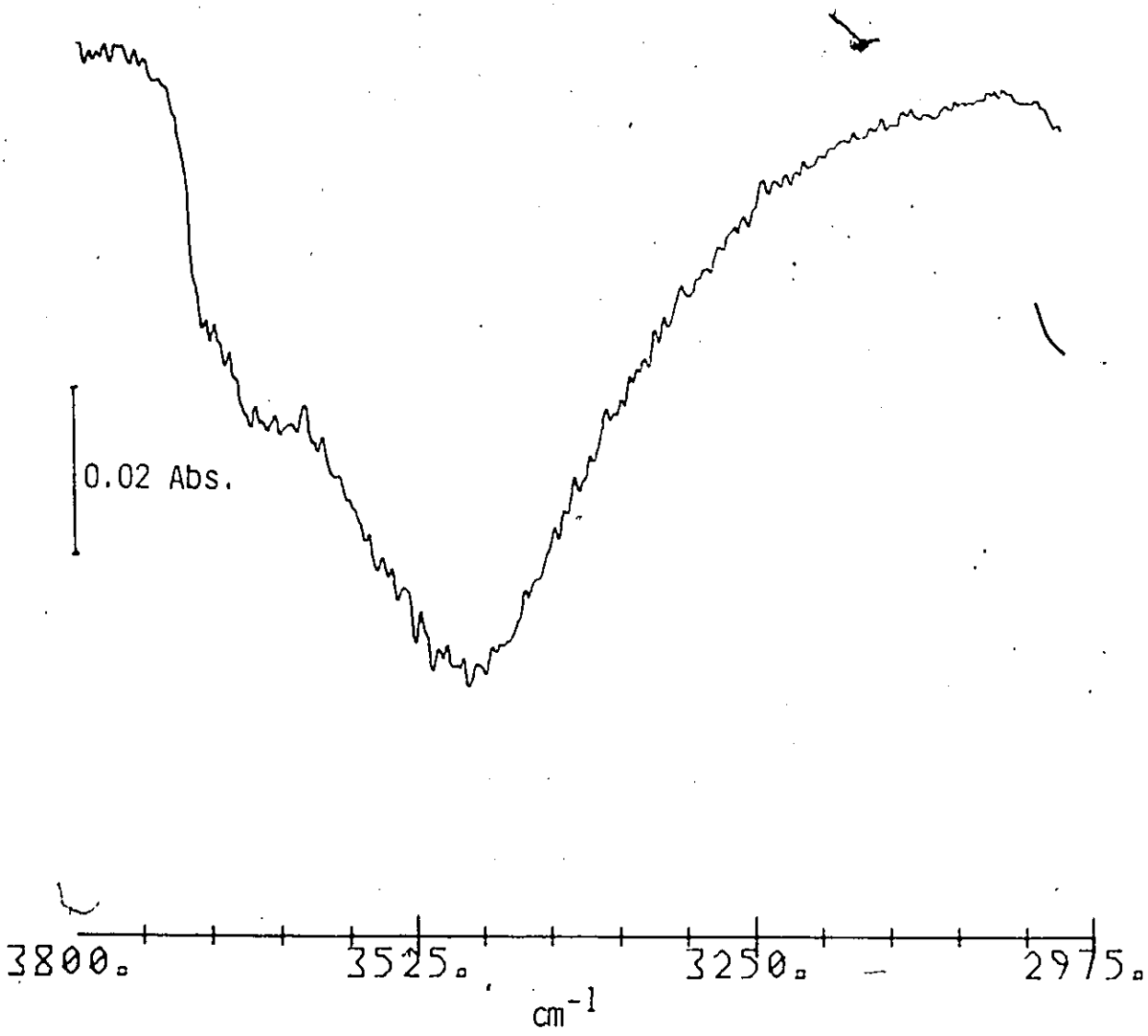


Figure 4-9
Difference spectrum in the OH stretching region for a silica which had been degassed at 150°C, reacted with triethylborane for 24 hrs and then with $TiCl_4$ i.e. the spectrum shows the change in the OH region as a result of an additional reaction with $TiCl_4$.

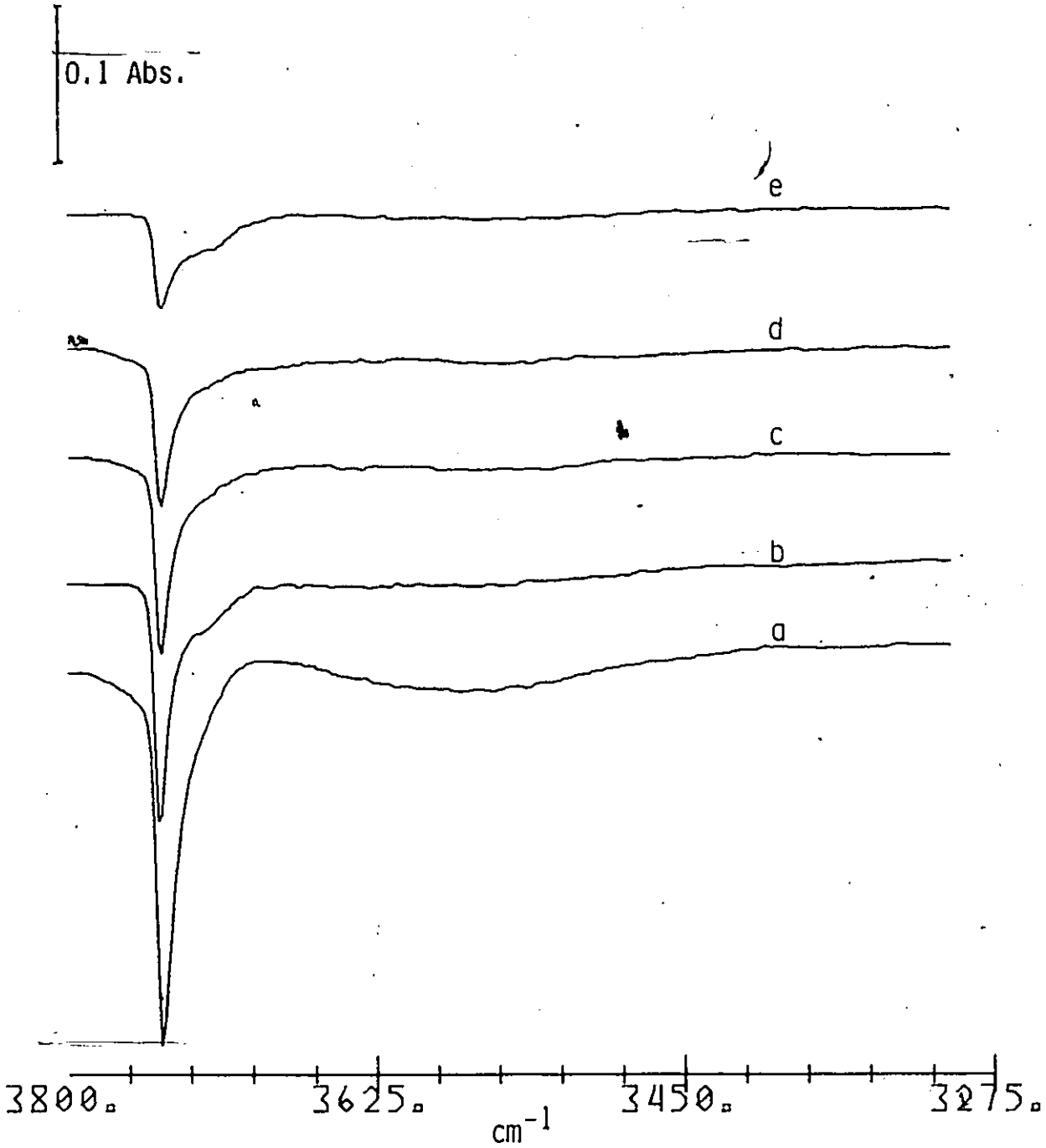


Figure 4-10
Time resolved difference spectra for a silica (10mg/cm$^2$) which had been degassed at 150°C and then reacted with triethylborane. See text for details. The difference spectrum are for a two hour interval after a total elapsed time of a) 2 hrs; b) 4 hrs; c) 6 hrs; d) 8 hrs and e) 10 hrs.

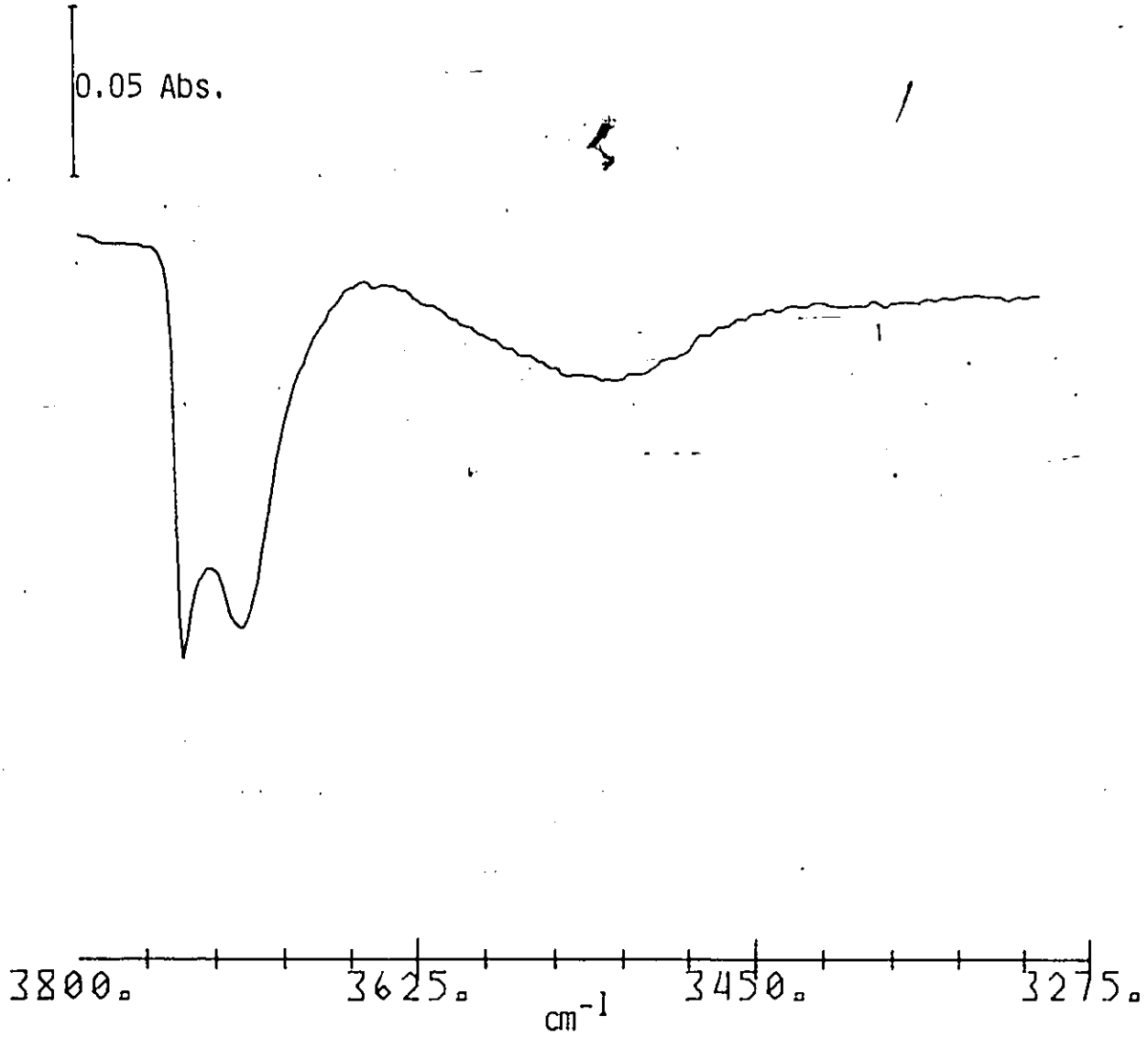


Figure 4-11
Difference spectrum of the sample in Figure 4-10 showing the change in the OH region in the final 14 hrs of a 24 hrs reaction with triethylborane.

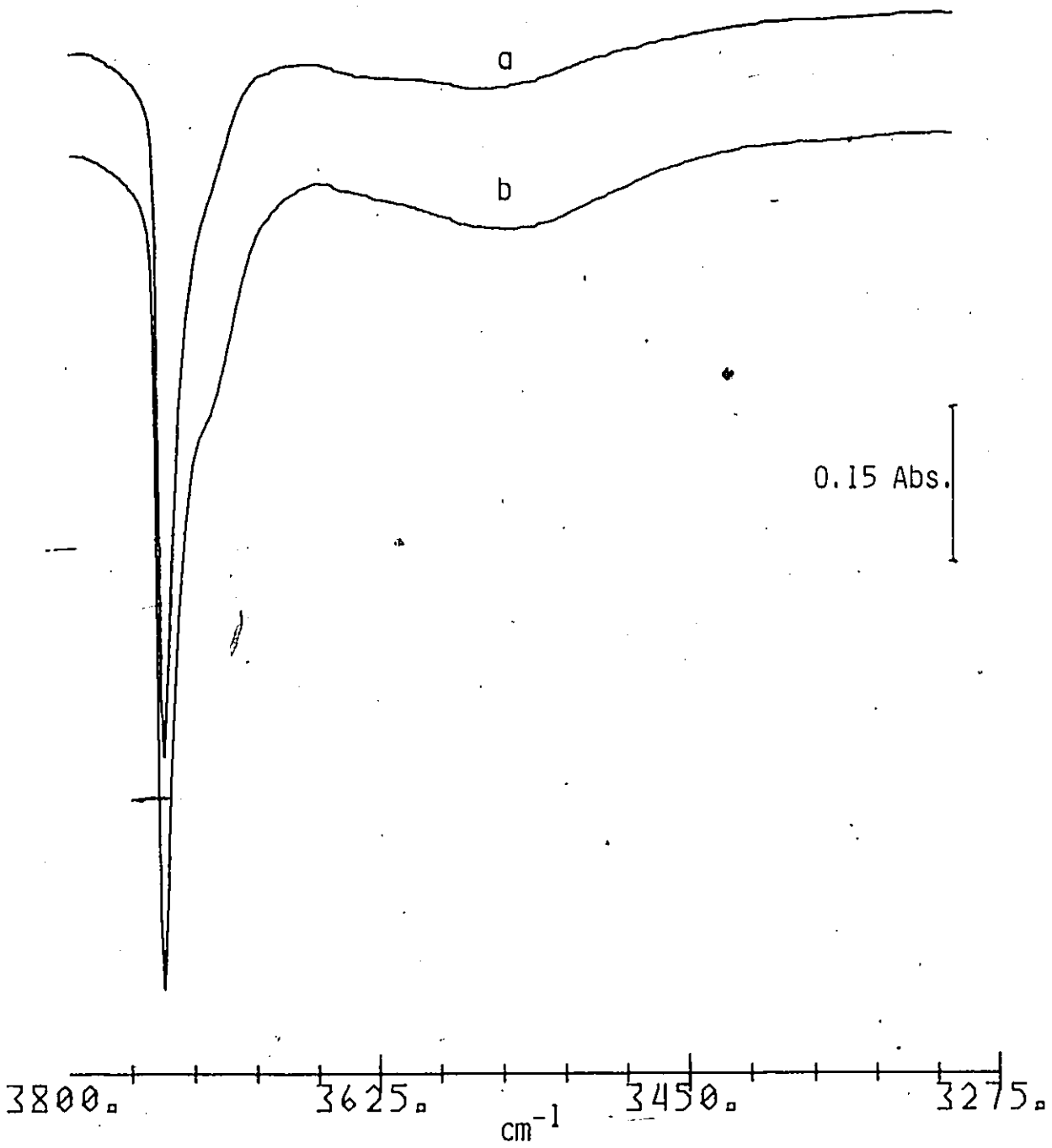


Figure 4-12
a) Difference spectrum for the sample in Figure 4-10 showing the change in the OH region during the first 10 hrs. of reaction with triethylborane.
b) Difference spectrum showing the change in the OH region during the 24 hrs of reaction.

Figure 4-13 shows the corresponding results for silica degassed at 150°C and partially exchanged with $D_2O$. The peaks due to the adsorbate were as before and so, too, was the change in the OH region. The changes in the OD region are shown in figures 4-14 and 4-15. The three peaks due to deuterated hydroxyls that reacted with TEB are at 2761, 2740 and 2625 $cm^{-1}$ while those due to reaction with titanium tetrachloride are at 2690 and 2570 $cm^{-1}$.

When 18 torr of $H_2O$ was added at 25°C to silica which had been treated with TEB a weak peak appeared at 3748 $cm^{-1}$ along with an intense broad band at 3300 $cm^{-1}$ but the peaks assigned to adsorbed TEB did not change significantly. Heating the sample to 200°C in $H_2O$ reduced the intensity of the peaks due to TEB and the OH peak at 3748 increased significantly. Finally heating at 380°C in water removed all the TEB peaks and left peaks at 3748, 3700, 1460 and 1379 $cm^{-1}$ (Figure 4-16). The TEB treated silica is quite thermally stable and decomposition of the surface just began at 200°C and new peaks appeared at 2620, 2598, 2578, 2508, 2285 and 1568 $cm^{-1}$ (Figure 4-17). The addition of 28 torr of $O_2$ produced an immediate change in the spectrum of TEB treated silica. The ultimate result after 24 hrs shown in Figure 4-18 was a strong band at 2984 $cm^{-1}$ and two weaker ones at 2940 and 2888 $cm^{-1}$. The 1400 - 1300 $cm^{-1}$ region was completely absorbing at this stage.

During the reaction of TEB with silica at 25°C ethane was detected by mass spectrometry. After the reaction of TEB with silica a sample portion of the gas phase was condensed in a liquid nitrogen trap connected to the inlet of the mass spectrometer. The condensed gases were slowly warmed up and ethane (m.p. -183°C) was detected first and, as the trap warmed further, the excess TEB (m.p. -93°C) was detected.

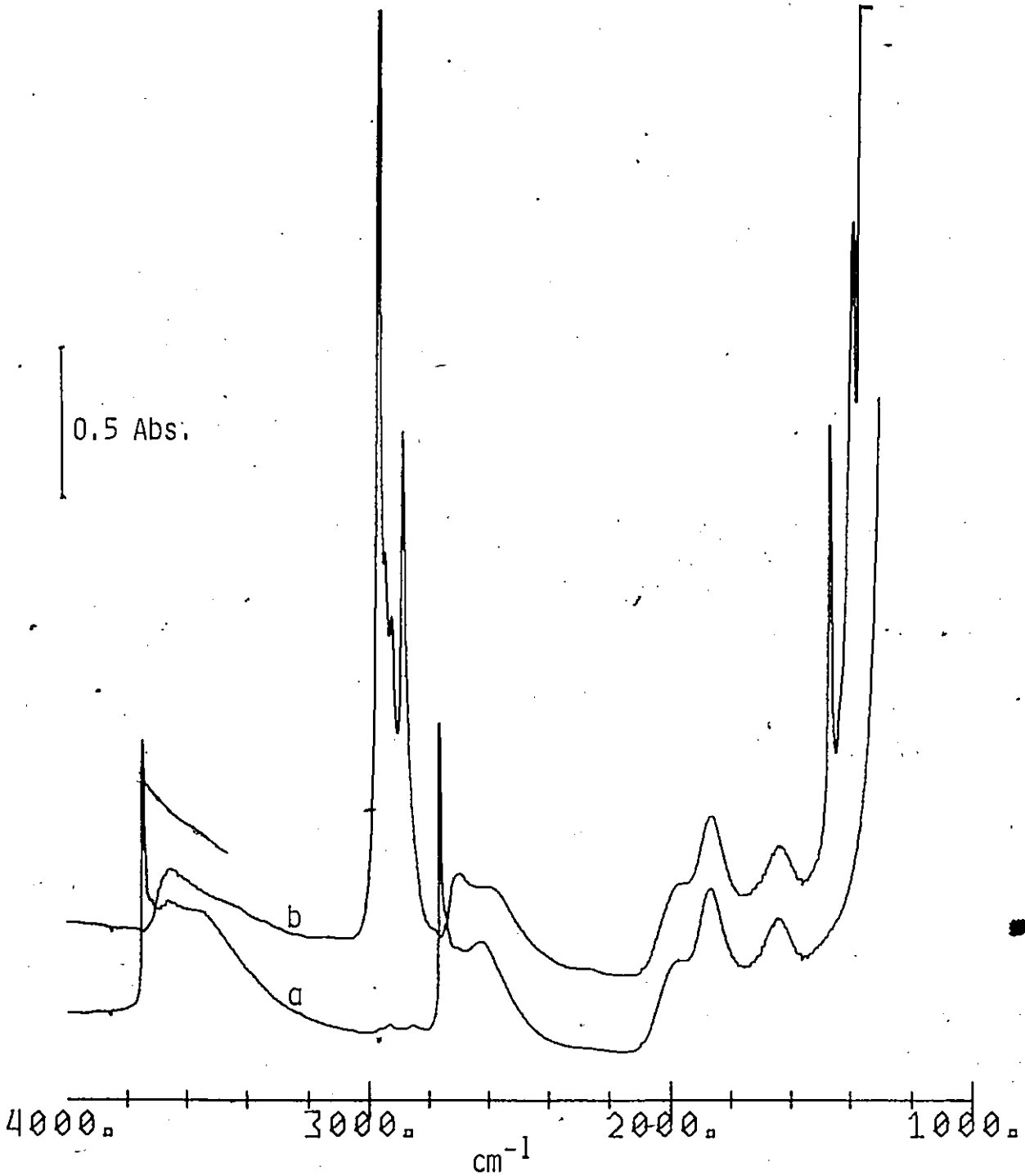


Figure 4-13
a) Infrared spectrum of a silica (20mg/cm$^2$) which had been partially exchanged with $D_2O$ at 150°C and degassed at 150°C for 1 hr.
b) After reaction of a) with triethylborane for 24 hrs and evacuation for 1 hr.

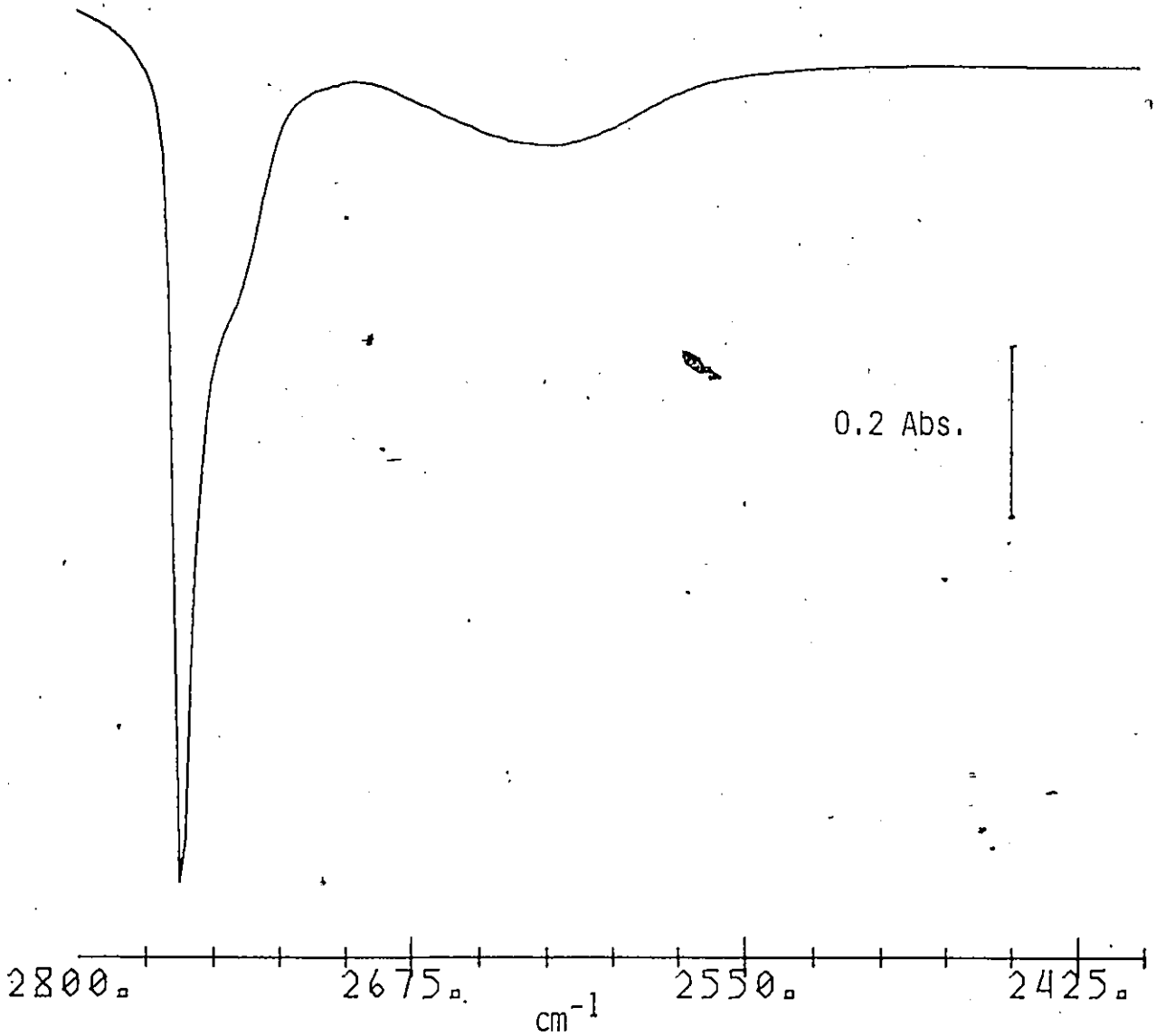


Figure 4-14
Difference spectrum in the OD stretching region for Figure 4-13b minus Figure 4-13a.

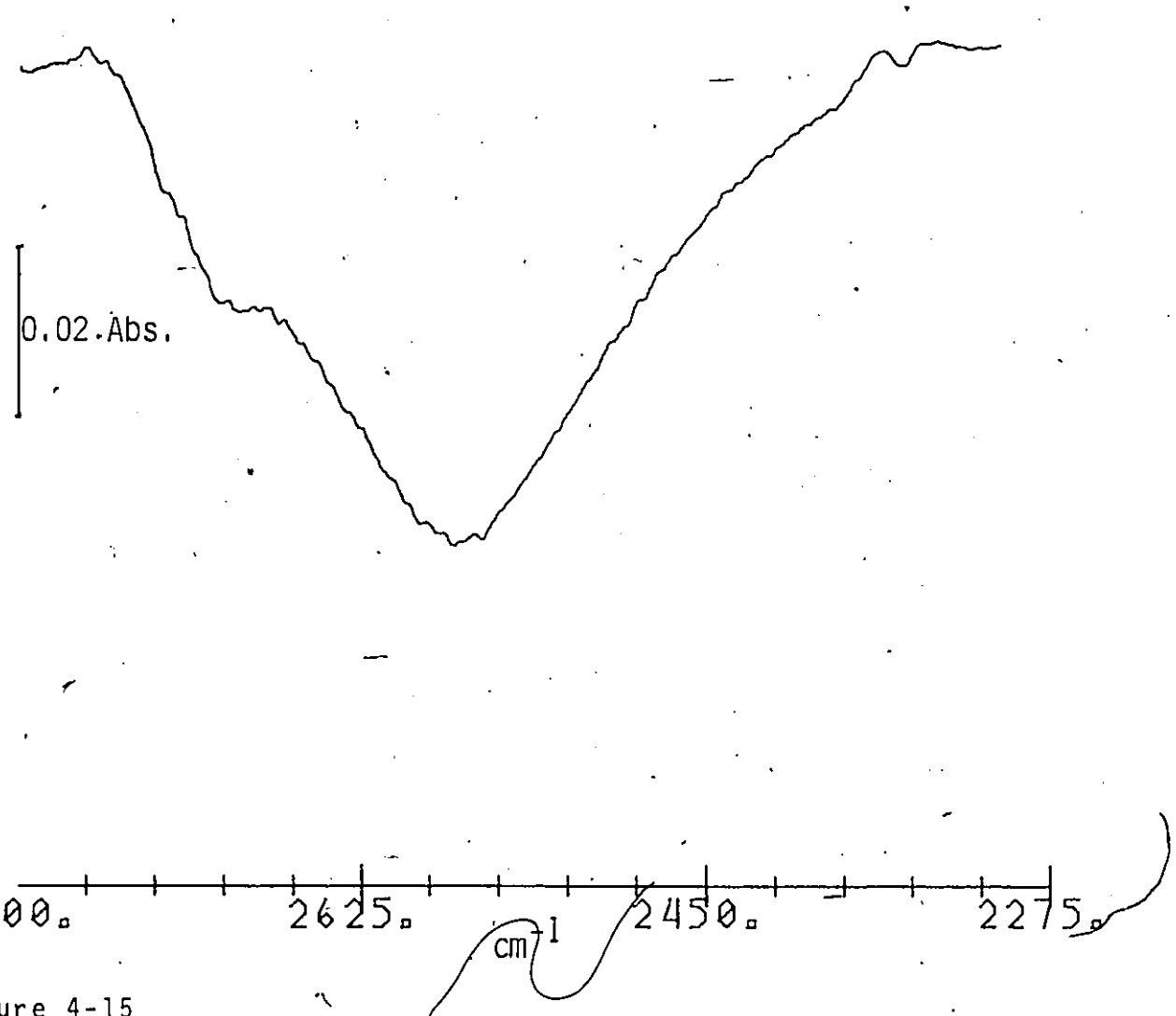


Figure 4-15
Difference spectrum in the OD stretching region for the sample from Figure 4-13b after reaction with $TiCl_4$.

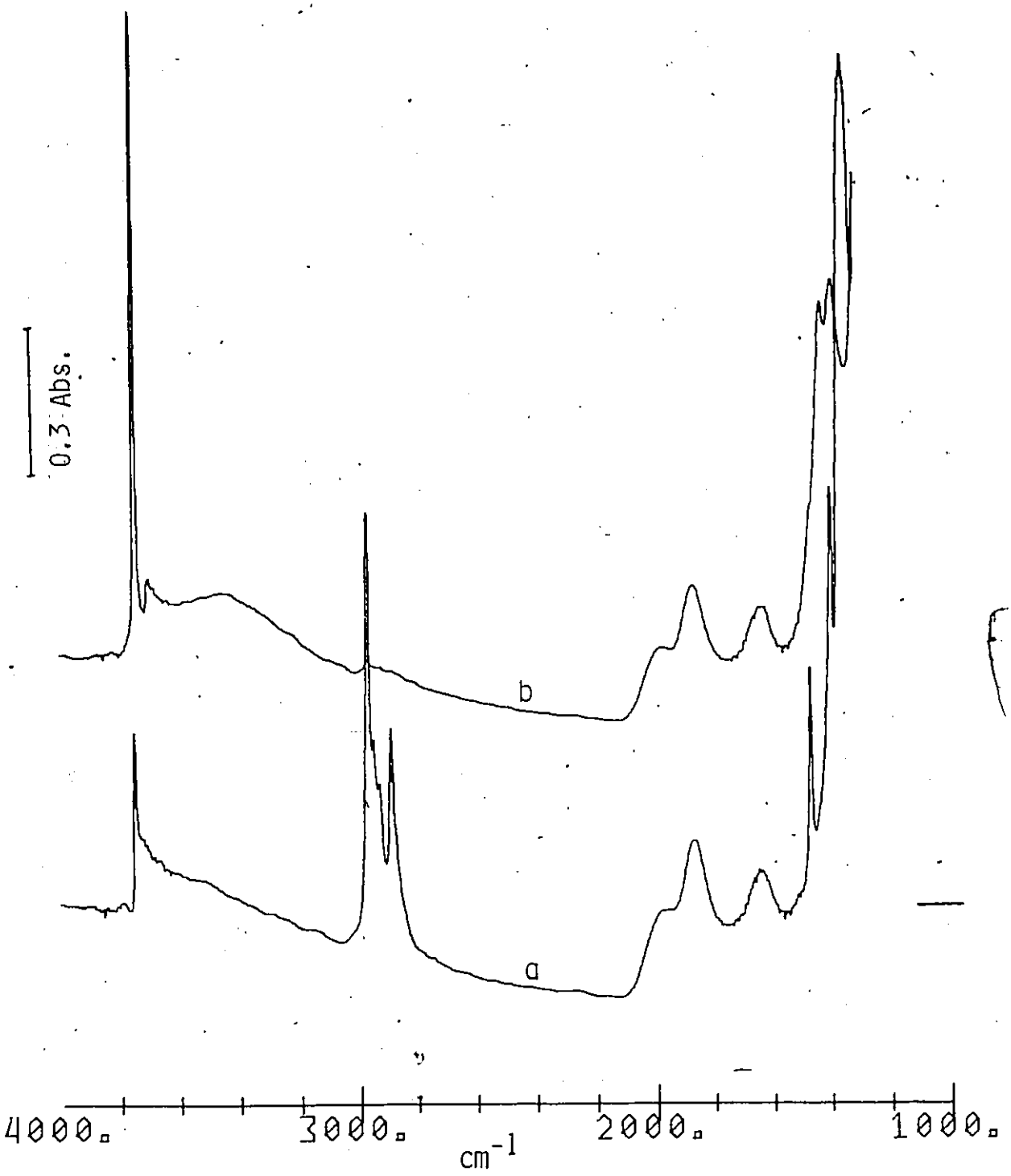


Figure 4-16
Infrared spectrum of a silica (10mg/cm$^2$) which had been degassed at 450°C, reacted with triethylborane and then hydrolyzed:
a) After hydrolysis at 200°C for 1 hr and evacuation at 25°C for 5 min.
b) After hydrolysis at 380°C for 3 hrs and evacualtion at 200°C for 1 hr.

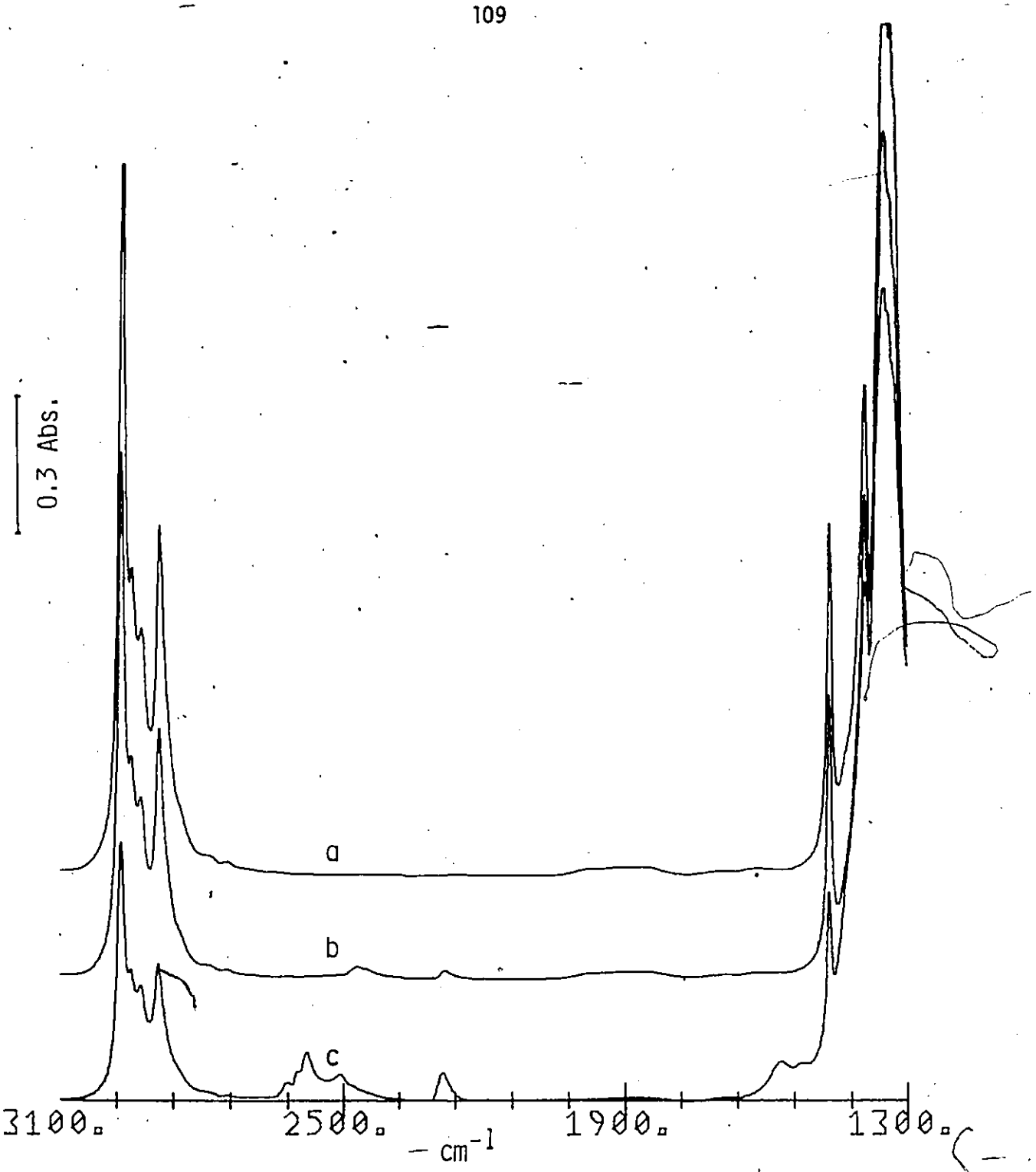


Figure 4-17
Infrared spectrum of a silica (10mg/cm$^2$) degassed at 450°C and reacted with triethylborane followed evacuation for 1 hr at a) 200°C; b) 300°C and c) 400°C.

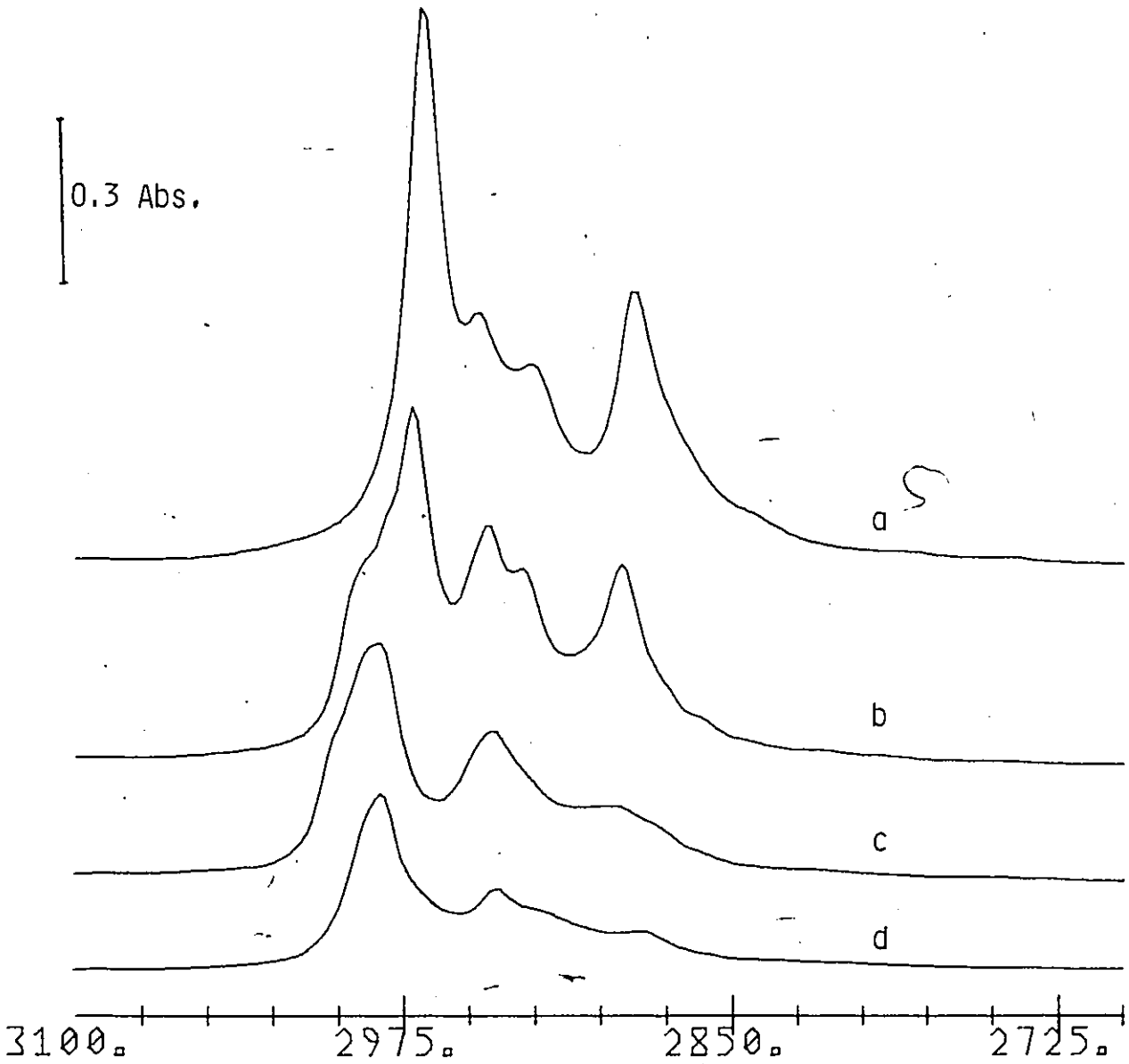


Figure 4-18
Infrared spectrum in the 3200-2700cm$^{-1}$ region showing the changes after the addition of 28 torr of oxygen to a silica which had been treated with triethylborane
a) Spectrum before the addition of $O_2$
b) $O_2$ for 5 min.
c) $O_2$ for 24 hrs.
d) evacuation for 1 hr at 25°C.

Discussion

The change in the frequency of the isolated hydroxyl from 3748 to 3700cm$^{-1}$ following the immediate introduction of TEB to the cell indicates that the interaction with adsorbed TEB is weak. The shift is of the magnitude expected for weakly interacting non-polar liquids such as carbon tetrachloride, hexane, nitrogen and carbon monoxide[139, 140]. It might be expected that the interaction was between the electron deficient boron in TEB and the oxygen of the hydroxyl group.

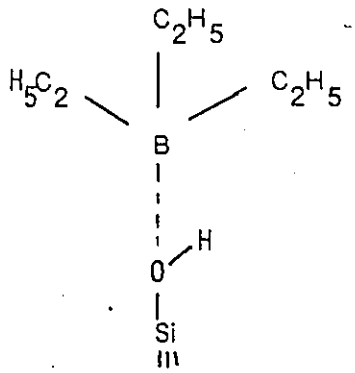

However, as will be shown, the subsequent reaction was selective with respect to the type of hydroxyl, which is contrary to the situation with the analagous boron trichloride previously mentioned.

Two possible reactions between TEB and silica may be envisaged:

(1)

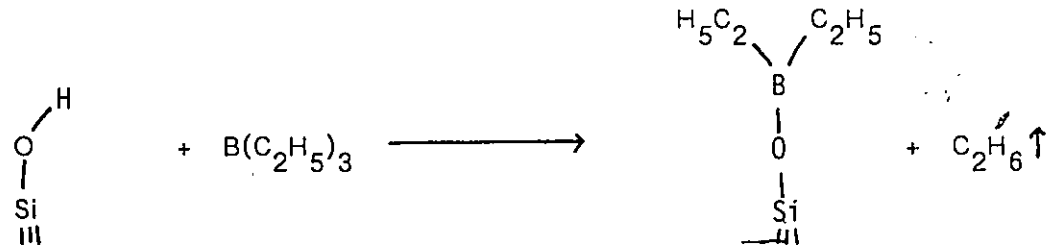

(2) 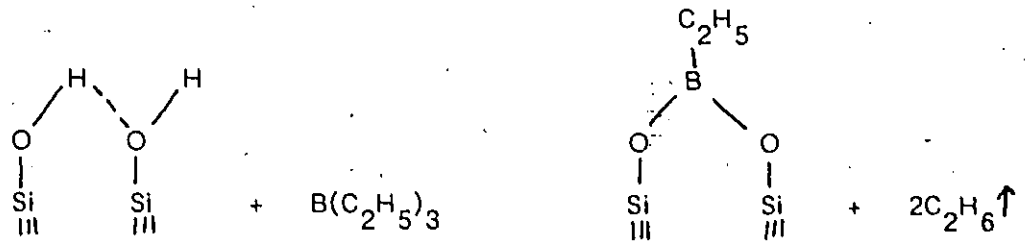

It will be shown that the results support the notion that reaction (1) was the sole reaction on silica. The assignment of the observed bands was made by analogy with those for gaseous TEB[141, 142]. The two intense bands at 2967 and 2887 $cm^{-1}$ are the antisymmetric and symmetric stretch of - $CH_3$ while those at 2946 and 2924 $cm^{-1}$ are the corresponding - $CH_2$ - stretching modes. The bands observed at 1465 and 1389 $cm^{-1}$, respectively are assignable as the - $CH_3$ antisymmetric and symmetric deformations, respectively. The intense band at 1345$cm^{1}$ is attributed to the sole B-O stretch and that at 940 $cm^{-1}$ as possibly a C-C stretch or a symmetric -$BC_2$ stretch. The observation of a single B-O stretch precludes the possibility that $(\equiv SiO)_2B$ is present since this species would have two BO stretches and these frequencies would be different from that of $\equiv SiOB$. Furthermore, the relative intensities of the 1465, 1389 and 1345 $cm^{-1}$ bands were the same whether the sample had been degassed at 450°C or 150°C; in the latter case more paired hydroxyls should be present for possible reaction with TEB to yield $(\equiv SiO)_2B$.

The spectrum of a thin film of silica reacted with TEB showed additional bands in the 1100 $cm^{-1}$ region, where a broad band centred at 1110 $cm^{-1}$ and another at 1060 $cm^{-1}$ with a shoulder at 1020 $cm^{-1}$ were observed. The band at 1110$cm^{-1}$ might be the -$BC_2$ asymmetric stretch which for TEB occurs at 1120$cm^{-1}$. The 1060 $cm^{-1}$ band could be the $\equiv SiO$ stretch of $\equiv SiOB$ which is expected to lie between 1200 and 1000 $cm^{-1}$ since those for Si-OSi, Si-OC and Si-OTi, reported in the previous Chapter, lie in this region.

It has been established that when silica is degassed at 500°C, all paired hydroxyls are removed and that the density of isolated hydroxyls on the surface is about 1.2-1.4 per 100 $nm^2$. These remaining hydroxyls are isolated in the sense that they are too far away from each other for hydrogen bonding but nevertheless there is a range of environments for the hydroxyls[66]. This view is supported by the present results (Figure 4-7) where the peak for those hydroxyls which reacted with TEB shows a slight asymmetry to low frequency.

The difference spectrum in Figure 4-8, which shows the hydroxyls groups that reacted with TEB on a 150°C degassed silica, was very different from a similar difference spectrum for a silica which had been degassed at 500°C. Here, in addition to a band at 3748$cm^{-1}$, a pronounced shoulder was observed at 3720$cm^{-1}$ as well as a broad band at 3550 $cm^{-1}$. The disappearance of these three bands has been analyzed by time resolved spectroscopy. This study, shown in Figures 4-10 and 4-11, showed that in the first 2 hrs of reaction, a band at 3748 $cm^{-1}$, with asymmetry to low frequency, and a broad band near 3550 $cm^{-1}$ disappeared. In the succeeding 8 hrs however, while the band 3748 $cm^{-1}$ was still disappearing, no proportionately strong band was apparent at 3550 $cm^{-1}$. After 10 hrs approximately 80% of the isolated hydroxyls had reacted. In the final 14 hrs the spectrum (Figure 4-11) revealed that a proportionally large amount of hydroxyls, with a band at 3717 $cm^{-1}$ and a broad peak centered at 3525$cm^{-1}$, had reacted compared to the isolated hydroxyls.

The intensities of the broad bands at 3550 and 3525 $cm^{-1}$, in Figures 4-10a and 4-11, respectively, are approximately the same. However, whereas there was an intense band at 3717 $cm^{-1}$ in Figure 4-11 there was only a slight assymmetry at this frequency on the tail of the isolated hydroxyl band in 4-10a. Even though the bands at 3720 and 3500 $cm^{-1}$ may be removed by degassing at

450°C their absence in Figure 4-7 and the relationship of their intensities indicate that the three bands at 3717, 3550 and 3525 $cm^{-1}$ are associated with at least two different kinds of hydroxyl groups.

One implication of the above results is that the 3550 $cm^{-1}$ band is due to three or more hydrogen-bonded hydroxyls (see Chapter 1.) and that the 3717 and 3525 $cm^{-1}$ bands are due to a different type of hydrogen-bonded species.

Peaks at 3720 and 3520 $cm^{-1}$ in the infrared spectrum of silica have been reported by Volkov et al.[43] and Morrow et al.[32]. Volkov assigned these bands to either an unsymmetrically perturbed water molecule or to a water dimer. Morrow et al. assigned these bands to a pair of hydrogen bonded hydroxyls which were generated during the rehydration of highly dehydroxylated silica.

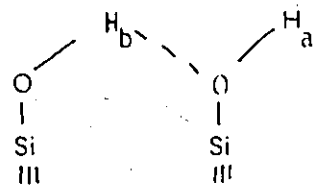


$\nu(OH_b)$ 3520 $cm^{-1}$

$\nu(OH_a)$ 3720 $cm^{-1}$

In agreement with their work with $D_2O$, the present results in Figures 4-13 and 4-14 showed that for partial H/D exchange no additional bands are found in the 3700 $cm^{-1}$ region as one would expect if a water dimer were present.

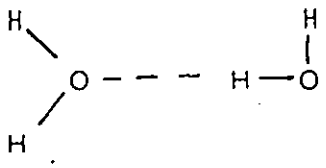


In further agreement with Morrow we find in the - OD region of the spectrum a

band at 2740cm$^{-1}$ corresponding to the 3720cm$^{-1}$ band. No time resolved work was done with the deuterated sample so the corresponding low frequency band which Morrow found at 2610 cm$^{-1}$ is not assigned here. This band would overlap in Figure 4-14 with the OD band for the hydrogen-bonded groups of OD at 2625 cm$^{-1}$ and this probably accounts for the broad band observed here in the present case.

The suggestion that the 3720 and 3520 cm$^{-1}$ bands could be due to strongly adsorbed water may have some validity in case of gels and is supported by the solid-state nuclear magnetic resonance studies of Maciel and Sindorf[59]. However, aerosil silicas are very different from gels and it has been well established that water is completely removed from aerosils by degassing at 25°C because the deformation mode of $H_2O$ at 1627 cm$^{-1}$ in the infrared spectrum of an aerosil disappears completely. Further, TEB reacts readily with only one of the hydrogens of $H_2O$ to produce $(C_2H_5)_2$ BOH[143] and reaction of the second hydrogen to yield $[(C_2H_5)_2B]_2O$ requires moderate temperatures and a carboxylic acid catalyst. Thus if water were present a peak at 3700cm$^{-1}$ for >BOH should have been created.

Figures 4-9 and 4-15 show the resulting disappearance of -OH and -OD groups, respectively, when a silica degassed at 150°C was reacted with TEB and then with titanium tetrachloride. The removal of bands at 3645 and 3480 cm$^{-1}$ is consistent with perturbed hydroxyl groups in the interstices formed by interparticle contact in the silica. These hydroxyls are inaccessible to the more bulky TEB but some can react with $TiCl_4$. The $D_2O$ exchanged sample showed that not all the hydroxyl groups accessible to $D_2O$ are accessible to TEB or $TiCl_4$.

Triethylborane treated silica was fairly stable to hydrolysis as is shown in Figure 4-16. The hydrolysis was minimal at 25°C and slow at 200°C when a band at 3748 cm$^{-1}$ due to ≡SiOH began to appear and the peaks due to adsorbed TEB

showed a slight decrease. Hydrolysis was rapid at 380°C and the bands at 3700, 1460 and 1379 $cm^{-1}$ indicate a $\equiv SiOB(OH)_2$ species or boric acid was produced along with $\equiv SiOH$.

The surface of the TEB treated silica showed considerable thermal stability and Figure 4-17 shows that decomposition did not begin until about 300°C. Bands in the 2600 - 2500 $cm^{-1}$ region due to BH species appeared and a band at 2285 $cm^{-1}$ indicative of $\equiv SiH$ show that pyrolysis was the probable cause of decomposition.

The addition of oxygen to TEB treated silica shown in Figure 4-18 indicates that oxidation of the surface species was occuring. The final bands observed in Figure 4-18d can be assigned to an ethoxy ($-O\ CH_2CH_3$) species attached either to boron or silicon. Further speculation is not warranted.

Conclusions

Triethylborane reacts with hydroxyl groups on silica which are of three types : isolated, hydrogen bonded groups of three or more hydroxyls and hydrogen bonded pairs. The reactions occur at different rates with the first two types reacting fastest and the hydrogen bonded pairs the slowest. The product of these reactions is the same, i.e., $\equiv SiOB\ (C_2H_5)_2$ and the reactions may be presented as shown:

$$\equiv SiOH + B(C_2H_5)_3 \longrightarrow \equiv SiOB(C_2H_5)_2 + C_2H_6\uparrow$$

$\nu(OH)$ 3748 $cm^{-1}$

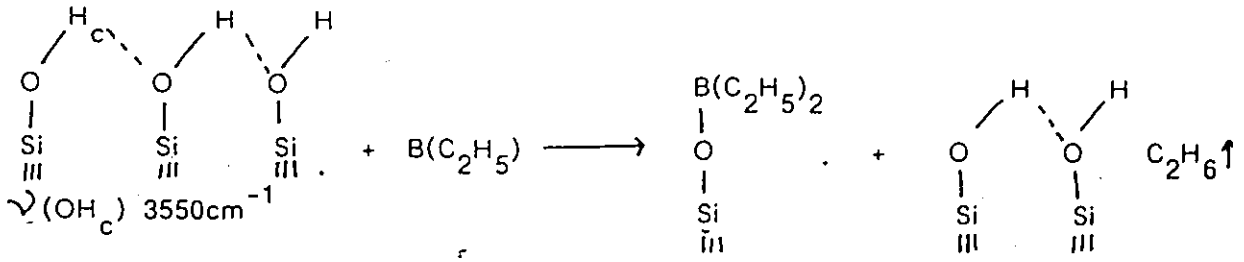

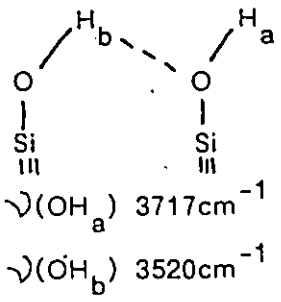


$$+\ 2B(C_2H_5)_3 \longrightarrow 2 \equiv SiOB(C_2H_5)_2 + 2C_2H_6\uparrow$$

The reaction of hydrogen-bonded groups could, in principle, leave hydrogen-bonded pairs which are sterically hindered from further reaction with TEB. However there is no way to ascertain this from the present available data.

The relative rates of reaction for the hydroxyls cannot be rationalized in terms of the scheme outlined by Hockey for the chlorosilanes and boron trichloride. It is possible that steric effects and O-H bond strengths (or acidity) play complex roles in the observed results. Further speculation cannot be made here with the present data.

# CHAPTER 5

## THE REACTIONS OF DIBORANE WITH SILICA

### Introduction

Diborane was one of the first probe molecules which was used to determine the concentrations of hydroxyl groups on silica surfaces[144-8]. It was believed to react with the surface hydroxyls (isolated, hydrogen-bonded pairs and geminal pair )in the following ways:

(1) $\equiv Si\text{-}OH + \frac{1}{2}B_2H_6 \longrightarrow \equiv SiOBH_2 + H_2\uparrow \quad R = 2$

(2)

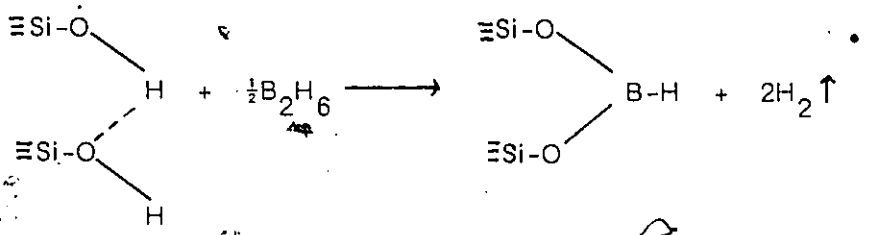

$R = 4$

(3)

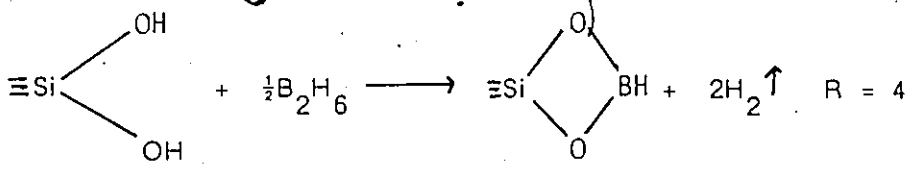

$R = 4$

With very highly hydrated silicas an additional reaction was believed to occur:

(4) $3 \equiv Si\ OH + \frac{1}{2}\ B_2\ H_6 \longrightarrow (\equiv SiO)_3B + 3H_2\uparrow$

$R = 6$

The ratio of hydrogen evolved to diborane consumed (R) for a known mass of silica in these hydrolyses was related to the concentrations of the surface hydroxyls.

The above reactions were originally proposed on the basis of the values of R which were obtained using silica gel. This was further substantiated after

additional work by Weiss, Shapiro and Knight[145], who noted that for deuterated diborane ($B_2D_6$) only HD was evolved so that the reaction was indeed between diborane and the surface silanols with, one molecule of hydrogen gas being evolved for each -OH reacted. Later work, however, by Naccache et al.[146, 147] with silica gels gave different R values for which they proposed the following set of reactions:

(5) $\equiv SiOH + B_2H_6 \longrightarrow \equiv Si\text{-}O\text{-}B_2H_5 + H_2\uparrow \quad R = 1$

(6) $\equiv Si\text{-}OH\text{----}O\begin{matrix}H\\H\end{matrix} + B_2H_6 \longrightarrow SiOH\text{----}O\begin{matrix}BH_2\\BH_2\end{matrix} + 2H_2\uparrow$

$R = 2$

The structure of the $\equiv SiOB_2H_5$ species was not discussed.

To this point there was no hard evidence to prove the existence of any of the proposed surface species obtained after reaction with diborane until Mathieu and Imelik[149] reported R values and corresponding infrared spectra for the reaction of diborane with silica gels degassed at 150°C and 600°C. The R value for the silica degassed at 150°C was 2 and the infrared spectrum had an intense band at 2580$cm^{-1}$ with a weak shoulder at 2510$cm^{-1}$ which they assigned to the species $\equiv Si\text{-}OH\text{----}O(BH_2)_2$ in reaction (6). The value of R for the silica degassed at 600°C was 1.0 and exhibited infrared bands of two types: (I) at 2625 and 2515$cm^{-1}$ and (II) at 2560 with a doublet near 2465$cm^{-1}$. During evacuation of the diborane following the reaction, type I bands decreased while type II increased and on this basis Mathieu and Imelik assigned type I to physically adsorbed diborane and II to $\equiv SiOBH_2BH_3(X)$.

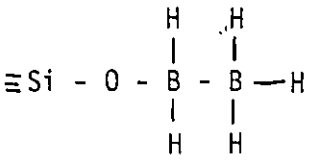

( X )

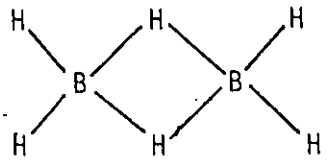

( Y )

This species contains tetravalent boron, which is unknown for boron compounds. It is known that diborane (Y) and other higher boranes contain hydrogen bridges and that these bridges have IR frequences around 2200 and 1600cm$^{-1}$; however, Imelik does not report the observation of any infrared bands in these regions.

Baverez and Bastik[150] also reported IR spectra and R values for silica gels and aerosils. The R values obtained were slightly higher than those of Mathieu and Imelik for the gels but their IR spectra were significantly different. The IR spectra by Baverez and Bastik were better resolved and for both the gel and aerosil degassed at either 200 or 450$^{o}$C they observed type I bands at 2597 and 2520cm$^{-1}$ and type II bands at 2560, 2479 and 2452cm$^{-1}$, and these two types behaved similarly to those observed by Mathieu and Imelik. In addition however, Baverez found in all reactions a new band, type III at 2585cm$^{-1}$, which was independent of the behaviour of types I and II bands, and weak bands at 2110, 2090, 1560 and 1535 which mimiced the behaviour of type I bands. Type I bands were assigned to the hydrogen bridged diborane (Y) which was co-ordinated to a lone pair of electrons on surface oxygens (N) and type II to $BH_3$ also coordinated to surface oxygen (M), and these two species were in equilibrium because N or M could be made to dominate the spectrum by readding or evacuating diborane.

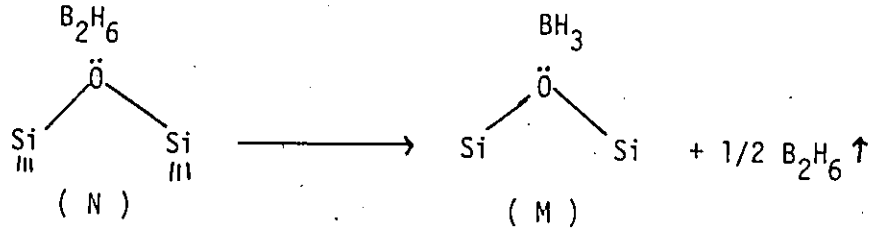


The exact mode of coordination of species (N) was not explained and the assignments of the spectra of N and M was speculative and vague. The type III band at 2585cm$^{-1}$ which was most intense with silica degassed at 200°C was assigned to the species produced in reaction 2.

Following the above studies, Fripiat and Van Tongelen[148] reported a similar investigation for silica gels degassed at 150°C. They proposed that in addition to reaction (1) two other processes were taking place:

(7)

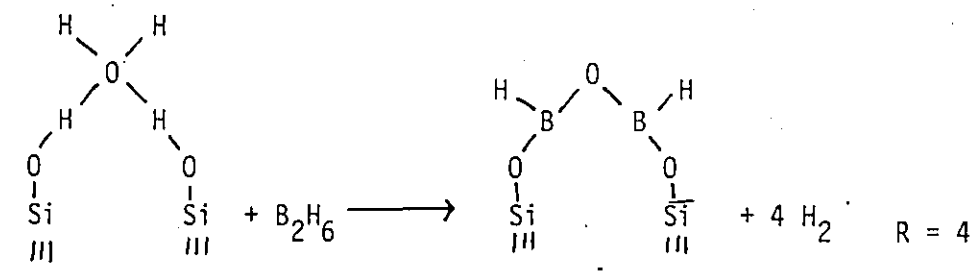


(8)

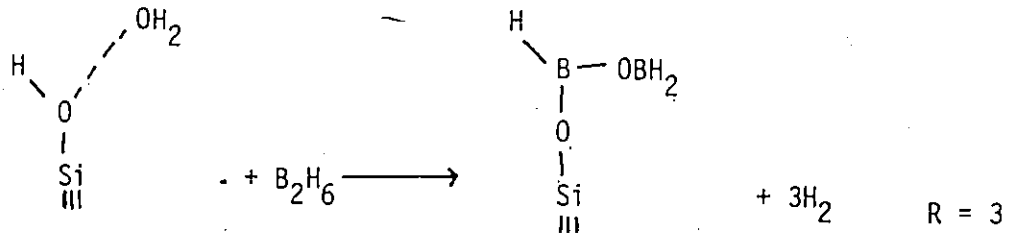


The most recent report concerning silica treated with diborane found in the

literature is that by Maschenko[151] for gels degassed at 150 and 800°C. For the gel which was degassed at 150°C, after treatment with diborane the IR spectrum had bands at 2585, 2373, 2487 and 2467cm$^{-1}$ in addition to a weak band at 2290cm$^{-1}$ and an intense band in the 1300-1400cm$^{-1}$ region. In contrast, the silica gel degassed at 800°C exhibited intense bands at 2578, 2487, 2467, 2290, 1387 and 1362cm$^{-1}$. The band at 2585cm$^{-1}$, in agreement with other authors, was assigned to the species produced in reaction (2) while the bands at 2578, 2487 and 2467 cm$^{-1}$ were assigned to the species $\equiv SiOBH_2$ in reaction (1). The species $\equiv SiOBH_2$ would be expected to have only two bands in the 2600-2400cm$^{-1}$ region, namely, the antisymmetric B-H stretch and, at lower frequency, the symmetric stretch. The author postulated that three bands are observed because the doublet at 2487 and 2467cm$^{-1}$ corresponds to two types of $-BH_2$ for which the force constants of the asymmetric vibration were different from that of the symmetric vibration. They therefore proposed that a second reaction to produce $-BH_2$ occurs:

(9)

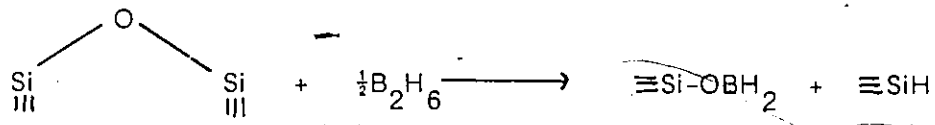

Reactive siloxanes are known to be generated by the high temperature degassing of silica and, in support of the above reaction, Mashchenko assigned the band at 2290cm$^{-1}$ to a $\equiv Si-H$ species which is known to have IR bands in this region. Finally, the bands at 1387 and 1362cm$^{-1}$ were assigned to B-O stretches but the nature of these species were not defined. It is interesting that Mashchenko does not observe nor does he comment on the bands at 2597 and 2570cm$^{-1}$ observed by Mathieu and Imelik[149] and Baverez and Bastik[150].

Several species produced in the reactions of diborane with silica gels and aerosils have been proposed in the studies described above and some of the shortcomings of these have been mentioned. Up to the present time no

unambiguous assignments have been made regarding the observed infrared data and similar observations by different authors have been assigned to dissimilar species. One of the problems with regards to the IR spectra of adsorbed diborane is that the bands are broadened due to the isotopic abundance of boron, i.e., 20% B-10 and 80% B-11. Another problem is that different gels and aerosils were used in the above investigations. In the present investigation a complete assignment of all the surface species formed by diborane on silica was attempted using infrared and Raman spectroscopies (Part I). In order to obtain a complete assignment it was necessary to use in addition to normal isotopic abundance diborane ($^{n}B_2H_6$) pure $^{10}B_2H_6$, $^{10}B_2D_6$, and oxygen-18 exchanged silica. Early attempts in this study to characterize the surface species involved the reaction of the borane surface species with amines, alcohols and alkenes and additionally the reaction of borane carbonyl ($H_3B{:}CO$) with silica. These early attempts gave inconclusive results and will only be briefly reported at the end of this chapter (Part II).

Experimental

All silica samples used were previously calcined at 500°C in air except for samples that were degassed at 150°C, in which case uncalcined silica was used. Oxygen-18 exchanged silica was prepared by four 12 hours exposures of the sample to 15 torr of 99%$H_2O^{18}$ at 420°C for 48 hours at which point there was better than 90% exchange of $\equiv SiO^{16}H$ to $\equiv SiO^{18}H$. All infrared experiments were carried out in the conventional type quartz infrared cell since it was found that extensive reaction occurred between the walls of pyrex cells and diborane at 100°C. For this reason, after each experiment the quartz cell was heated in air at 1000°C to oxidize any borane species on the cell walls which would otherwise

contaminate silica samples subsequently degassed in the cell. Infrared spectra in Part I were recorded using either a Perkin-Elmer 13G, a Perkin-Elmer 283 or a Bomen DA3-02 FTIR spectrometer, while those in Part II were obtained exclusively from the 283 spectrometer. The borane treated silicas refered to in Part II were silicas degassed at 1000°C which were treated with diborane at 25°C and evacuated at that temperature for 1 hr.

## Part I The Nature of Chemisorbed Diborane on Silica

### Results

A difference was observed in the extent of the reaction between silica degassed at 500°C and diborane depending on whether the spectrum was recorded on the 283 or FTIR spectrometer. When 10-20 torr of diborane was left in contact with silica which was positioned in the infrared beam, after 30 minutes approximately 5-10% of the hydroxyl groups had reacted on the sample in the 283 spectrometer and no reaction had occured with that in the FTIR spectrometer. Morrow and Moran[152] have reported that, with black samples, heating in the infrared beam of a dispersive instrument can be severe and Volkov et al.[43] have reported similar results for white samples. Using the extent of reaction of diborane with silica at known temperatures it has been estimated that under the above conditions the temperature of the sample in the 283 spectrometer was approximately 50°C, slightly cooler in the 13G spectometer and near ambient in the FTIR spectrometer. It is therefore concluded that under the above conditions diborane does not react with surface hydroxyls at 25°C; however, as will be discussed later it does react at this temperature with surface siloxanes generated by high temperature dehydroxylation of silica.

Exposure of a silica sample at 100°C to 10-20 torr of diborane resulted in

complete reaction of all accessible hydroxyl groups in 15 minutes and the spectra were the same whichever infrared spectrometer was used. Figure 5-1a shows the IR spectrum from 2700-1300cm$^{-1}$ after reaction of a silica degassed at 500°C with excess $^{n}B_2H_6$ at 100°C. Infrared bands were observed in the BH stretch region at 2597, 2565 and 2516cm$^{-1}$; in the region of BHB bridge vibrations at 2092, 1983, 1700, 1563, 1545 and 1524cm$^{-1}$ and in the region of B-O stretch at 1336cm$^{-1}$. Evacuation at room temperature caused a gradual change in the spectrum and the ultimate result is shown after evacuation at 100°C in Figure 5-1b where all the bands for BHB bridges have disappeared and new BH and BO stretches have appeared. A weak band which remained unchanged in the presence of diborane as well as after evacuation was observed at 2280cm$^{-1}$.

Figures 5-2a - d more clearly show the changes that occurred in the BH stretching region after reaction with $^{10}B_2H_6$ and evacuation. These spectra show that bands A diminished in intensity upon prolonged evacuation and at the same time bands B grew while a band C appeared to remain unchanged. These changes are most clearly illustrated in Figure 5-3a which is the difference spectrum 2b-2c. The peaks pointing up are those disappearing and those pointing down are being created. The bands marked A* and B* are almost coincident as shown in Figure 5-2b and c and since B* is more intense than A* the net difference in Figure 5-3a is the appearance of B*. The band marked C in Figure 5-2a - d is in fact not changing with evacuation and so does not appear in Figure 5-3a. Figure 5-3b shows the corresponding difference spectrum for $^{n}B_2H_6$.

The changes shown in Figure 5-1, 5-2 and 5-3 were reversible with the addition and evacuation of diborane and indicate that there is an equilibrium between the species responsible for bands A and those responsible for bands B and that, furthermore, in the former species, there are BHB bridges but none in the

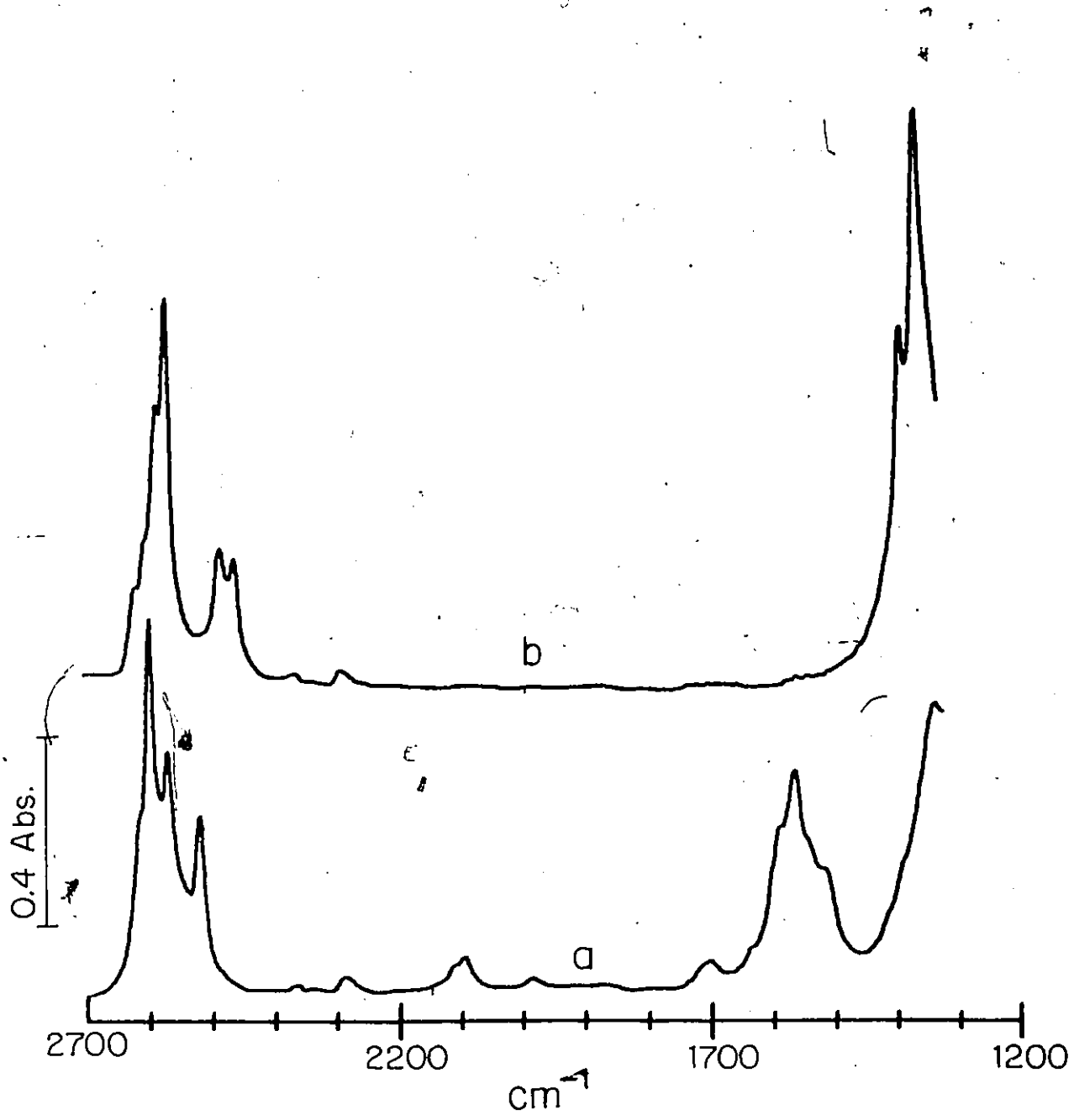


Figure 5-1
Infrared spectrum of $^{n}B_2H_6$ adsorbed on a silica (10mg/cm$^2$) which had been degassed at 500°C for 1 hr.
a) After the addition of 10 torr of $^{n}B_2H_6$ to the sample at 100°C for 30 min. (the gas phase contribution and the silica background have been subtracted)
b) After evacuation of a) for 30 min. at 100°C.

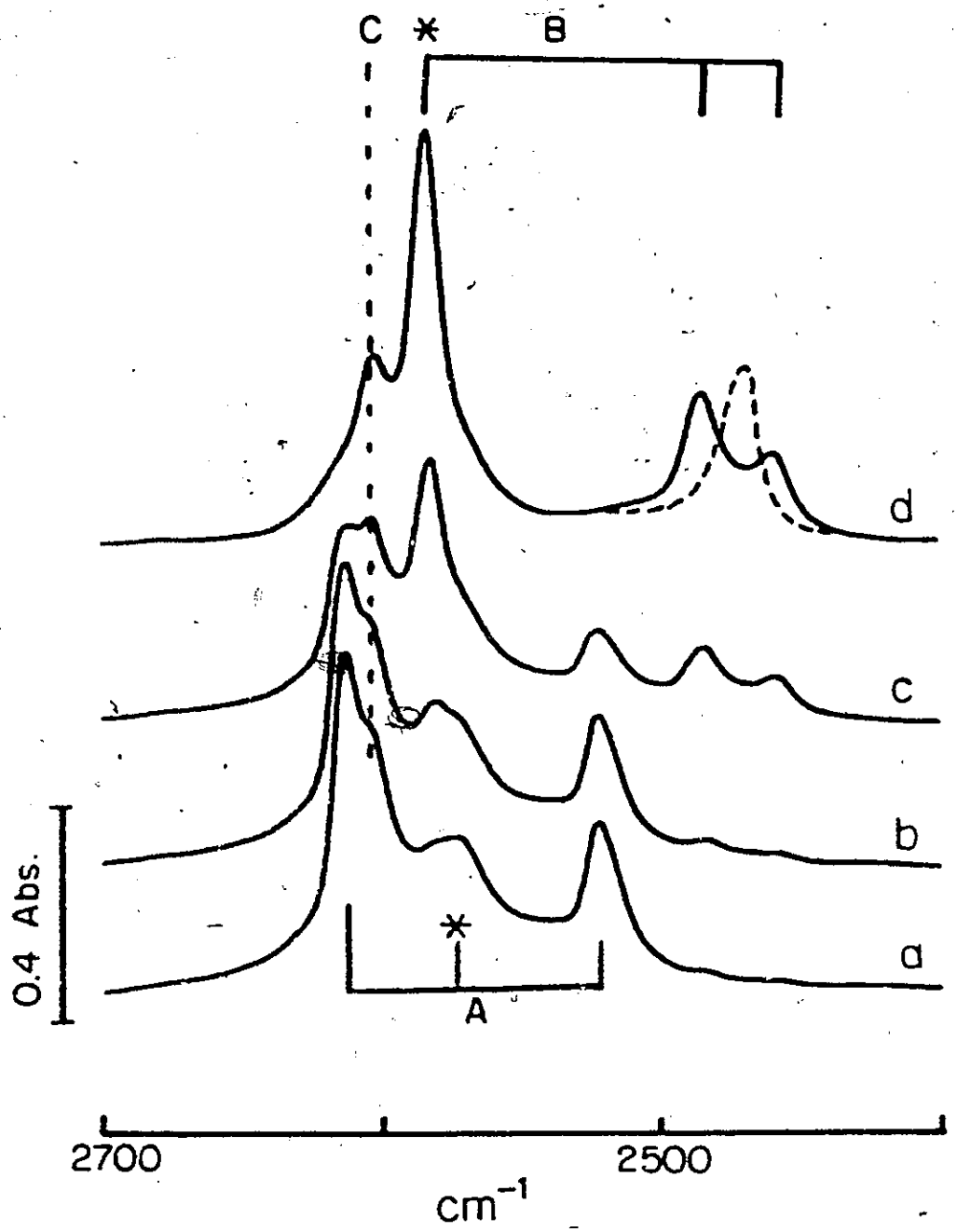


Figure 5-2
Infrared spectra in the BH stretching region for adsorbed $^{10}B_2H_6$
a) Conditions as in Figure 5-1a
b) Evacuation at 25°C for 1 min.
c) Evacuation at 100°C for 5 min.
d) Evacuation at 100°C for 30 min.
Bands due to species A, B and C are explained in the text.
The dashed spectrum is that for oxygen-18 exchanged silica.

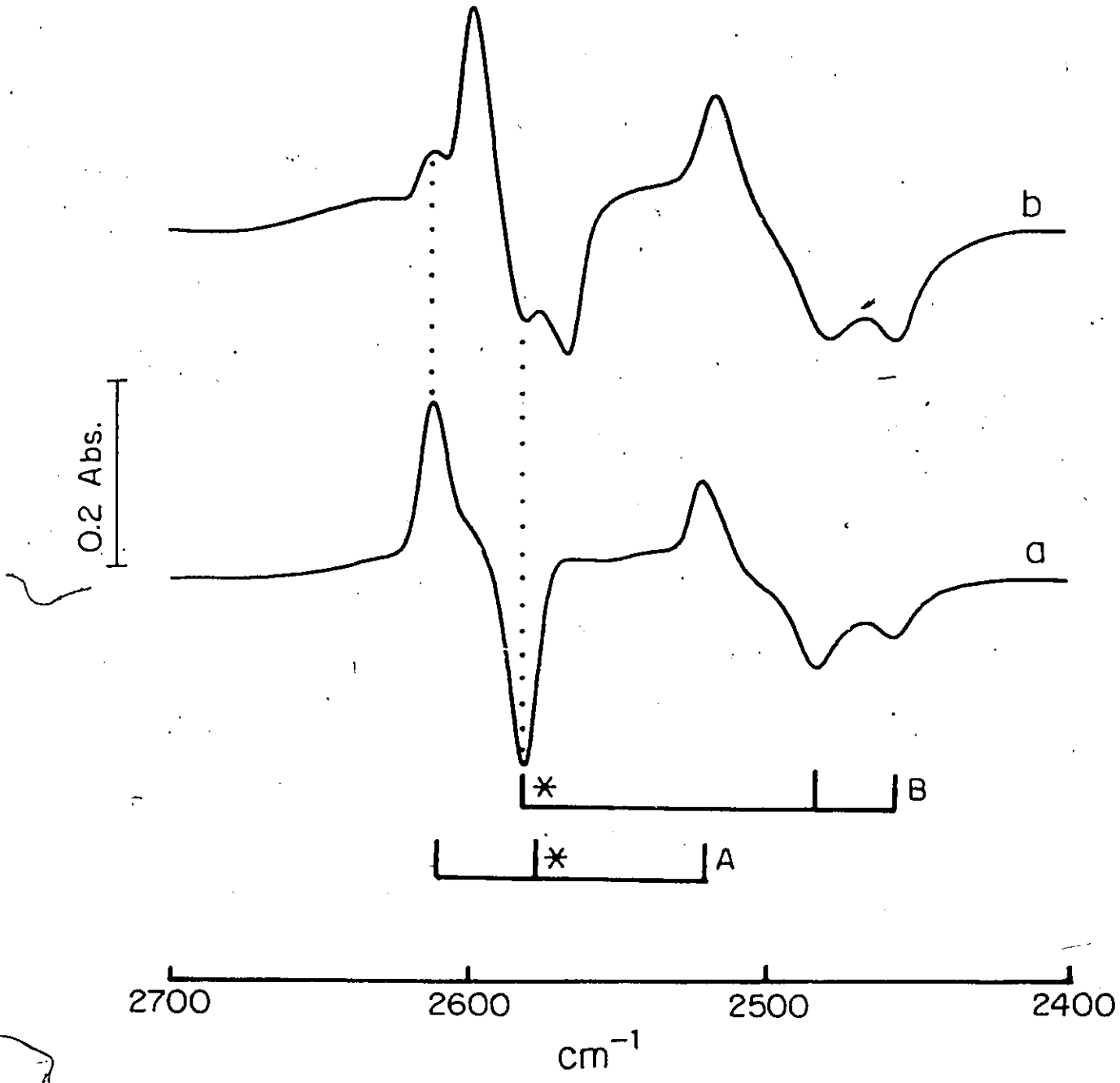


Figure 5-3
a) Difference spectrum Figure 5-2b minus Figure 5-2c.
b) A similar difference spectrum for $^{n}B_2H_6$.

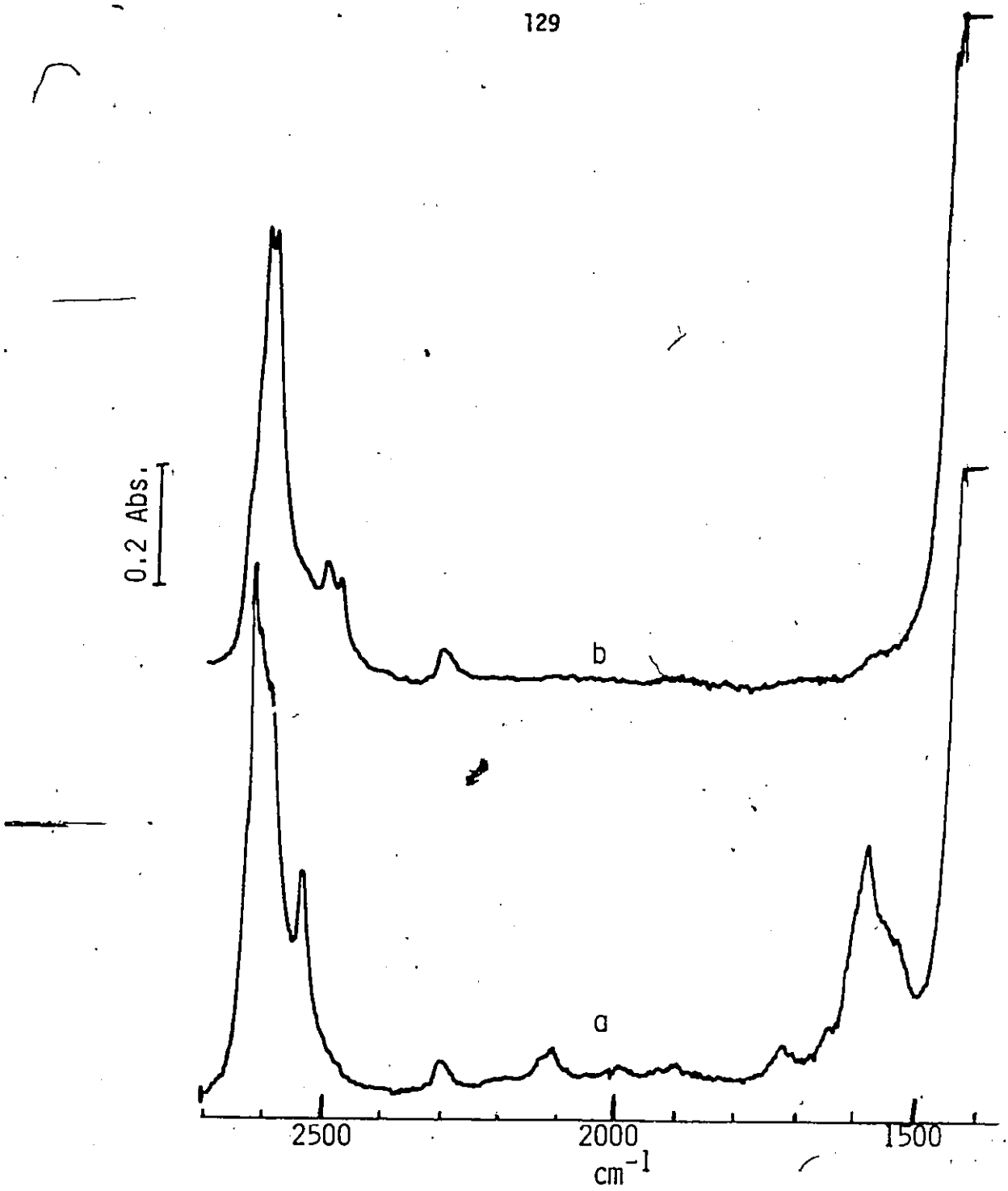


Figure 5-4
Infrared spectrum of $^{n}B_2H_6$ adsorbed on a silica (10mg/cm$^2$) which had been degassed at 150°C for 1 hr.
a) After the addition of 15 torr of $^{n}B_2H_6$ to the sample at 100°C for 1 hr. (gas phase and silica background contributions have been subtracted)
b) After evacuation of a) at 100°C for 1 hr. The 1400-1300 region was totally absorbing in spectra a) and b).

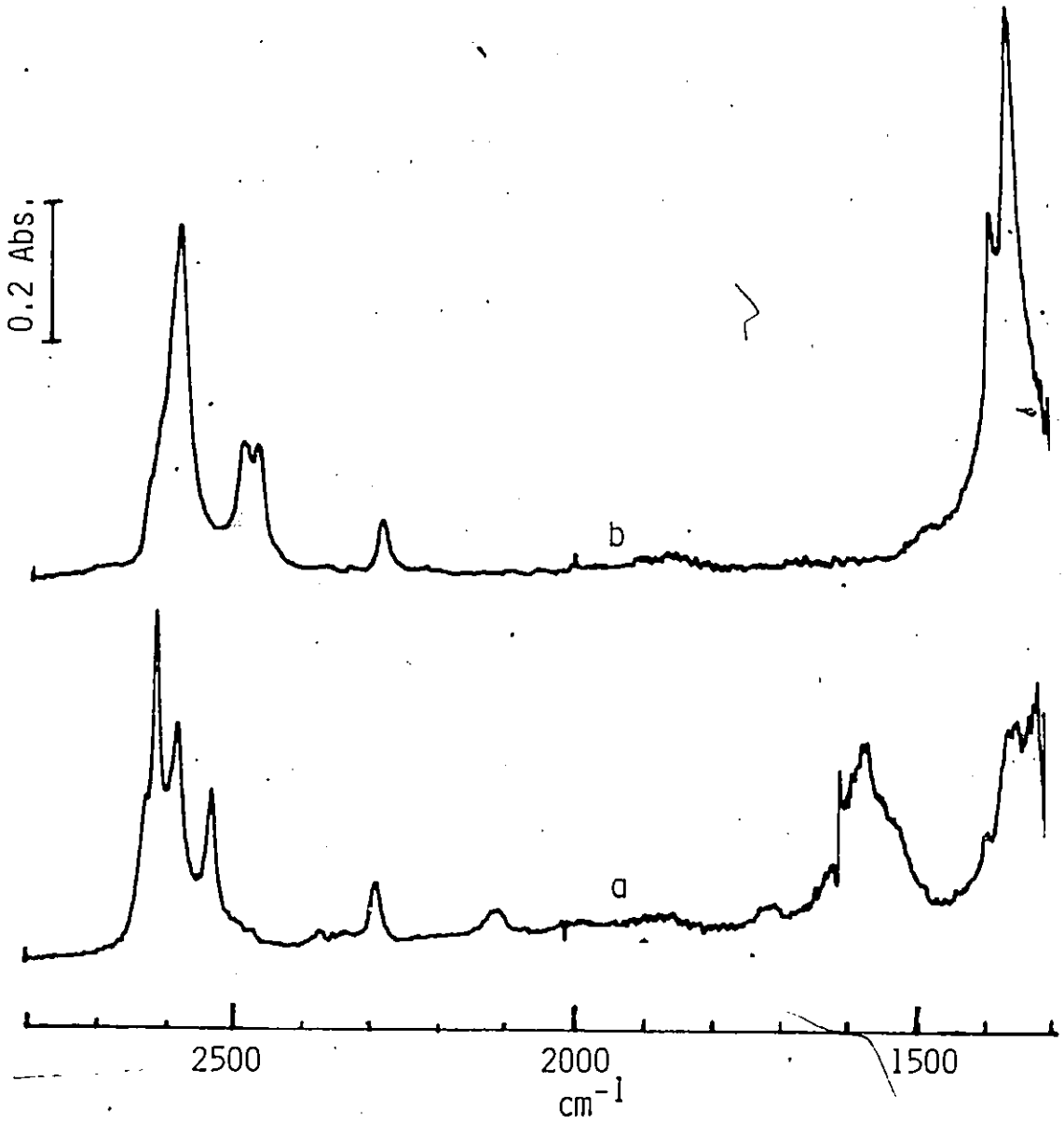


Figure 5-5
a) Infrared spectrum under the same conditions as in Figure 5-4a except the sample had been degassed at 1000°C.
b) After evacuation of a) at 100°C for 1 hr.

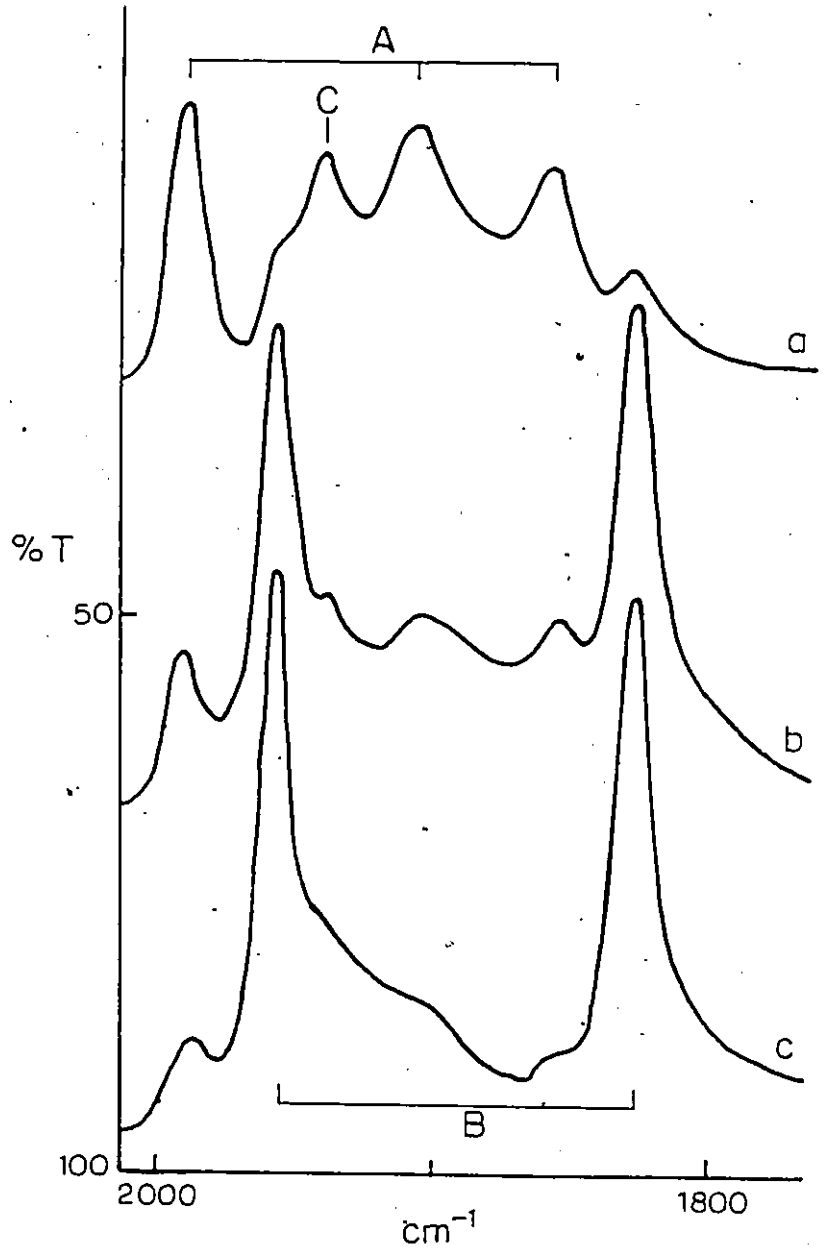


Figure 5-6
Infrared spectrum of $^{10}B_2D_6$ adsorbed on a silica (40mg/cm$^2$) degassed at 1000°C.
a) In the prescence of 10 torr of $^{10}B_2D_6$ at 20°C.
b) After evacuation at 20°C for 5 hrs.
c) After evacuation at 20°C for 24 hrs.
The % T scale refers to c) and the other spectra have been displaced.

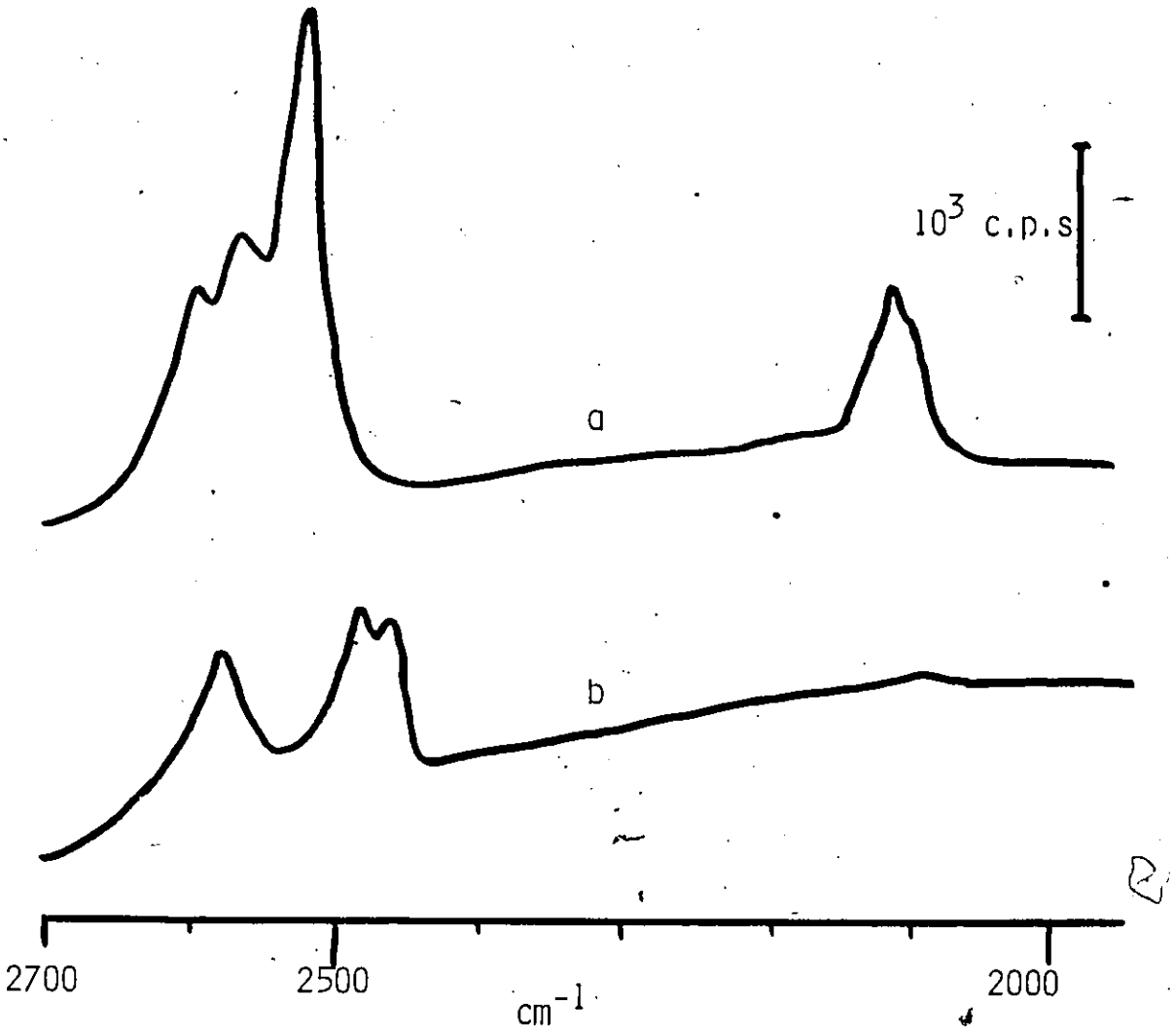


Figure 5-7
Raman spectra of $^{n}B_2H_6$ adsorbed on a silica degassed at 480°C for 1 hr.
a) After the addition of 10 torr $^{n}B_2H_6$ and heating the sample in the laser beam at 500mW for 16 hrs.
b) After evacuation of a) at 100°C for 15 min.

Table 5-1

Frequencies of infrared and Raman bands assigned to species A, B, C produced by the adsorption of diborane on silica.

| Species | $^{10}B_2H_6$ | $^{11}B_2H_6$ | $^{10}B_2D_6$ | $^{11}B_2D_6$ | $^{10}B_2H_3D_3$ [a] |
|---|---|---|---|---|---|
| A | 2612 | 2597 | 1986 | 1966 | 2565 |
| | 2574 | 2565 | 1908 | 1890 | 1912 |
| | 2522 | 2516 | 1860 | 1848 | |
| | 2097 | 2092 | | | |
| | 1992 | 1983 | | | |
| | 1717 | 1700 | | | |
| | 1575 | 1563 | | | |
| | 1545 | 1545 | | | |
| | 1524 | 1526 | | | |
| | 1340 | 1336 | | | |
| B | 2583 | 2565 | 1956 | 1940 | 2563 |
| | 2484 | 2479 | 1831 | 1821 | 2488 |
| | 2459 | 2456 | | | 1890 |
| | 1386 | 1356 | 1340 | | |
| C | 2602 | 2585 | 1950 | 1936 | 2602 |
| | 1400 | 1380 | | | 1950 |
| | 927 | 910 | | | |

a) Data of Morrow and McFarlane ref. 153.

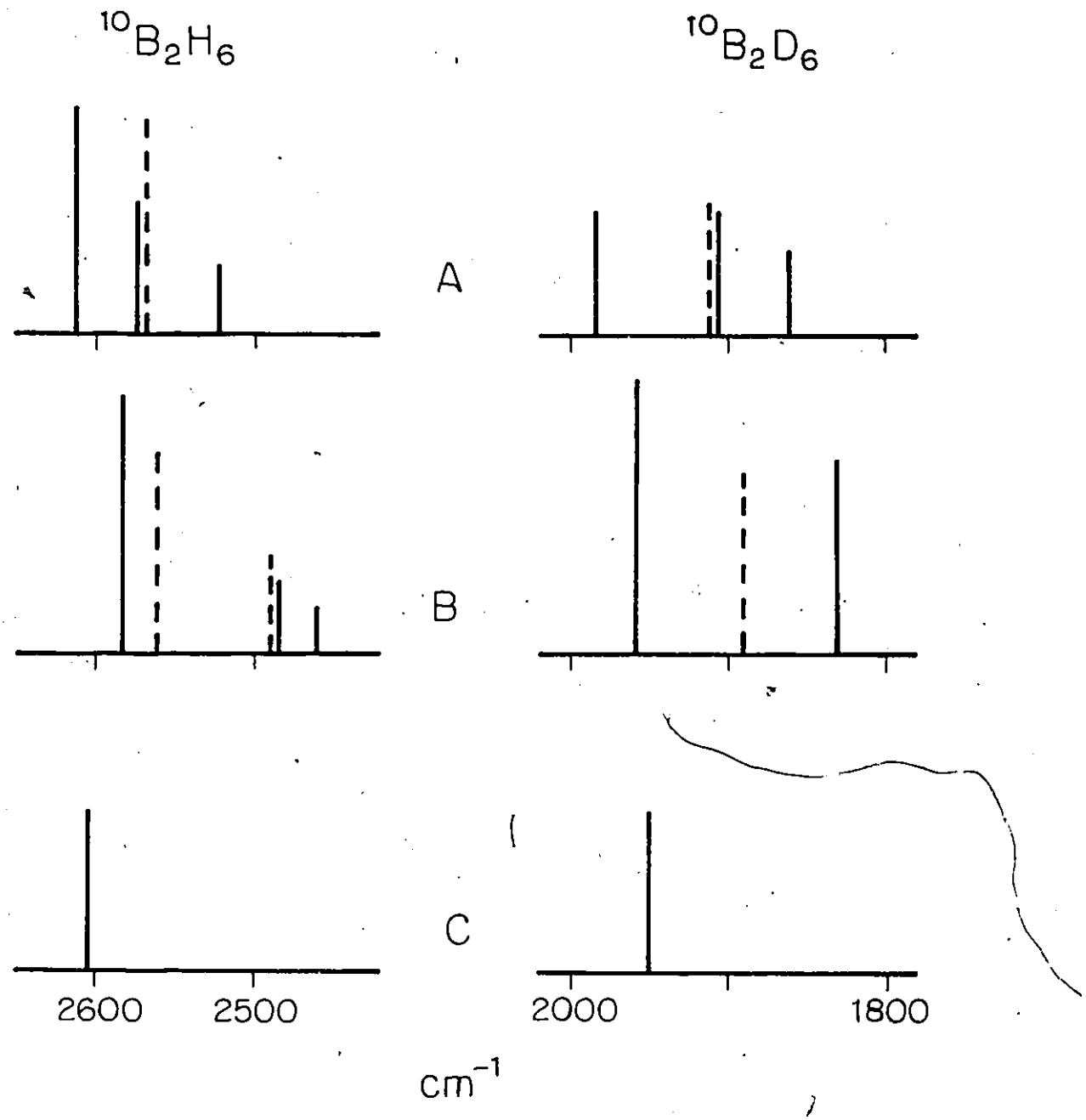


Figure 5-8
Bar graph representation of the $^{10}BH$ and $^{10}BD$ stretching modes for species A, B and C. The dashed lines show the new band positions for mixed H/D species.

latter. Difference spectra, similar to those in Figure 5-3 were obtained for any two stages in a series of spectra recorded during evacuation although the absolute intensities were different. From this it may be concluded that one species is responsible for bands A and one species for bands B and that these species are in an equilibrium with each other that involves gaseous diborane i.e.

$$A \underset{+B_2H_6}{\overset{-B_2H_6}{\rightleftharpoons}} B$$

In addition to this, a third species C is present which remains unchanged and independent of the presence of excess gaseous diborane.

Spectra corresponding to those of Figure 5-1 are shown in Figures 5-4 and 5-5 for silicas degassed at 150°C and 1000°C and reacted with $^{n}B_2H_6$. Spectra were also obtained with $^{n}B_2D_6$ and $^{10}B_2D_6$ and in the case of the latter is shown in Figure 5-6. Figure 5-7 shows the corresponding Raman spectra for the sample in Figure 5-1a and 1b from 2700-2000cm$^{-1}$. No low frequency Raman bands were observed. Table 5-1 lists all the band frequencies for species A, B and C and Figure 5-8 shows bar graphs of the BH(D) stretches listed in Table 5-1.

Discussion

It has been shown that diborane at a pressure of 10-20 torr does not react with silica at 25°C but that heating by the infrared beam of a dispersive infrared spectrometer caused some reaction to occur. This observation might have been an important unknown factor in the discrepancies of earlier work, all of which used dispersive infrared spectrometers. The heating caused by the IR beam was also shown to influence the spectrum observed after the reaction with silica and the evacuation of diborane. Nevertheless, the spectra observed in this work most closely resembled those reported by Baverez and Bastik but the use of

$^{10}B_2H_6$, $^{10}B_2D_6$ and the recording of the spectrum in the presence of gaseous diborane was unique to this work.

The appearance of species A and a small amount of species C in the presence of gaseous diborane, after the complete reaction of all accessible hydroxyl groups and the observed equilibrium between species A and B, indicate that species A and B are not simply coordinated $B_2H_6$ and $BH_3$ as postulated by Baverez and Bastik. However, in view of the decreasing amounts of species C generated on silica degassed at higher temperatures, this species, in agreement with Baverez and Bastick, is assigned to $(\equiv SiO)_2BH$ as in reaction (2). At high diborane coverage of silica, the B-O stretching region from 1400-1300cm$^{-1}$ was totally absorbing, as shown in Figure 5-4. At lower coverages, using $^{10}B_2H_6$, bands due to $(\equiv SiO)_2BH$ were observed at 1400 and 927cm$^{-1}$. These bands have been assigned, in accordance with similar bands observed for cyclic boroxine[154], to the $-BO_2$ antisymmetric stretch and B-H deformation mode, respectively, of $(\equiv SiO)_2BH$. It is clear that the small amounts of species C generated cannot account for the reaction of all hydroxyl groups with diborane especially in those silicas degassed at 500 and 1000°C which have very few hydrogen-bonded paired hydroxyls. The observations that species A contains BHB bridges and the equilbrium involving species A and B and gaseous diborane suggest the following scheme:

(10)

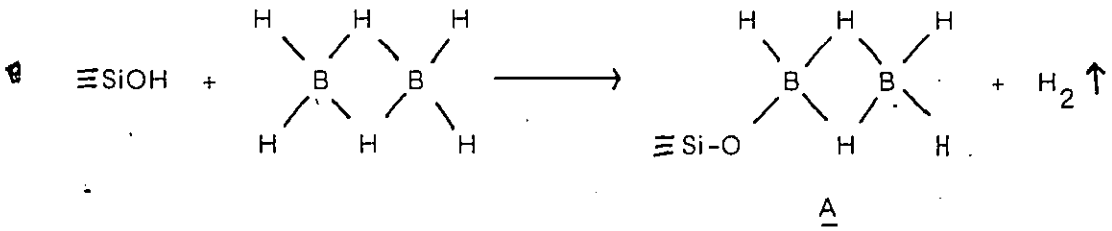


A

(11)

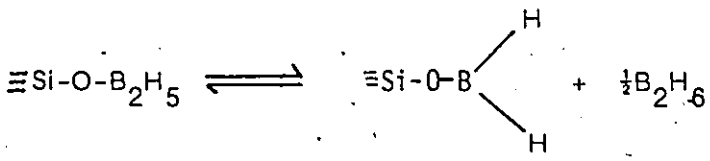

A B

While the infrared bands observed for species A might be interpreted in terms of diborane coordinated in some manner to a lone pair of electrons the assignment of the B bands to coordinated $BH_3$ is not plausible because the observed BH stretches (2580-2450cm$^{-1}$) are higher than those normally observed for coordinated $BH_3$ (2450-2350)[155-9]. The species $\equiv SiOB_2H_5$ shown in reaction (10) would be expected, by comparison with $B_2H_6$[160], to have three BH stretches of terminal BH groups in the region 2600-2500cm$^{-1}$ and several BHB bridging vibrations around 2100, 1900, 1750 and 1500cm$^{-1}$ and a single B-O stretch at 1336cm$^{-1}$, as observed. Partial exchange of $\equiv SiOB_2H_6$ with $B_2D_6$ or the reaction of silica with $B_2H_3D_3$ would be expected to produce one additional band midway in frequency between the antisymmetric and symmetric terminal $BH_2$ stretches (2612 and 2522cm$^{-1}$, respectively, for $^{10}B$) and, indeed, a new band was observed at 2565cm$^{-1}$. The above arguments also apply to the fully deuterated species and the results are as expected.

The species B, $\equiv SiOBH_2$, would be expected to have two IR peaks in the region of BH stretch but in fact three peaks were observed. It is this observation that has been the cause of the ambiguity in the previous attempts to assign this species. The formation of species B using $^{10}B_2D_6$ lends support to the above assignment as in this case only two BD stretches are observed and futhermore, as expected, upon partial deuteration only one new band midway between

these two was observed (Figure 5-8). In contrast, the partial deuteration produces two new bands in the BH stretching region. Further support for the assignment of species B comes from the results of Morrow[153] who report that upon 50% deuteration of species B three bands were observed in the region of B-O stretch at 1386, 1361 and 1340cm$^{-1}$ (using $^{10}B_2H_3D_3$) and the ratio of their intensities was that which would be expected for the abundance of a species $BX_2$ where the probability of X being either H or D was 50%.

Data from the BD and BO stretch regions appear to support the assignment of species B to $\equiv SiOBD_2$ while the BH stretch infrared data obtained appear to contradict this assignment. To clarify this, diborane was reacted with silica for which the $\equiv Si^{16}OH$ groups had been exchanged to give $\equiv Si^{18}OH$. In this case, while the spectrum for species A remained the same, that for species B now contained only two bands (Figure 5-2d). The band assignable to the antisymmetric stretch of $\equiv SiOBH_2$ was unchanged in frequency after oxygen-18 exchange while a single band appeared at the midpoint of the doublet at 2470cm$^{-1}$ (Fig 5-2d). Partial deuteration of the $\equiv Si^{18}OBH_2$ species produced a single band at 2546cm$^{-1}$ and although this was not at the midpoint of the symmetric (2470cm$^{-1}$) antisymmetric (2583cm$^{-1}$) frequencies, i.e., 2527cm$^{-1}$, it offers some further encouragement for the assignment. These observations with oxygen-16 and -18 silica may be rationalized in terms of one component of the doublet being a combination band involving the B-O stretch, which was intensified by Fermi resonance with the other component at 2470cm$^{-1}$. Such a combination band could be composed of the B-O$^{16}$ stretch at 1386cm$^{-1}$ and a band at approximately 2470-1386 = 1084cm$^{-1}$ which is close to the expected -BH deformation mode and which was not observed because the silica is opaque in this region.

Although diborane does not react with surface $\equiv SiOH$ groups at 25°C there

was a reaction at this temperature with the siloxane groups created by degassing silica at temperatures greater than 400°C. This reaction was particularly noticeable for silica degassed at 1000°C. When approximately 0.1-5.0 torr of diborane was added to this sample at 25°C a band at 2280cm$^{-1}$ assigned to ≡SiH grew in unison with the bands due to ≡SiOBH$_2$ and the disappearance of the bands due to the reactive siloxane[30-32] at 908 and 888cm$^{-1}$. Only very weak bands due to ≡SiOB$_2$H$_5$ appeared because there was almost no excess diborane present. Diborane thus has a third mode of dissociative chemisorption which is shown in reaction (9) as proposed by Mashtchenko. Additional evidence for the assignment of the band at 2280cm$^{-1}$ to ≡SiH is given by the results obtained here when using $^{10}B_2D_6$ when this band now shifts to 1662cm$^{-1}$ which, is the expected frequency for SiH/D[161, 162].

Conclusions

At pressures of 10-20 torr diborane did not react at 25°C with the hydroxyl groups on silica. It did, however, react at this temperature with the siloxane bridges produced as a result of the high temperature dehydroxylation of silica, to give ≡SiOBH$_2$ (≡SiOB$_2$H$_5$ in the presence of excess gaseous diborane) and ≡SiH. At 100°C diborane reacted rapidly with hydrogen bonded and isolated hydroxyl groups to produce (≡SiO)$_2$BH and ≡SiOB$_2$H$_5$ as shown in reactions (2) and (10), respectively. The species ≡SiOB$_2$H$_5$ was predominant in the presence of gaseous diborane at 25°C but in the absence of diborane ≡SiOBH$_2$ was the favoured species. The assignment of the above species, based on the extensive infrared data obtained, is virtually complete. The assignment of the species ≡SiOBH$_2$ was complicated by the presence of infrared combination bands but the weight of evidence presented strongly supports the present assignments.

## Part II The Chemisorption of borane carbonyl and some reactions of diborane treated silica

In the early stages of the present investigation into the nature of chemisorbed diborane on silica the reactions of some amines, alcohols and alkenes with the borane treated silica were studied. The results of these studies presented here remain difficult to interpret because the above reactions were carried out when what are now known to be $\equiv SiOBH_2$ and $\equiv SiOB_2H_5$ were present simultaneously and in varying relative concentrations. The reaction of borane carbonyl with silica was also studied to determine if this reactant would give the same adsorbed species as did diborane, and hence a clue to the identity of this species, but the results were disappointing. Nevertheless results of the study of these reactions are briefly presented here for the sake of completeness.

### A. The Reaction of Silica With Borane Carbonyl

Borane carbonyl ($H_3B{:}CO$) prepared as previously described always contained traces of diborane due to thermal decomposition. While distillation was used in attempts to remove most of the diborane impurity, analysis of the gas remaining after exposure of silica to $H_3B{:}CO$ always showed significant amounts of $B_2H_6$ in the infrared spectrum of the gas phase. The fact, therefore, that exposure of a silica degassed at 1000°C to 10 torr of $H_3B{:}CO$ at 25°C produced $\equiv SiOBH_2$, $\equiv SiH$ and traces of $\equiv SiOB_2H_5$ (i.e., the spectrum was identical to that produced with diborane itself) could not be assumed to have arisen from a reaction solely of $H_3B{:}CO$ with $\equiv SiOH$. In spite of this the results did provide some reinforcement for the intuitive belief that $\equiv SiOBH_2$ was being produced in the reaction of $\equiv SiOH$ and diborane.

B. Reactions with Amines

i) Ammonia

The addition of 10 torr of ammonia ($NH_3$) to diborane treated silica resulted in the immediate disappearance of the bands due to $\equiv SiOBH_2$ and $\equiv SiOB_2H_5$ which were replaced by new bands at 2400, 2800, 3400, 3500 and a broad band at 3100cm$^{-1}$ (Figure 5-9a). Evacuation of the cell caused these bands to gradually decrease, and new bands at 3560, 3460, 2585, 2565, 2540 and 2490cm$^{-1}$ grew in unison. A band at 1610cm$^{-1}$ (not shown) present upon the addition of $NH_3$ did not change with evacuation. If the reaction was carried out using deuterated ammonia ($ND_3$) the new bands on addition of $ND_3$ appeared at 2760, 2575, 2530, 2400 and 2300cm$^{-1}$ and those upon evacuation were at 2560, 2480 and 2460cm$^{-1}$ with those at 2760, 2575 and 2530cm$^{-1}$ remaining unchanged.

ii) Pyridine

The addition of 4 torr of pyridine to the silica sample treated with diborane removed the IR bands due to $\equiv SiOBH_2$ and $\equiv SiOB_2H_6$ and caused the appearance of an intense broad band centered at 3000cm$^{-1}$ and two weaker bands at 2390 and 2290cm$^{-1}$. Evacuation of the cell at 25°C reduced the intense band at 3000cm$^{-1}$ to a weak peak while the bands at 2390 and 2290cm$^{-1}$ remained unchanged. Further evacuation at 150°C lead to a dramatic decrease in these three bands and the partial restoration of the original spectrum due to $\equiv SiOBH_2$.

iii) Trimethylamine

The exposure of borane treated silica to trimethylamine followed by evacuation at 25°C generated several sharp bands in the 3000-2800cm$^{-1}$ region attributable to adsorbed trimethylamine and two moderately strong bands at 2380 and 2300cm$^{-1}$ while the original BH bands disappeared.

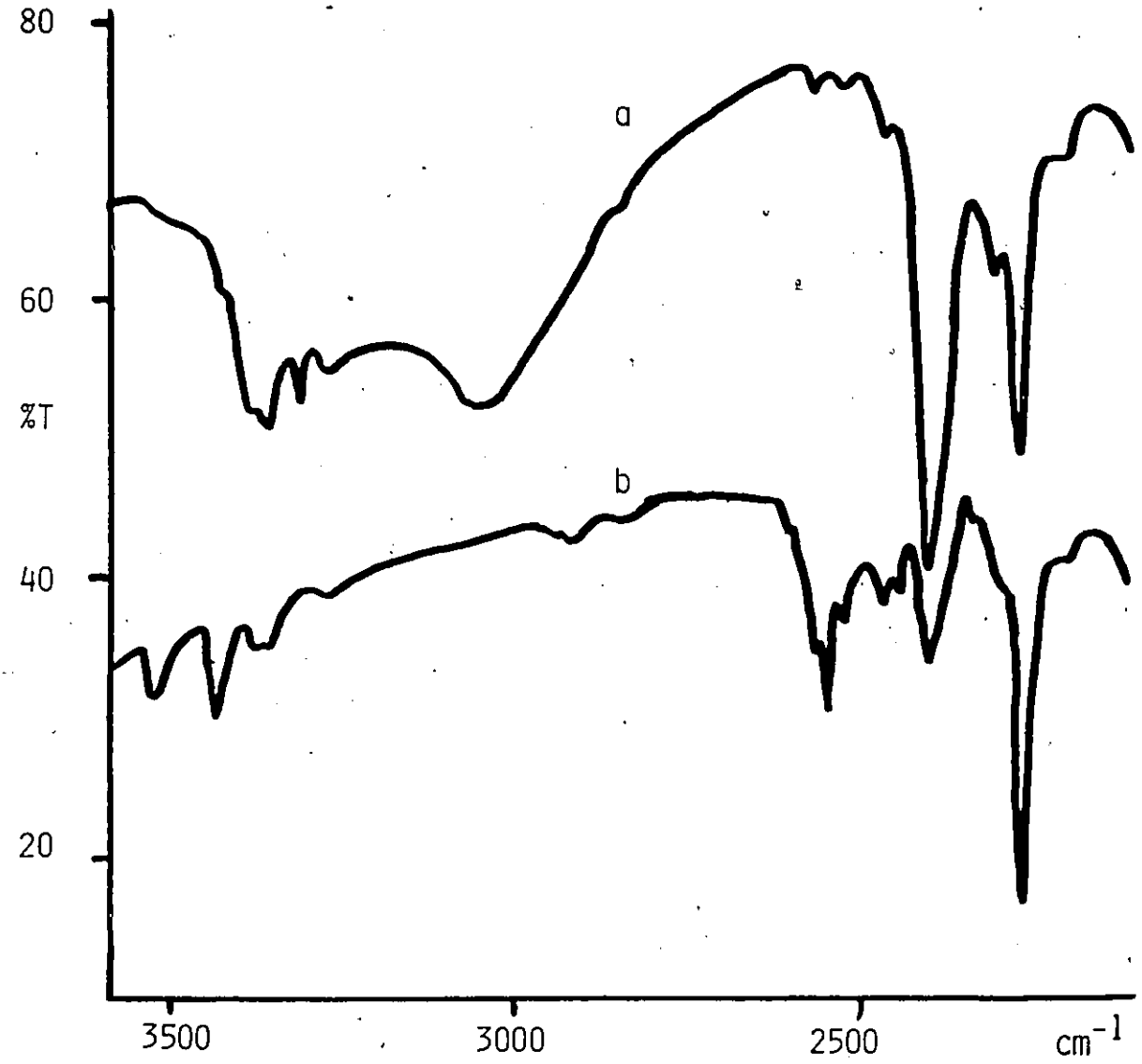


Figure 5-9
Infrared spectra of diborane treated silica
a) After the addition of 10 torr of $NH_3$
b) After evacuation of a) for 1 hr.
The vertical scale refers to a) and b) had been displaced by 40% T.

Discussion

Ammonia and its substituted amines are known to react with the borane-tetrahydrofuran ($H_3B$:THF) adduct to form amine-boranes[163, 164]

$$THF : BH_3 + AN: \longrightarrow AN: BH_3 + THF$$

AN: - an amine

while the adducts formed with substituted amine are stable that with ammonia undergoes slow thermal conversions at 25°C:

$$2\ H_3N : BH_3 \longrightarrow [\ BH_2(NH_3)_2]^+\ BH_4^-$$

$$H_3N : BH_3 \longrightarrow H_2N = BH_2 + H_2$$

The analysis of the infrared spectrum of the borane treated silica after reaction with ammonia is difficult because the expected adduct, $\equiv Si\text{-}OBH_2{:}NH_3$, and the products of its thermal decomposition (which may be accelerated in the heat of the infrared beam of the 283 spectrometer) would all be expected to have similar NH and BH stretching frequencies. Any speculation about the nature of the species produced here would be fruitless given the limited data available and the unknown extent of any possible decomposition of the species initially formed.

The adducts of $BH_3$ with pyridine and trimethyl amine are known to have antisymmetric and symmetric BH stretches around 2330 and 2280cm$^{-1}$ and the observation of two moderately strong bands in this region after the adsorption of these amines on borane treated silica indicates that the corresponding adducts were being formed with $\equiv SiOBH_2$. The formation of adducts in the present case indicates that the boron atom, as would be expected, still retained strong Lewis acidity with respect to the basic amines.

C. Reactions With Methanol and Cyclopentanol

The spectrum obtained after reaction of diborane treated silica with

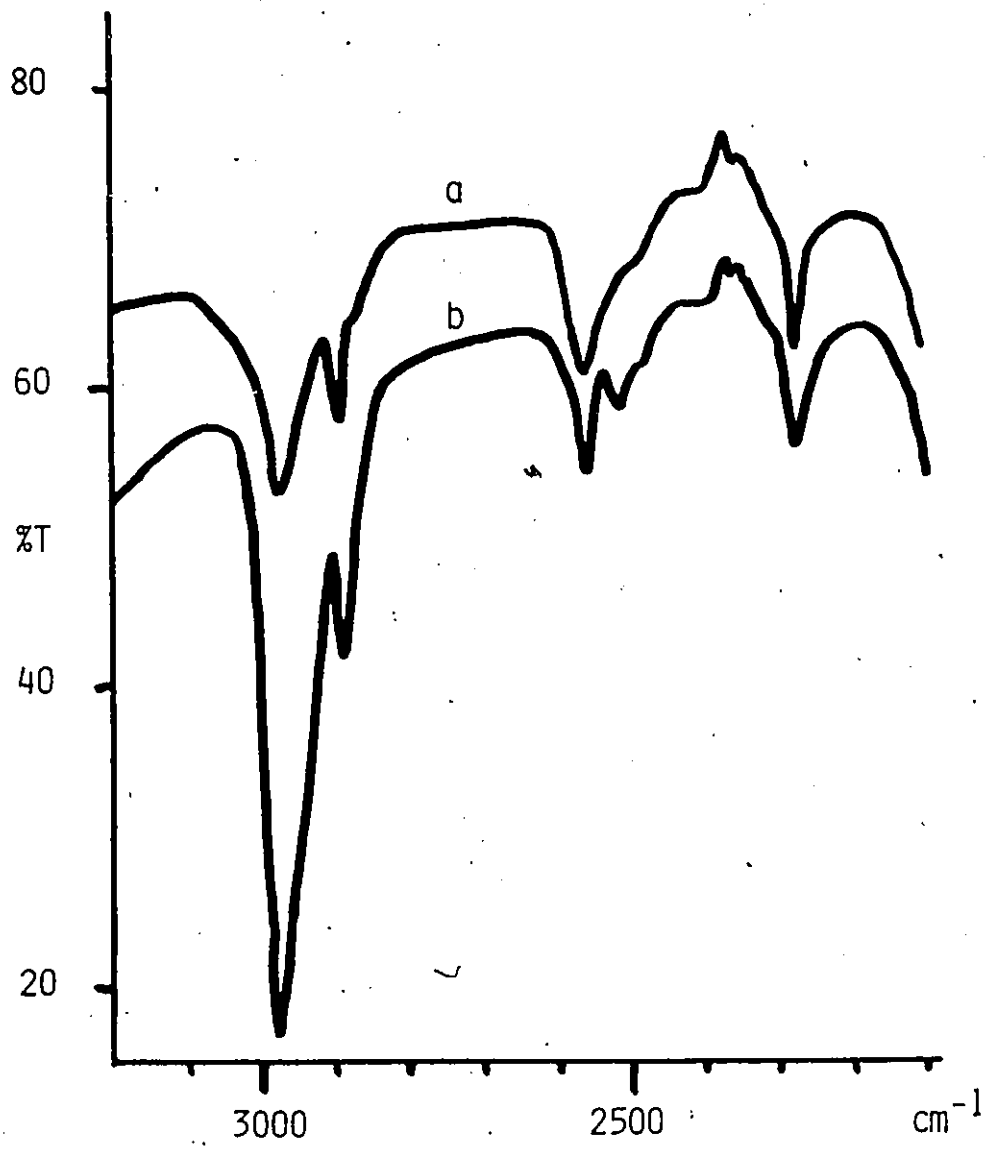


Figure 5-10
Infrared spectra of diborane treated silica after reaction with and evacuation of:
a) Methanol
b) Cyclopentanol
The % T scale refers to a) and b) has been displaced by 10% T.

either methanol ($CH_3OH$) or cyclopentanol ($C_5H_9OH$) were similar. After the addition of 3 torr of methanol followed by evacuation new bands were observed at 2980, 2890 and 2560cm$^{-1}$ with shoulders at 2870 and 2500cm$^{-1}$ while in the case of cyclopentanol the bands were at 2970, 2880, 2555 and 2510cm$^{-1}$ (Figure 5-10). If it was assumed that the reaction of these alcohols was one in which BH bonds were being replaced by $B\text{-}OCH_3$ or $B\text{-}OC_5H_9$ and that the single band at 2560cm$^{-1}$ was that of the remaining =BH species, this would indicate that there was not much difference in steric hindrance involved in the reaction with a small methanol molecule versus a large cyclopentanol molecule. This argument strongly favours $\equiv SiOBH_2$ since, if only one molecule of the alcohol reacts, the steric hindrance by replacing one hydrogen with $-OC_5H_9$ or $-OC_3$ would be about the same whereas replacing two or more hydrogens with these groups would create much greater steric hindrance in the case of $-OC_5H_9$ so such a reaction might not occur and the spectra would be different.

D. Reaction with Alkenes

The reaction of borane treated silica with 2-methly-2-butene (I), 1,3-butadiene (II) or ethylene (III) resulted in the disappearance of all bands in the BH stretching region and there were no bands at 1600cm$^{-1}$ or above 3000cm$^{-1}$ which are indicative of the presence of adsorbed alkenes.

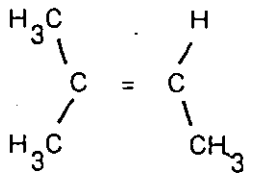

I

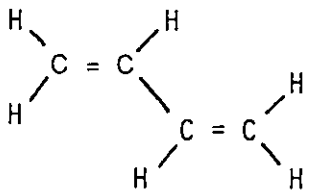

II

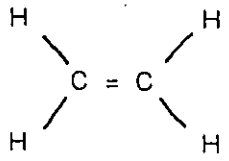

III

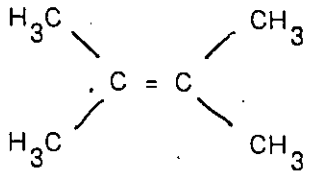

IV

The only infrared bands observed are those due to saturated hydrocarbons. By contrast, the reaction of 2,3-dimethyl-2-butene (IV) leaves a strong band at $2440cm^{-1}$ in addition to those due to saturated hydrocarbons.

It is well known that in tetrahydrofuran, I, II and III react to completion with $BH_3$ while IV reacts to only partial completion due to steric hindrance, i.e.,

$$R_2C = CR_2 + BH_3 \longrightarrow B(-CR_2 - CHR_2)_3$$

I, II, III $R = -H$, or $-CH_3$

$$(CH_3)_2C = C(CH_3)_2 + BH_3 \longrightarrow H_2B - \underset{\displaystyle CH(CH_3)_2}{\overset{\displaystyle |}{C}} - (CH_3)_2$$

IV

Similar reactions might be expected for diborane treated silica with species containing BH bonds and the presence of a single infrared band due to a BH species after reaction with IV is a strong indication that a borane species with only two attached hydrogens, i.e., $\equiv SiOBH_2$ was initially present. If three hydrogen were initially present then IV would have reacted to give $-BH_2R$ and two infrared active B-H stretches should have been observed. Finally, the absence of infrared bands due to unsaturated hydrocarbons after reaction of the borane treated silica with II might be rationalized as follows:

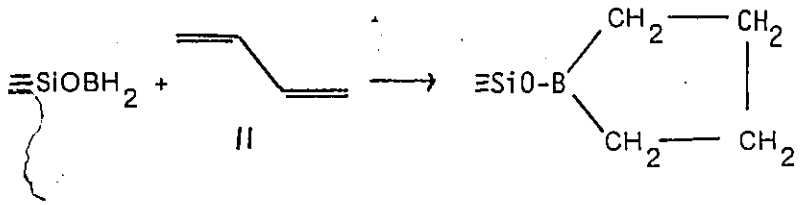

Such ring forming reactions as this are known to occur with dialkenes and $BH_3$[165, 166].

# CHAPTER 6

# THE ADSORPTION OF DIBORANE ON $\gamma$-ALUMINA

## Introduction

Only three infrared spectroscopic studies of the adsorption of diborane on alumina, done between 1974 and 1977, appear in the literature [151, 167, 168]. Similar spectra were observed in each case but definitive assignments for the postulated surface species were not made. In the previous Chapter, new insight was given into the nature of diborane adsorbed on silica and with this knowledge it was felt that a new study relating to diborane and alumina was warranted.

The first infrared study of diborane adsorbed on alumina was reported by Mashchenko[151], who observed that, for an alumina degassed at 600°C, upon addition of diborane the hydroxyl bands at 3700, 3742 and 3800 $cm^{-1}$ decreased and new infrared peaks appeared at 2570, 2495, 2200, 1460, 1365, 1325, 1250, 1200 and 1155 $cm^{-1}$. Mashchenko assigned the peaks at 2570, 2495, 2200, 1460 and 1155 to $AlBH_4$ formed according to the following reaction:

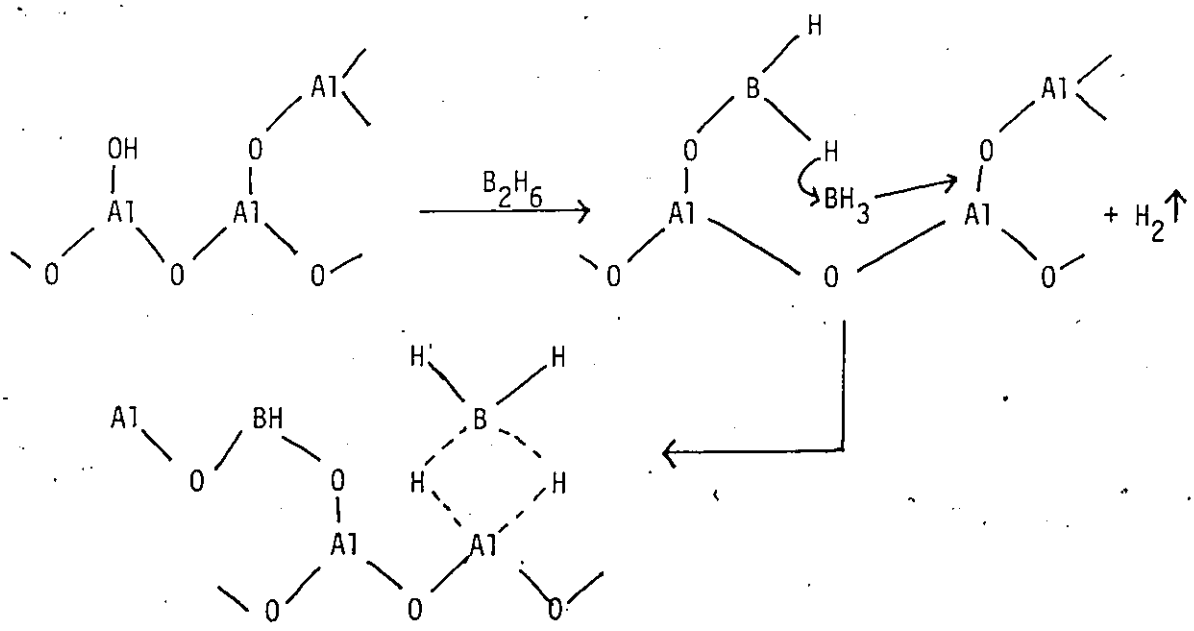

The other bands at 1365, 1325, 1250 and 1200 $cm^{-1}$ were assigned to "vibrations of B-O bonds with various force constants and possibly, with various types of symmetry". No assignment was made in the 2600-2400 $cm^{-1}$ spectral region for the BH stretch of the $(\equiv AlO)_2BH$ species and the disappearance of the hydroxyl bands was not discussed in terms of the reactions proposed.

The other studies by Matsuda et al.[167, 168] reported that diborane adsorbed on a 450°C degassed alumina produced new infrared bands at 2580, 2485, 2170, 1470, 1370, 1330, 1260, 1190 and 1150 $cm^{-1}$. Matsuda associated the bands from 2580 -1470$cm^{-1}$ with B-H bonds and those from 1370 - 1150 $cm^{-1}$ with B-O bonds. By comparison with the infrared spectrum of aluminum borohydride Matsuda et al. assigned the bands at 2170 and 1470 $cm^{-1}$ to $\equiv AlBH_4$ but did not discuss how such a species would be formed. The bands at 2580, 2485, 1370 and 1150 $cm^{-1}$ were attributed to the species $-OBH_2$ produced in reaction (2).

(2) $B_2H_6 + 2\ O\text{-}H \longrightarrow 2\ O\text{-}B(H)(H) + 2H_2\uparrow$

No assignments were made for the bands at 1330, 1260 and 1190 $cm^{-1}$ and no consideration was given to the changes in the hydroxyl region of the spectrum from 3800 - 3500 $cm^{-1}$.

Although both Matsuda and Maschenko agreed that a $AlBH_4$ species was produced upon adsorption of diborane on alumina they differed in the assignment of a second species to $-OBH_2$ or $(\equiv Al\ O)_2BH$ respectively. Neither author tried to interpret the observed infrared spectrum in the 3800-3500$cm^{-1}$ and 1400-1100$cm^{-1}$ regions. Therefore, a more thorough investigation into the nature of adsorbed diborane was carried out using infrared and Raman spectroscopies. In

addition, boron -10 diborane was used in an attempt to obtain better resolved infrared spectra.

The adsorption of diborane on titanium dioxide ($TiO_2$, anatase) was cursorily investigated. High surface area anatase has only two types of hydroxyl groups, one which is acidic and the other which is basic in character. Anatase is also reported to have two types of Lewis acid sites. One type is a weak Lewis site and involves a Ti-O-Ti species while the other a strong site involving incompletely co-ordinated surface $Ti^{4+}$. Both types of Lewis sites are reported to be formed by dehydroxylation of anatase above 150°C. An excellent review of the surface properties of titanium oxides has been published by Parfitt[169]. Anatase presents a less complicated surface than does alumina but has similar surface sites, i.e., basic and acidic hydroxyl groups and strong and weak Lewis acid sites. It seemed reasonable that an investigation of the adsorption of diborane on anatase might have given valuable insights of the corresponding reaction with alumina. This however was not the case. Nevertheless, these results using anatase along with those obtained with alumina are presented in Part I of this Chapter.

Weiss and Shapiro[170] and others[171] have reported that diborane treated silica-aluminas catalyzed the polymerization of acetylene to benzene. Weiss also observed that during the polymerization the silica-alumina which was initially white changed to a violet colour. The species producing this violet colour has not been identified up to the present time. An investigation was undertaken to determine the source of this violet colour generated by the reaction of acetylene over a borated silica-alumina and also to determine if a similar colour change could be observed with a diborane treated alumina or offretite. The results of these investigations are present in Part II of this Chapter.

Experimental

The Degussa alumina was calcined in air at 550°C before degassing except where the sample was degassed at 150°C, in which case an uncalcined sample was used. Degussa anatase was calcined at 500°C in air before degassing at 150°C. The anatase was then heated in 300 torr of oxygen at 400°C to remove any further organic impurities, cooled to 25°C in oxygen and then evacuated at 25°C for 15 minutes.

For infrared experiments 100 mg of the sample was pressed at $10^7$ Pa pressure into a 2.5 cm disc whereas for Raman experiments 150 mg was used and pressed at the same pressure into a 1 cm disc. Infrared spectra were recorded on both the Perkin-Elmer 283 and the Bomem DA3-02 FTIR spectrometers. The Raman spectra were recorded using the 4880Å (blue line) of the argon ion laser to avoid possible fluorescence problems of blue chromophores adsorbed on samples in several experiments involving the reaction of acetylene with diborane treated oxides.

In Part II references are made to diborane treated oxides and their preparations are listed below.

i) Alumina: Borated alumina was prepared by degassing alumina at 450°C and reacting this sample with diborane at 100°C for 1 hr followed by evacuation at 100°C for 30 minutes.

ii) Silica: Diborane treated silica was prepared in the same manner as for alumina except the sample was initially degassed at 500°C.

iii) Silica - alumina: Davisson silica-alumina (13% $Al_2O_3$) was degassed at 300°C for 1 hr and then exposed to diborane at 25°C for 15 min. Evacuation at 25°C for 1 hr produced borane treated silica-alumina.

iv) Offretite: The $H^+$ exchanged form of this zeolite having a silica to

alumina ratio of 80:1 was degassed at 500°C. Similar treatment with diborane as in (iii) produced the required borated offretite.

Results and Discussion:

Part I

i) The Adsorption of diborane on alumina

Figure 6-1a shows the infrared spectrum of alumina which had been degassed at 450°C while Figures 6-1b and 6-1c show the spectrum after exposure to the sample and evacuation of diborane at 25°C and 100°C, respectively. Figure 6-2a and 6-2b show the spectral subtractions for Figures 6-1b - 6-1a and 6-1c - 6-1a, respectively. The corresponding spectra for alumina degassed at 150°C and 920°C are shown in Figures 6-3 to 6-6. The infrared bands observed in all the above spectra are quite broad and considerable overlapping of the bands is apparent. It will be shown that this was not simply due to the overlap of boron -10 and boron -11 bands as a result of employing $^{n}B_2H_6$ but in fact to the presence of several species with similar infrared band frequencies.

The changes observed in the O-H stretch region of the infrared spectrum of alumina degassed at 450°C and 150°C and then reacted with diborane at 25°C are shown in Figures 6-1 to 6-4. For the alumina degassed at 450°C, Figure 6-2a shows that the hydroxyl groups with bands at 3790, 3773 and 3735cm$^{-1}$ corresponding to hydroxyls of types Ib, Ia and IIb had reacted. These are the most basic hydroxyls on alumina (order of increasing basicity : III < IIa < IIb < Ia < Ib) and basic hydroxyl groups are the ones expected to react with the Lewis acid, diborane. Figure 6-4a shows that hydroxyls with infrared bands at 3738 and 3687cm$^{-1}$ with a weak shoulder at 3777cm$^{-1}$ had reacted on alumina degassed at 150°C and treated with diborane. As was mentioned in Chapter 1, hydroxyl pairs of

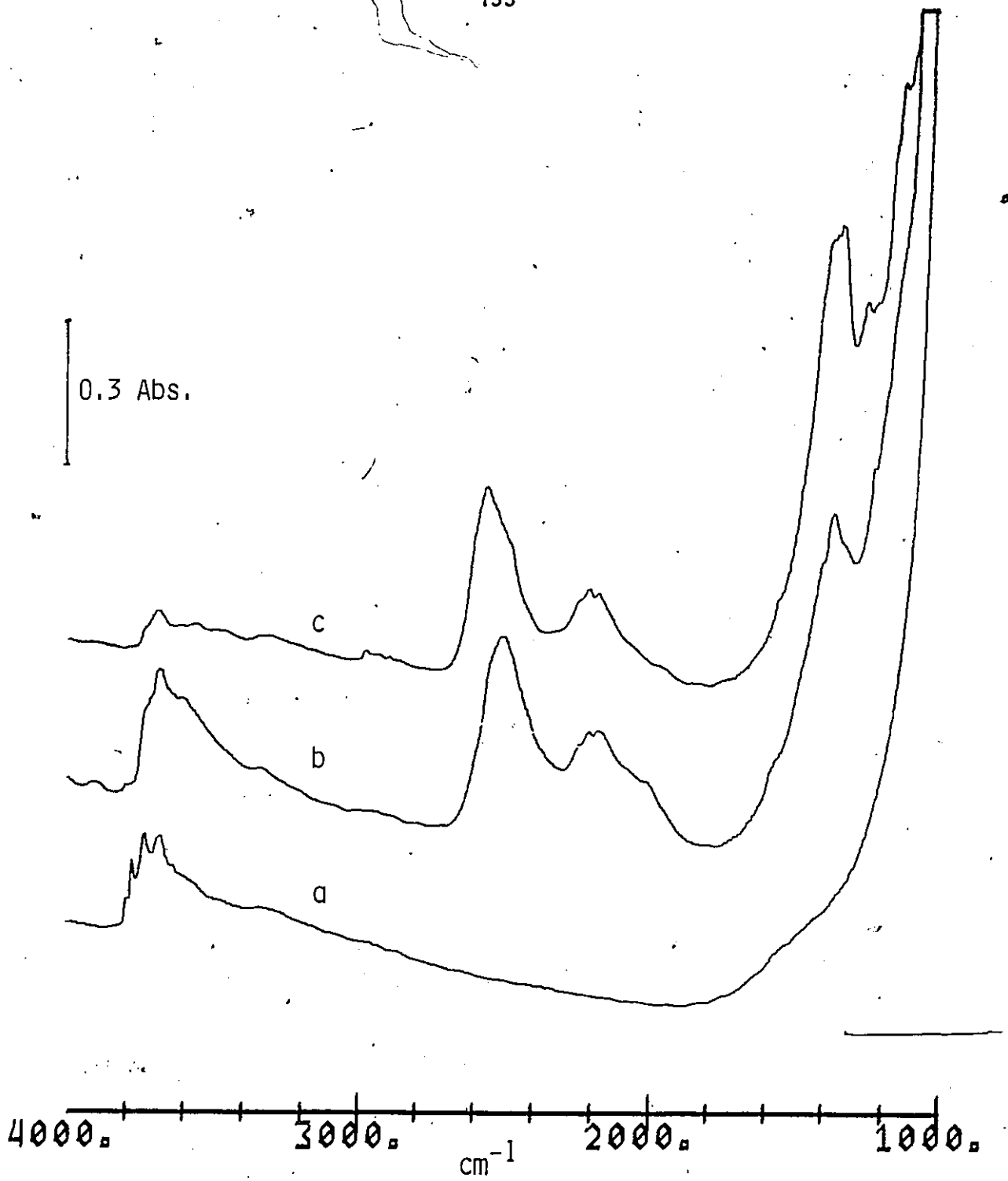


Figure 6-1
a) Infrared spectrum of an alumina degassed at 450°C for 1 hr.
b) After reaction of a) with 10 torr of $^{n}B_2H_6$ for 1 min. at 25°C and evacuation for 15 min.
c) After reaction of b) with $^{n}B_2H_6$ at 100°C for 1 hr. and evacuation at 100°C for 30 min.

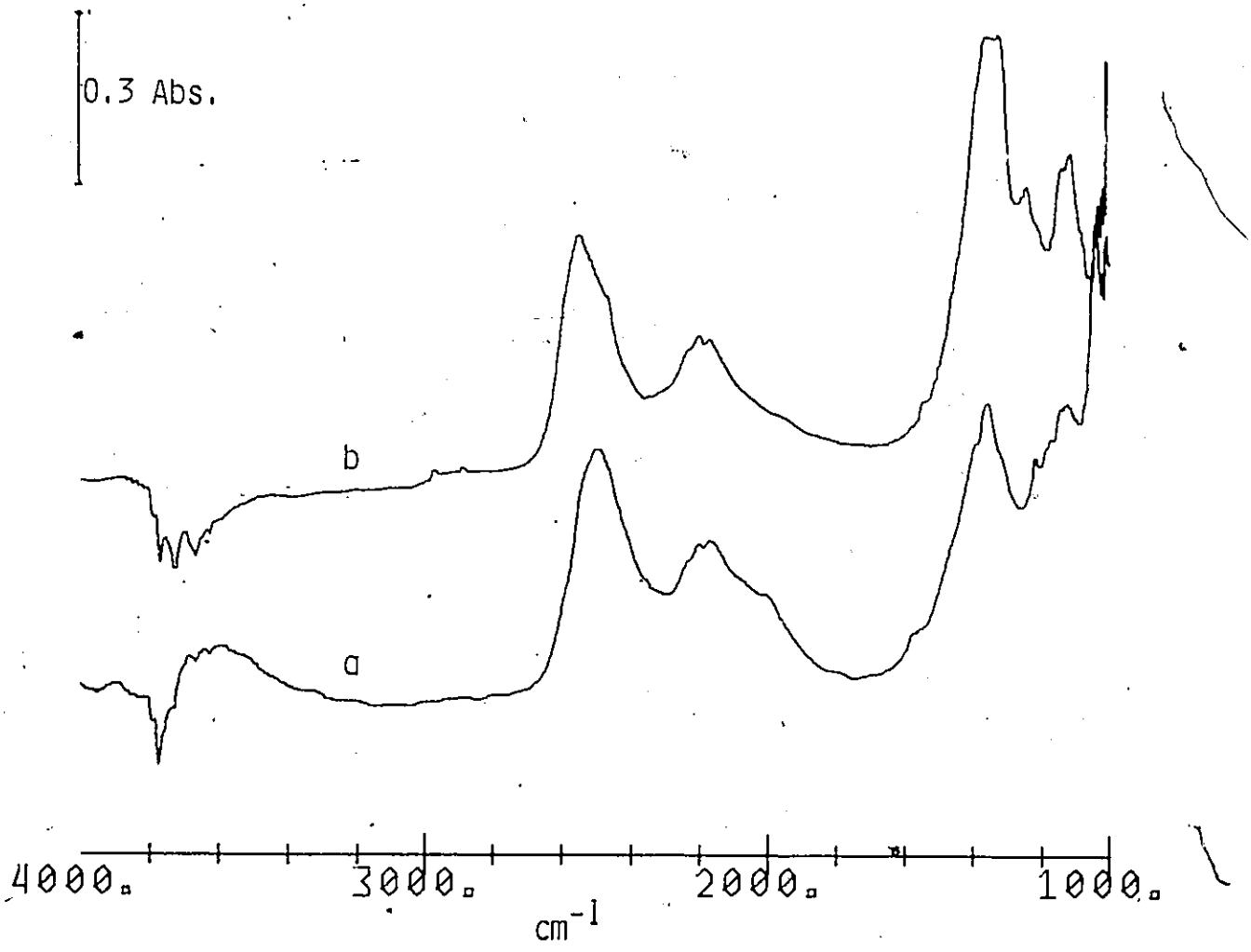


Figure 6-2
Difference spectra for $^{n}B_2H_6$ reacted with an alumina which had been degassed at 450°C
a) Figure 6-1b minus Figure 6-1a
b) Figure 6-1c minus Figure 6-1a.

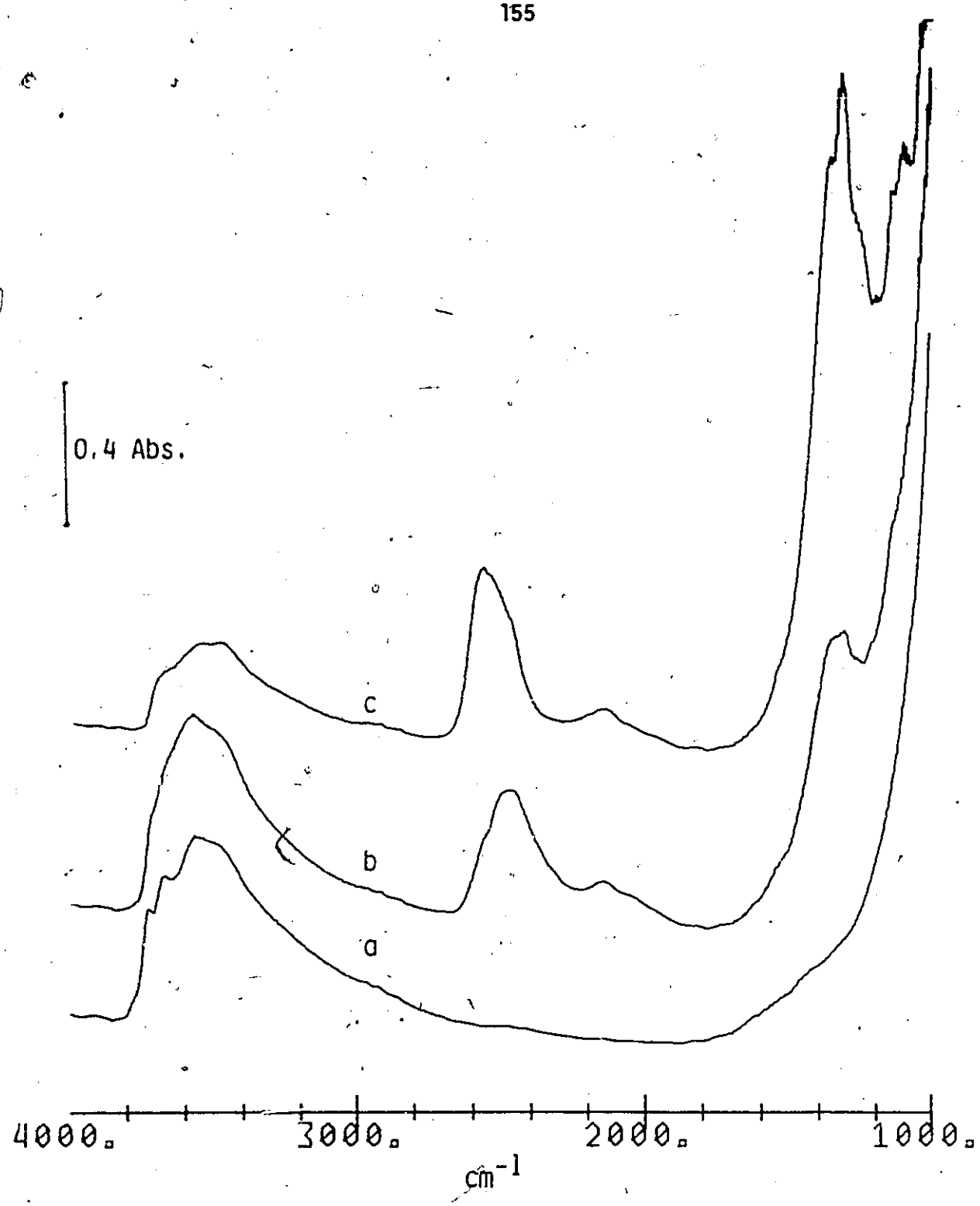


Figure 6-3
a) Infrared spectrum of alumina degassed at 150°C for 1 hr.
b) After reaction of a) with $^{n}B_2H_6$ at 25°C for 1 min. followed by evacuation for 15 min.
c) After reaction of b) with $^{n}B_2H_6$ at 100°C for 30 min.

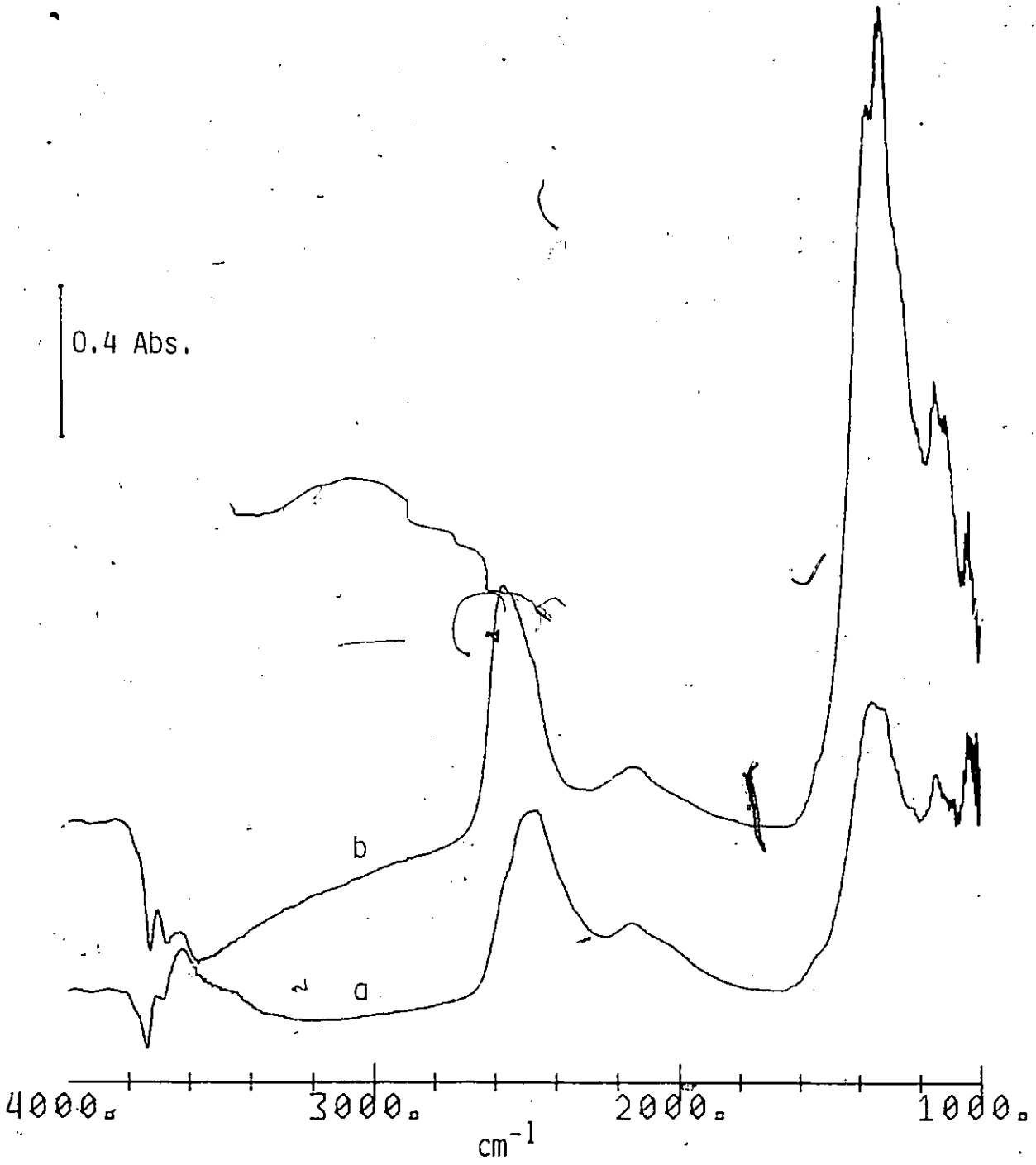


Figure 6-4
Difference spectra for a 150°C degassed
a) Figure 6-3b minus Figure 6-3a
b) Figure 6-3c minus Figure 6-3a.

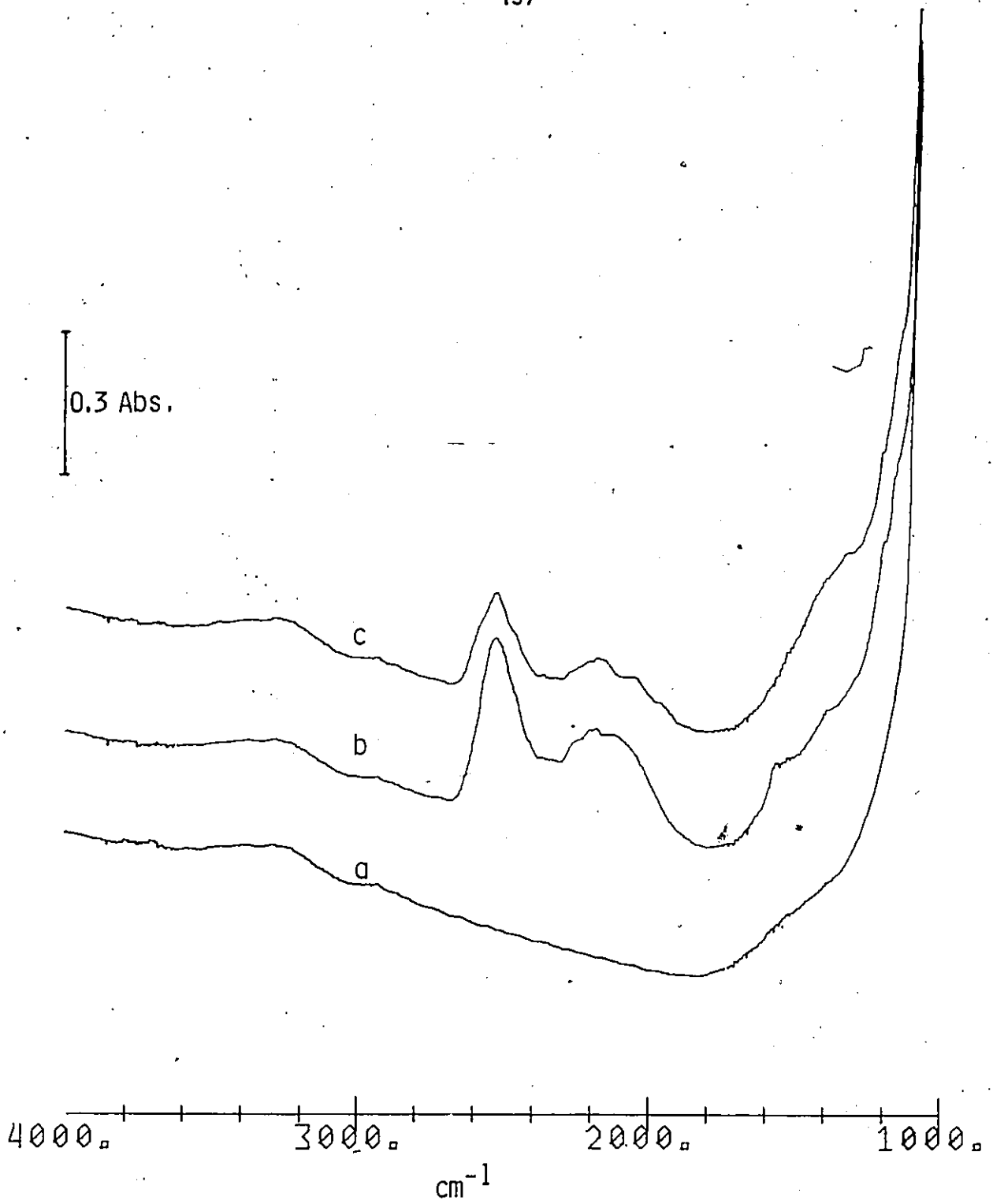


Figure 6-5
a) Infrared spectrum of an alumina degassed at 920 C for 1 hr.
b) After reaction of a) with $^{n}B_2H_6$ at 25 C for 1 min. and evacuation for 5 min.
c) After evacuation of b) for 1 hr. at 100 C.

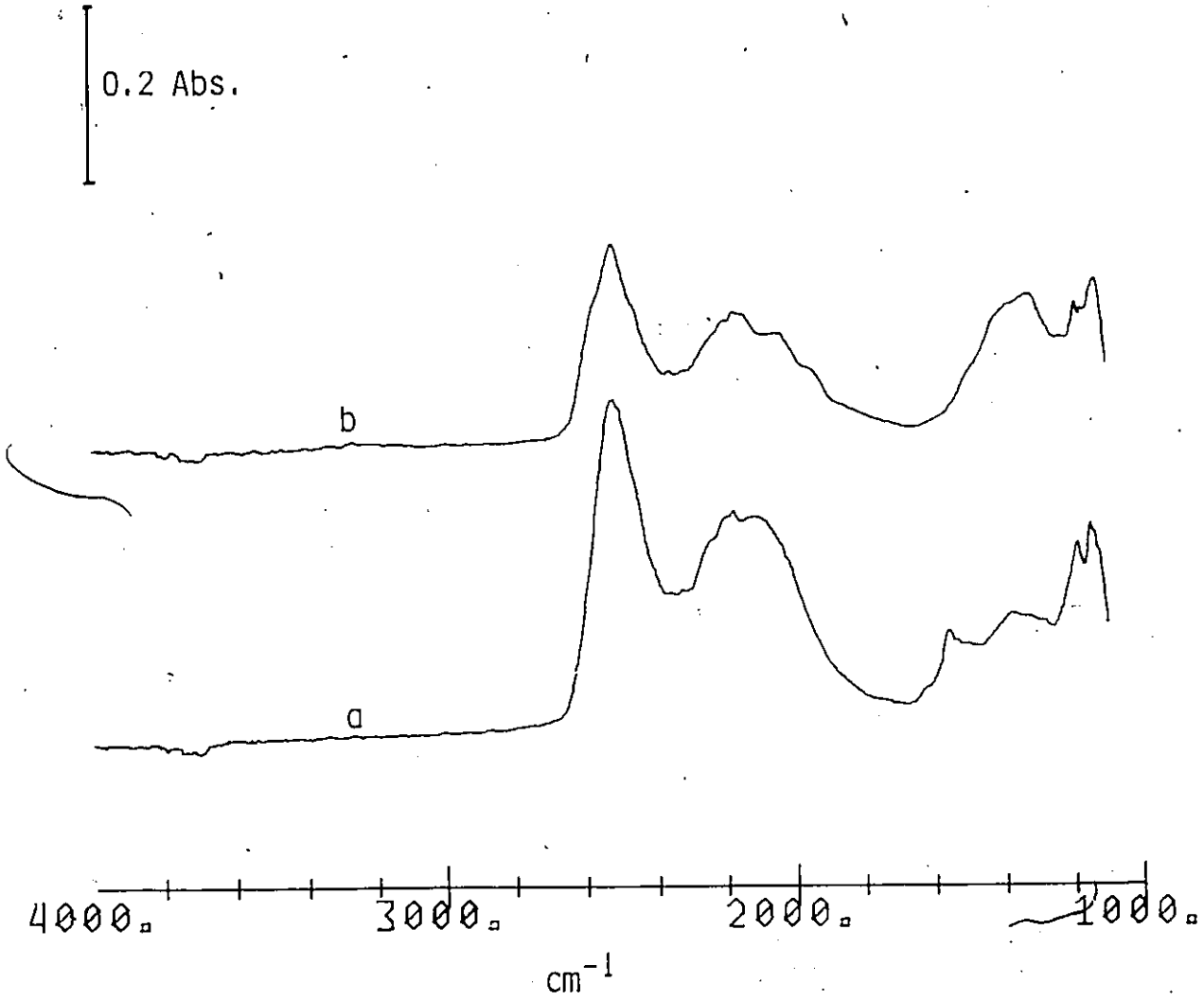


Figure 6-6
Difference spectra for a 920 C degassed alumina which had been reacted with $^{n}B_2H_6$.
a) Figure 6-5b minus Figure 6-5a.
b) Figure 6-5c minus Figure 6-5a.

the types Ia - IIa and IIb - III are present on a highly hydroxylated alumina. The IR bands at 3777, 3738 and 3687cm$^{-1}$ are assignable to perturbed types Ia, IIb and III hydroxyls, respectively. The band which appears at 3625cm$^{-1}$ in Figure 6-4a might be hydroxyl groups of types IIa and IIb which are most abundant on highly hydroxylated alumina and which are further perturbed by the borane species formed on alumina. Finally, after reaction with diborane at 100°C, all the accessible hydroxyl groups (acid and basic ones) on the two alumina samples have reacted.

The changes in the hydroxyl stretching region of the spectrum indicate that diborane reacts at 25°C with the more basic hydroxyl groups on alumina degassed at 450°C. For alumina degassed at 150°C, neighbouring hydroxyl pairs of the types Ia - IIa and IIb - III may be reacting since Infrared bands due to strongly perturbed hydroxyls disappeared after reaction with diborane. An identification of the adsorbed B-H species is needed to determine whether the neighbouring hydroxyls reacted as pairs or single hydroxyl groups with a molecule of diborane.

The spectrum observed after the adsorption of diborane at 25°C on alumina degassed at 450°C is similar to that of Mashchenko[151] and of Matsuda et al.[167, 168] in the 2600-1600 cm$^{-1}$ region but was different in some respects in the 1500-1100 cm$^{-1}$ region. The infrared spectrum of the alumina used by Mashchenko and Matsuda showed several peaks in the 1400-1200 cm$^{-1}$ region before reaction with diborane and these peaks are probably due to a bicarbonate species on the alumina surface. Neither of these authors report calcining the aluminas before degassing and the adsorption of atmospheric carbon dioxide to form carbonates and bicarbonates on alumina is a well known phenomenon. Both authors used aluminas with much higher surface areas than that used here and this might

account for some of the differences between their work and that presented here.

The infrared spectrum of diborane adsorbed on alumina did not change with the presence or absence of excess diborane. The spectrum did change slightly, however, if the borane treated sample was degassed at 100°C but this was due to the removal of a small amount of the adsorbed species. Although this observation is very different from that in the case of silica, it does not automatically imply that $\equiv AlOBH_2$ species do not exist on alumina. The electron deficiency on the boron atom might be satisfied by the greater electron density on the oxygen atom in $\equiv Al-O$ compared to that in $\equiv SiO$ so that $\equiv AlOB_2H_5$ with BHB bridges would not be very stable.

The bands in the infrared spectrum of adsorbed diborane on alumina are just as broad and overlapped whether the reaction was with $^{n}B_2H_6$ or $^{10}B_2H_6$ at 25°C or 100°C. Table 6-1 lists the frequencies of the broad bands and weak shoulders observed for the reactions of diborane at 25°C and 100°C. Assignments of these bands to possible surface species is extremely difficult given the quality of the spectra obtained. Nevertheless, tentative assignments which have some consistency in all the observed spectra can be attempted.

The broad band around 2200cm$^{-1}$, produced by the reaction of diborane with alumina at 25°C, was significantly different for alumina degassed at 150, 450 or 920°C. This band changed little upon further reaction at 100°C with diborane or evacuation at 100°C for 1 hour. This band may be assigned to AlHB bridge stretches in $\equiv AlBH_4$(I) formed by the dissociative chemisorption of diborane on a pair of Lewis acid and base sites.

Table 6-1

Frequencies of infrared bands observed after the reaction of diborane with alumina at 25 C (upper table) and at 100 C (lower table)

| $Al_2O_3$ degassed at 920 °C / $cm^{-1}$ | | $Al_2O_3$ degassed at 450°C / $cm^{-1}$ | | $Al_2O_3$ degassed at 150°C / $cm^{-1}$ |
|---|---|---|---|---|
| $^nB_2H_6$ | $^{10}B_2H_6$ | $^nB_2H_6$ | $^{10}B_2H_6$ | $^nB_2H_6$ |
| 2514 s | 2523 s | 2535 sh | 2588 sh | 2562 sh |
| 2460 sh | 2463 sh | 2492 s | 2517 s | 2473 s |
| 2228 sh | 2237 | | 2470 sh | 2154 |
| 2196 sh | | 2230 sh | 2244 sh | 1340 br |
| 2174 | 2178 | 2202 | 2214 | 1144 |
| 2116 br | 2127 | 2168 | 2178 | |
| 1554 | 1554 | 2022 sh | 2025 sh | |
| 1350 br | 1350 br | 1560 | 1560 | |
| 1187 | 1193 | 1387 sh | 1427 sh | |
| 1146 | 1146 | 1355 s | 1390 s | |
| 1135 sh | | 1216 w | 1352 sh | |
| | | 1138 s | 1154 | |
| 2561 sh | | 2551 s | 2559 s | 2571 s |
| 2510 s | | 2466 sh | 2480 sh | 2472 sh |
| 2460 sh | | 2230 sh | 2244 sh | 2151 |
| 2196 sh | | 2202 | 2214 | 1362 |
| 2170 | | 2171 | 2178 | 1316 s |
| 2144 sh | | 1560 | 1560 | 1270 sh |
| 2054 | | 1360 br | 1406 s | 1144 |
| 1962 sh | | | 1346 s | |
| 1464 w | | 1244 | 1280 | |
| 1350 br | | 1140 s | 1142 s | |
| 1187 | | | | |
| 1131 br | | | | |

s- strong, w- weak, sh- shoulder, br- broad.

(3)

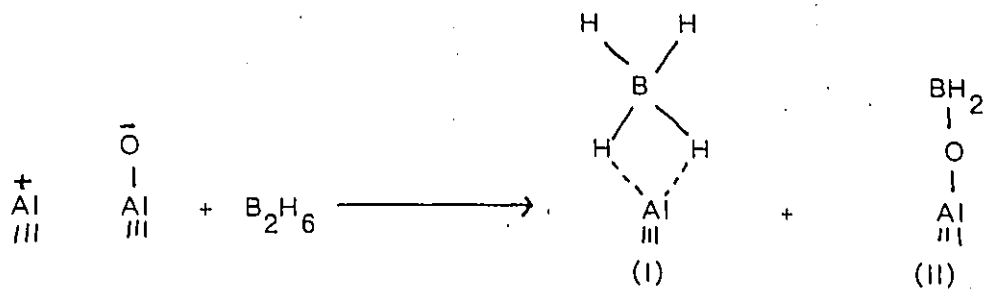


The difference in the intensity of the 2200cm$^{-1}$ band for alumina degassed at 450$^{o}$C compared to that degassed at 150$^{o}$C is a measure of the increasing number of Lewis sites being formed as a result of condensation of neighbouring hydroxyl groups. In the case of alumina degassed at 920$^{o}$C the 2200 cm$^{-1}$ band was much broader and this might be explained by the formation of stronger Lewis sites with a range of strengths which, as was mentioned earlier, only begin to form at temperatures above 400$^{o}$C.

The species $\equiv AlOBH_2$(II) formed in reaction (3) would be expected to have, like $\equiv SiOBH_2$, two bands due to B-H stretching in the 2600 - 2400 cm$^{-1}$ region. No distinct bands are observed for this species. Figure 6-6b does show in this region shoulders at 2561 and 2460 cm$^{-1}$ on either side of the band at 2510 cm$^{-1}$. The antisymmetric and symmetric stretches of $\equiv AlBH_4$, by analogy with those for $Al(BH_4)_3$[172], are expected near 2550 and 2490 cm$^{-1}$ and it is possible that the 2510 and 2460 cm$^{-1}$ bands are due to this species while the band at 2561 cm$^{-1}$ is antisymmetric stretch of $\equiv AlOBH_2$. The symmetric stretch of $\equiv AlOBH_2$ would be expected to occur near 2470 cm$^{-1}$ and it could be that this band was buried within the overlapping bands in this region. There is a broad band in Figure 6-6b from 1500 - 1300 cm$^{-1}$ and withjn this region several bands are expected for $\equiv AlBH_4$, namely, the AlHB bridges stretch near 1500 and the $BH_2$ rock near 1390 cm$^{-1}$. The

B-O stretch of $AlOBH_2$ is also expected in the 1300 - 1400 $cm^{-1}$ region. The band observed at 1187 $cm^{-1}$ might be another AlHB bridge vibration which is also expected in this region, while the band at 1131 $cm^{-1}$ is possibly an unusually high $BH_2$ deformation mode of $\equiv AlOBH_2$. Since no non-condensable gas (i.e., hydrogen) was detected at liquid nitrogen temperature this was further support for the proposed reaction (3) on alumina degassed at 920°C.

Alumina degassed at 150°C and reacted with diborane at 100°C has only a weak infrared band near 2200$cm^{-1}$ due to a $\equiv AlBH_4$ species but it has a strong peak for a B-H stretch which is at higher frequency than that observed with alumina degassed at either 450 or 920°C. In view of the previous discussion concerning the changes in the hydroxyl region for this sample, the band observed at 2571 $cm^{-1}$ is assigned the B-H stretch of $O_2BH$ (III).

(4)

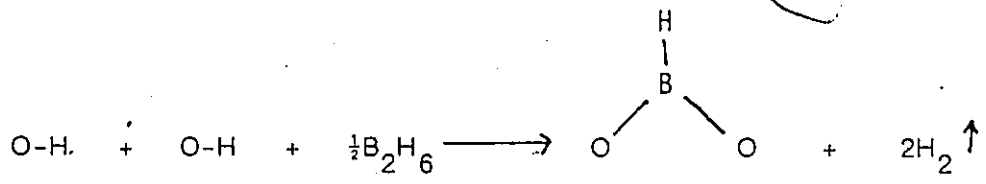


type III type IIb III

The same spectrum shows a band at 2472 $cm^{-1}$, which is the expected position of the symmetric BH stretch for $AlOBH_2$. The observation, therefore, of two bands in the B-O stretch region at 1362 and 1316 $cm^{-1}$ may be attributed to the asymmetric B-O stretch of $O_2BH$ and the B-O stretch of $\equiv AlOBH_2$ respectively. Again, a weak band at 1144 may be assigned, as before, to the $BH_2$ deformation mode of $AlOBH_2$.

The spectrum after reaction at 100°C of alumina, which had been degassed at 450°C, has some elements of the corresponding spectra for aluminas which had been degassed at 150 and 900°C. The only significant additional feature for the

450°C degassed sample was a band at 1244cm $^{-1}$. This band does not lie close to any known frequencies for $Al(BH_4)_3$, $B_2H_6$, $BH_3$ adducts or B-O species. It does appear to have a B10/B11 shift of about 36cm$^{-1}$, which is unusually large for any BH vibrational mode. No reasonable assignment can be suggested for this infrared band.

No additional information about the adsorption of diborane on alumina was found by using Raman spectroscopy. The Raman spectrum (not shown) showed identical broad bands in the 2600-1600cm$^{-1}$ region to those in the infrared spectrum and there were no bands observed between 1600 and 100cm$^{-1}$.

To conclude, the assignments of the surface species $AlBH_4$, $AlOBH_2$ and $O_2BH$ are only tentative because the observed infrared and Raman bands were very broad. This broadness is possibly due to a wide range in types of hydroxyl groups and Lewis sites on the alumina surface, which leads to surface species with similar structure but different force constants for vibrations and hence infrared frequencies.

ii) The adsorption of diborane on anatase

The reaction of diborane with $TiO_2$ (anatase) yielded very little useful information. Upon addition of 10 torr of diborane to $TiO_2$ degassed at 150°C, the sample which was initially white changed to an intense blue colour and was no longer transparent to infrared radiation above 1000cm$^{-1}$. A non-condensable gas, presumably hydrogen, was found to be produced in this reaction. If 10 torr of oxygen was added to the borane treated sample the blue colour immediately disappeared and the sample became infrared transparent again.

The original infrared spectrum of anatase showed two peaks at 3715 and 3665cm$^{-1}$. The hydroxyl groups with a band at 3715cm$^{-1}$ are relatively basic

while that at 3665 $cm^{-1}$ is acidic and they are similar to the hydroxyl groups of type Ia and IIa, respectively, on alumina. Degassing $TiO_2$ at 150°C is sufficient to remove hydrogen-bonded water but does not form strong Lewis sites[169]. After the addition of oxygen to the borane treated $TiO_2$ no new absorptions bands were observed in the hydroxyl stretching region however, there was a strong band at 2580 $cm^{-1}$ and an intense broad absorption from 1500 to 1000 $cm^{-1}$. No information was gained by using a thin film of $TiO_2$ because in these experiments, while the film did not become totally absorbing after turning blue, the spectrum was featureless and since the hydroxyl bands were too weak to be observed initially no information regarding their fate was obtained.

The Raman spectrum of $TiO_2$ was recorded before and after reaction with diborane and the only difference observed in the spectrum was a ten fold decrease in the peaks due to the lattice modes of $TiO_2$ after the addition of diborane. Upon the addition of oxygen, when the colour of the sample went from blue to white, the peaks due to the lattice modes of $TiO_2$ increased. No other peaks were observed at any stage in the reaction.

The changes in intensity of the TiO lattice modes with diborane might indicate a disruption of Ti-O-Ti bonds in anatase. Dicyclopentadienyl-titanium borohydride has an intense violet colour[173], and it is possible that such borohydride species are responsible for the blue colour in the present case. Further speculation is not warranted.

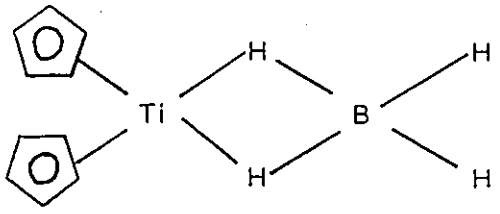


dicyclopentadienyltitanium borohydride

Part II

The Reaction of Acetylene with borated oxides:

The addition of acetylene ($C_2H_2$) to borane treated alumina, offretite or silica-alumina resulted in the initially white sample changing to a violet colour, but with a borane treated silica the addition of acetylene did not cause any colour change. Although the infrared spectra of the borane treated alumina, offretite and silica-alumina were different, the infrared and Raman spectra after reaction of these samples with acetylene were quite similar. It is convenient to examine the reaction of acetylene with the borated alumina first and then to discuss any differences observed using the other oxides.

Upon adding 5 torr of acetylene to the borated alumina the sample turned pink and weak infrared bands developed at 3073, 3044, 2968 and 2884 $cm^{-1}$ in addition to strong bands at 1604, 1426, 1310 and 1252 $cm^{-1}$ (Figure 6-7a and 6-8). Figure 6-8 also shows that the relatively strong infrared bands at 2560 and 2466 $cm^{-1}$ had diminished. After exposure to acetylene for 14 hrs the intensities of the bands in Figure 6-8 had increased and the sample now had a violet colour. At this point the intensities of infrared bands at 2200 and 2173$cm^{-1}$, which were unchanged upon initial exposure of the sample to acetylene, had begun to decrease. Evacuation at 25°C for 5 hrs caused no change in either the infrared spectrum or colour of the sample. Upon readding acetylene and heating the sample to 100°C for 2 hrs the sample had an intense violet colour and infrared bands notably at 3063, 2946, 2913, 2877, 1920, 1462 and 1421 $cm^{-1}$ were observed (Figure 6-9). In the B-H region of the IR spectrum bands at 2558, 2476, 2200 and 2172 $cm^{-1}$ had decreased with the appearance of this intense violet colour.

The Raman spectrum of the violet sample after heating with acetylene at 100°C (above), shown in Figure 6-10, exhibited two very strong peaks at 1115 and

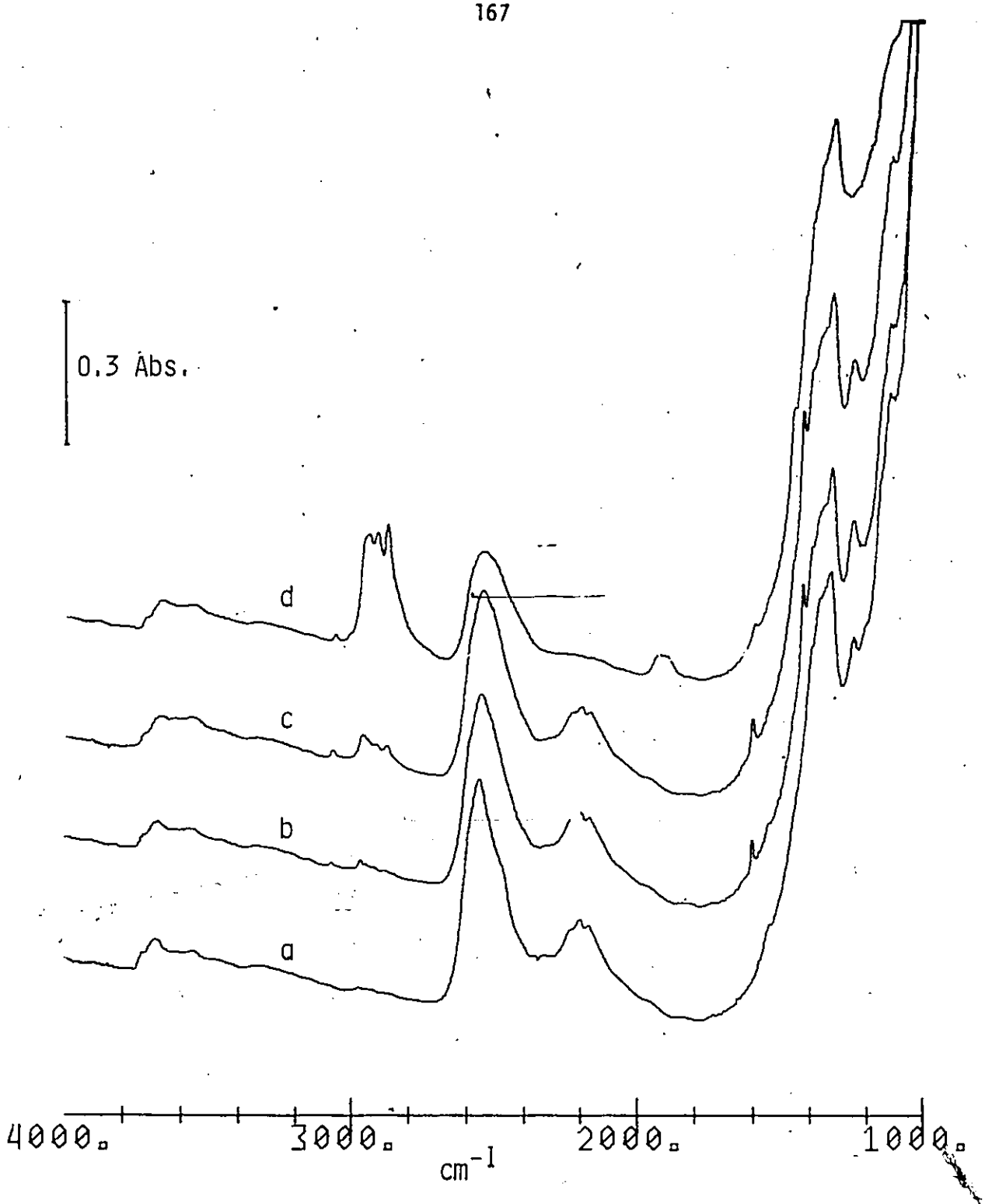


Figure 6-7
a) Infrared spectrum of alumina which had been degassed at 450°C for 1 hr. and reacted at 100°C with $^{n}B_2H_6$ followed by evacuation at 100°C for 1 hr.
b) After the addition to a) of 5 torr of $C_2H_2$ for 5 min. and evacuation for 5 min.
c) After 14 hrs. exposure of b) to 5 torr of $C_2H_2$ and evacuation for 5 min.
d) After heating c) in the presence of 5 torr of $C_2H_2$ at 100°C for 1 hr. and evacuation at 25°C for 5 min.

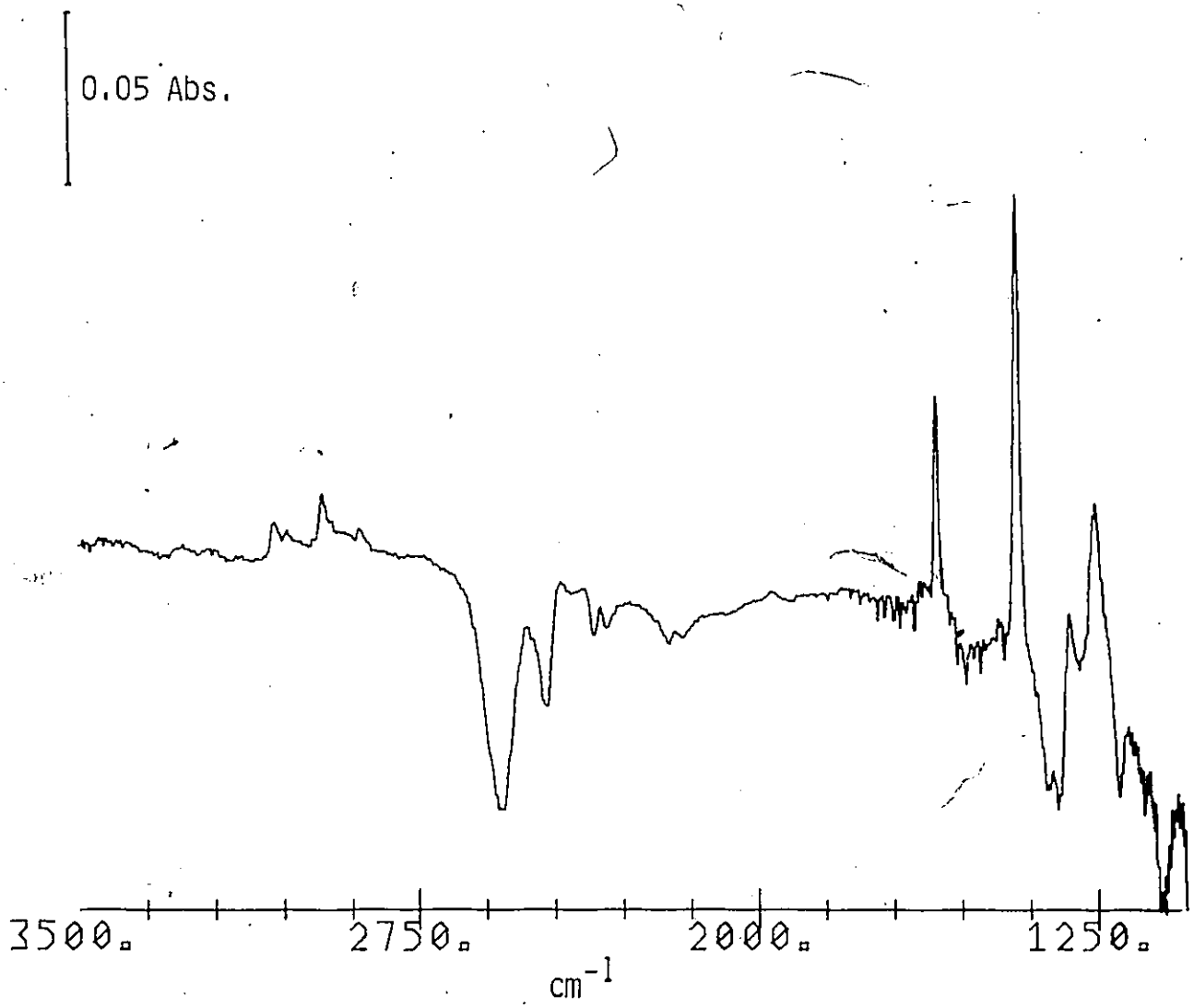


Figure 6-8
Difference spectrum Figure 6-7b minus Figure 6-7a.

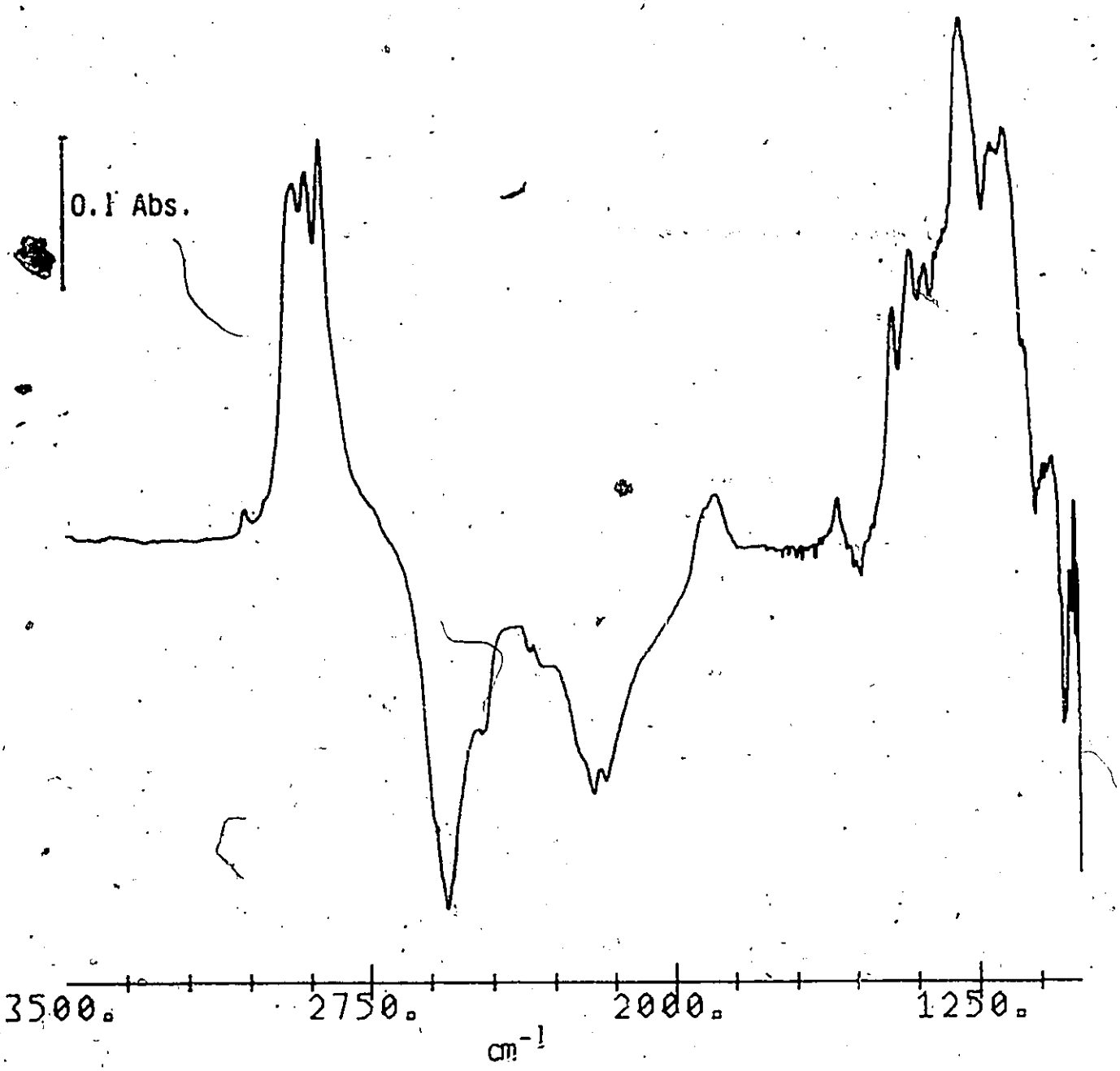


Figure 6-9
Difference spectrum for Figure 6-7d minus Figure 6-7a

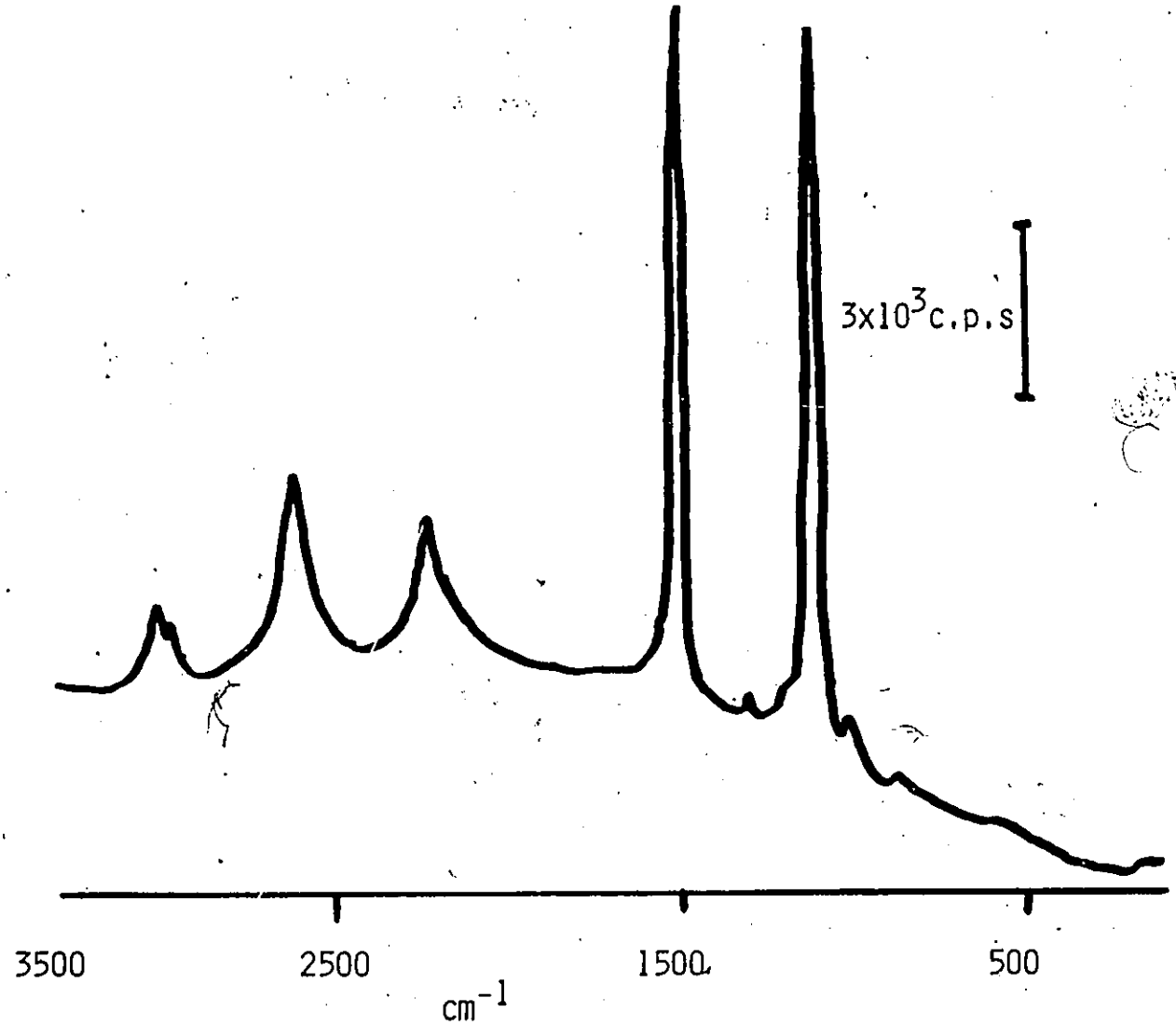


Figure 6-10
Raman spectrum of a diborane treated alumina which had been reacted with 20 torr of $C_2H_2$ at 25°C for 14 hrs.

1505 $cm^{-1}$ with weaker ones at 1000, 1300, 2225, 2610, 2965 and 3010 $cm^{-1}$. In no stage of the reaction with acetylene was gaseous benzene detected by either infrared or mass spectroscopy. (Benzene had been found for this reaction by Weiss when silica-alumina was used).

Intense Raman bands at 1505 and 1115 $cm^{-1}$ are very characteristic of polyacetylene. Shirakawa et al.[174, 175] have reported the Raman and infrared spectra of polyacetylenes and they assigned intense bands at 1500 and 1100 $cm^{-1}$ to carbon-carbon double and single bond vibrations, respectively, and a weaker band at 1016 $cm^{-1}$ to an out of plane C-H deformation mode.

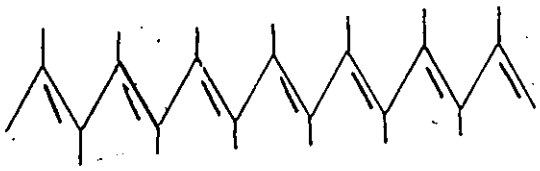

trans-polyacetylene

The corresponding bands for cis-polyacetylene are reported to be 1552, 1262 and 920 $cm^{-1}$. Furthermore, Shirakawa noted that thin films of trans-and cis-polyacetylene are deep blue and clear red, respectively. The Raman spectrum of the violet alumina sample was identical between 1600 - 800 $cm^{-1}$ to that reported by Shirakawa for trans-polyacetylene and the violet species observed on reacting borated alumina with acetylene is assigned to this polymer.

Shirakawa et al. assigned only one IR band in the C-H stretching region at 3013 $cm^{-1}$ to trans-polyacetylene and no bands were observed in the 1600-1500$cm^{-1}$ region of the IR spectrum for C=C stretch. The observation of additional infrared bands in the C-H and C=C stretching region in the present case indicates that a second reaction not involving the formation of polyacetylene was occuring. Holliday et al.[176] reported that trivinylborane [$B-(CH=CH_2)_3$] had strong IR bands at 3069, 3030, 2986, 2962, 1606 and 1421 $cm^{-1}$. The presence of

infrared bands in the present instance at 3063, 1606 and 1421 $cm^{-1}$ indicates that some vinyl ($-CH=CH_2$) species were being produced, at least initially, since the band at 1606 $cm^{-1}$ does disappear after heating the sample in acetylene at 100°C.

Figures 6-11 and 6-12 show the infrared spectrum of offretite and silica-alumina before and after reactions with diborane and acetylene. In the case of offretite it is noteworthy that the most acidic hydroxyls with infrared band at 3600 and 3558$cm^{-1}$ reacted with diborane at 25°C while the least acidic one did not react (recall the cases with alumina). The infrared spectrum in the B-H stretching region did not change even after prolonged evacuation of the borane treated offretite. The observation of IR bands at 2585, 2545 and 2442 $cm^{-1}$ along with a band at 1560 $cm^{-1}$ (not shown) indicated the formation of a bridged boron species, i.e., $\equiv SiOB_2H_5$, as with silica. This species, $\equiv SiOB_2H_5$, was most likely formed inside cages within the offretite framework (since the acidic hydroxyls are known to be in these cages) and this could account for the unusual stability of this $\equiv SiOB_2H_5$ when compared to that on silica. Several bands in the 2200-2300 $cm^{-1}$ region are observed in the IR spectrum of the borated offretite and are possibly different $\equiv SiH$ species but do not warrant further speculation. After exposure of the diborane treated offretite to acetylene the sample immediately turned a deep violet colour and IR bands at 3075, 2975, 2930 and 2895 $cm^{-1}$ were observed along with an intense band at 1615 $cm^{-1}$ (not shown). The Raman spectrum of this blue coloured offretite was identical to that obtained with alumina.

The diborane treated silica-alumina (Figure 6-12) also turned violet upon exposure to acetylene but the change in colour occurred over a period of about 15 minutes and the new infrared bands were at 3075, 2970, 2890 with a strong band at 1610 $cm^{-1}$ (not shown). The Raman spectrum of this violet coloured sample was also similar to that obtained with alumina. No gaseous benzene was detected after

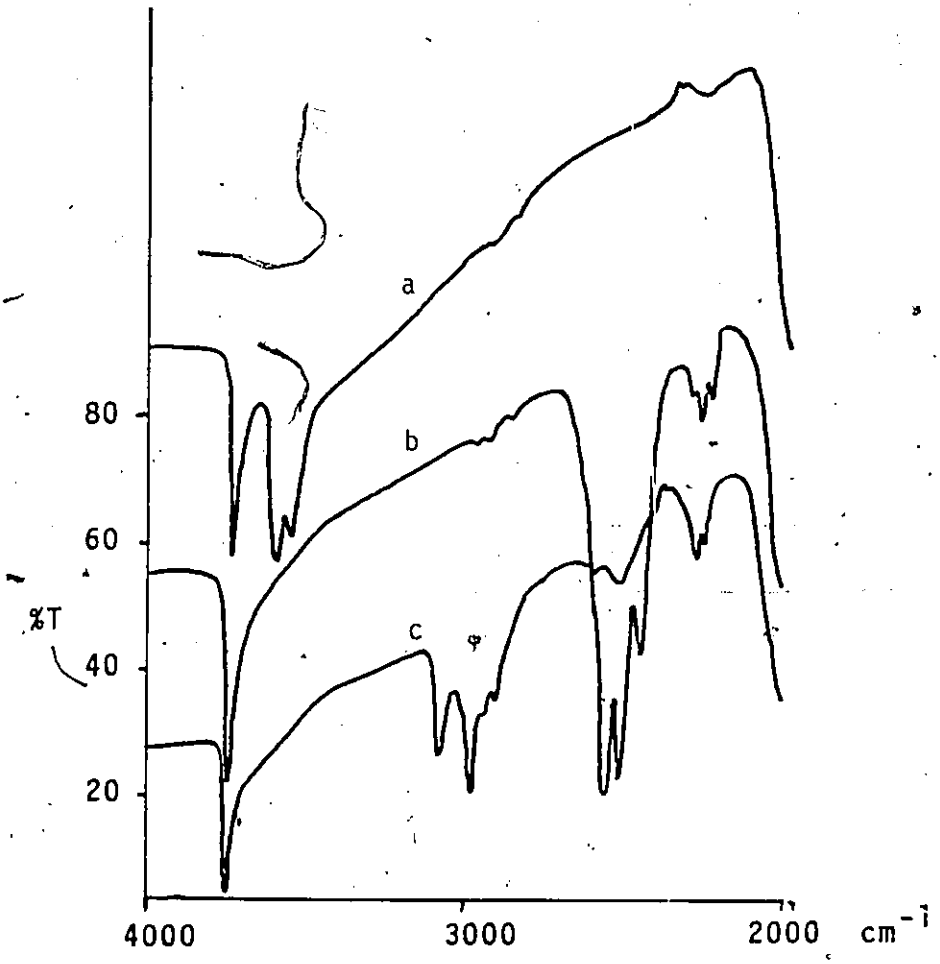


Figure 6-11
a) Infrared spectrum of $H^+$ - offretite which had been degassed at 500°C for 1 hr.,
b) After the reaction of a) with $^nB_2H_6$ at 25°C and evacuation for 1 hr.
c) After exposure of b) to 10 torr of $C_2H_2$ for 1 hr and evacuation for 10 min.
The % T scale refers to c) and a) and b) have been displaced.

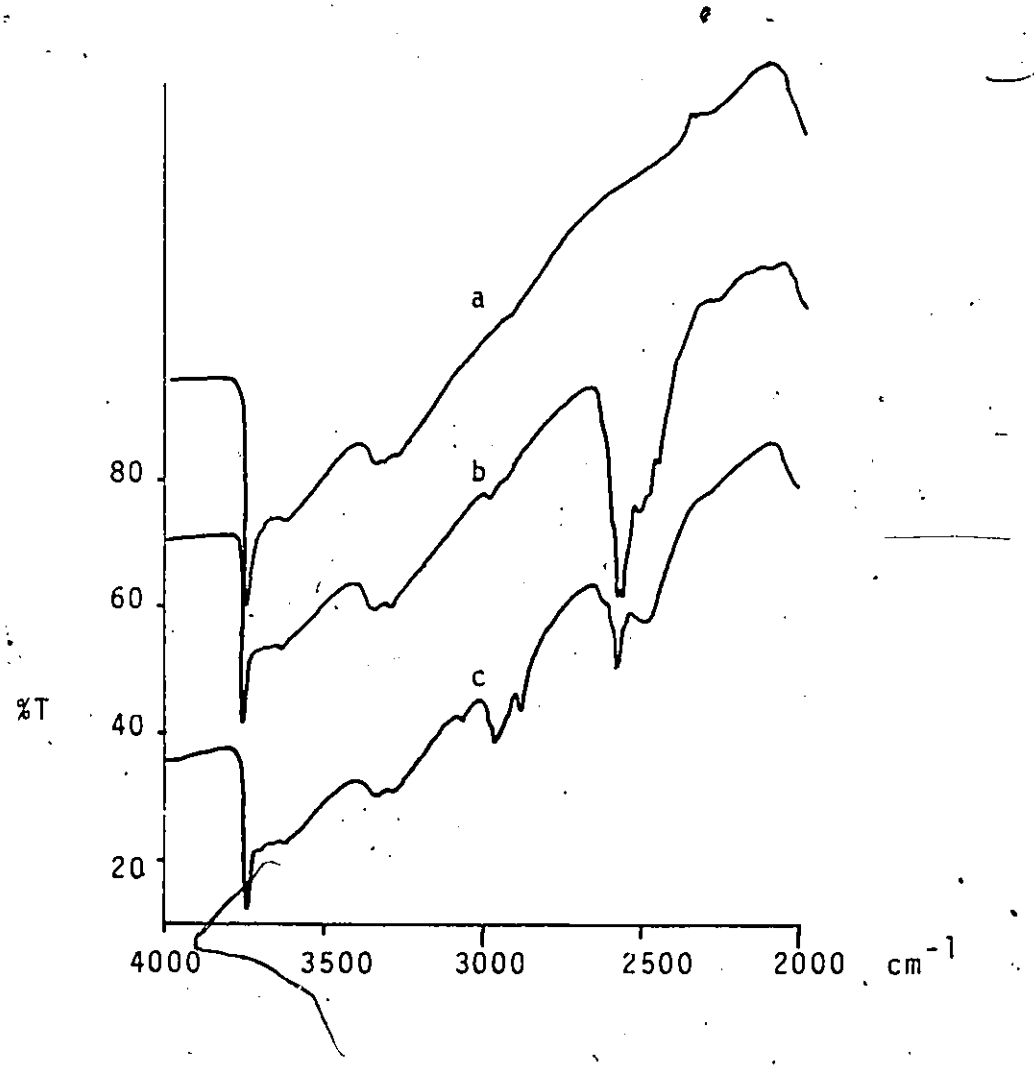


Figure 6-12
a) Infrared spectrum of Davisson silica-alumina which had been degassed at 300°C for 1 hr.
b) After exposure of a) to $^{n}B_2H_6$ and evacuation at 25°C
c) After exposure of b) to 15 torr of acetylene for 30 min. and evacuation for 10 min.
The % T scale refers to c) and a) and b) have been displaced.

adding acetylene to either the borated offretite or silica-alumina.

The infrared spectrum of diborane treated silica after exposure to acetylene had very intense bands at 3073, 2971, 1607 and 1430cm$^{-1}$ in addition to a number of bands in the B-H stretching region around 2500cm$^{-1}$. The sample remained white, which meant therefore that no polyacetylene was produced. The spectrum shown in Figure 6-13 is complex and it is apparent that, in addition to vinyl groups attached to boron, other boron species may also be present.

The adsorption of acetylene on alumina has been investigated by Yates and Luccesi[177] using infrared spectroscopy and they postulated two adsorbed species. One species was strongly adsorbed acetylene in an "end-on" configuration involving hydrogen bonding through the acetylenic hydrogen atom and a less strongly adsorbed species in a side-on interaction involving the $\pi$-electrons of acetylene. Bhasin et al.[178] support the assignments of Yates and additionally observed that a coloured product was formed and evidence for polymerization of acetylene was given by the observation of a C=C stretch near 1600cm$^{-1}$ in the infrared spectrum.

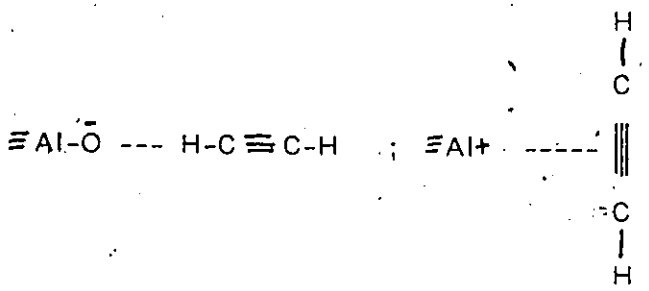

Heaviside et al.[179] have reported a Raman study of the reactions of acetylene with alumina degassed at various temperatures and with potassium exchanged zeolite-X. The spectra reported by Heaviside et al., which were very similar to those obtained in the present studies, were attributed to trans-polyacetylene. Heaviside et al. report that despite the intensity of the colour, and of the Raman spectrum, the actual amount of the

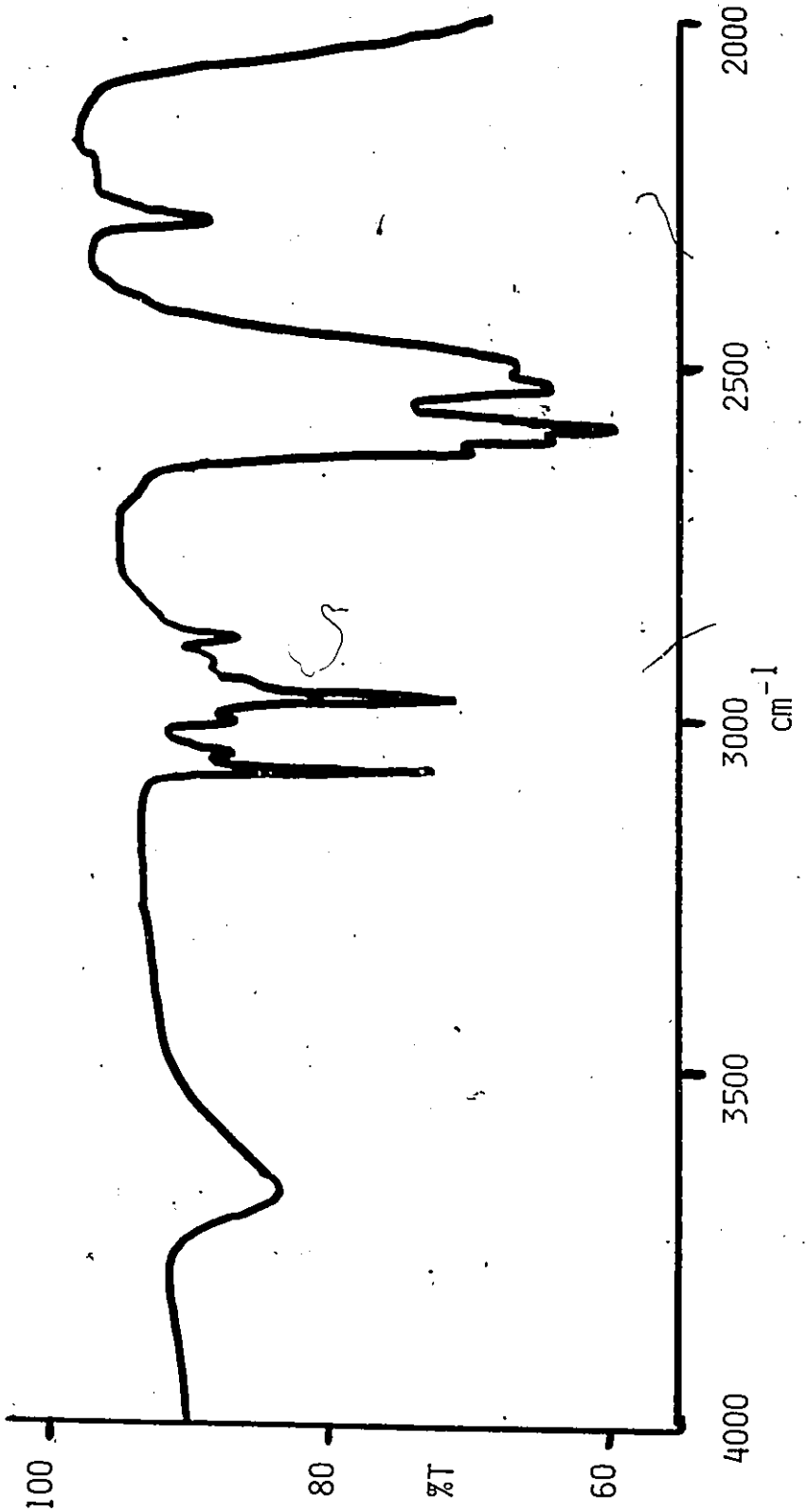


Figure 6-13
Infrared spectrum of a diborane treated silica which had been exposed to 10 torr of $C_2H_6$ for 1 hr. and evacuated for 1 hr.

polyene formed was very small, approximately 0.5 mg / g of alumina. The intensity of the colour and the Raman spectrum were reported to increase with the degassing temperature of the alumina and Heaviside et al. interpreted this observation in terms of $\rangle C=CH_2$ co-ordinated to a pair of Lewis acid sites (of which there are an increasing number at higher degassing temperature) and that polymerization proceeds on this anchored vinyl group.

Acetylene polymerizes to trans-polyacetylene on diborane treated alumina, offretite and silica-alumina but not on diborane treated silica. The polymerization appears to be fastest on borated offretite and slowest on alumina but in the latter case could be increased significantly by heating the borated alumina in acetylene at 100°C. Side reactions involving the formation of vinylboranes $[-B-(CH=CH_2)x;\ x=1,2]$ also occurred on the diborane treated alumina, offretite and silica-alumina but appeared to be the sole reactions of borane treated silica. A comparison between untreated alumina and diborane treated alumina showed that the adsorption of diborane promoted the polymerization of acetylene since the untreated sample gave only a faint discolouration while the borated sample gave an intense violet colour under the same conditions. Although no benzene was detected during the production of purple coloured trans-polyacetylene, the observation of a purple colour by Weiss et al.[170] during the polymerization of acetylene over diborane treated silica-alumina was quite probably also due to polyacetylene produced in a side reaction.

A final observation can be made relative to the adsorbed species produced by diborane on alumina. In Figure 6-8 two bands at 2560 and 2466 $cm^{-1}$ were found to decrease after exposure of borane treated alumina to acetylene while a band at 1604 $cm^{-1}$ appeared and the bands from 2200-2100$cm^{-1}$ assigned to $AlBH_4$ were unchanged. The similarity in the IR bands observed after the addition of

acetylene to both borated silica and alumina at 25°C (i.e., bands at 3073, 2968, 1604 and 1426 $cm^{-1}$ with alumina versus 3073, 2971, 1607 and 1430 with silica) indicates the formation of similar vinyl borane species. The bands at 2560 and 2466 $cm^{-1}$ are close to the expected frequencies for $-BH_2$ groups and the above observations provide additional support for the formation $OBH_2$ species on alumina like those on silica upon the adsorption of diborane.

# CHAPTER 7

## THE ADSORPTION OF TRIMETHYLGALLIUM ON SILICA AND ITS REACTIONS WITH $NH_3$, $PH_3$, $AsH_3$, $H_2O$, HCN AND HCl

### Introduction

Many hydrogen sequestering reagents such as $SiCl_xMe_{4-x}$[Me=$CH_3$, x=1-4], $GeCl_xMe_{4-x}$, $Al_2Me_6$, $(Me_3Si)_2NH$, $BCl_3$, $TiCl_4$ and most recently in this work $(C_2H_5)_3B$, have been used as probes to study the nature of the hydroxyl groups on silica surfaces and to chemically modify these surfaces for other purposes[8, 17, 24, 28, 47, 91-97, 122, 123, 126]. It has been reported[92-95, 126] that trimethylaluminum (which exists as the dimer $Al_2Me_6$ at 25°C) when exposed to silica reacts first with the normal siloxane sites (distinct from siloxanes generated on highly degassed silica surfaces) and then with ≡SiOH groups i.e. the following reactions occur in sequence:

(1) $\equiv Si\text{-}O\text{-}Si + \frac{1}{2}Al_2Me_6 \longrightarrow \equiv SiOAlMe_2 + \equiv Si\text{-}Me$

(2) $\equiv Si\text{-}OH + \frac{1}{2}Al_2Me_6 \longrightarrow \equiv SiOAlMe_2 + CH_4\uparrow$

Trimethylgallium [$Ga(CH_3)_3$, TMG], unlike the aluminum analogue, is a monomer at 25°C and the aim of the present study was to use the techniques of infrared and Raman spectroscopies to determine whether TMG reacts with silica in the same manner as $Al_2Me_6$.

Trimethylgallium is used extensively in the semi-conductor industry to produce GaN, GaP and GaAs semi-conductors via reactions with ammonia, arsine and phosphine ($NH_3$, $PH_3$, $ASH_3$), respectively[180-182]. Possible mechanisms for these reactions have been proposed by several authors[181-3]. In the present study infrared and Raman spectroscopies were also used to determine if $MH_3$(M=N,P,As)

would react with TMG adsorbed on silica to produce GaM and to investigate the mechanisms of these reactions. Gallium doped oxides are reported to have unusual catalytic properties[184, 185a] and two such cases for silica were cursorily investigated and are briefly reported in this chapter.

Tubis et al.[184] have studied the reaction of TMG with silica. They observed new infrared bands after reaction at 3012, 2960 and 2915cm$^{-1}$ which they assigned to species I and II in the following reactions:

(3) $\equiv SiOH + GaMe_3 \longrightarrow \underset{I}{\equiv SiOGaMe_2} + CH_4\uparrow$

(4) 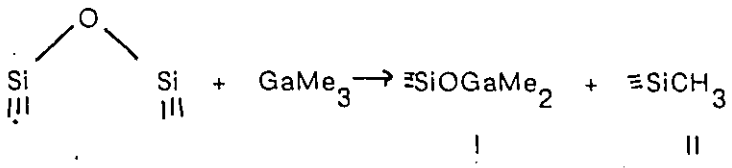

Since the band at 3012cm$^{-1}$ was removed by the admission of air this band was assigned to a Ga-$CH_3$ vibration whereas the band at 2960 and 2915cm$^{-1}$ were attributed to $\equiv SiCH_3$ which would be more stable in the presence of oxygen and water. The authors also studied the reactions of the TMG treated silica with hydrogen chloride (HCl) and suggested that the following reaction occurred with species I:

(5) $\equiv SiOGaMe_2 + 2HCl \longrightarrow \equiv SiOGaCl_2 + 2CH_4\uparrow$

On the basis of new evidence from this study it will be shown that the conclusions of Tubis et al. are incorrect.

The results obtained in these investigations are presented in two parts. Part I deals with the adsorption of TMG on silica and the subsequent reactions of this treated surface with $H_2O$, $NH_3$, $PH_3$ and $AsH_3$, and the catalytic activity of gallium doped silica, while Part II will be devoted to the reactions of HCN and

HCl with TMG treated silica.

Experimental

The silica used in most of these experiments was calcined at 550°C and then degassed at 500°C for 1 hr, and any exceptions to this will be specifically stated. The silica discs used in IR studies contained 5-10mg/cm$^2$ of silica while those for Raman studies contained 100mg/cm$^2$ . Thin silica films were prepared as previously described. $\beta$ - gallium oxide ($Ga_2O_3$) was used as supplied (Alfa-Ventron 99.99%) and self-supporting discs containing approximately 2mg/cm$^2$ of $Ga_2O_3$ were used in infrared studies while discs containing 100mg/cm$^2$ were used in Raman studies. Oxygen-18 exchanged silica was prepared by repeated exposure and evacuation of $H_2O^{18}$ to silica at 420°C until the desired degree of exchange ($SiO^{18}H/SiO^{16}H$) was achieved and the sample was then finally degassed at 420°C for 1 hr. Deuterated silica ( $\equiv$SiOD) was prepared in a similar manner to the oxygen-18 samples except that $D_2O$ was used.

Results and Discussion

Part I

(i) The Adsorption of TMG on Silica

When silica was exposed to 5 torr of TMG at 25°C the IR band of $\equiv$SiOH at 3748cm$^{-1}$ disappeared immediately and new bands appeared at 3016, 2967, 2910, 2400 and 1410cm$^{-1}$ (Figures 7-1a and 7-1b). The bands at 2967, 2910, 2400 and 1410cm$^{-1}$ were diminished slightly by evacuation for 10 minutes while that at 3016cm$^{-1}$ disappeared (Figure 7-1c). Infrared and mass spectrometric analysis of the gas phase showed only the presence of excess $GaMe_3$ and $CH_4$ (IR bands for $CH_4$ at 3016 and 1307cm$^{-1}$). When deuterated silica was exposed to TMG, $CH_3D$ with no trace of $CH_4$ was detected. The IR bands at 2967, 2910, 2400 and 1410cm$^{-1}$ shown

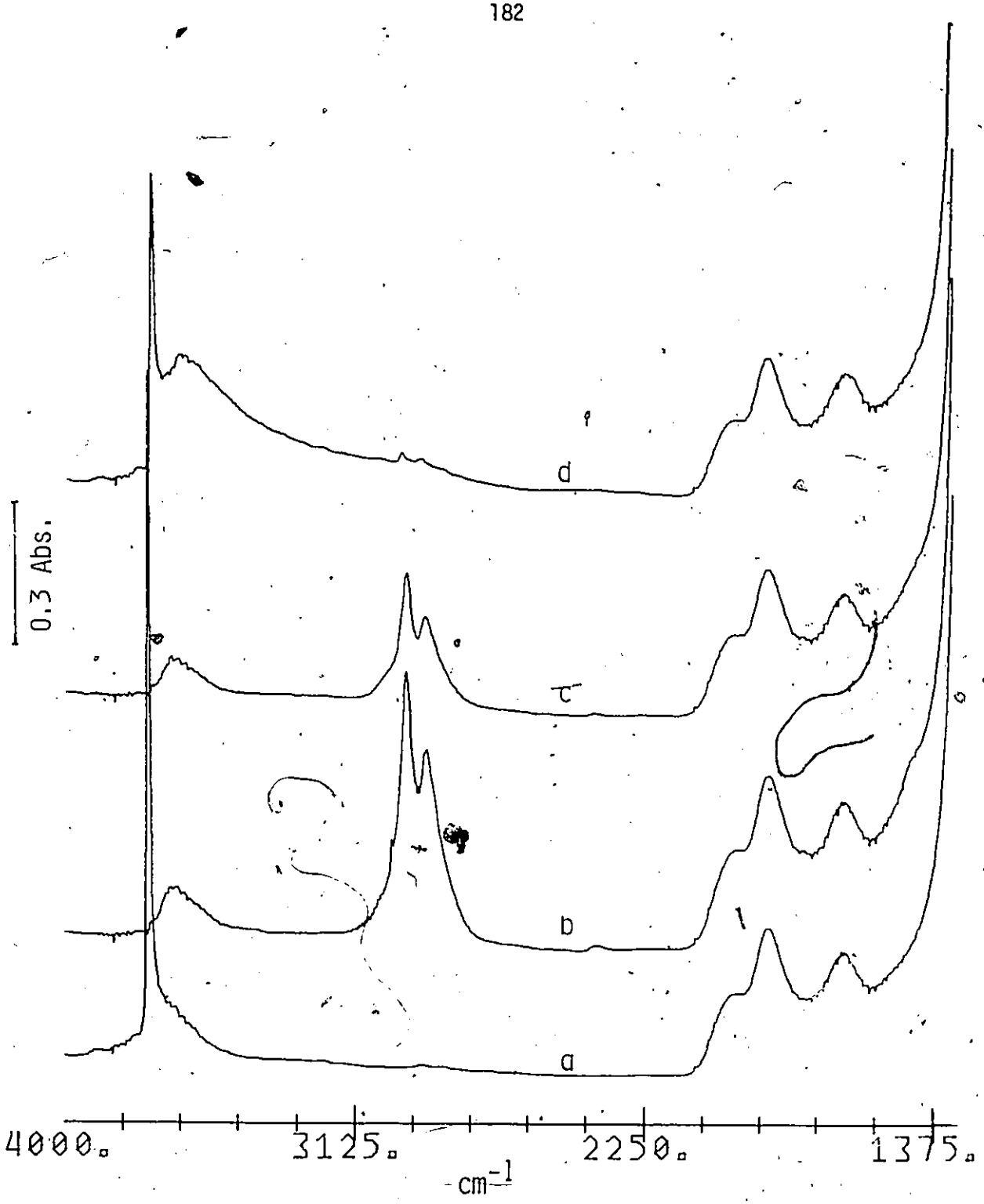


Figure 7-1
a) Infrared spectrum of silica (10mg/cm$^2$) degassed at 500°C
b) After the addition of 5 torr of trimethylgallium at 25°C to a)
c) Evacuation of b) for 10 min.
d) Following hydrolysis of c) at 200°C in 18 torr of $H_2O$ for 14 hrs and evacuation at 200°C for 1 hr.

in the difference spectrum (Figure 7-2) did not change even after 48 hrs evacuation at 25°C and are therefore due to a strongly adsorbed species. The broad band at 3650cm$^{-1}$ after reaction with TMG (Figure 7-1c) is due to the inaccessible surface hydroxyl groups[26, 28]. Figures 7-3a and 7-3b show the spectrum of a thin silica film before and after reaction with TMG while Figure 7-3c shows the corresponding difference spectrum. The new bands observed after the adsorption of TMG on a thin silica film are at 1210, 1002, 745, 703 and 606cm$^{-1}$ (The peaks at 745, 703 and 606cm$^{-1}$ were also observed using self-supporting discs containing 5mg/cm$^2$ of silica). The shoulder at 960cm$^{-1}$ is an artefact due to the disappearance of the band at 980cm$^{-1}$ attributable to the Si-O stretching mode of ≡SiOH.

Figures 7-4 and 7-5 show the infrared spectra of silica which had been degassed at 150 and 1000°C, respectively, before and after reaction with TMG. Figure 7-4b shows that a larger amount of residual inaccessible hydroxyls remained after reaction of TMG with a silica degassed at 150°C compared to one degassed at 500°C but that the 2967 and 2910cm$^{-1}$ bands were about 20% more intense in the former case. For a silica degassed at 1000°C (Figure 7-5) there was no band due to residual inaccessible hydroxyls and the bands at 2967 and 2905cm$^{-1}$ were about one half as intense compared to that for the 500°C degassed silica. The IR bands at 908 and 888cm$^{-1}$ due to the reactive siloxanes generated at 1000°C also disappeared, probably via reaction (4).

The Raman spectrum from 100-3100cm$^{-1}$ is shown for a 480°C degassed silica before and after reaction with $GaMe_3$ (Figures 7-6a and 7-6b). The new bands which appeared after reaction were observed at 140, 440, 555, 610, 1210 and (inset) 2910, and 2970cm$^{-1}$. The band at 980cm$^{-1}$ which disappeared after reaction with TMG is attributed to the Si-O stretch of ≡SiOH whose Raman band at

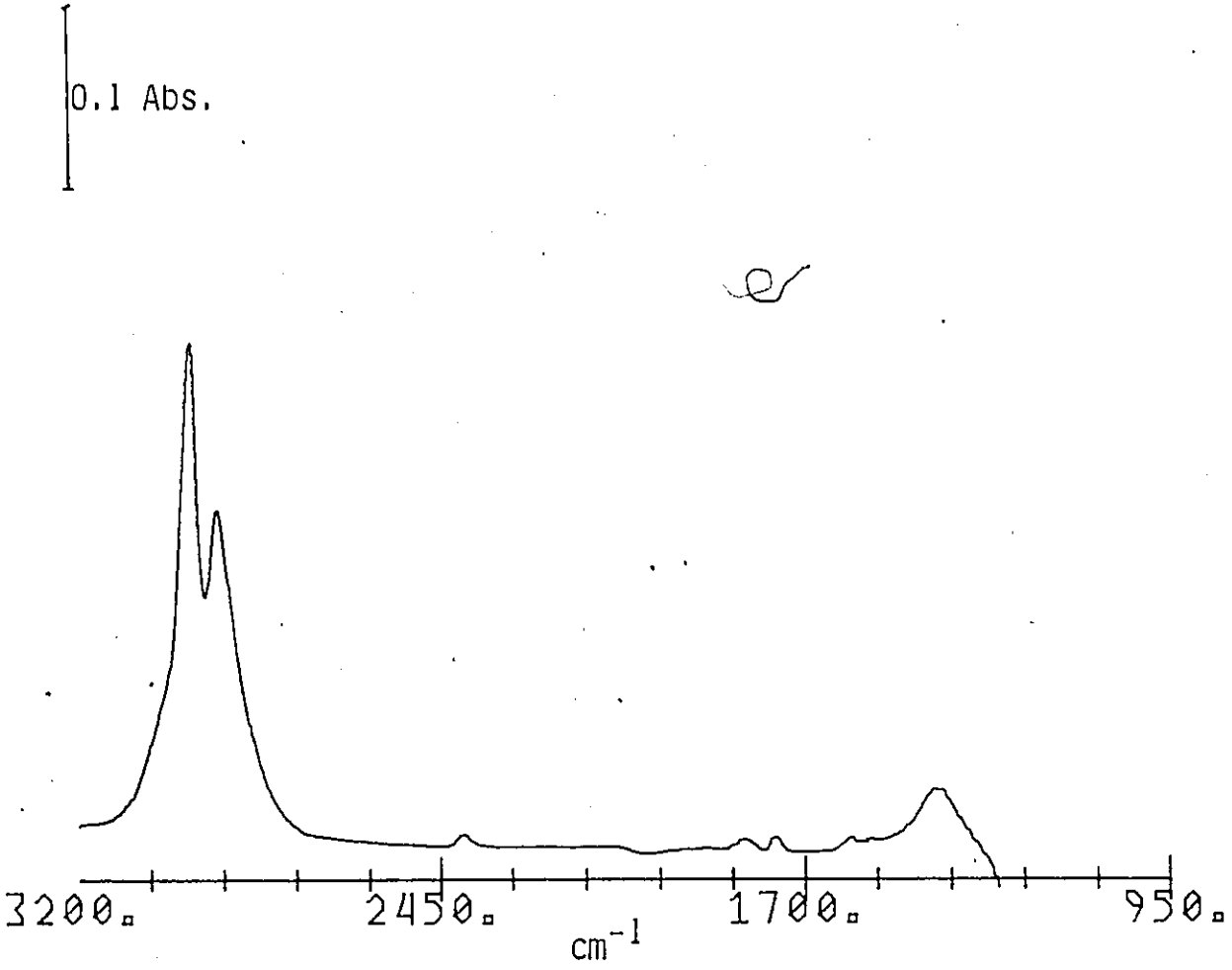


Figure 7-2
Difference spectrum Figure 7-1c minus Figure 7-1a in the region 3200-1300cm$^{-1}$.

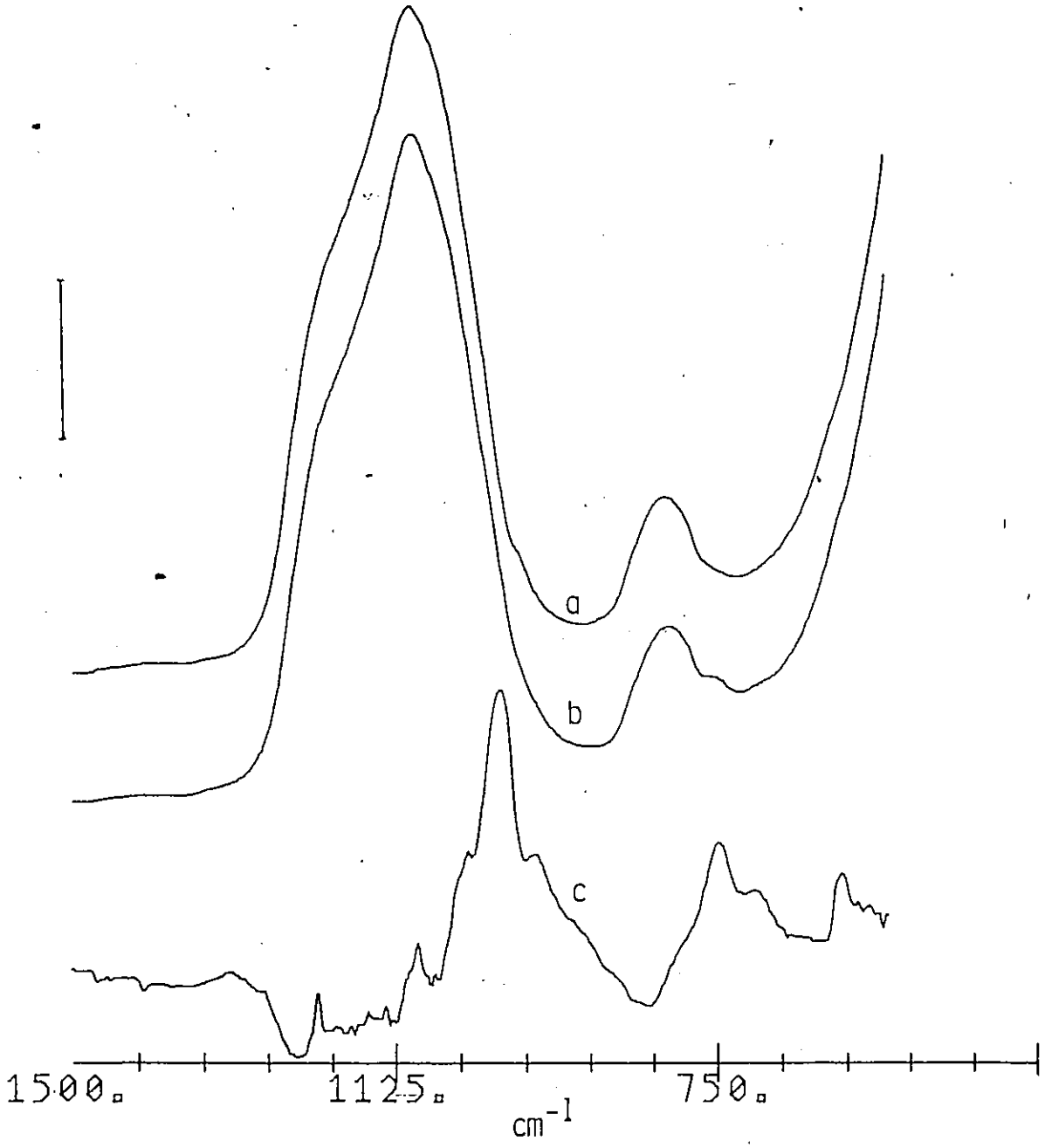


Figure 7-3
a) Infrared spectrum of a thin silica film which had been degassed at 500°C for 1 hr.
b) Spectrum after reaction with trimethylgallium at 25°C and evacuation for 10 min.
c) Difference spectrum b) minus a)
The bar at left represents 0.3 absorbance units for a) and b) and 0.05 for c).

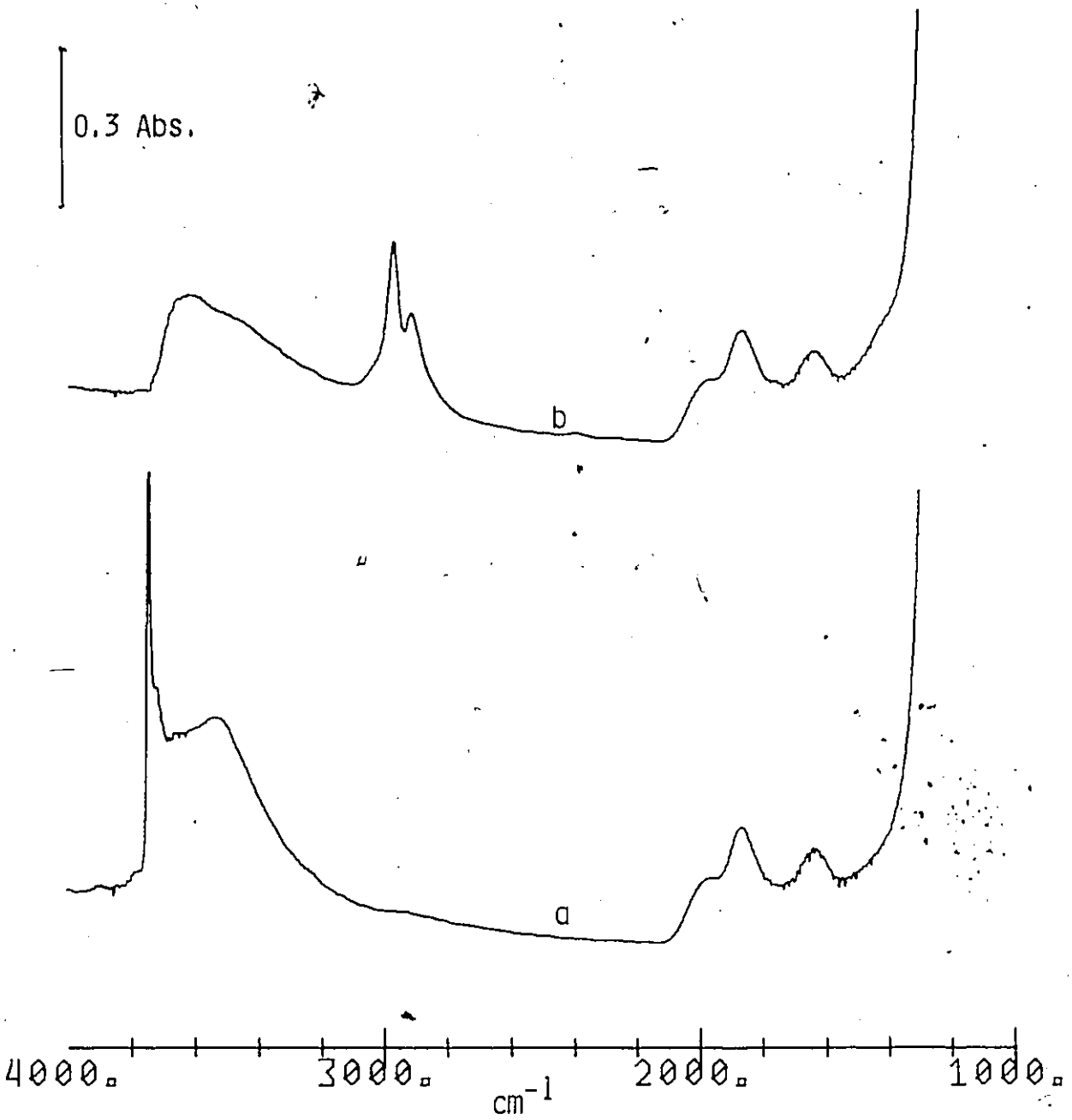


Figure 7-4
a) Infrared spectrum of a silica (10mg/cm$^2$) degassed at 150°C for 1 hr.
b) Following reaction of a) with excess trimethylgallium at 25°C and evacuation for 10 min.

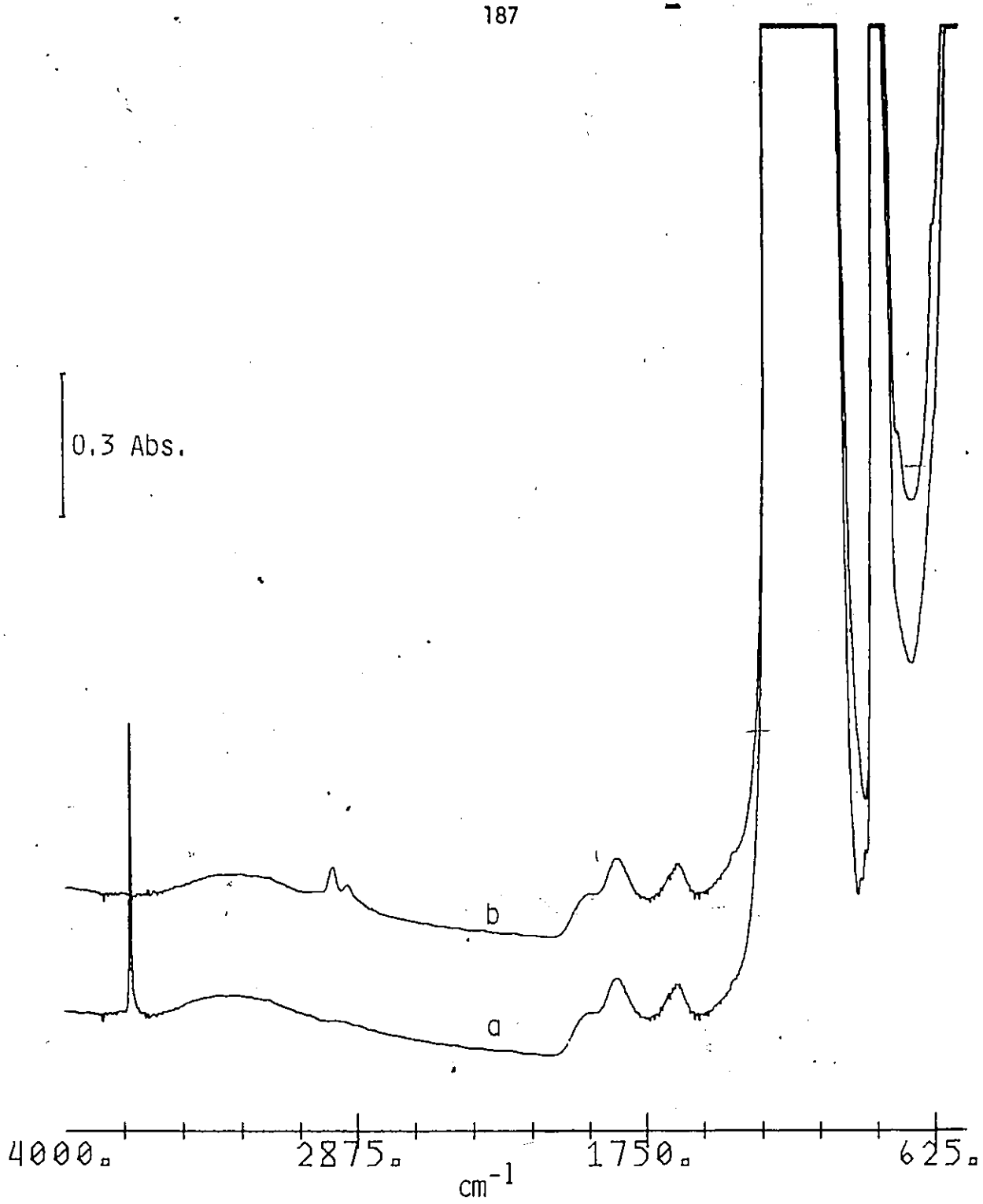


Figure 7-5
a) Infrared spectrum of a silica (5mg/cm$^2$) which had been degassed at 1000°C for 1 hr.
b) Spectrum obtained after reaction with trimethylgallium and evacuation for 10 min. at 25°C.

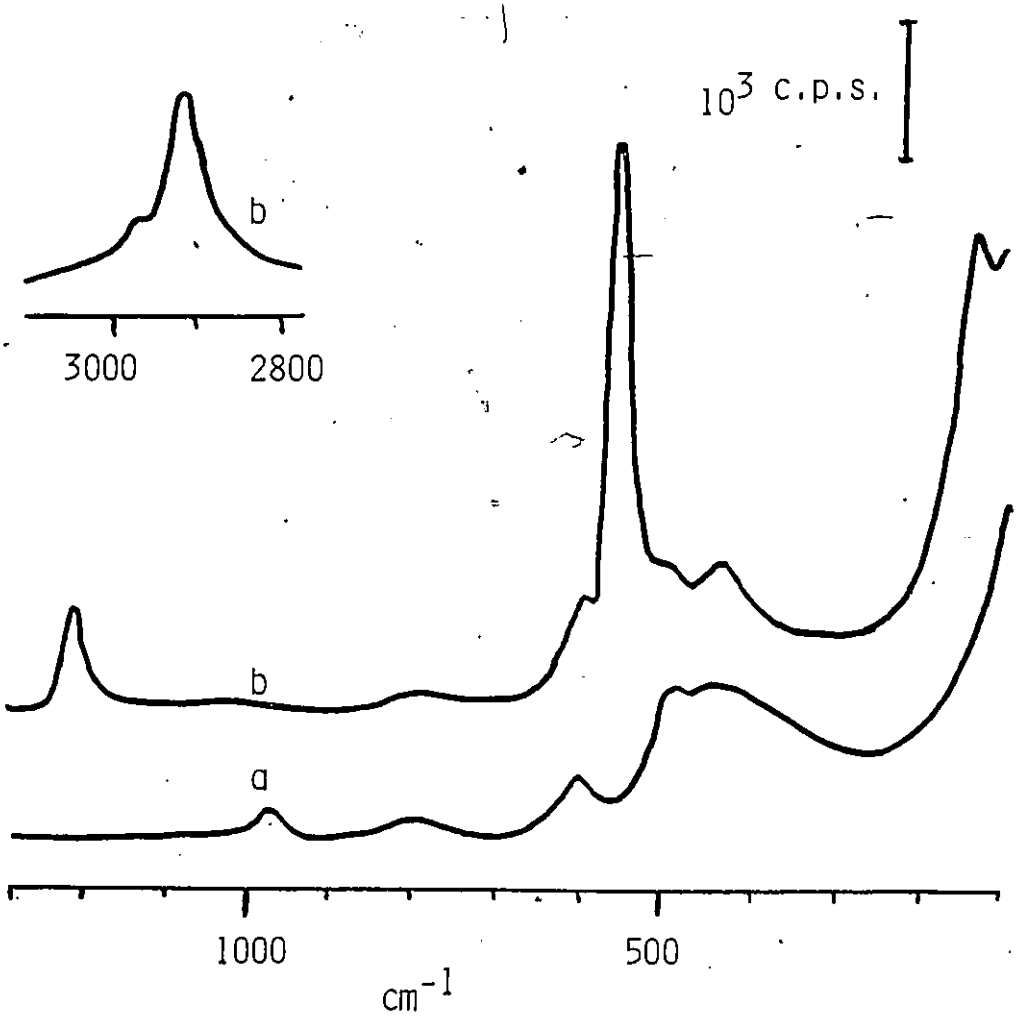


Figure 7-6
a) The Raman spectrum of a silica degassed at 480°C for 1 hr.
b) After reaction with trimethylgallium and 10 min. evacuation at 25°C.
Inset shows the region from 3100-2700$cm^{-1}$ of curve b).

3748cm$^{-1}$ due to the OH stretch (not shown) also disappeared.

The addition of 18 torr of water at 25°C resulted in a small decrease in the intensity of the IR bands at 2967 and 2905cm$^{-1}$, an increase in the absorption near 3700cm$^{-1}$ (presumably due to the formation of ≡Si-OH or ≡GaOH), and the generation of a small quantity of methane. While there was little further change after prolonged exposure at 25°C, heating the sample to 200°C in the presence of water completely removed the bands at 2967 and 2910cm$^{-1}$ and left sharp weak bands at 2983 and 2925cm$^{-1}$. A large quantity of methane was generated during the hydrolysis at 200°C; the ≡SiOH band at 3748cm$^{-1}$ was almost completely restored and there was an increased absorbance around 3650cm$^{-1}$ possibly due to GaOH (Figure 7-1d). The ratio of $CH_4$ produced by hydrolysis of the $GaMe_3$ treated silica to that generated in the initial adsorption of $GaMe_3$ was 2.0 ∓ 0.1. If the TMG treated silica was heated at temperatures between 100-300°C in a closed cell or under continuous evacuation, $CH_4$ (quantity increasing with temperature) was produced and the intensity of the bands at 2967 and 2910cm$^{-1}$ decreased while that of a band at 2980cm$^{-1}$ increased. Hydrolysis then yielded a smaller quantity of methane than that produced by the hydrolysis of the unheated TMG treated silica, a smaller OH intensity and more intense bands at 2983 and 2925cm$^{-1}$. Heating the TMG treated silica beyond 300°C resulted in the generation of a large quantity of methane and the sample turned grey, indicating thermal decomposition of the surface species. No ≡SiOH was generated at any temperature during heating of the TMG treated silica alone.

The addition of oxygen at 25°C to the TMG treated silica resulted in the immediate disappearance of the bands at 2967 and 2910cm$^{-1}$, the generation of a small quantity of methane, and new IR bands attributable[185 b] to ≡SiOCH$_3$ were observed. Additional bands were observed in the 3700-3500cm$^{-1}$ region which might

be due to ≡SiOH, ≡GaOH or adsorbed water. It is speculated that Ga-C bonds were cleaved by oxygen to form GaO and $OCH_3$ and that the latter subsequently formed ≡$SiOCH_3$, or that methyl groups are generated which then react with the silica surface to produce the ≡$SiOCH_3$ species.

It is evident that more than one strongly adsorbed species are formed by the reaction of TMG with silica. Silica which has been degassed at 500°C or higher possess hydroxyl groups only of the isolated type and the immediate disappearance of these hydroxyls upon the addition of TMG indicates that ≡$SiOGaMe_2$ is being formed according to reaction (3). That methane was generated by this reaction was substantiated by infrared and mass spectrometries and it is therefore clear that the "3012"$cm^{-1}$ infrared band observed by Tubis et.al. was in fact due to gaseous methane and not to species I, ≡$SiOGaMe_2$.

By comparison with the infrared and Raman spectra of $GaMe_3$ and $GaMe_3$ adducts[186-190] the observed infrared and Raman spectra of $GaMe_3$ adsorbed on silica can be assigned. The 2967 and 2910$cm^{-1}$ bands (IR and Raman) are assigned respectively to the antisymmetric and symmetric stretch of $-CH_3$ in ≡$SiOGaMe_2$ while the bands at 1410 and 1210$cm^{-1}$ are the corresponding deformation modes. The weak band observed at 2400$cm^{-1}$ is quite probably an overtone of the symmetric deformation mode at 1210$cm^{-1}$. The IR band at 1002$cm^{-1}$ is due to the antisymmetric Si-O-Ga stretching mode while the bands at 745 and 703$cm^{-1}$ are $-CH_3$ rocking modes. The IR and Raman bands at 610 and 555$cm^{-1}$ are assigned to the antisymmetric and symmetric $GaC_2$ stretching modes. The Raman band at 440$cm^{-1}$ is probably the symmetric Si-O-Ga stretching mode which is expected to occur near here (a similar mode near here is observed for SiOTi, SiOGe and SiOSi[122]) while that at 140$cm^{-1}$ is possibly the superposition of several $SiOGaC_2$ deformation modes which should occur nearby.

Further support for the above assignment comes from the observation that the ratio of the quantity of methane produced by the adsorption of TMG on silica to that produced in the subsequent hydrolysis at 200°C was 2.0 ∓ 0.1. If the hydrolysis takes place as shown in reaction (5) and if reaction (3) were the sole reaction of $GaMe_3$ with silica, the ratio would be 2 but if reactions (3) and (4) occur to equal extents the ratio would be 4.

(5) $\equiv SiOGaMe_2 + 3H_2O \longrightarrow \equiv SiOH + Ga(OH)_3 + 2CH_4\uparrow$

The methane ratios observed mean that reaction (3) was the dominant one and very little reaction occurred between $GaMe_3$ and the normal siloxane bridges, unlike the case reported for $Al_2Me_6$.

The infrared band observed at 2983 and 2925$cm^{-1}$ after hydrolysis can possibly be assigned to $\equiv SiCH_3$. IR bands at these frequencies were observed by Yates et al.[93] after the high temperature degassing of $Al_2Me_6$ on silica, and by Low[191] for reactive silicas, and have been assigned to $\equiv SiCH_3$. It was observed that these bands could be increased in intensity by heating the $GaMe_3$ treated silica before hydrolysis so it was impossible to determine whether these bands were due to $\equiv SiCH_3$ formed as a result of reaction (4) or as a result of partial decomposition due to heating of the surface during hydrolysis at 200°C. It has been noted, however, that the intensities of the 2983$cm^{-1}$ band were 0.01, 0.045 and 0.07 absorbance units for silicas which had been degassed at 150, 500 and 1000°C, respectively, reacted with TMG, and then hydrolyzed. Part of the increase in the intensity here can be accounted for by the increasing amounts of reactive siloxane sites which are generated by degassing above 400°C and which would then react according to reaction (4) to yield $\equiv SiCH_3$.

Tubis et al.[184] had reported that the ratios of $GaMe_3$ consumed to methane

produced were in the range of 0.5 - 0.7 and that this indicated significant reaction of $GaMe_3$ with siloxane sites according to reaction (4) (if reaction (3) occurred as frequently as (4) the ratio would be 0.5, whereas if only (4) occurred the ratio would be 1). The $GaMe_3$ consumed and methane produced was determined by using a Toepler pump which gave the amount of $CH_4$ produced directly and the amount of $GaMe_3$ consumed by the difference between that which was added initially to the reaction chamber to the excess condensed in a liquid nitrogen trap placed in the forepart of the Toepler pump. It has been observed in the present study that a large quantity of TMG was physiosorbed on the silica reacted with $GaMe_3$ and that this was present even after evacuation of the excess $GaMe_3$ to 0.1 torr but was removed completely after pumping for 10 minutes to $10^{-4}$ torr. It is apparent therefore that unless the Toepler pump is used to reduced the pressure to much less than 0.1 torr significant errors in the measured amounts of $GaMe_3$ consumed will occur and lead to ratios less than 1. The ratios observed by Tubis et al. for $GaMe_3$ consumed to $CH_4$ produced could mean that there was still considerable physiosorbed $GaMe_3$ (the authors do not specify to what pressures their system was Toepler pumped) or that significant reaction was occuring between siloxane sites and $GaMe_3$. The latter observation might be due to the silica used, which was different from that employed in the present studies, or the higher pressures of TMG used by Tubis et al. which might lead to increased reaction rates with siloxane groups.

The evidence presented here indicates that trimethylgallium reacts with the hydroxyl groups on silica (paired and unpaired) to give $\equiv SiOGa(CH_3)_2$ and that this is the predominant reaction. Some reaction between trimethyl gallium and siloxane sites of the normal type may occur but only to a very small extent. Reaction of siloxane sites produced by the high temperature degassing of silica

occurs with $GaMe_3$ but again the amount of reaction is small since there are very few of these sites being produced even at 1000°C.

ii) Reactions with Lewis bases

Trivalent gallium in the species $\equiv SiOGaMe_2$, as might be expected, exhibits strong Lewis acidity and this was most clearly demonstrated by the adsorption of pyridine on the trimethylgallium treated silica. Upon exposure of TMG-$SiO_2$ to 1 torr of pyridine followed by evacuation at 25°C for 14 hrs new IR bands due to pyridine where observed in the 3000$cm^{-1}$ region and there was a change in the relative intensities of the 2967 and 2910$cm^{-1}$ bands. In addition, new bands were observed at 1612, 1492 and 1452$cm^{-1}$ and are assigned in accordance with the results of Parry[192] to Lewis bound pyridine (Figure 7-7). These bands remained unchanged even after evacuation at 200°C for 2 hrs.

(6) $\equiv SiOGaMe_2$ + 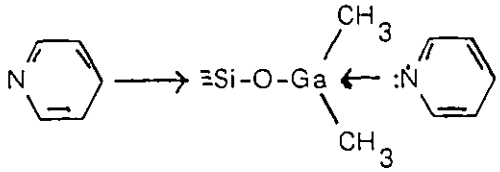 → 

The Lewis acidity of $\equiv SiOGaMe_2$ was also shown by its reaction with the Lewis bases $NH_3$, $PH_3$ and $AsH_3$. The reactions of $PH_3$ and $AsH_3$ with TMG-$SiO_2$ are similar and relatively simple compared to the case with $NH_3$ and will be dealt with first.

The addition of 10 torr of $PH_3$ or $AsH_3$ to TMG-$SiO_2$ at 25°C resulted in the immediate generation of a small quantity of $CH_4$, a slight decrease in the intensities of the IR bands at 2967 and 2910$cm^{-1}$ and a slight regeneration of the IR band due to $\equiv SiOH$. New IR bands were observed in the presence or absence of excess gaseous $MH_3$[M=P or As] in the region of M-H stretch at 2405, 2380 and 2365$cm^{-1}$ for $PH_3$ and at 2131 and 2220$cm^{-1}$ for $AsH_3$ (Figure 7-8B). In the Raman

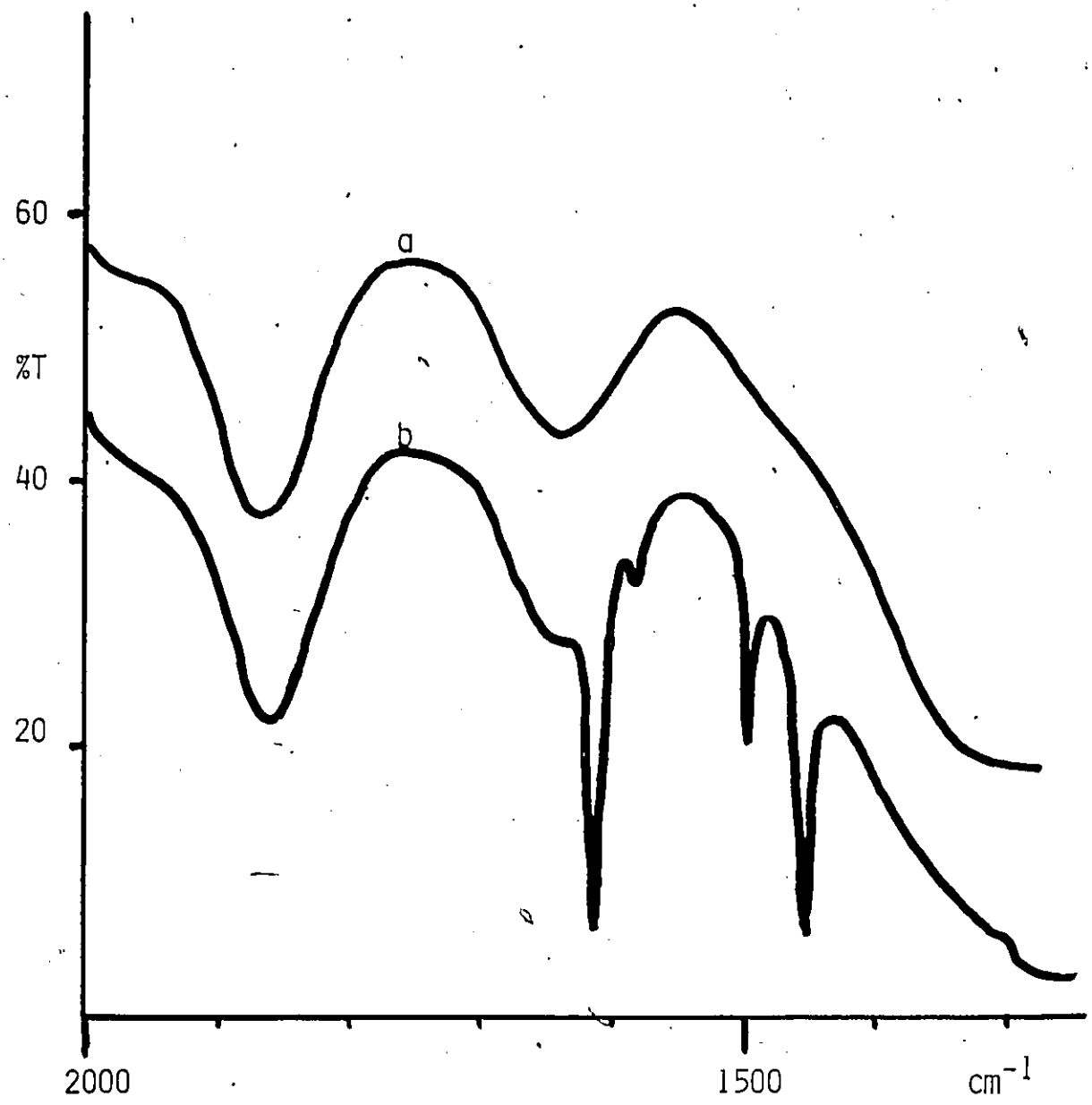


Figure 7-7
a) Infrared spectrum of trimethylgallium treated silica in the region 2000-1300cm$^{-1}$.
b) Spectrum of a) after the addition of 1 torr of pyridine and 14 hrs evacuation at 25°C.
The % T scale refers to b) and a) has been displaced.

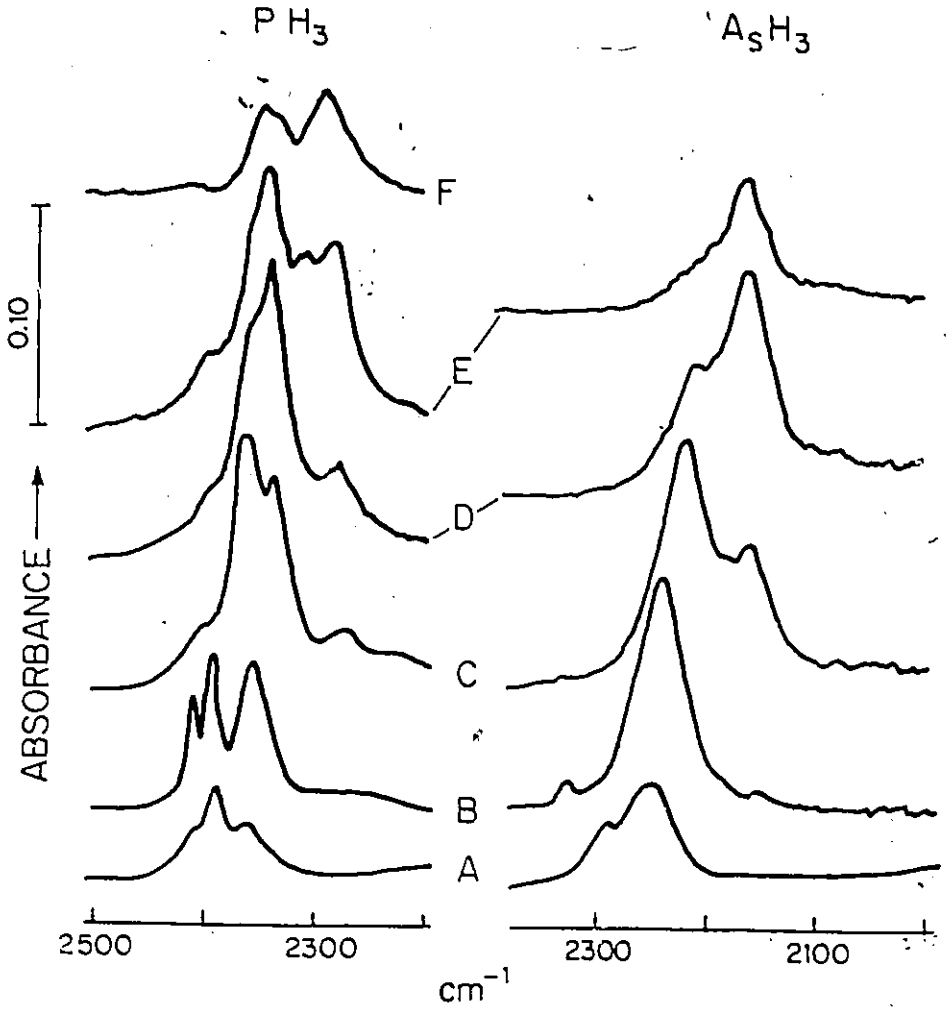


Figure 7-8
A) Raman spectrum observed after adding 15 torr of $PH_3$ or $AsH_3$ to trimethylgallium treated silica
B) Infrared spectrum of a sample similar to A) but after evacuation for 5 min.
C) Infrared spectrum after heating sample B) in the presence of the gaseous hydride at 100°C ($PH_3$) or 125°C ($AsH_3$)
For $PH_3$, curves D, E and F refer to subsequent heating at 200°C for 30 min., 200°C for 18 hrs., and 250°C for 1 hr respectively. For $AsH_3$, curves D and E refer to subsequent heating at 125°C for 18 hrs and 200°C for 4 hrs respectively.

spectrum, the same three bands around 2400cm$^{-1}$ were observed for $PH_3$ with low frequency bands at 290 and 240cm$^{-1}$ while for $AsH_3$ the new bands were at 2180 and 2150cm$^{-1}$ with the corresponding low frequency bands at 270 and 210cm$^{-1}$ (Figure 7-8A). The Raman bands due to $\equiv SiOGaMe_2$ remained virtually unchanged.

Upon heating the sample to 100°C in the presence of $PH_3$ or $AsH_3$ additional amounts of $CH_4$ were generated, there was a substantial increase in the amount of $\equiv SiOH$ regenerated, the bands at 2967 and 2910cm$^{-1}$ diminished and there were additional changes in the P-H and As-H stretching regions (Figure 7-8C). These changes continued upon heating to 200°C, at which stage most of the $-GaMe_2$ had reacted and 60% of the $\equiv SiOH$ originally present before reaction with TMG had been regenerated(Figures7-8D -F). All As-H and Ga-Me IR bandshad disappeared after heating to 250°C in the reaction with $AsH_3$ but in reactions with $PH_3$ the corresponding bands disappeared at 300°C. There were in both cases weak residual bands at 2983 and 2925cm$^{-1}$ which are assigned as in the previous section to $\equiv SiCH_3$ produced by some thermal decomposition of $\equiv SiOGaMe_2$. During the heating of the samples in $AsH_3$ or $PH_3$ the samples had a pale yellow colour at 100°C which developed at 250-300°C into a deep reddish-brown colour which is characteristic of gallium arsenide and gallium phosphide. Raman spectra of the samples during the heating process with $PH_3$ or $AsH_3$ were not obtainable because of the increased fluorescence background created by heating the samples.

The M-H stretching modes of gaseous $PH_3$ and $AsH_3$ are at 2323, 2328 cm$^{-1}$ and 2116, 2123 cm$^{-1}$, respectively, so that new bands observed at 25°C with TMG-$SiO_2$ in the presence or the absence of excess $MH_3$ are due to strongly adsorbed M-H species. Durig et al.[190] have reported the infrared and Raman spectrum of the trimethylgallium-phosphine adduct ($(CH_3)_3Ga:PH_3$) and they have assigned bands observed at 2381 and 2364 cm$^{-1}$ to antisymmetric and symmmetric P-H

stretches and bands at 316 and 279cm$^{-1}$ to the Ga:$PH_3$ rocking mode and Ga-P stretching mode, respectively. By anology with the assignment of Durig, the bands observed with $PH_3$ at 2380, 2368, 290 and 240cm$^{-1}$ are attributed to the above vibrational modes. The IR band observed at 2405cm$^{-1}$ after exposure of TMG-$SiO_2$ to $PH_3$ might be due to a splitting of the doubly degenerate $PH_3$ antisymmetric stretch or an overtone of the $CH_3$ symmetric deformation mode at 1210cm$^{-1}$ which has been intensified by Fermi resonance with the mode at 2380cm$^{-1}$. Further speculation on this point is not warranted. The IR or Raman spectrum of the adduct between arsine and trimethylgallium has not been reported. Nevertheless, a similar assignment to that with $PH_3$ may be made for the Raman bands appearing at 2180, 2150cm$^{-1}$ (2220, 2131cm$^{-1}$ IR) and 270 and 210cm$^{-1}$ after exposure of TMG-$SiO_2$ to $AsH_3$. No speculation is attempted into the reasons for the difference in frequencies of the IR and Raman bands in the 2200cm$^{-1}$ region.

From the above assignments and observations it is clear that an overlapping series of chemical changes beginning with mainly coordinated $MH_3$ at 25°C and ending with GaM at 300°C is taking place. A systematic study of the various changes was not attempted for this reason. Some possible reaction paths are shown below:

(7) $\equiv Si\text{-}O\text{-}GaMe_2 + MH_3 \longrightarrow \equiv SiOGa(Me)(Me) \leftarrow :MH_3$

$\equiv SiOGaMeMH_2 + CH_4$ ; $>GaMeMH_2 + \equiv SiOH$

$\equiv SiOH,\ GaM,\ CH_4$

The gradual changes in the MH stretching region with increasing temperature shown in Figure 7-8 might be due to various -$GaMH_x$ (x = 1-3) species produced in the above reactions. Schyler and Ring[181] have proposed a similar scheme for the

reactions for the systems $GaMe_3/PH_3$ and $GaMe_3/AsH_3$ above 200°C.

Upon the addition of 10 torr of $NH_3$ to TMG-$SiO_2$, new infrared bands (Figure 7-9b) appeared at 3370, 3340, 3290, 3219, 3175 and 1640$cm^{-1}$ and the relative intensities of the 2967 and 2910$cm^{-1}$ bands changed drastically. No methane or ≡SiOH was generated as was observed for $AsH_3$ or $PH_3$. Evacuation of the excess $NH_3$ caused a slight decrease in the intensities of the new bands but no further changes were produced by prolonged evacuation. Upon heating the sample in the presence of ammonia a series of spectral changes was observed (Figure 7-10a-c). The sharp band at 3016$cm^{-1}$ due to $CH_4$ appeared upon heating the sample with $NH_3$ at 100°C but a peak 3745$cm^{-1}$ due to ≡SiOH did not appear until 200°C. As the sample was heated from 100-200°C the 1640$cm^{-1}$ band decreased while a band at 1510$cm^{-1}$ increased, but beyond 200°C the 1510$cm^{-1}$ band began to decrease and new bands appeared at 3450$cm^{-1}$, 1550 and 931$cm^{-1}$. If heating was continued to 520°C, the infrared spectrum showed strong bands at 3748 (80% of its original intensity), 3520, 3450, 1552 and 931$cm^{-1}$ and weak bands at 2983 and 2915$cm^{-1}$ (Figure 7-11). The Raman spectrum of TMG-$SiO_2$ after the addition of 10 torr of $NH_3$ followed by prolonged evacuation showed almost no change except for a new band at 3290$cm^{-1}$ and a shift in the -$GaC_2$ deformation mode at 140$cm^{-1}$ to 165$cm^{-1}$.

Ammonia, like pyridine, is expected to co-ordinate to the electron deficient gallium in ≡SiO$GaMe_2$ via its lone pair of electrons and the infrared and Raman spectra observed after exposure of TMG-$SiO_2$ to $NH_3$ at 25°C can be explained in terms of this. Durig et al.[189] have assigned the IR and Raman spectrum of the trimethylgallium-ammonia adduct and the spectra observed in the present case can be assigned by analogy. The strong IR bands at 3370 and 3290$cm^{-1}$ are attributed to the antisymmetric and symmetric -$NH_3$ stretch (values

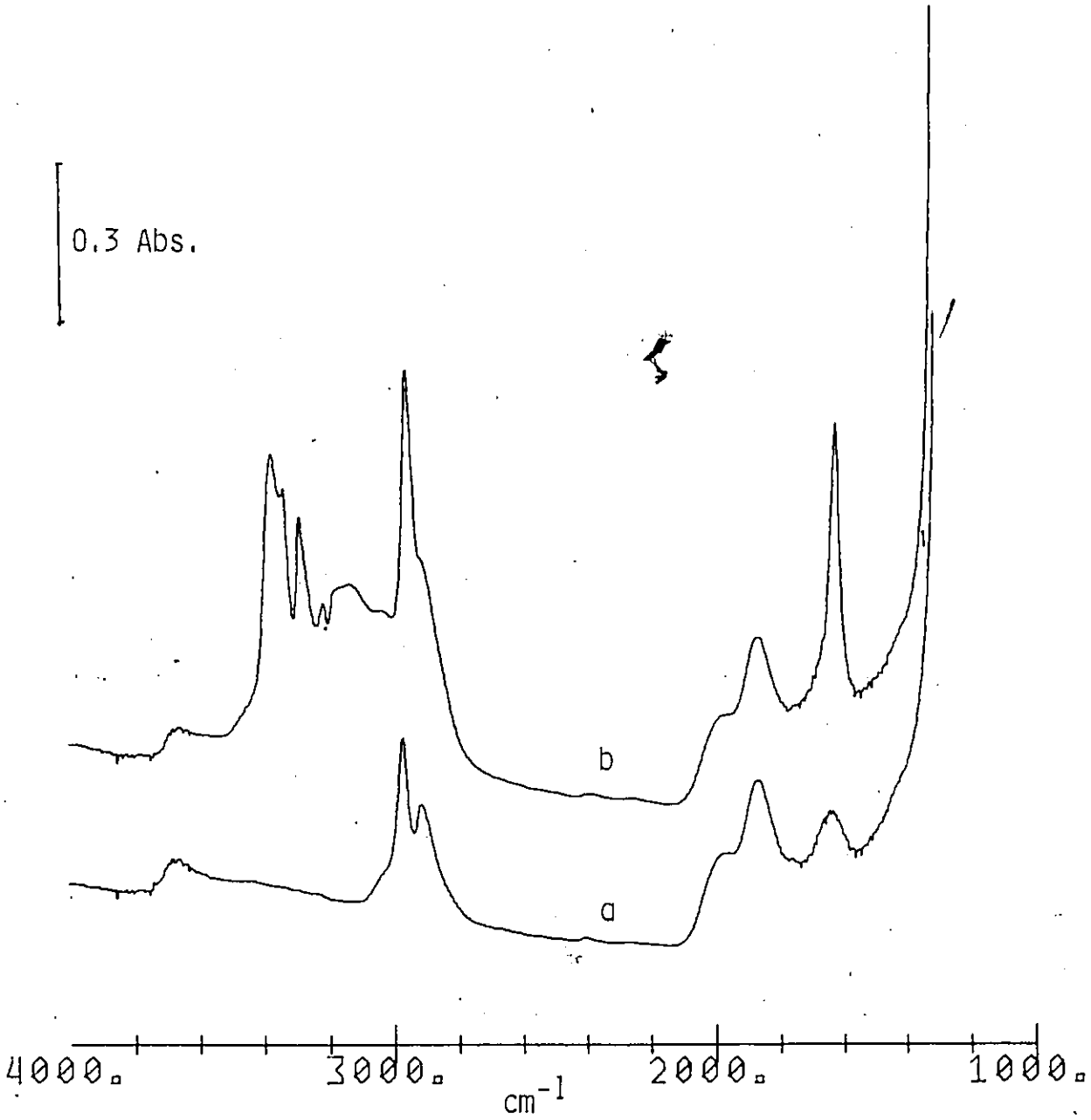


Figure 7-9
a) Infrared spectrum of trimethylgallium treated silica
b) Spectrum after the addition of 5 torr of $NH_3$ to a).

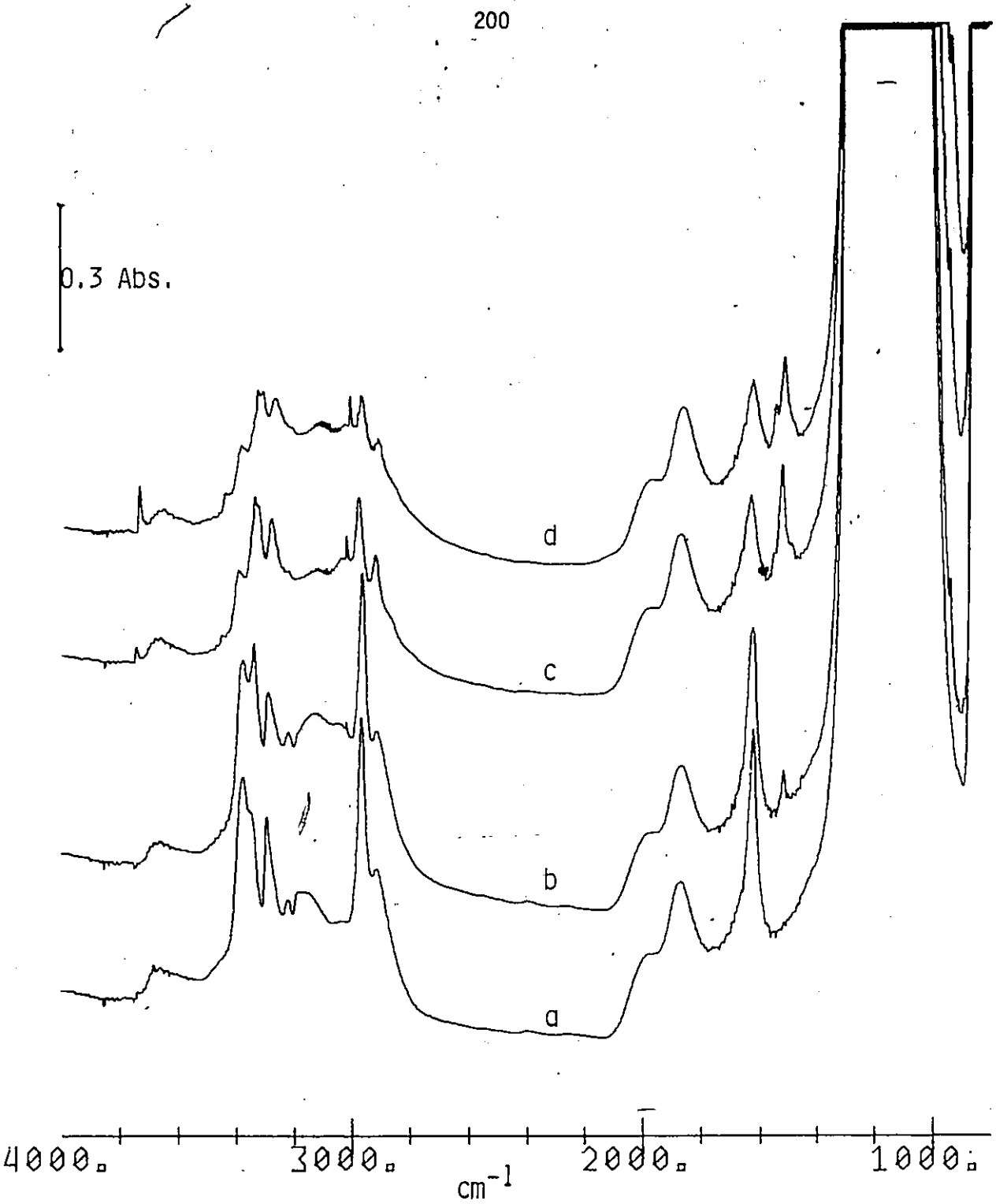


Figure 7-10
a) Infrared spectrum of sample for Figure 7-9b following evacuation at 25°C for 5 min.
b) Spectrum of a) following the readdition of 10 torr of $NH_3$ and heating at 100°C for 1 hr.
c) After heating b) in $NH_3$ at 200°C for 1 hr.
d) After heating c) at 300°C for 1 hr.

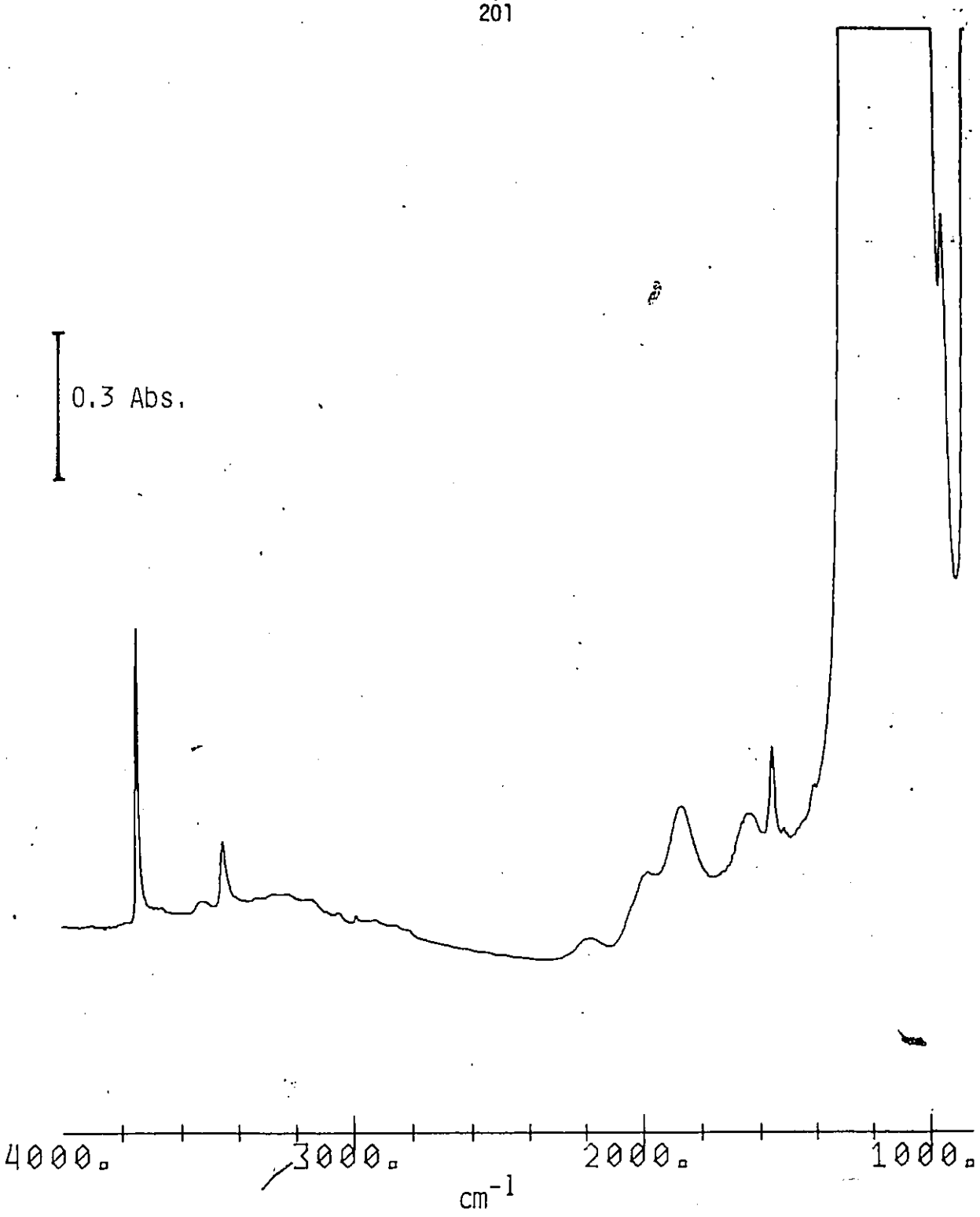


Figure 7-11
Infrared spectrum of the sample from Figure 7-10d after heating in $NH_3$ at 520°C for 14 hrs. followed by evacuation at 520°C for 1 hr.

for gaseous $NH_3$ are 3444, 3337$cm^{-1}$ respectively) while that at 1640$cm^{-1}$ is assigned to the antisymmetric deformation mode. The band at 3219$cm^{-1}$ is quite probably an overtone of the $-NH_3$ antisymmetric deformation at 1640$cm^{-1}$. Durig observed bands for $Me_3Ga{:}NH_3$ at 3348, and 3187$cm^{-1}$ but did not make any assignment of these bands and correspondingly there is not sufficient information to assign the new IR band observed in the present case at 3340 and 3175$cm^{-1}$.

One distinct difference between the reactions of TMG-$SiO_2$ with $NH_3$ from that with either $PH_3$ or $AsH_3$ is that a considerable quantity of $CH_4$ was liberated before any $\equiv$SiOH was regenerated. The next step in the reaction after the coordination of $NH_3$ to form $\equiv SiOGaMe_2NH_3$ therefore appears to be the generation of $CH_4$ and the formation of $\equiv SiOGaMeNH_2$. Further support for this is given by the growth of a new band at 1510$cm^{-1}$ which could be assigned to the antisymmetric $-NH_2$ stretch for the above species and that this 1510$cm^{-1}$ band decreased with an increase in the band due to $\equiv$SiOH. The following reaction scheme is therefore proposed:

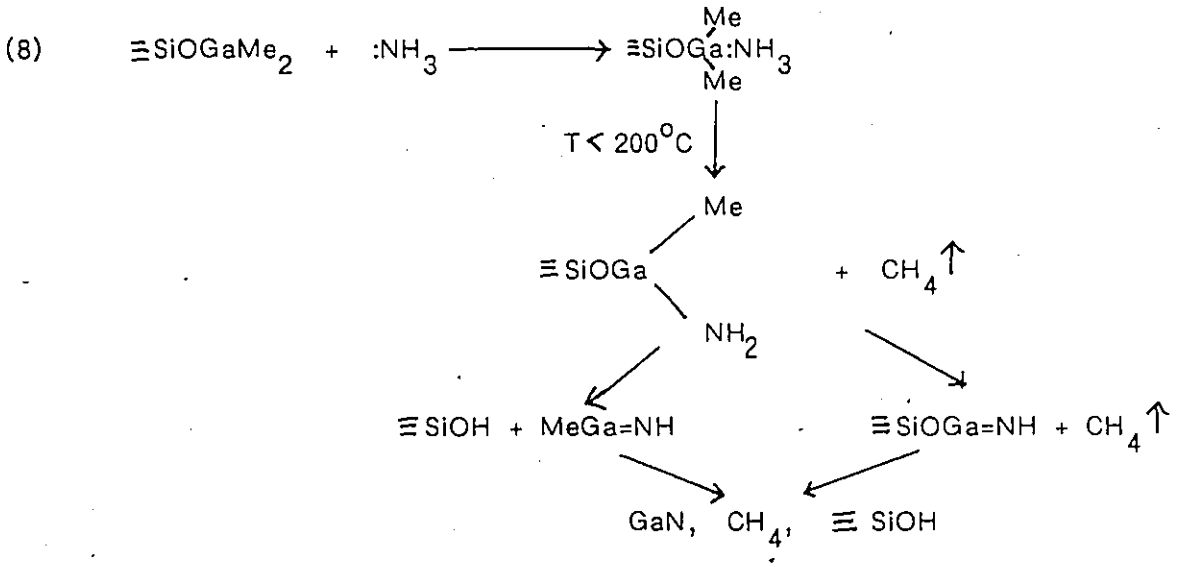


The strong IR bands that remained at 3520, 3400, 1552 and 931$cm^{-1}$ after heating

at 520°C are very characteristic of $\equiv SiNH_2$. This species is known to be formed by the reaction of ammonia with silica at 650°C via the following reaction[130] and it is possible that this reaction was also occuring in the present case.

$$\equiv SiOH + NH_3 \xrightarrow{650^\circ C} \equiv SiNH_2 + H_2O$$

iii) Catalytic Activity of TMG Treated Silica

Gallium oxide is known to catalyze the deuterium exchange and cis-trans isomerization of alkenes[193, 194]. The chemical similarities of gallium oxide to alumina suggest that it might also catalyze the Claus reaction as does alumina[195, 196a,b].

Claus reaction: $2H_2S + SO_2 \longrightarrow \frac{3}{n}S_n + 2H_2O$

Silica treated with trimethylgallium and then hydrolyzed, according to the results presented earlier, would be expected to produce silica with its normal SiOH group and $Ga(OH)_3$, although this latter species has not been positively identified. In any event the silica would contain highly dispersed oxidized gallium of some form, and some preliminary experiments were done to ascertain whether this oxidized gallium catalyzed the deuteration of propene and the Claus reaction.

The sample used in these catalytic studies consisted of silica which had been degassed at 500°C, reacted with trimethylgallium at 25°C and then hydrolyzed at 200°C followed by evacuation at 200°C. For studying the deuteration of propene ($C_3H_6$), 400 torr of a 1:4 mixture of propene and $D_2$ were exposed to the sample at 200°C (which is in the mid-range of temperatures used by Carleton et al.[193, 194] with gallium oxide) for up to 14hrs. The infrared spectra of the sample showed a diminution with time of the $\equiv SiOH$ and $\equiv GaOH$ bands at 3748 and

3650cm$^{-1}$ and a growth in new bands due to ≡SiOD and ≡GaOD at 2765 and 2670cm$^{-1}$. The infrared spectrum of the gas phase showed a decrease in the bands originally present for propene and growth in a band at slightly different frequencies in the C-H stretching region and completely new set of bands around 2250cm$^{-1}$ which are attributable to CD stretches. A mass spectrum of the gas phase showed additional peaks from 1-6 mass units higher than those for propene, corresponding to propene where one to six hydrogens have been substituted by deuterium. A detailed analysis of the gaseous products to determine their structures was not undertaken. It is possible that in addition to deuterated propene some deuterated propane ($C_3H_8$) may also have been produced but this could not be determined. If the trimethylgallium treated silica was hydrolyzed with $D_2O$ to produce SiOD and GaOD and then reacted with only propene at 200°C, first the GaOD was converted to GaOH and then the ≡SiOD to ≡SiOH and partially deuterated propene was detected by IR spectroscopy. This result indicated that the exchange reaction with $D_2/C_3H_6$ mixtures might be occuring via ≡SiOD and ≡GaOD groups generated by exchange of the corresponding -OH species with gaseous $D_2$.

It seems that hydrolyzed trimethylgallium treated silica catalyzes the deuteration of propene. Carleton et al.[193, 194] have reported that the deuteration of propene appeared to involve ≡GaOH with a band at 3650cm$^{-1}$ and its ability to exchange with $D_2$ and $D_2O$, which is in agreement with the above results. The authors, however, did not present any evidence for a direct exchange between the hydroxyl groups and propene. Evidence has been presented here, however, for the direct H/D exchange between propene, ≡SiOD and ≡GaOD. Silica itself was not found to catalyze the deuteration of propene in a $C_3H_6/D_2$ mixture and no ≡SiOD groups were formed. Silica does not undergo H/D exchange with $D_2$ but alumina[111] does, and it might be expected in the present case that GaOH first exchanges with

$D_2$ to produce GaOD which then exchanges with propene.

The reaction of the hydrolyzed TMG-$SiO_2$ with sulphur dioxide ($SO_2$) and hydrogen sulphide ($H_2S$) at 25°C was investigated using infrared and Raman spectroscopies. The addition of 5 torr of $SO_2$ to the sample produced no changes in the infrared spectrum except for the appearance of peaks due to gaseous $SO_2$. The addition of 15 torr of a 2/1 mixture of $H_2S$ and $SO_2$ produced a broad IR band around 3500$cm^{-1}$. The Raman spectrum of the sample did not change upon addition of 5 torr of $SO_2$ but, upon the addition of 3 torr of the 2/1 mixture of $H_2S$ and $SO_2$, strong new peaks appeared at 158, 227 and 480$cm^{-1}$ along with a weaker band at 405$cm^{-1}$ and these bands were not removed by prolonged evacuation at 25°C. The Raman spectrum of a 480°C degassed silica did not change upon exposure under the same conditions to the $H_2S/SO_2$ mixture whereas alumina degassed at the same temperature produced bands identical to those observed using hydrolyzed TMG-$SiO_2$.

Sulphur ($S_8$) is known[196b] to have intense Raman bands at 152. 218 and 475$cm^{-1}$ with weaker ones at 238 and 437$cm^{-1}$ and it appears, therefore, that the Claus reaction producing sulphur is promoted by the presence of oxidized gallium on silica. The broad band observed at 3500$cm^{-1}$ in the IR spectrum after the addition of the $H_2S/SO_2$ mixture might be due to either hydrogen sulphide or $H_2O$ (produced in the Claus reaction) hydrogen-bonded to the ≡SiOH or ≡GaOH groups. These reactions were not investigated to any further depth since the original impetus for this study was only to determine if hydrolyzed TMG-$SiO_2$ exhibited catalytic properties in the deuteration of propylene and the Claus reaction. There was also no convenient way to determine the relative efficiences of hydrolyzed TMG-$SiO_2$ and alumina for the above reactions.

The detailed mechanism for the above reactions have not been investigated. The structure of the adsorbed species produced by $D_2$, $C_3H_6$, $H_2S$ and $SO_2$ on

hydrolyzed TMG-$SiO_2$ is not known and further investigations are needed.

Part II

(I) The Reaction of HCl with TMG-Silica

Upon the addition of 5-10 torr of HCl to TMG-$SiO_2$, within 1 minute the 2967 and 2910$cm^{-1}$ infrared bands of the species $\equiv SiOGaMe_2$ disappeared, a broad band at 3250$cm^{-1}$ appeared with a shoulder at 3550$cm^{-1}$ along with a weak peak at 3748$cm^{-1}$ (approximately 10% of the initial OH intensity before the TMG reaction) due to regenerated $\equiv SiOH$, and a quantity of gaseous methane (sharp IR peak at 3016$cm^{-1}$) equal to that generated in the initial reaction of the silica with TMG was produced (Figure 7-12a). Spectral subtraction of the spectrum immediately after exposure to HCl from that before reaction with HCl (not shown) clearly shows that there was a weak peak at 1613$cm^{-1}$ and a strong one at 955$cm^{-1}$. The subtraction also showed that the peaks at 745, 703 and 606$cm^{-1}$ were replaced by new ones at 758 and 600$cm^{-1}$. Evacuation of the cell at this point reduced the intensities of the bands at 3748 and 3250$cm^{-1}$ and new IR bands also present in Figure 7-12a were more clearly observed at 2990, 2933 and 2913$cm^{-1}$ with very weak bands at 3054 and 2795$cm^{-1}$. Evacuation also removed the weak band at 1613$cm^{-1}$ but the other bands at 955, 758 and 600$cm^{-1}$ remained unchanged.

If HCl was left in contact with TMG-$SiO_2$ for more than 1 minute additional spectral changes occurredslowly over the next 12 hrs. The IR bands at 3748$cm^{-1}$ (15% of the original intensity) and at 3250$cm^{-1}$ increased in intensity, a weak broad band appeared at 2370$cm^{-1}$ and weak bands at 2983 and 2915$cm^{-1}$ assigned to $\equiv SiCH_3$ remained in the $-CH_3$ stretching region (Figure 7-12b). More methane was also evolved in an amount equal to that produced in the first minute, the bands in the 800 to 500 $cm^{-1}$ region disappeared, and strong new bands were

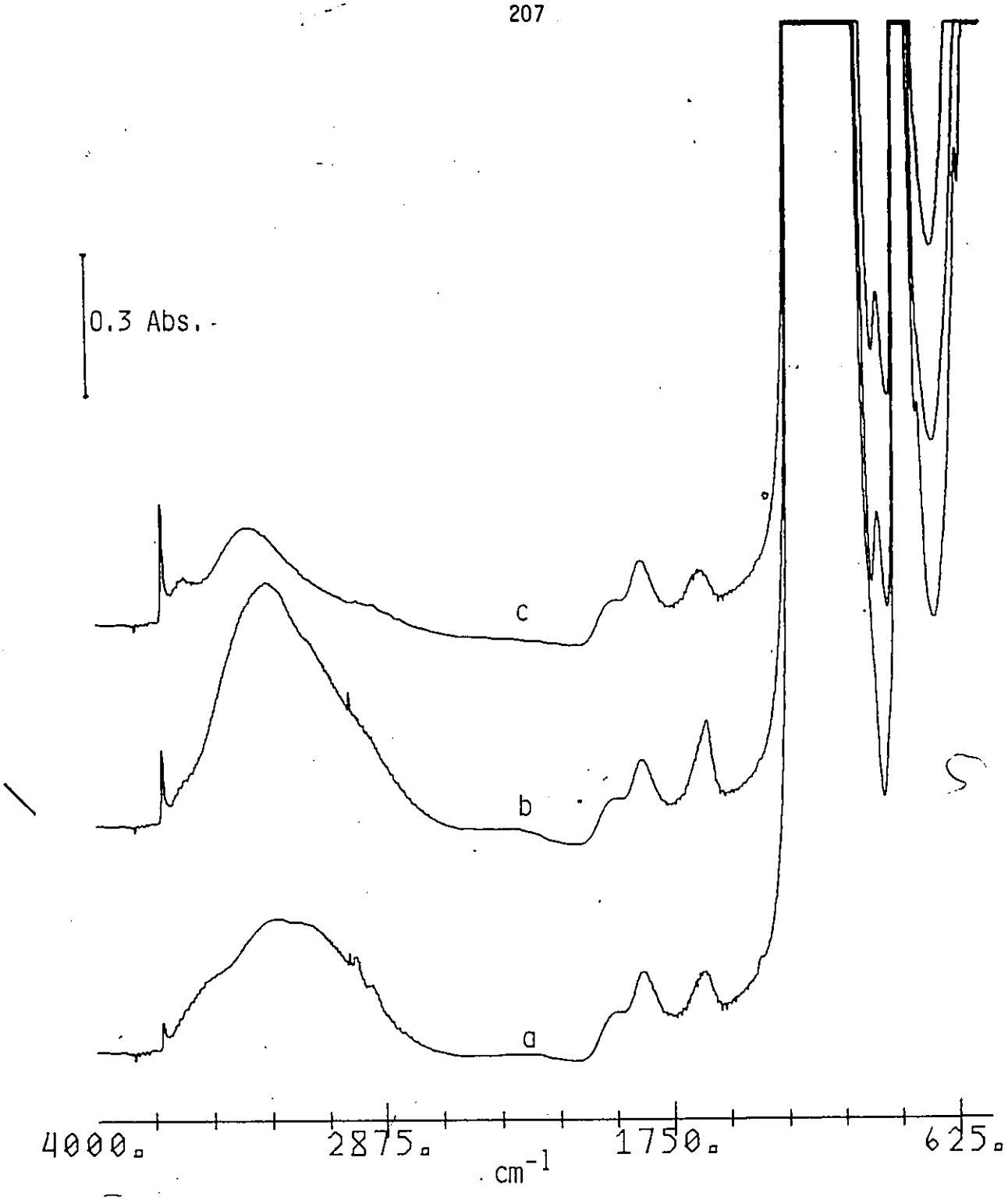


Figure 7-12
a) Infrared spectrum of trimethylgallium treated silica 1 min. after the addition of 5 torr of HCl.
b) Spectrum of a) after 12 hrs exposure to HCl
c) Following evacuation of b) for 1 hr at 25°C.

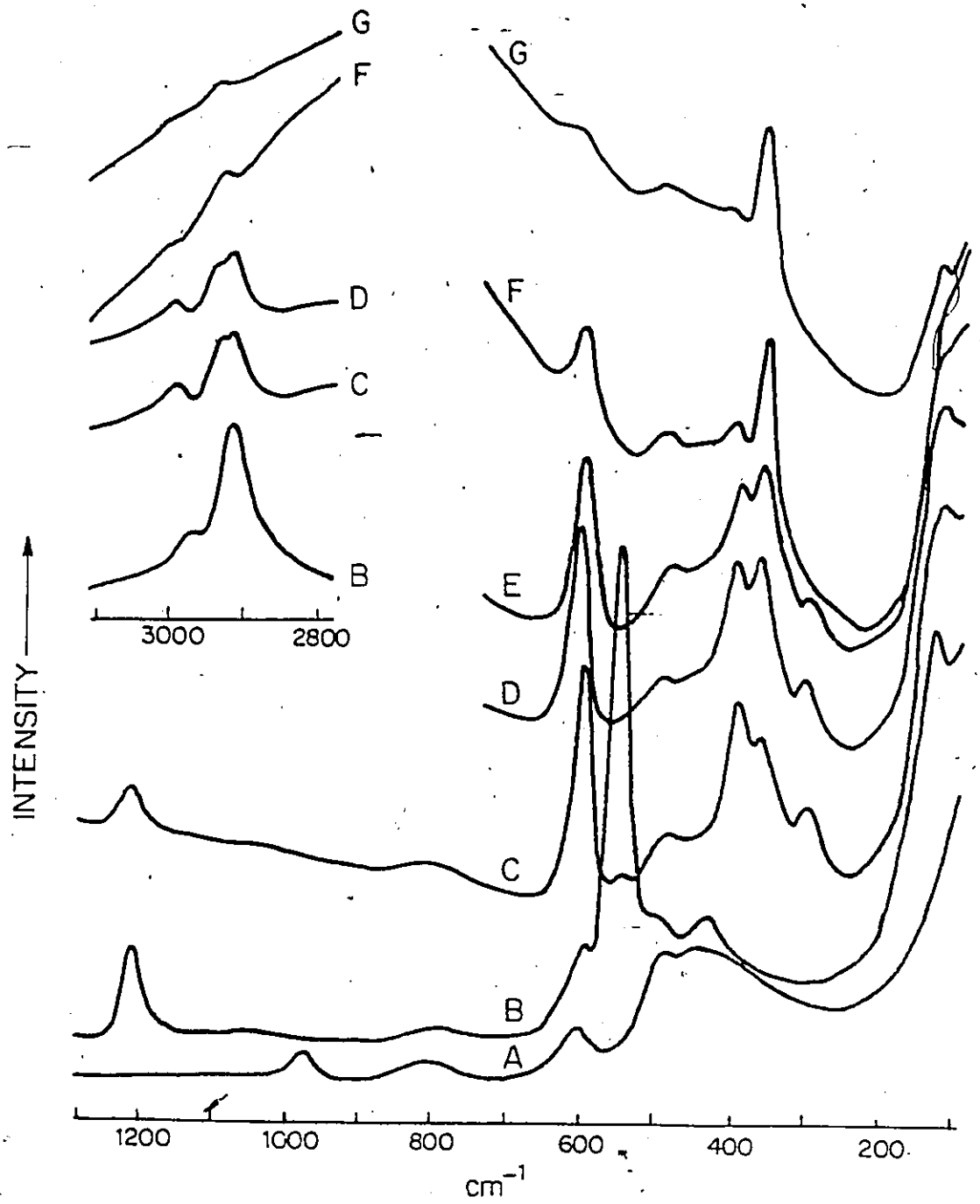


Figure 7-13
A) Raman spectrum of a silica degassed at 500°C for 1 hr.
B) Spectrum of a) after treatment with trimethylgalluim
C) After the addition of 15 torr of HCl to b) for 10 min.
D) 30 min. exposure of c) to HCl
E) 60 min. exposure
F) Spectrum after "heating" e) in the IR beam of the 283 spectrometer for 30 min.
G) After 24 hrs exposure to HCl at 25°C of a sample similar to b).

observed at 1610 and 925cm$^{-1}$.

Evacuation of the gas phase (after 12 hrs exposure to HCl) resulted in a decrease in the intensities of the bands at 3748, 3250, 2370 and 1610cm$^{-1}$ while that at 925cm$^{-1}$ increased. During evacuation for 1 hr the bands at 3250 and 1610cm$^{-1}$ continued to decrease while those at 3748 and 925cm$^{-1}$ increased (Figure 7-12c). After evacuation for 1 hr the 1610cm$^{-1}$ band was not detectable but the 3250cm$^{-1}$ peak continued its steady decline and that at 925cm$^{-1}$ decreased slowly while the $\equiv$SiOH band 3748cm$^{-1}$ continued to grow slowly. Prolonged evacuation eventually return 40% of the $\equiv$SiOH intensity and only a weak band remained at 925cm$^{-1}$ but the band at 3250cm$^{-1}$ was still moderately strong. The changes observed upon the evacuation of HCl were completely reversible. Furthermore, with increasing pressure of HCl from 2-30 torr the IR bands at 3250 and 1610cm$^{-1}$ increased drastically and in unison with the decrease in the band at 925cm$^{-1}$ while that at 3748cm$^{-1}$ increased only slightly. These results indicate that two or more species with IR bands at 3748, 3250, 2370, 1610 and 925cm$^{-1}$ are in equilibrium and that the position of this equilibrium depends on the pressure of HCl.

The Raman spectrum of TMG-$SiO_2$ changed drastically upon the addition of 10 torr of HCl. The $\equiv$SiOGaMe$_2$ bands below 700cm$^{-1}$ were replaced by new ones at 610, 410, 370, 305 and 125cm$^{-1}$ while the band present initially at 1210cm$^{-1}$ shifted to 1230cm$^{-1}$. At this point the band for the symmetric -$CH_3$ stretch for $\equiv$SiOGaMe$_2$ was replaced by a doublet (Figure 7-13b and c). Additional changes over the next 14 hrs are shown in Figures 7-13d - g. The band at 370cm$^{-1}$ grew with time but it is difficult to judge whether the 125cm$^{-1}$ band changed because of the increasing background fluorescence. It was clear, however, that all other bands (including that at 1230cm$^{-1}$ not shown) decreased to zero intensity, leaving

only the bands at 370 and 125cm$^{-1}$. No Raman spectrum following evacuation of the HCl is available because no Raman signals could be extracted from the fluorescence background which grew enormously following the evacuation.

The infrared and Raman studies indicate that there is a fast initial reaction of HCl with TMG-silica producing one molecule of methane per $\equiv SiOGaMe_2$ and that a second, much slower reaction also occurs with HCl to eliminate a second molecule of methane. The fast reaction might be either or both of the following reactions:

(9) $\equiv SiOGaMe_2 + HCl \longrightarrow \underset{III}{\equiv SiOGaMeCl} + CH_4\uparrow$

(10) $\equiv SiOGaMe_2 + 2HCl \longrightarrow \equiv SiOH + \underset{IV}{GaMe_2Cl}$

The infrared and Raman bands from 3000 - 2700cm$^{-1}$ and at 1230, 758 and 600cm$^{-1}$ (760cm$^{-1}$ Raman) may be attributed to the $-CH_3$ stretches, deformation and rocking modes and the Ga-C stretch, respectively, of either species III or IV. Species IV would be expected to be hydrogen bonded to the $\equiv SiOH$ group since this species was not removed upon evacuation. This might also account in part for the broad band at 3250cm$^{-1}$ where hydrogen-bonded OH stretches occur. It is more difficult to rationalize the presence of a broad band at 3250cm$^{-1}$ in the case of species III. Species III could, however, account for the IR band at 955cm$^{-1}$ which could be attributed to the $\equiv Si-O$ stretch of this species. Hydrogen-bonded $\equiv SiOH$ should also have a band in this region due to the $\equiv Si-O$ stretch but it is expected to be much broader than the band observed here.

The Raman bands at 410 and 305cm$^{-1}$ could be GaCl(Me) stretching modes of

either species III or IV. The band at 125cm$^{-1}$ is possibly the superposition of several expected low frequency deformation modes. In the case of species IV the 410cm$^{-1}$ Raman band might be due to the symmetric -$GaCl_2$ stretching mode. Gallium trichloride is a planar molecule with a strong Raman band at 382cm$^{-1}$ for the symmetric $GaCl_3$ stretch and a weak one at 465cm$^{-1}$ for the corresponding antisymmetric stretch[197-199]. These vibrational modes for coordinated $GaCl_3$ are at 360 and 400cm$^{-1}$ [198, 200], respectively, and for $BrGaCl_2$ between 460 and 382cm$^{-1}$ [199, 201]. Gallium trichloride exists as a dimer at 25°C and the Ga-Cl-Ga bridge modes occur near 300cm$^{-1}$ [197, 199]. It might be expected that the band at 305cm$^{-1}$ observed in this instance could be due to dimeric species IV with Ga-Cl-Ga bridges, however, other evidence to be presented opposes this view.

Since there is an equivalence in the amounts of methane evolved in the slow and fast reactions, and since all the vibrational modes for Ga - $CH_3$ disappear completely, the possible reactions in the slow step are:

(11) $\equiv SiOGaMeCl + HCl \longrightarrow \equiv SiOGaCl_2 + CH_4\uparrow$

(12) $\equiv SiOGaMeCl + 2HCl \longrightarrow \equiv SiOH + GaCl_3 + CH_4\uparrow$

(13) $GaMeCl_2 + HCl \longrightarrow GaCl_3 + CH_4\uparrow$

The Raman spectrum observed after completion of the slow step exhibited bands only at 370 and 125cm$^{-1}$. This might support the formation of either $\equiv SiOGaCl_2$ or monomeric $GaCl_3$ since no bands were observed for dimeric $GaCl_3$ at 300cm$^{-1}$. The observation that no dimeric $GaCl_3$ was formed is a strong indication that dimeric $GaMeCl_2$ was probably not formed in the fast reaction and that the band at 305cm$^{-1}$ must be due to some other species. It seems likely, however, that reaction (10) or (12) must occur at some stage since a significant quantity of isolated $\equiv SiOH$ (IR band at 3748cm$^{-1}$) and possibly hydrogen-bonded $\equiv SiOH$ (band

at 3250cm$^{-1}$) were observed.

Thus far no firm assignments of the IR bands at 3250, 2370, 1610 and 925cm$^{-1}$ have been made. An attempt at such an assignment was made by investigating the reaction of deuterium chloride (DCl) with TMG-$SiO_2$. With the addition of 10 torr of DCl to TMG-$SiO_2$ for 14 hrs, $CH_3D$ was produced in the same ratio as $CH_4$ using HCl. A weak IR band at 2765cm$^{-1}$ due to $\equiv$SiOD with a broad band a 2400cm$^{-1}$ were observed along with a moderately strong peak at 925cm$^{-1}$. No infrared bands were observed at 3748, 3250, 2370 or 1610cm$^{-1}$. New IR bands which were observed at 758 and 600cm$^{-1}$ immediately upon the addition of DCl disappeared as they did with HCl after 14 hrs (Figures 7-14a and b). After the reactions with DCl were complete, evacuation of the DCl and $CH_3D$ followed by the addition of a 1:1 mixture of DCl and HCl produced $\equiv$SiOH/D IR bands at 3748 and 2765cm$^{-1}$ along with intense broad bands at 3250cm$^{-1}$ and 2400cm$^{-1}$. A new strong infrared band also appeared at 1418cm$^{-1}$. The observation of a band at 1418cm$^{-1}$ with 1:1 HCl/DCl is the first indication that the bands at 3250/1610cm$^{-1}$ and 2400cm$^{-1}$ might be due to two hydrogens attached to an oxygen i.e. the species is either a protonated hydroxyl group ($-OH_2^+$) or water ($H_2O$). Water has antisymmetric and symmetric stretching modes at 3756 and 3657cm$^{-1}$ respectively and a bending mode at 1595cm$^{-1}$ [202, 203]. The corresponding bands for $D_2O$ are reported at 2788, 2671 and 1178cm$^{-1}$ [203]. The H-O-D bending mode in HDO occurs at 1402cm$^{-1}$, almost midway between that of $H_2O$ and $D_2O$[203]. Thus, the observation of an infrared band at 1418cm$^{-1}$ ((1610 + 1198)/2= 1404cm$^{-1}$) is good evidence for the presence of water. This argument does not negate the possibility of the formation of a protonated hydroxyl group since it would also be expected to have an HOD bending mode near here. However, such a protonated silanol has never been reported. Furthermore, the formation of $\equiv SiOH_2^+$ would also involve the formation of $GaCl_4^-$, which has

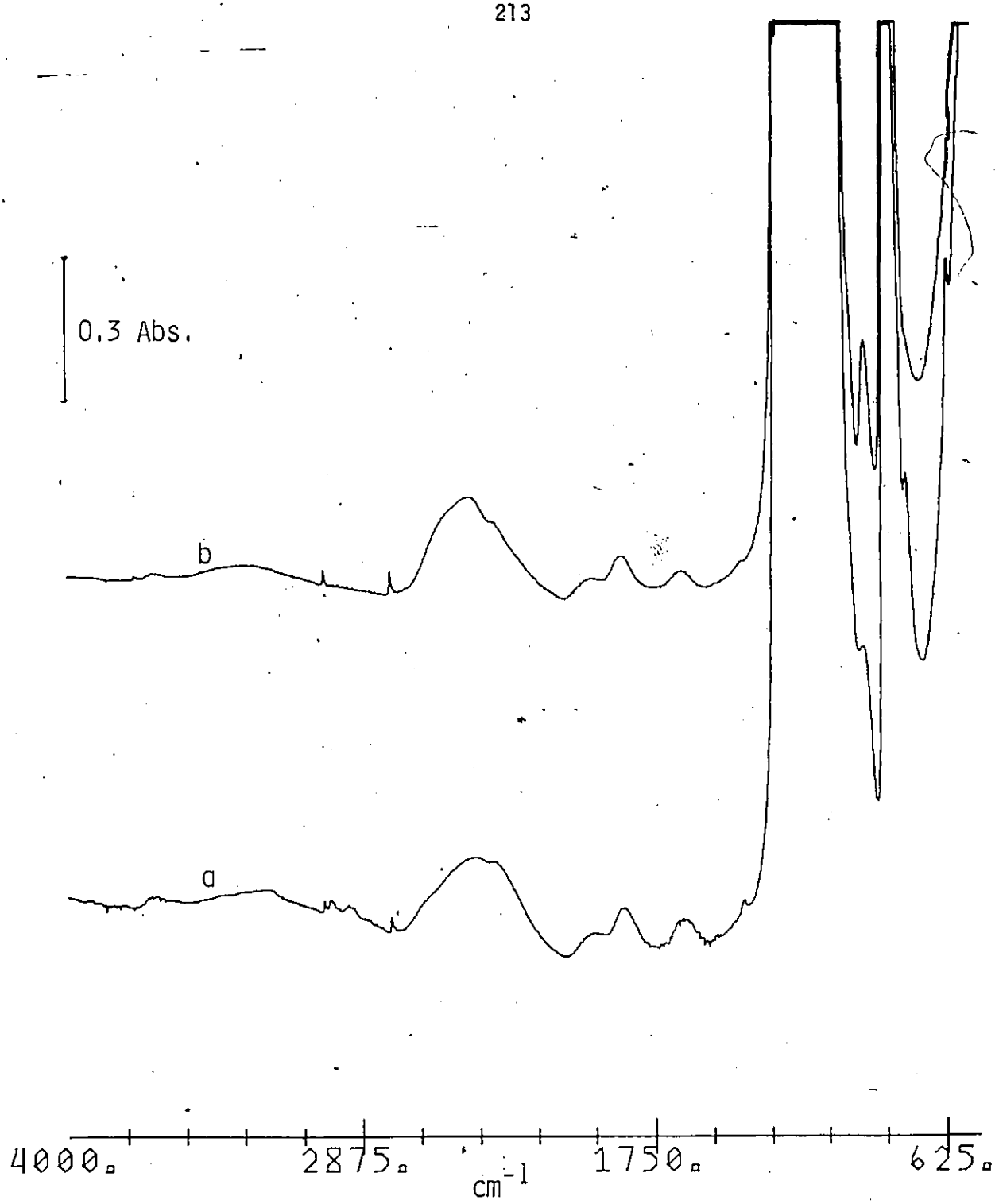


Figure 7-14
a) Infrared spectrum of a silica treated with trimethylgallium, after 30 min. exposure to 10 torr of DCl
b) After 14 hrs exposure of a) to DCl.

completely different Raman bands[205] from those observed here.

In order to determine whether the oxygen atom involved in the $OH_2$ species came from $\equiv SiOGaMe_2$ species formed via $\equiv SiOH$ or from lattice $\equiv Si-O-Si\equiv$ (or if the HCl contained traces of $H_2O$), experiments were performed with silica in which the hydroxyl groups were partially or completely exchanged with oxygen-18 water to yield $\equiv Si^{18}OH$. In the case of the partially exchanged sample the ratio of $\equiv Si^{16}OH$ / $\equiv Si^{18}OH$ observed after reaction of TMG-$SiO_2$ with HCl was the same as that observed before reaction of the silica with TMG. When a completely exchanged silica was used, only $\equiv Si^{18}OH$ was produced after reaction with HCl. The 1610$cm^{-1}$ IR band shifted to 1602$cm^{-1}$ while that at 925$cm^{-1}$ with oxygen-18 shifted to 889$cm^{-1}$. The shift in the band at 1610$cm^{-1}$ to 1602$cm^{-1}$ is of the magnitude expected for $H_2O$ (1595 and 1586$cm^{-1}$, respectively[205a]). The shift in the band at 925$cm^{-1}$ to 889$cm^{-1}$ is that which can be predicted for an $\equiv Si-O$ stretch based on a difference in reduced mass ($\mu$):

$$\sqrt{\frac{\mu SiO^{18}}{\mu SiO^{16}}} = \frac{\nu Si^{16}O}{\nu SiO^{18}} = 1.037 = \frac{925}{892}$$

If HBr was reacted with TMG-$SiO_2$ all the infrared bands due to $Ga-CH_3$ disappeared within 1 minute. Twice as much methane as was generated in the initial reaction of the silica with TMG was produced. The infrared spectrum after the reaction with HBr showed peaks at 3748, 3550, 3280, 1672, 1598 and a weak band at 907$cm^{-1}$. Evacuation of the cell for 10 minutes increased the intensities of the band at 3748 and 907$cm^{-1}$ but diminished those at 3280, 1672 and 1598. As was the case with HCl, the evacuation and re-addition of HBr produced completely reversible changes in the infrared specturm of the sample.

The observed shift in the infrared bands at 925 with $O^{18}/O^{16}$ and Br/Cl

substitutions but no shift with D/H substitution favours the assignment of this IR band to a $\equiv SiOGaX_2$ species (X = Br, Cl). The behaviour of the IR bands at 925, 1600, 3250 and 3748cm$^{-1}$ in the presence or absence of gaseous HX indicates that there might be reversible cleavage of the Si-O-Ga bond and that HX hydrogen-bonds to the species thus produced. A possible reaction might be:

(15) $\equiv SiOGaCl_2 + HCl \text{ (excess)} \rightleftharpoons \equiv Si\text{-}OH \text{ ----} Cl\text{-}H + GaCl_3$

Although HCl does not hydrogen-bond to the $\equiv SiOH$ groups on pure silica, the presence of $GaCl_3$ on the silica surface might make such an interaction possible and could cause the following reaction:

(16) $\equiv SiOH \text{ ----} H\text{-}Cl + GaCl_3 \longrightarrow \equiv SiCl + H_2O{:}GaCl_3$

The species $\equiv SiCl$ would be expected to have an IR band near 712cm$^{-1}$ [205b] but no such band was observed in the present investigation. Roziere et al.[200] have reported that the adduct $H_2O{:}GaCl_3$ exhibits strong IR bands at 3290 and 1615cm$^{-1}$ with a weak band at 2350cm$^{-1}$ assignable, respectively, to the $H_2O$ stretching modes ( 2 bands near 3290cm$^{-1}$), the HOH bending mode, and a combination of the bending and rocking modes of $H_2O$ (the rocking mode was observed as strong band at 770cm$^{-1}$). The authors also report an intense Raman band at 365cm$^{-1}$ with weaker ones at 418, 404, 320 and 169cm$^{-1}$ for $H_2O{:}GaCl_3$. These were assigned, to respectively, the Ga-Cl symmetric and antisymmetric stretches, Ga-O stretch, and the overtone and fundamental of the Ga-Cl deformation. Similar infrared and Raman data were reported by these author for $H_2O{:}GaBr_3$. The observation of Raman and infrared bands in this investigation near those reported for $H_2O{:}GaCl_3$ provides support for the existence of this species produced by the reactions of $\equiv SiOGaCl_2$ with excess HCl (reactions (15) and (16)).

Further support for reactions (15) and (16) comes from a study of the reaction of $GaCl_3$ / $Ga_2Cl_6$ with silica. When silica was exposed to the vapour pressure of solid gallium chloride at 25°C (predominantly $Ga_2Cl_6$ in the vapour phase) the IR band due to isolated ≡SiOH disappeared and an intense band was observed at 940cm$^{-1}$ and two weaker bands also appeared at 1604 and 1416cm$^{-1}$ (Figure 7-15a). No other IR bands were observed and the spectrum did not change upon prolonged evacuation. Upon the addition of 30 torr of HCl to this sample new peaks appeared at 3748cm$^{-1}$, 3320, 1606cm$^{-1}$ and the band at 940cm$^{-1}$ shifted to 925cm$^{-1}$ and was very weak. Exposure to HCl for 14 hrs increased the intensity of the peaks at 3748, 3350 and 1606cm$^{-1}$ while a very weak peak was observed at 917cm$^{-1}$ (Figure 7-15b). Evacuation at 25°C for 1 minute increased the intensities of the bands at 3748 and 917cm$^{-1}$ but decreased those at 3320 and 1606cm$^{-1}$ (Figure 7-15c). The corresponding Raman spectrum exhibited bands at 200, 325 and 415cm$^{-1}$ after evacuation of the excess $Ga_2Cl_6$ (Figure 7-16a). Upon the addition of 25 torr of HCl bands at 370 and 130cm$^{-1}$ appeared and increased in intensity while those at 415, 325 and 200cm$^{-1}$ decreased (Figures 7-16b and c). After 14 hrs exposure to HCl the only peaks remaining were those at 370 and 130cm$^{-1}$.

The changes in the infrared spectrum of silica treated with $Ga_2Cl_6$ and HCl support the assignment of an infrared band near 940cm$^{-1}$ to ≡SiOGaCl$_2$ which might be formed by either reaction (11) or (17).

(17) ≡SiOH + $GaCl_3$ ⟶ ≡SiOGaCl$_2$ + HCl↑

The Raman bands observed at 370 and 125cm$^{-1}$ after the reaction of excess HCl with TMG-Silica for 14 hrs or with $Ga_2Cl_6$ treated silica must therefore be assigned, based on the above evidence, not to ≡SiOGaCl$_2$ as proposed earlier but to $GaCl_3$,

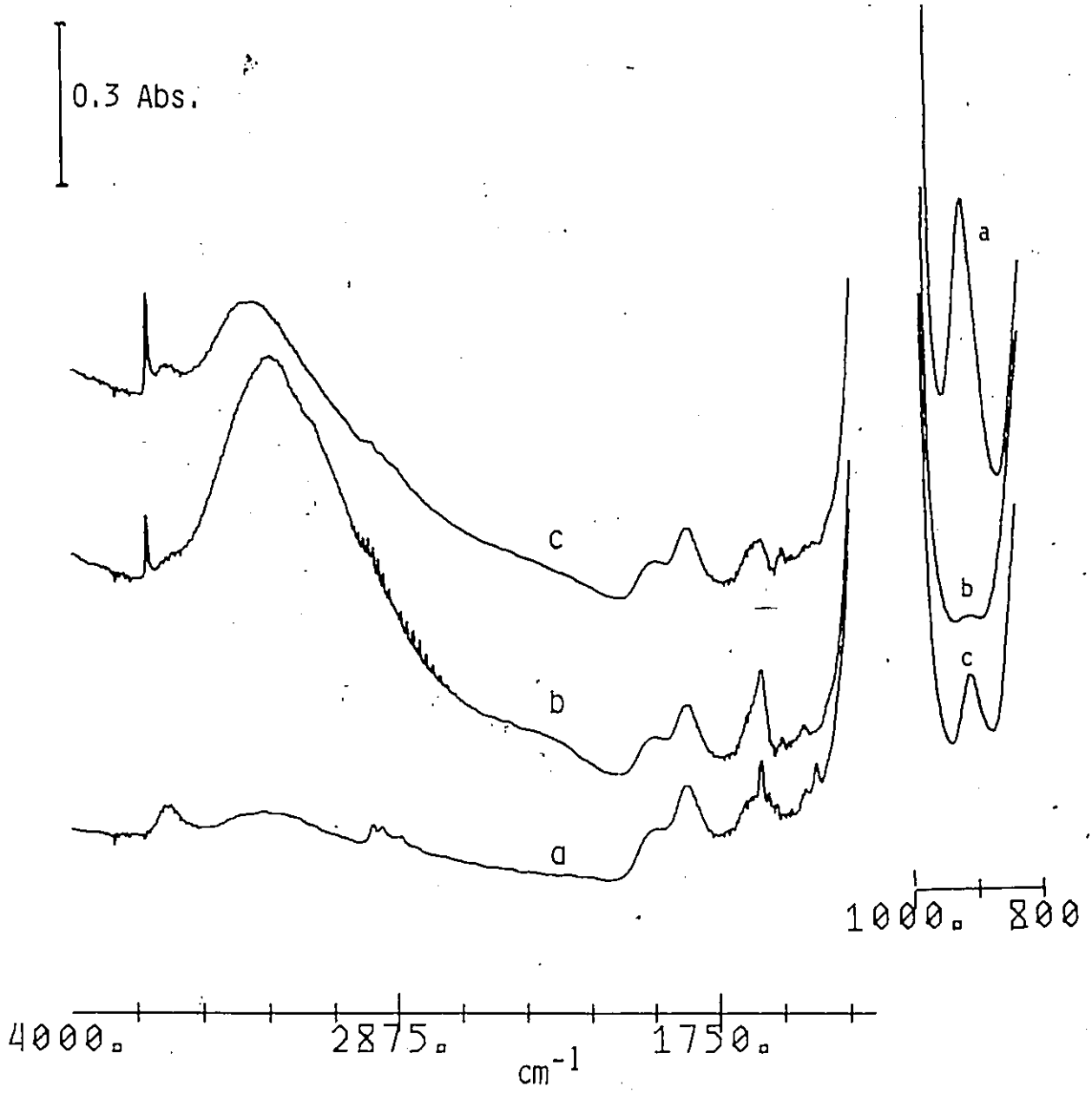


Figure 7-15
a) Infrared spectrum of a silica (7mg/cm$^2$) which had been degassed at 500°C and then exposed to the vapour pressure of solid $Ga_2Cl_6$ at 25°C for 2 hrs followed by evacuation for 1 hr.
b) After exposure of a) to 30 torr of HCl for 14 hrs.
c) Following evacuation of b) for 10 min. at 25°C
Inset shows the region from 1000-800cm$^{-1}$. The bar at left represent 0.3 absorbance for the main curves and 0.8 for the inset.

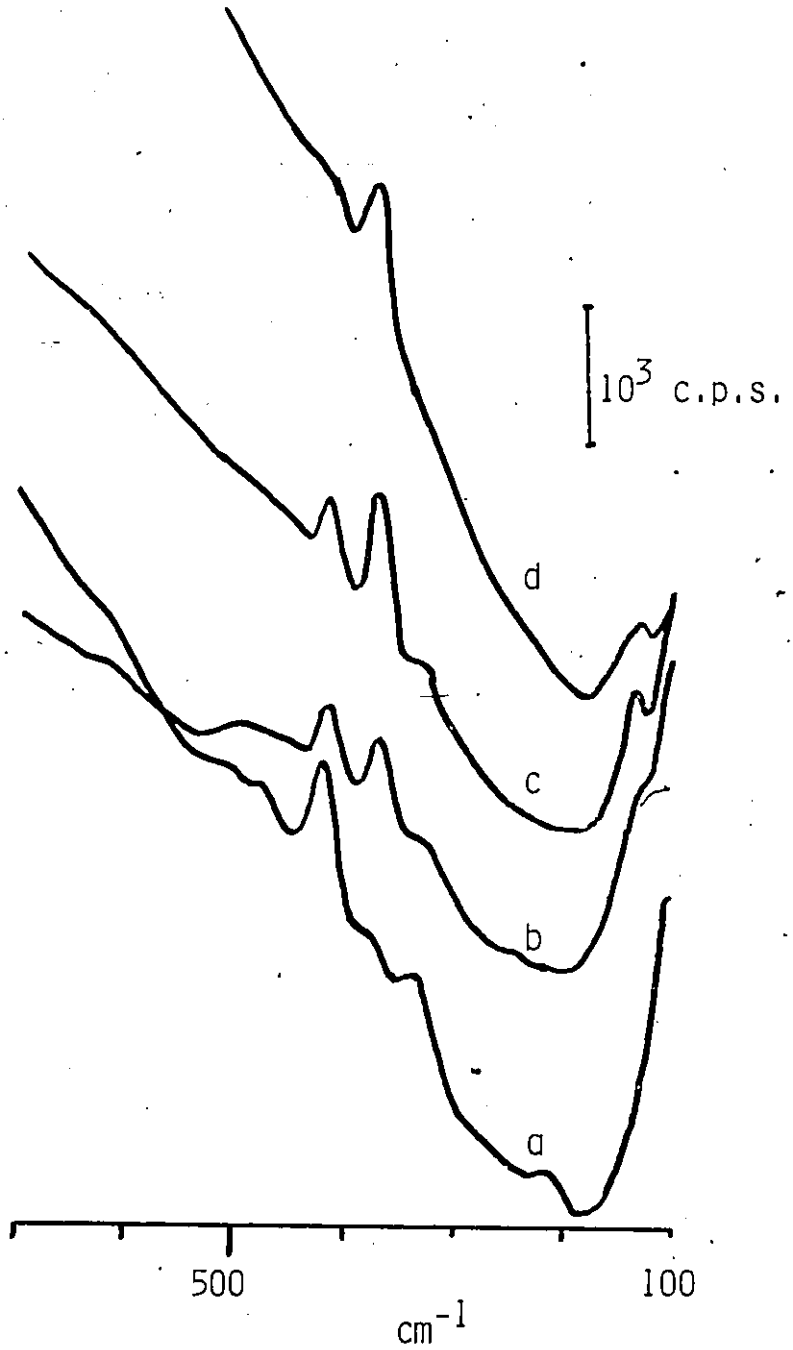


Figure 7-16
The Raman spectrum of a silica degassed at 480°C for 1 hr:
a) After exposure to the vapour pressure of solid $Ga_2Cl_6$ for 1 hr and evacuation for 5 min. at 25°C
b) Following the addition to a) of 25 torr of HCl for 30 min.
c) Exposure to HCl for 5 hrs.
d) Exposure for 14 hrs.

possibly as the adduct with water. The Raman bands observed at 410 and 305cm$^{-1}$ upon the exposure of TMG-$SiO_2$ to HCl are possibly due, therefore, to a mixture of $\equiv SiOGaCl_2$ and $\equiv SiOGaClMe$. Both of these species would be expected to have GaCl(Me) bands between 460 and 300cm$^{-1}$. The very weak Raman bands near 325 and 200cm$^{-1}$ after the reaction of $Ga_2Cl_6$ with silica might be due to some traces of $Ga_2Cl_6$ since the dimer does have bands close to these frequencies. The important observation is the appearance and growth of Raman bands at 370 and 130cm$^{-1}$ with the decline of that at 410cm$^{-1}$ upon exposure of the sample to excess HCl. This is a similar observation to that with TMG-$SiO_2$ and HCl and therefore supports the infrared assignment of a $\equiv SiOGaCl_2$ species which reacts according to reactions (15) and (16) to yield $\equiv SiOH$ and $H_2O{:}GaCl_3$.

Additional experiments were undertaken to examine the apparent propensity for reaction between HX and Ga-O bonds. Hydrogen chloride does not react with degassed silica but if TMG-$SiO_2$ was hydrolyzed and degassed at 200°C to produce $\equiv SiOH$ and $Ga(OH)_3$, the addition of HCl caused an immediate reduction in the intensity of the $\equiv SiOH$ infrared band at 3748 cm$^{-1}$. New IR bands appeared at 3400, 2370, 1690, 1616 and 927cm$^{-1}$ (Figures 7-17a and b). Evacuation of the cell for 5 minutes increased the intensity of the band at 3748cm$^{-1}$ but reduced the others (Figure 7-17c).

The reactions of HCl and HBr with gallium oxide degassed at 400°C are shown in Figures 7-18 and 7-19, respectively. In both instances intense peaks at 3400cm$^{-1}$ and, for HCl at 1694, 1608 and 1068 or for HBr at 1684, 1592 and 1044 were observed after exposure of the oxide to HX for 14 hrs. In both cases evacuation reduced the intensities of the bands at 3400cm$^{-1}$ and completely removed those around 1600cm$^{-1}$ and a strong band remained at 1090cm$^{-1}$. Using DCl, after 14 hrs exposure of the oxide new IR bands appeared at 2540, 1248 and

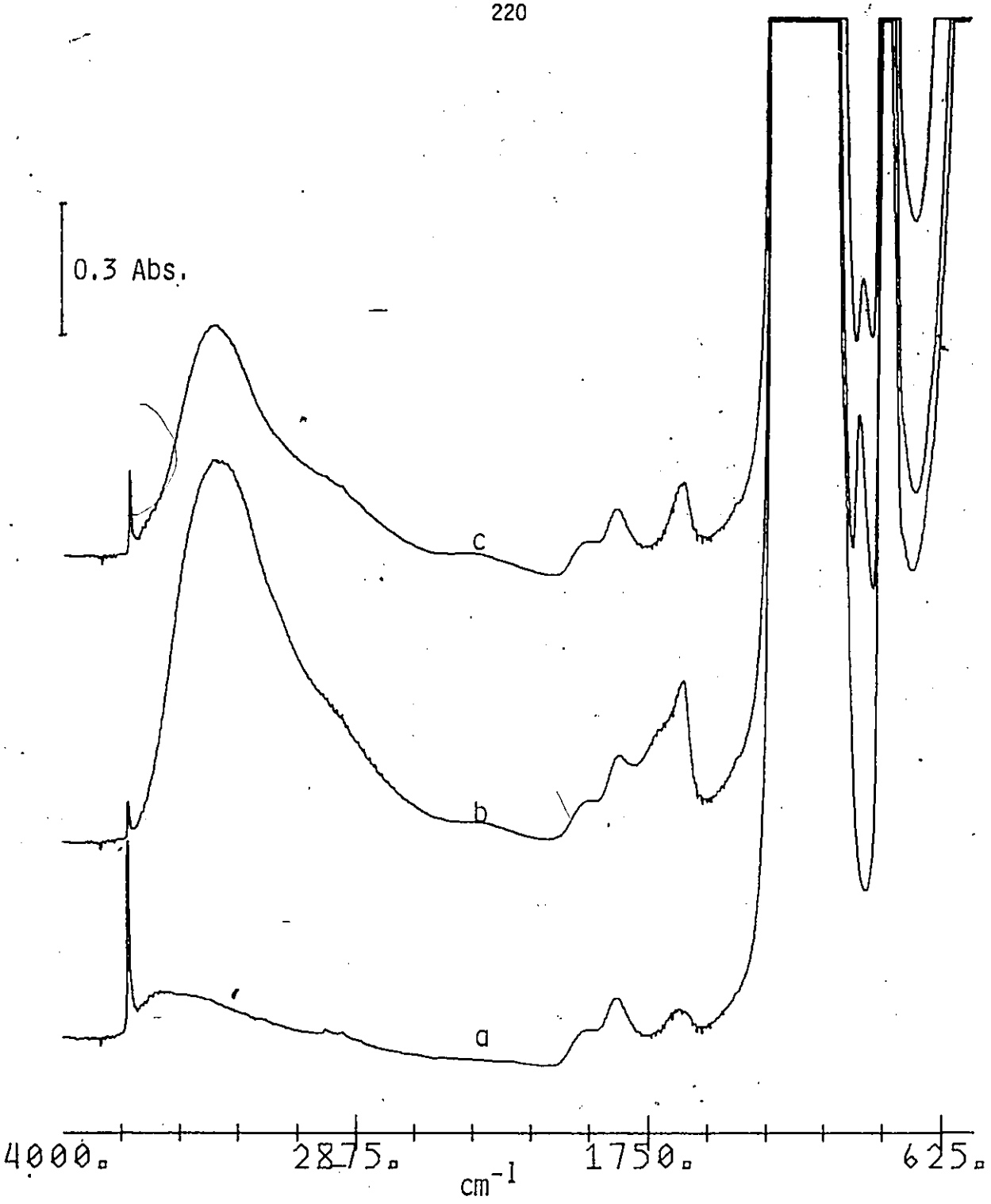


Figure 7-17
a) Infrared spectrum of trimethylgallium treated silica which had been hydrolyzed at 200°C for 14 hrs and then degassed at 200°C for 1 hr.
b) Spectrum following the addition of 10 torr of HCl to a).
c) After evacuation of b) for 35 min.

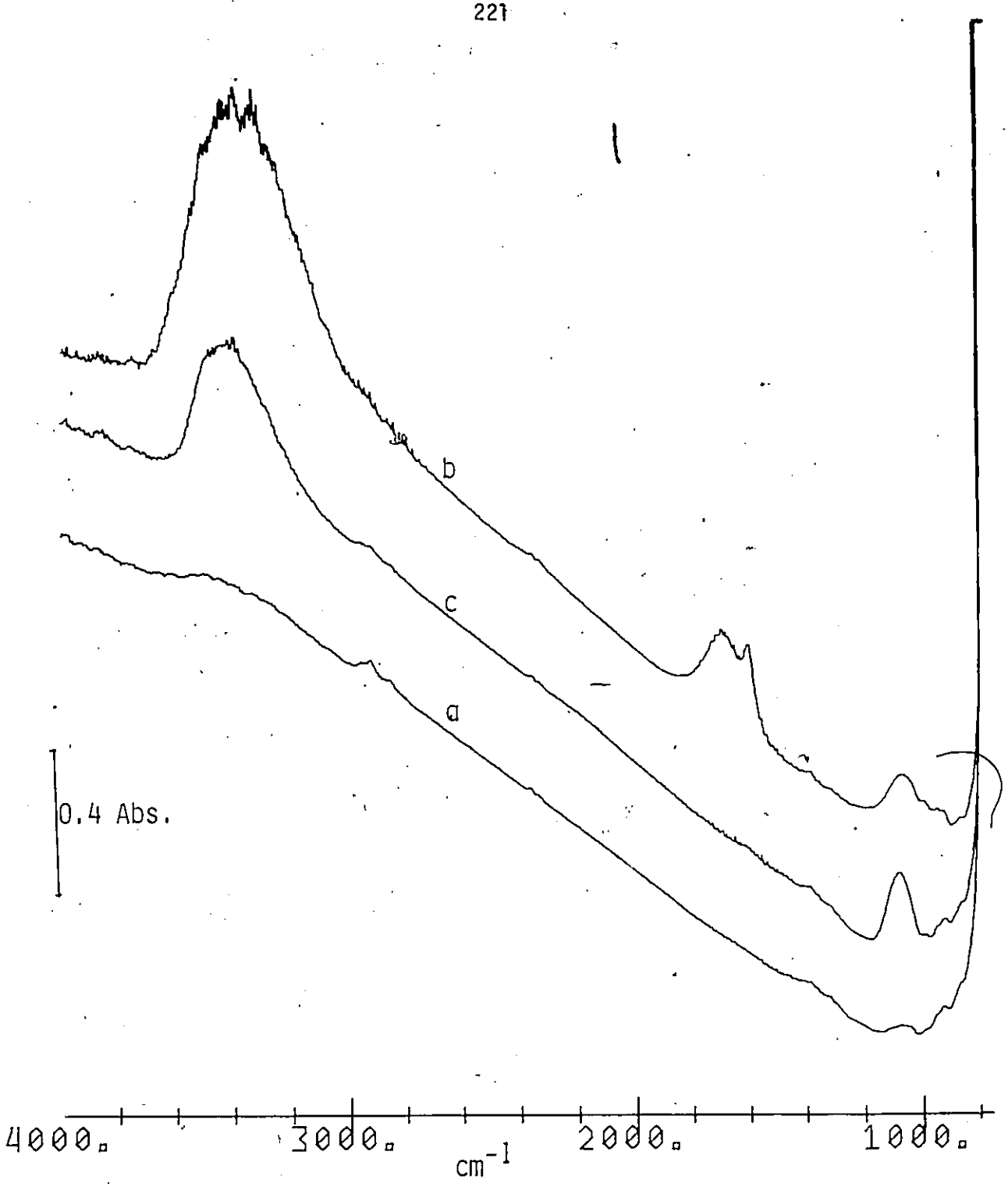


Figure 7-18
a) Infrared spectrum of gallium oxide degassed at 400°C for 1 hr.
b) Exposure of a) to 20 torr of HCl for 14 hrs.
c) Evacuation of b) for 2 min.

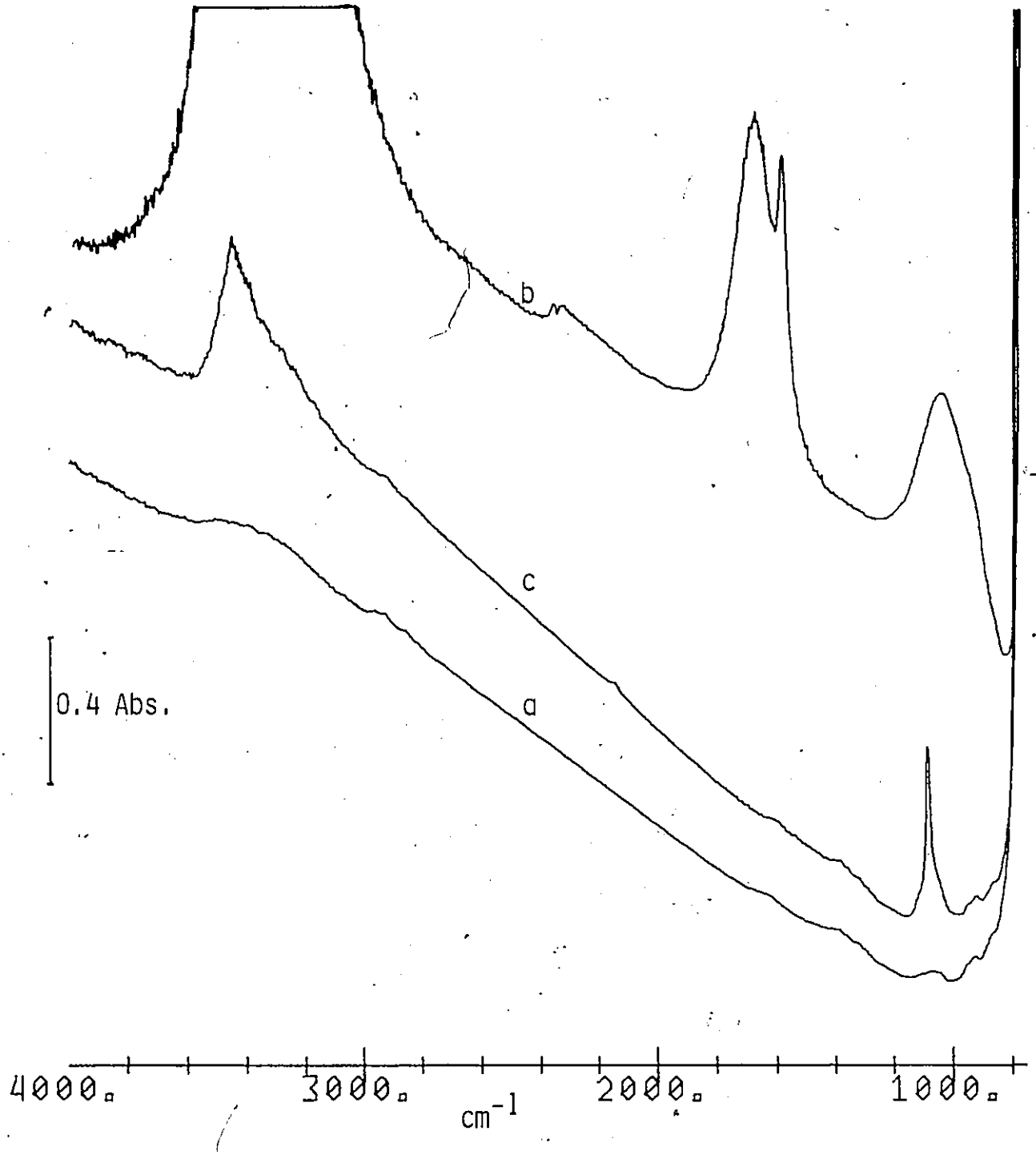


Figure 7-19
a) Infrared spectrum of gallium oxide degassed at 400°C
b) Exposure of a) to 10 torr of HBr for 14 hrs.
c) Evacuation of b) for 5 min. The peak around 3500cm$^{-1}$ is flat-topped because it is totaly absorbing at that point on a 0-2 absorbance scale.

1190cm$^{-1}$. The bands at 1248 and 1190cm$^{-1}$ were removed by evacuation for 1hr while that at 2540 decreased slightly and a new band appeared at 833cm$^{-1}$. A 1:1 mixture of HCl/DCl added to this sample produced new bands at 1468 and 1428cm$^{-1}$. This result strongly supports the assignment of the bands near 3400 and 1600cm$^{-1}$ to $H_2O$ for reasons mentioned earlier, and since there were two HOH deformation bands, it must be assumed that there were two different adsorption sites for water or that there were two forms of adsorbed water (i.e., one form may be more strongly hydrogen-bonded than the other). The observation of a band at 1090cm$^{-1}$ after evacuation of adsorbed HCl in the present case, which shifts with D/H substitution to 833cm$^{-1}$ but not with Br/Cl substitution favours the assignment of this band to the Ga-O stretching mode of a Ga-OH species

The above experiments with gallium oxide treated with HX show that water is generated most likely by cleavage of the Ga-O bond to give $H_2O$ and possibly Ga-X. The appearance of a Ga-X species could not be confirmed because the Raman spectrum of the oxide after exposure to HX had a very large fluorescence background. The reaction of HCl with hydrolyzed TMG-$SiO_2$ illustrates that apart from any reaction of HCl with the surface $Ga(OH)_3$, the presence of the gallium species produced (possibly $GaCl_3$) facilitates an interaction between ≡SiOH groups and HCl.

In summary, the weight of evidence, although not conclusive, indicates that the species ≡$SiOGaMe_2$ reacts within 1 minute with HCl to eliminate one methyl group as methane and that over the next 14 hrs the second methyl group is eliminated as methane. The ratio of methane produced in the reaction of TMG-$SiO_2$ with HCl to that produced in the reaction of TMG with silica was thus found to be 2.0 ± 0.1, which is in agreement with the value of 2.08 reported by Tubis

et al.[184] for the same reaction. Such a ratio is compatible with a reaction of HCl with $\equiv SiOGaMe_2$ to produce either $\equiv SiOGaCl_2$ or $GaCl_3$ and $\equiv SiOH$. Tubis et al. do not report any infrared spectra after reaction of the $\equiv SiOGaMe_2$ surface species with HCl and so their assignment of the species produced to $\equiv SiOGaCl_2$ based solely on methane ratios is not conclusive.

It has been shown in the present investigation that in the reaction of HCl with TMG-$SiO_2$, $\equiv SiOH$ groups were partially regenerated and the surface species $\equiv SiOGaCl_2$ and $GaCl_3$ (the latter being possibly present as the adduct $H_2O:GaCl_3$) were produced. Further, there is a complex relationship between the species $\equiv SiOH$, $\equiv SiOGaCl_2$ and $H_2O:GaCl_3$ and the presence of excess gaseous HCl which may be interpreted in terms of reactions (15) and (16). Support for the above hypothesis was given by an investigation of the behaviour of silica treated with $Ga_2Cl_6$ followed by reaction with excess HCl. In this case the $SiO_2$-$Ga_2Cl_6$ system had a similar behaviour toward HCl as did the TMG-$SiO_2$ system after treatment with excess HCl. While the reaction of HCl with TMG-$SiO_2$ has not been completely elucidated, evidence presented here shows that it is much more complex than indicated by Tubis et al..

(ii) The Reaction of HCN with TMG - Silica

In the studies reported thus far evidence has been presented for the formation of GaN, GaP, GaAs, $Ga(OH)_3$ and $GaCl_3$ produced by the reactions of the corresponding hydrogenous compounds with $\equiv SiOGaMe_2$. Gallium (III) cyanide ($Ga(CN)_3$) does not appear to exist although gallium (I) cyanide has been observed as a short lived species during the high temperature reaction of graphite with gallium and phosphorus nitride[206]. On the other hand, aluminum (III) cyanide has been produced by the reaction of excess HCN with ethereal $AlH_3$

to yield the adduct $(C_2H_5)_2O{:}Al(CN)_3$[207]. Hydrogen cyanide is also known to react with alkylaluminums to produce tetrameric dialkylaluminumcyanide $(R_2AlCN)_4$[208, 209]. Aluminum (I) cyanide has also been prepared under conditions similar to that used for gallium (I) cyanide. The only other compounds with Ga-CN bonds are those such as $K[Me_2Ga(CN)_2]$ formed by the reaction of $GaMe_3$ with $K_2[Hg(CN)_4]$[210]. The aim of the present investigation was to determine whether $-Ga(CN)_x$ (x=1-3) could be formed as a stable entity on the surface of silica via the reaction of HCN with $\equiv SiOGaMe_2$.

Upon the addition of 5 torr of HCN to TMG-$SiO_2$ a weak IR band at 3748cm$^{-1}$ due to regenerated $\equiv$SiOH appeared along with a broad band at 3650cm$^{-1}$ and a small quantity of methane was generated. An intense band was observed at 2203cm$^{-1}$ with a weaker one at 2104cm$^{-1}$ and there was a change in the relative intensities of the bands at 2967 and 2910cm$^{-1}$ (Figure 7-20a and b). Evacuation at 25$^{o}$C removed the IR bands due to HCN, $CH_4$ and that at 2104cm$^{-1}$ but no other changes were observed even after prolonged (1hr) evacuation. Re-addition of 20 torr of HCN resulted, over the next 24hrs, in a steady growth of the $\equiv$SiOH band at 3748cm$^{-1}$ and a broad band at 3500cm$^{-1}$ while the band at 2204cm$^{-1}$ decreased and that at 2104cm$^{-1}$ increased. The intensity of the $-CH_3$ stretches around 2900cm$^{-1}$ decreased and more methane was produced (Figure 7-20c). Again, evacuation removed only the bands due to $HC\equiv N$, $CH_4$ and that at 2104cm$^{-1}$. This band at 2104 cm$^{-1}$ could, however, be restored by the readdition of gaseous HCN. The amount of $\equiv$SiOH regenerated after 24hrs reaction was about 15% of that before addition of TMG and the amount of methane was about the same as that generated by the reaction of the silica with TMG(Figure 7-20d). There was a slight shift in the Ga-$CH_3$ stretching frequencies during the reaction with HCN with the peaks at 2967 and 2910cm$^{-1}$ shifting to 2971 and 2913cm$^{-1}$ with a weak shoulder at 2924cm$^{-1}$. The $-CH_3$ rocking

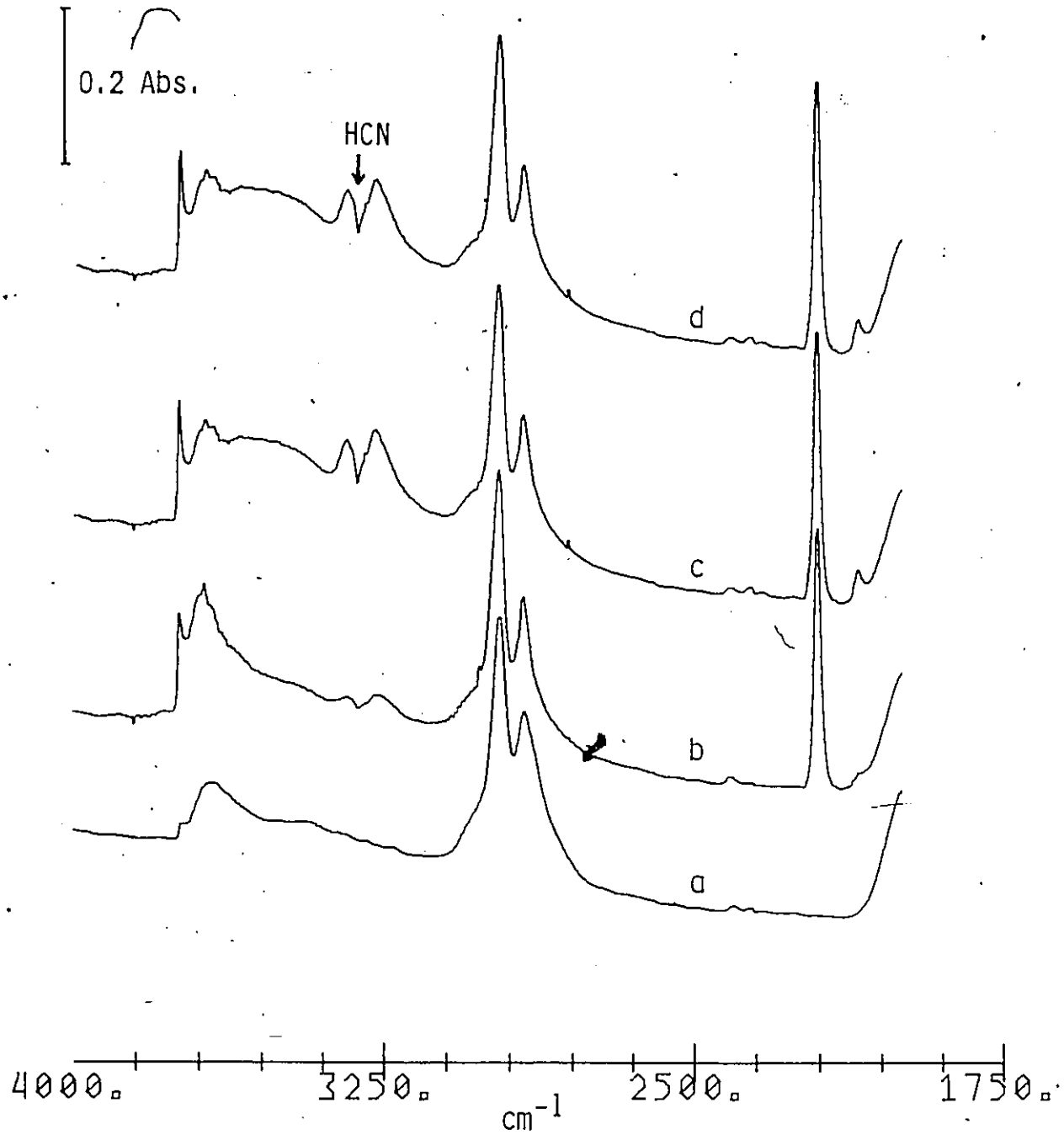


Figure 7-20
a) Infrared spectrum of trimethylgallium treated silica
b) Spectrum of a) following the addition of 5 torr of HCN
c) Evacuation of b) and the readdition of 20 torr of HCN
d) Spectrum of c) after 14 hrs exposure to HCN.

mode at 703cm$^{-1}$ was essentially removed after the addition of HCN but those at 745 and 606 remained virtually unchanged.

The Raman spectrum of TMG-Silica after the addition of 10 torr of HCN showed a decrease in intensity of the bands at 140cm$^{-1}$ and 440cm$^{-1}$ while the band at 610cm$^{-1}$ increased and that at 550cm$^{-1}$ remained unchanged. The bands at 2910 and 2967cm$^{-1}$ appeared unchanged even after 24 hrs exposure of the sample to HCN while the 1210cm$^{-1}$ peak shifted to 1215cm$^{-1}$. New bands also appeared at 2208 and 2105 cm$^{-1}$ and the latter band could be removed by evacuation at 25°C while all other bands remained unchanged.

The infrared and Raman studies indicate that HCN partially reacts with $\equiv SiOGaMe_2$ by two possible slow reactions e.g.,(9) and (10),proposed for the reaction of HCl. The $-CH_3$ profile in the infrared and Raman spectra was different from that observed with HCl after the elimination of one methyl group from $\equiv SiOGaMe_2$. The infrared band at 2204cm$^{-1}$ which appeared initially upon the addition of HCN might be assigned to HCN co-ordinated to gallium through the nitrogen atom. The adduct of HCN and the Lewis acid $BBr_3$ ($HCN:BBr_3$) has a strong infrared band at 2197cm$^{-1}$ which has been assigned to the C≡N stretch[211]. The corresponding C≡N stretches in $K[Me_2Ga(CN)_2]$ are reported[210] at 2138 and 2160cm$^{-1}$ whereas the C≡N stretch in gaseous HCN is at 2097cm$^{-1}$[212]. It therefore seems likely that a band at such a high frequency observed when HCN reacted with $\equiv SiOGaMe_2$ was due to the adduct produced in the following reaction:

(18) $\equiv SiOGaMe_2 + HCN \longrightarrow \equiv SiOGa(Me)(Me) \leftarrow :N\equiv CH$

Such adduct formation had been discussed earlier for $NH_3$, $PH_3$ and $AsH_3$.

It is known that -CN can form a dative bond through the lone pair of electrons on nitrogen to a Lewis acid site, e.g., in tetrameric $R_2AlCN$ mentioned earlier. Because of this adduct formation HCN might be reacting in a similar manner as did $PH_3$ and $AsH_3$ with $\equiv SiOGaMe_2$. Indeed, the $-CH_3$ profile bears some resemblance to that of these compounds coordinated to $\equiv SiOGaMe_2$ and the regeneration of a small amount of $\equiv SiOH$ and $CH_4$ is also consistent with the observations with these compounds. It is obvious, though, that at 25°C the reaction of HCN does not go to completion. Attempts to heat the sample in HCN resulted in a very complicated set of reactions since HCN also reacts with $\equiv SiOH$ groups to produce complex species[213] and so the effect of heating the sample in HCN was not investigated. Finally, the band at $2104cm^{-1}$ is quite close in frequency to that of gaseous HCN itself and its reversible removal upon evacuation is consistent with an assignment to physisorbed HCN. Hydrogen cyanide does not physisorb on silica to a significant extent under these conditions and the growth in this physisorbed species as the reaction with HCN procedes indicates that increased physisorption is being facilitated by the Ga-CN species being produced during the reaction.

It is concluded that HCN first coordinates via the nitrogen atom to the gallium in $\equiv SiOGaMe_2$ and reacts very slowly at 25°C to produce methane and $\equiv SiOH$. The nature of the product containing gallium is not known since the only $C\equiv N$ stretches observed have been assigned to coordinated and physisorbed HCN. However it seems logical that a Ga-CN or Ga-NC species was produced since $CH_4$ and $\equiv SiOH$ were generated. The data obtained do not allow further speculation on this point.

# CHAPTER 8

## THE REACTIONS OF TRIMETHYLGALLIUM WITH ALUMINA

### Introduction

In the previous chapter it was shown that trimethylgallium (TMG) reacted with isolated and hydrogen-bonded hydroxyls on silica to give the same products i.e. $\equiv SiOGaMe_2$ and $CH_4$ but that it reacted with siloxane bridges produced by high temperature dehydroxylation to yield $\equiv SiOGaMe_2$ and $\equiv SiMe$. The present investigation was done to determine if similar reactions occured on alumina involving $\equiv AlOH$ and $\equiv AlOAl\equiv$ groups.

The alumina used was Degussa Alumina Oxid C which, according to the manufacturer's specification, was mainly in the $\gamma$- form. This crystalline material, unlike aerosil silica, has an ordered surface of Al, O and H atoms and, as was previously discussed, the fully hydroxylated surface can possess five distinct types of hydroxyl groups. Dehydroxylation below 400°C proceeds orderly on this crystalline surface to produce weak Lewis acid and base sites while high temperature dehydroxylation proceeds with the migration of hydroxyl groups and anion vacancies to produce stronger Lewis sites.

This investigation asks two questions:

i) Can the different isolated hydroxyl groups be distinguished in their reactions with trimethylgallium, and

ii) how do the Lewis acid and base sites react with TMG and how does the relative acidity or basicity influence the reactions of these sites?

### Experimental

The alumina was used either untreated or calcined in air at 500°C. Discs

having masses of 100mg were pressed in a 2.5cm die at $10^7$Pa, then mounted in the IR cell previously described and degassed at temperatures of 150, 450 or 950°C for 1 hr (Samples A, B and C, respectively). All the infrared experiments were done using the Bomem FTIR. One Raman experiment was performed using 100mg of calcined alumina which was then degassed at 480°C. In all cases the sample was exposed to trimethylgallium at 25°C for 1 minute then evacuated at 25°C for 1 hr.

Results

Figures 8-1a and 8-1b show the infrared spectrum of an uncalcined alumina (Sample A) degassed at 150°C, before and after reaction with TMG. The difference spectrum in Figure 8-2 shows peaks going up, representing new spectral features at 3630, 2962, 2914, 2395, 1417 and 1211$cm^{-1}$ whereas the peak going down at 3735$cm^{-1}$ is due to surface hydroxyl groups which disappeared during the reaction. Figures 8-3a and 8-3b are the corresponding raw spectra for a calcined alumina degassed at 450°C (Sample B) and the difference spectrum is shown in Figure 8-4 New peaks are at 3630, 2960, 2913, 2400, 1430 and 1213$cm^{-1}$ while disappearing peaks are at 3790, 3773, 3730 and 3686$cm^{-1}$. Figure 8-5a and 8-5b show the same sequence of spectra for a calcined alumina which had been degassed at 950°C (Sample C) and the subtraction of 8-5b - 8-5a in Figure 8-6 shows new IR bands at 2963, 2939, 2900, 2836, 1435, 1385, 1214 and weak negative peaks at 3800 and 3730$cm^{-1}$. Figures 8-7a and 8-7b show the Raman spectrum of alumina before and after reaction with TMG. New peaks appeared at 2965, 2915, 1215, 595, 550$cm^{-1}$ and a weak shoulder appeared at 130$cm^{-1}$.

Samples A, B and C after reaction with TMG were hydrolyzed in 18 torr of water at 200°C for 2 hrs and a band at 3016$cm^{-1}$ indicating the presence of gaseous methane was observed. After evacuation at 200°C for 1 hr no bands were

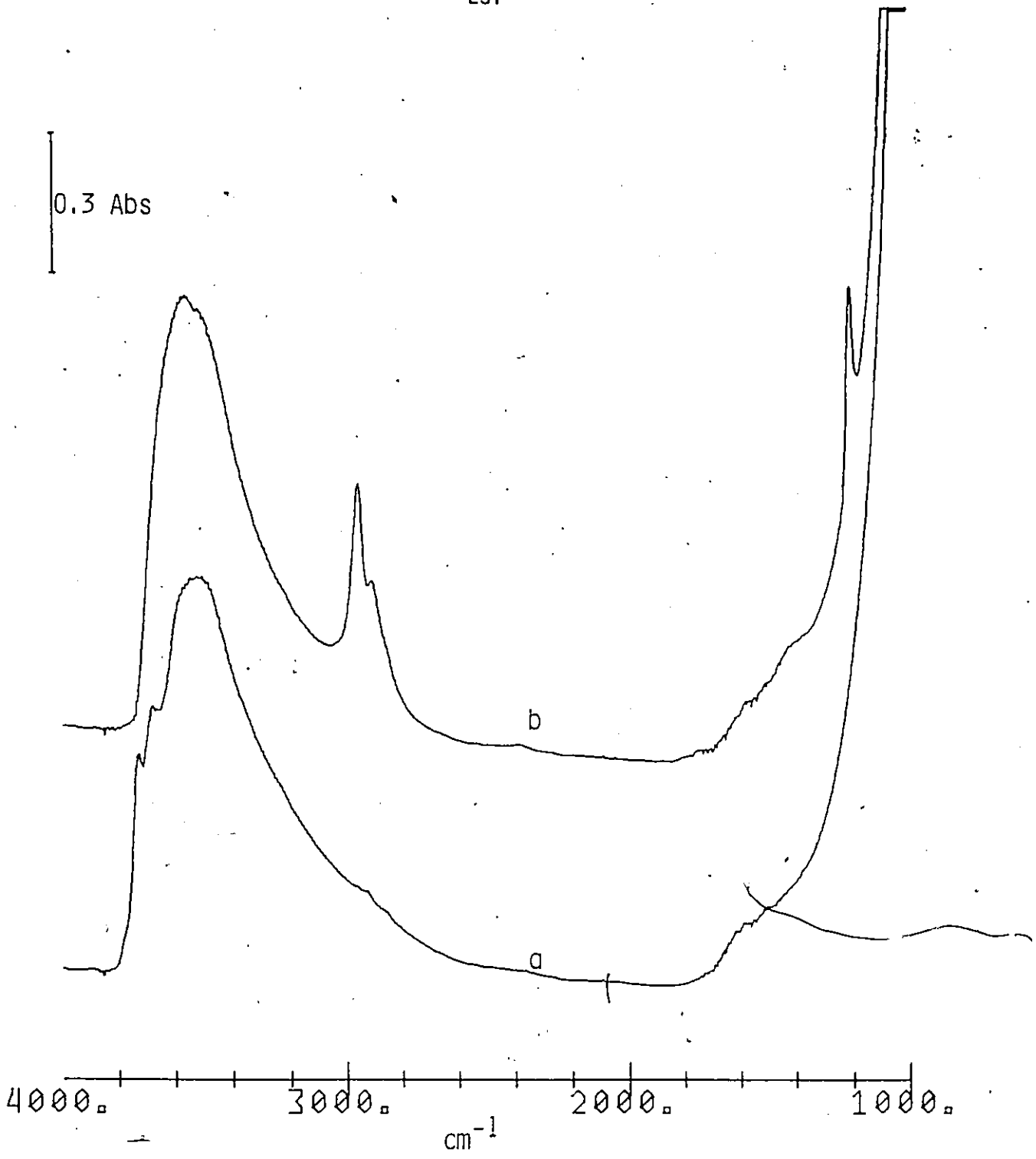


Figure 8-1
a) Infrared spectrum of an alumina degassed at 150°C for 1 hr.
b) After reaction of a) with excess trimethylgallium.

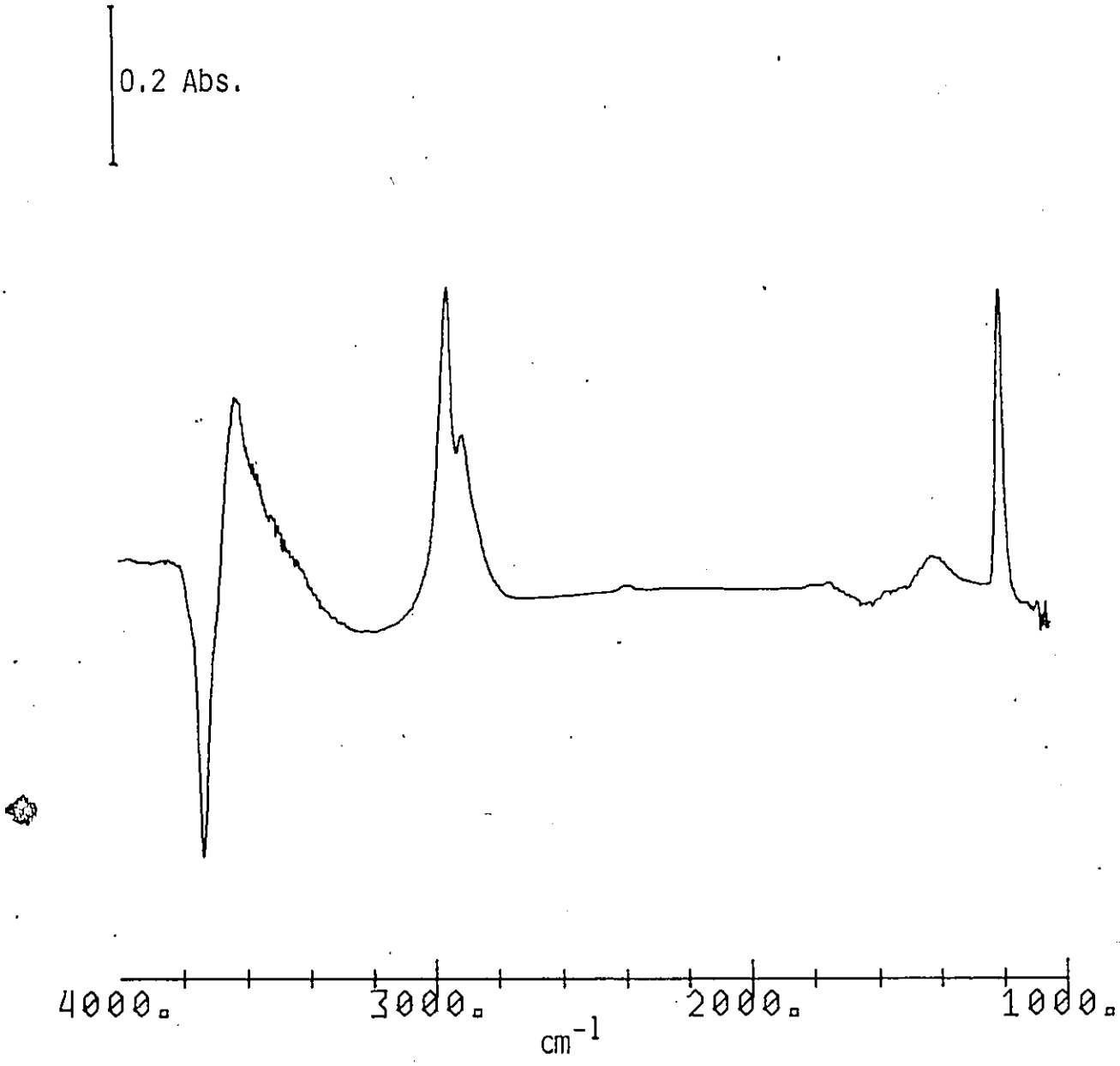


Figure 8-2
Difference spectrum Figure 8-1b minus Figure 8-1a (alumina degassed at 150°C).

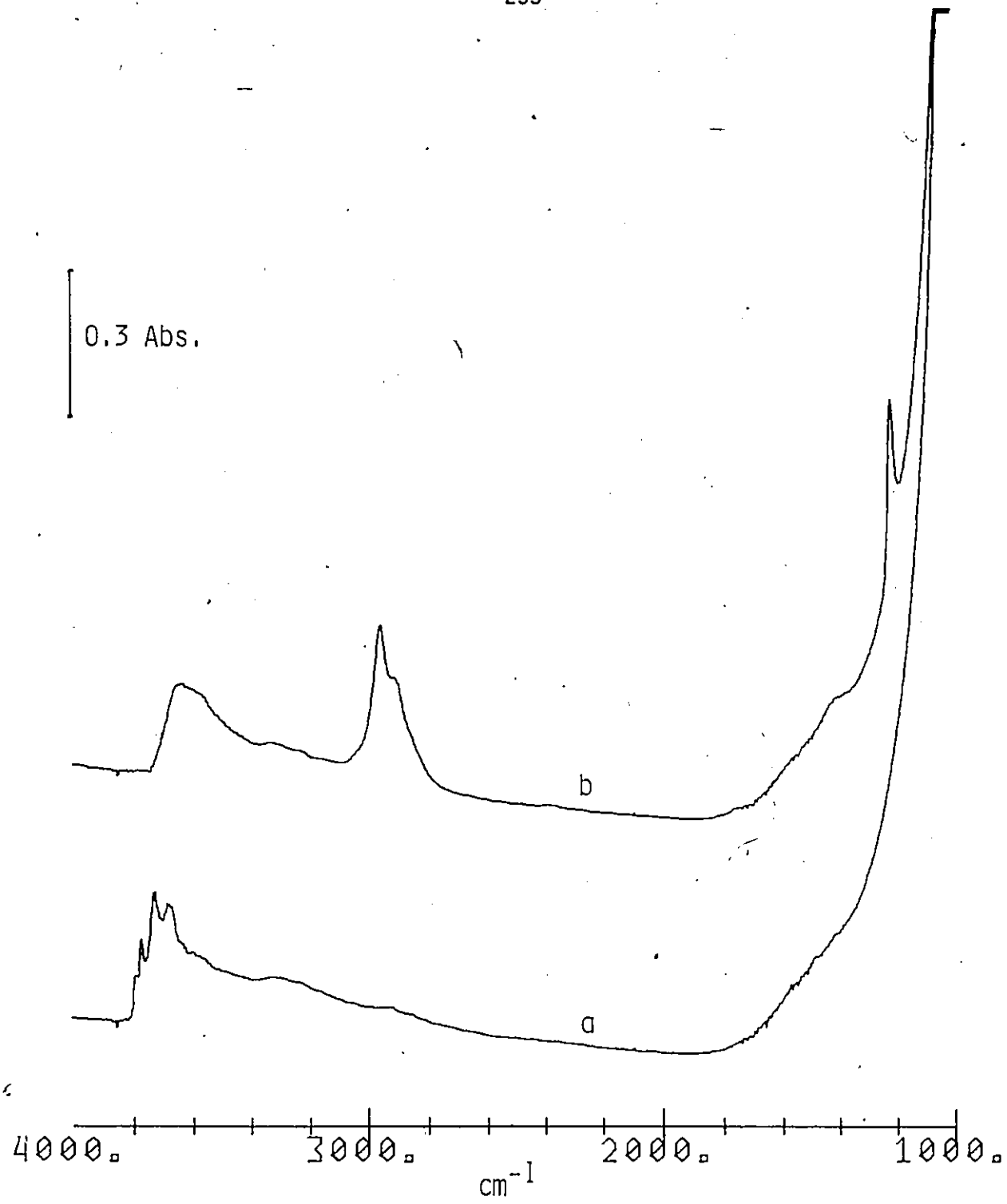


Figure 8-3
a) Infrared spectrum of alumina degassed at 450°C for 1 hr.
b) After reaction of a) with excess trimethylgallium.

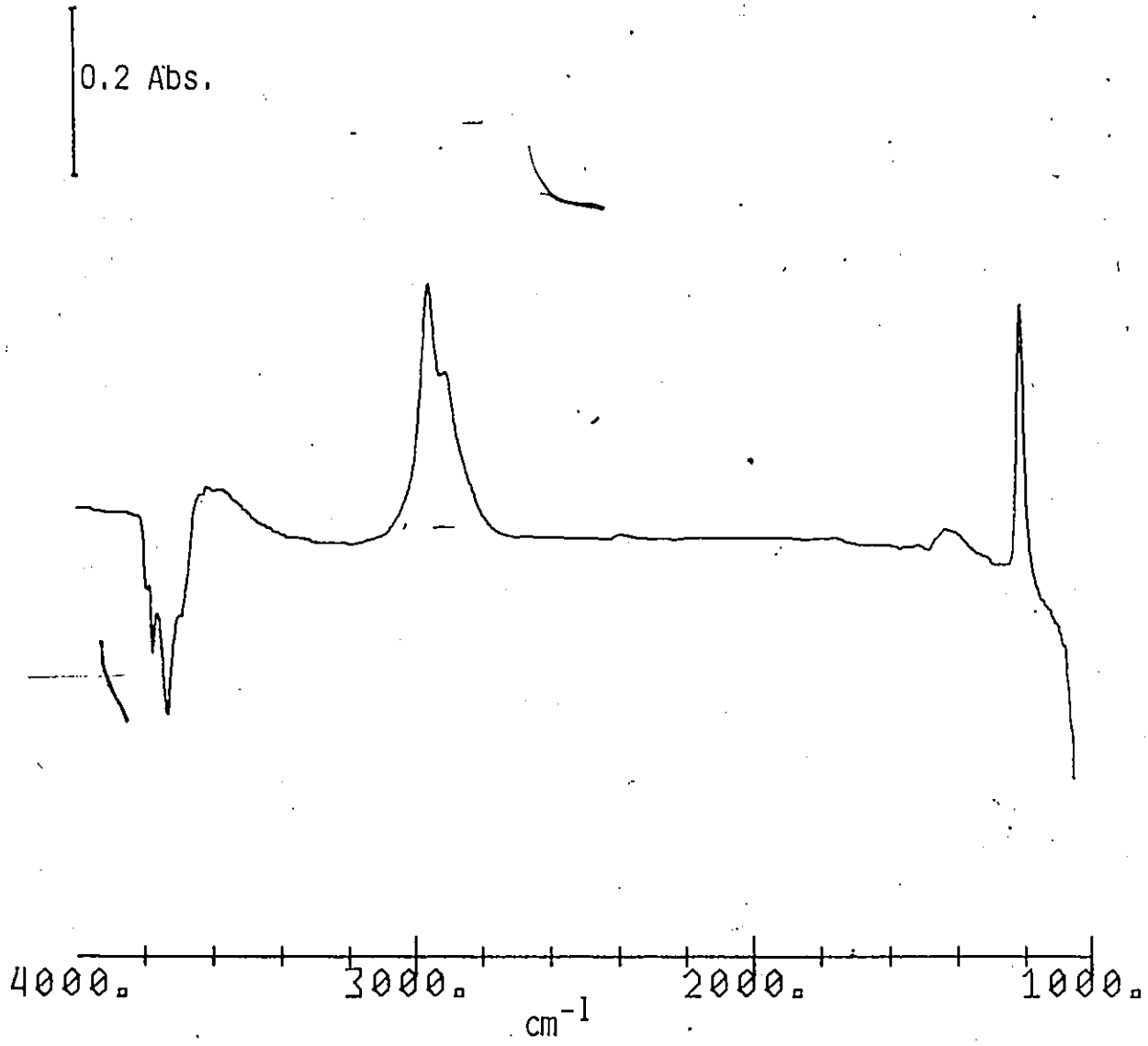


Figure 8-4
Difference spectrum Figure 8-3b minus Figure 8-3a (alumina degassed at 450°C).

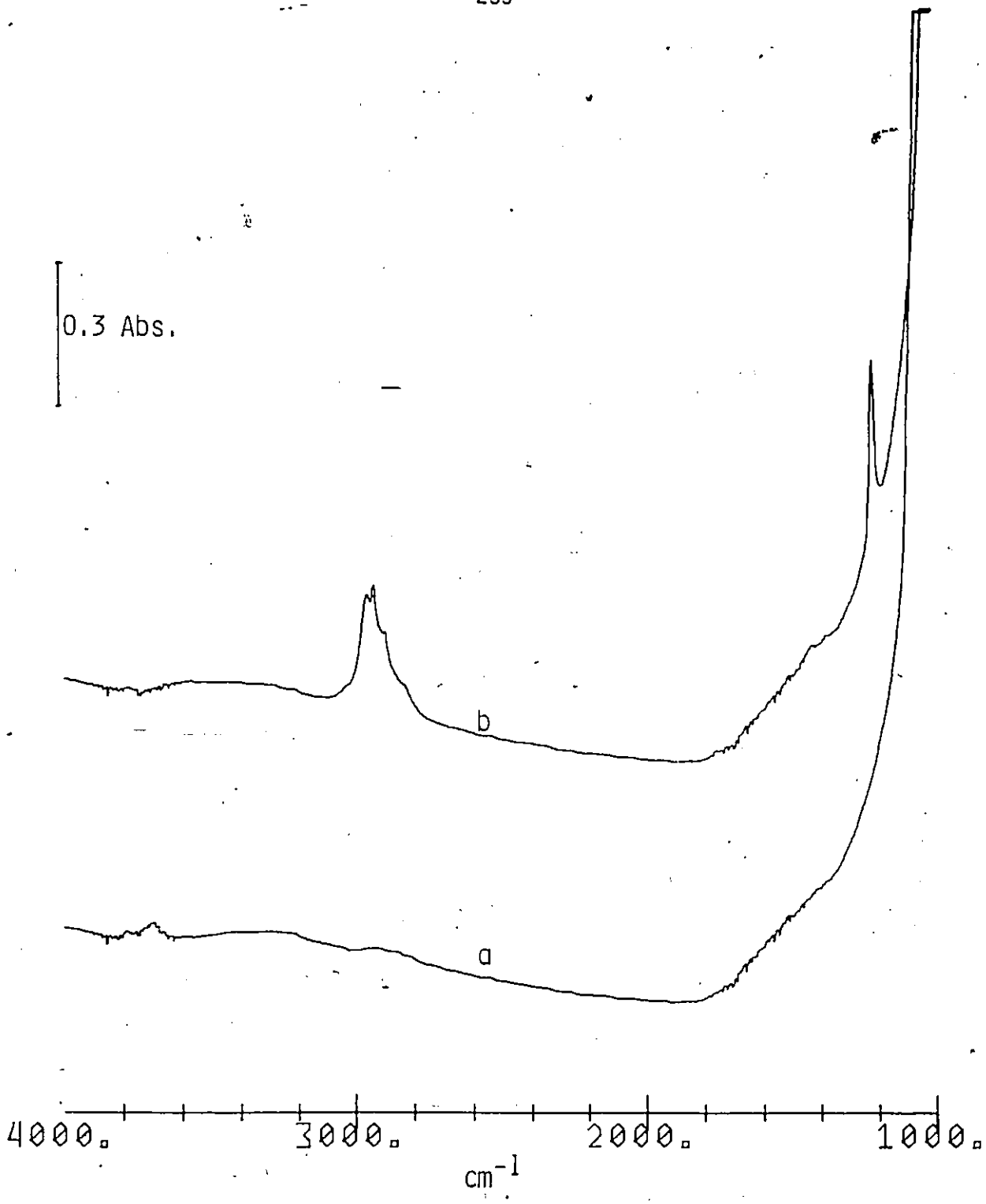


Figure 8-5
a) Infrared spectrum of alumina degassed at 950°C for 1 hr.
b) After reaction of a) with excess trimethylgallium.

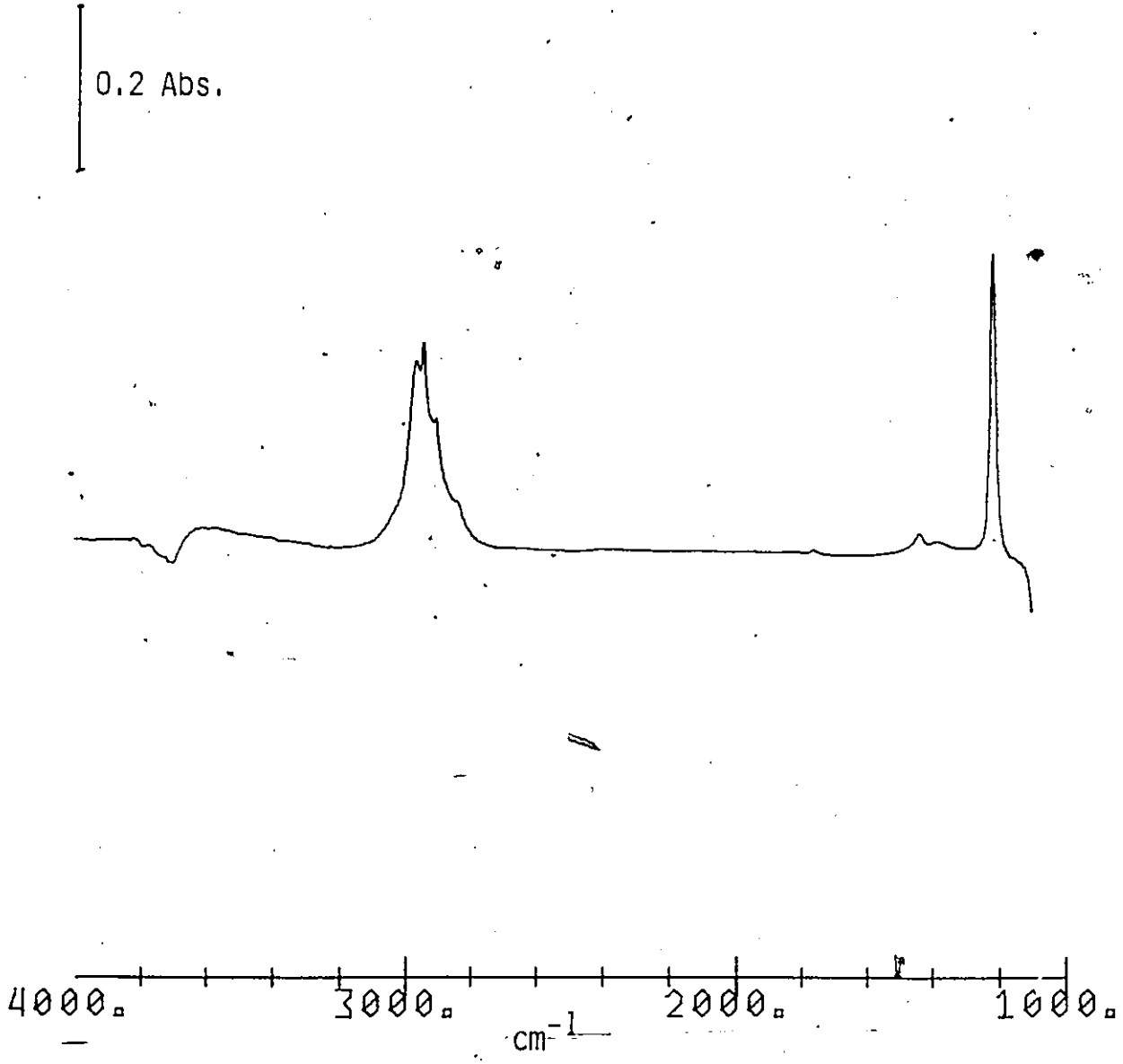


Figure 8-6
Difference spectrum Figure 8-5b minus Figure 8-5a (alumina degassed at 950°C).

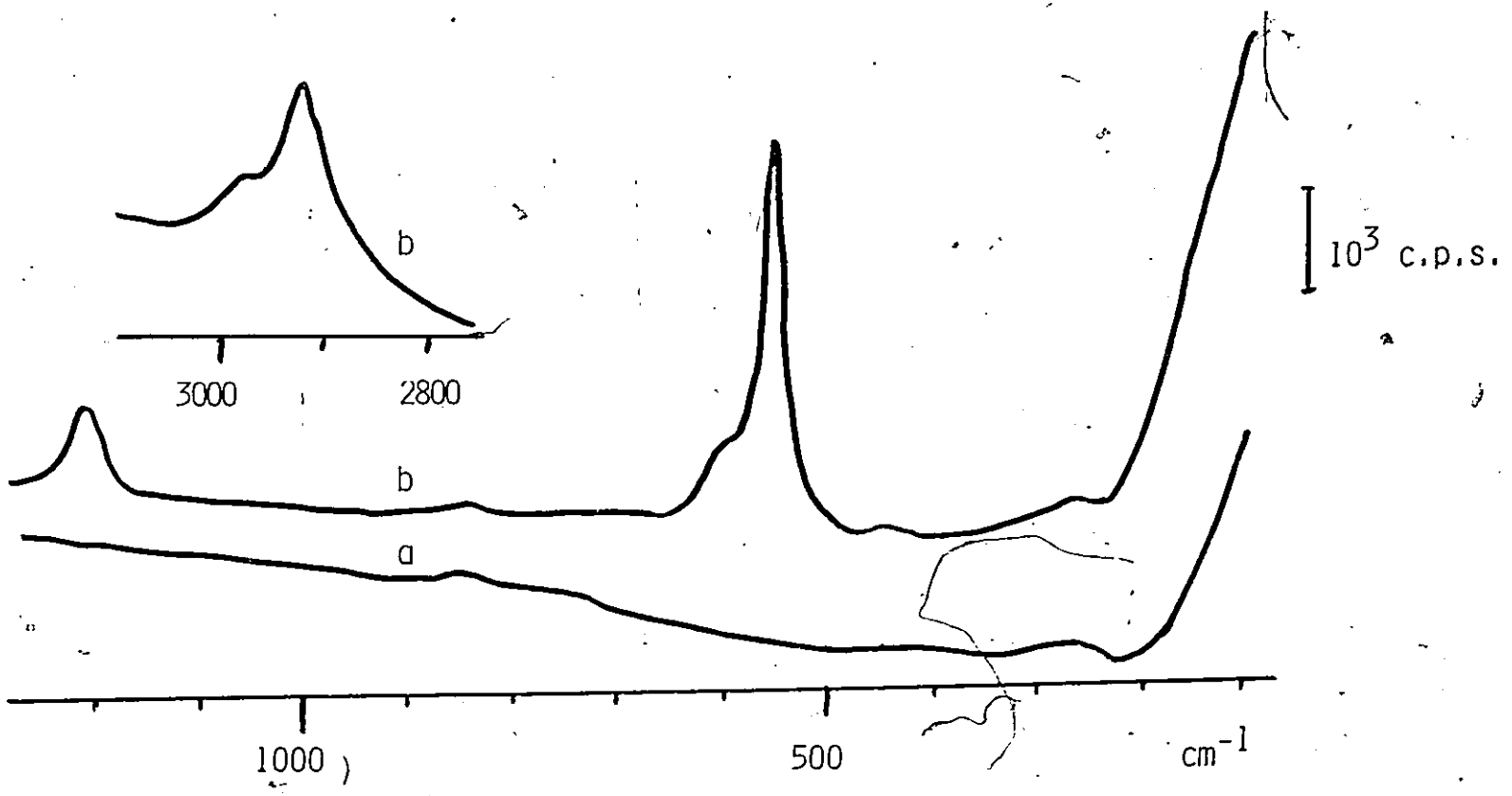


Figure 8-7
a) Raman spectrum of an alumina which had been degassed at 480°C for 1 hr.
b) After reaction of a) with trimethylgallium.
Inset shows the region from 3100-2700cm$^{-1}$ of curve b).

observed in the $-CH_3$ region. This is as expected since any $AlCH_3$ produced would be hydrolyzable, unlike $\equiv SiCH_3$ in the case with silica.

Discussion and Conclusions

The results for Samples A and B are similar but they are quite different from that for sample C. Knözinger[99] has shown, in a refinement of Peri's[105] work, that five types of isolated hydroxyl groups can be expected on an alumina surface (as disucssed in more detail in Chapter 1).

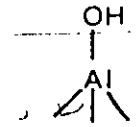


Ia 3760cm$^{-1}$

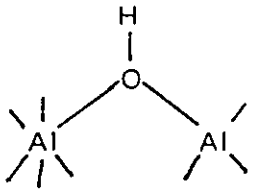


IIa 3730cm$^{-1}$

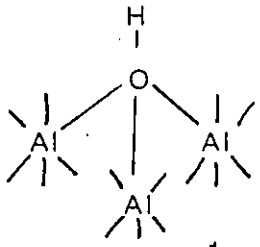


III 3700cm$^{-1}$

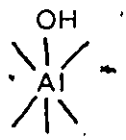


Ib 3785cm$^{-1}$

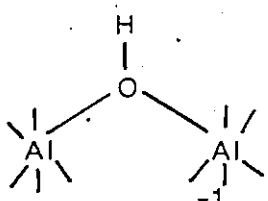


IIb 3740cm$^{-1}$

The surface hydroxyls on alumina might be expected to react in the same manner as those on silica to yield $-OGa(CH_3)_2$ and it is not expected that the frequencies of the $-CH_3$ stretches and deformations will be significantly shifted due to different coordinations of the oxygen atom. Indeed the results shown in Figures 8-1 to 8-4 bear out this hypothesis as the spectra of the reacted aluminas are similar in the $CH_3$ region from 3000-1200 while the reacted hydroxyls (negative peaks) 3800-3600 are different.

As was the case with silica, the 2962 and 2913cm$^{-1}$ bands can be assigned to the -$CH_3$ antisymmetric and symmetric stretch respectively of $AlOGaMe_2$ while the bands at 1417 and 1211cm$^{-1}$ are attributed to the antisymmetric and symmetric deformation modes of -$CH_3$ and the weak peak at 2400cm$^{-1}$ is quite probably an overtone of the symmetric -$CH_3$ deformation. The Raman spectrum showed three bands at 595, 550 and 130cm$^{-1}$ which may be assigned to the antisymmetric and symmetric stretches and the deformations, respectively, of -$GaC_2$. Three additional Raman bands were observed at 2965, 2915 and 1215cm$^{-1}$ coinciding with those in the infrared but no bands assignable to -AlOGa stretches were observed.

When alumina is dehydroxylated by degassing above 150°C the neighbouring pairs of hydroxyls may condense to eliminate water and produce a pair of coordinatively unsaturated oxygen and aluminum atoms, i.e., Lewis basic and acidic sites, respectively. In the present context pairs of hydroxyl groups of the types Ia/IIa and IIb/III would be condensed upon heating alumina from 150 to 450°C, i.e., Sample A to B, and Lewis acid and base sites should be created. If only the relative proportions of the hydroxyls were changed in Samples A and B it would not be very surprising that the spectrum of the adsorbed species remained the same, but Lewis acid and basic sites are being formed and the spectrum should show the formation of new surface species produced by the reaction of TMG with these sites. A possible reaction is:

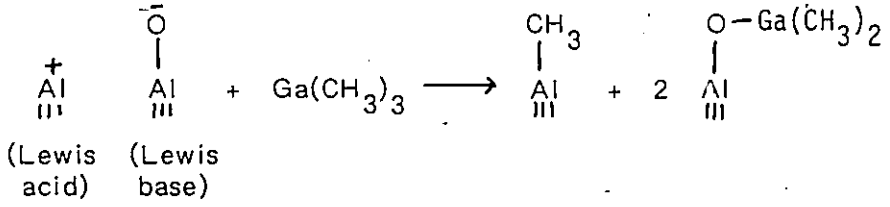


However, the -$CH_3$ stretching frequencies for -$AlCH_3$[127, 188] might be expected to

be very close to those of Ga-$CH_3$ and with the small number of Lewis sites formed at this temperature distinct bands for Al-$CH_3$ might not be detectable. Alternatively, Lewis sites produced by degassing alumina up to 400°C are not important catalytically and Knözinger argues that these neighbouring Lewis sites are weak and thus perhaps they do not react with TMG.

Dehydroxylation of alumina above 400°C produces strong Lewis acid and base sites due to the migration of surface hydroxyls and lattice cations. Sample C, which was degassed at 950°C, has very few hydroxyl groups remaining and is expected to have stronger Lewis acid and base sites than those produced by degassing at 450°C. The spectrum for adsorbed TMG on Sample C showed, in addition to peaks at 2962 and 2914$cm^{-1}$ due to AlOGa$(CH_3)_2$, new peaks at 2939, 2900 and 2836$cm^{-1}$, and these frequencies are comparable to those for the $CH_3$ stretching modes in $Al(CH_3)_3$[127, 188]. The intensity of the infrared band at 2939$cm^{-1}$ is comparable to that at 2963$cm^{-1}$ and a distinct peak at 2914$cm^{-1}$ is not observed. The similarity in the frequencies for -OGa$(CH_3)_2$ and Al-$CH_3$ and the width of the bands might thus appear to account for the difficulty in observing the IR bands for the latter species on Sample B.

From data given by Knözinger[99], estimates can be made about the number of hydroxyl groups and pairs of Lewis sites (Table 8-1) on alumina at various temperatures. If only two possible reactions of TMG with alumina are considered, i.e.,

(1) $\equiv Al\text{-}OH + Ga(CH_3)_3 \longrightarrow \equiv Al\text{-}O\text{-}Ga(CH_3)_2 + CH_4\uparrow$

(2) $\overset{+}{Al}_{III}\ \ \overset{\bar{O}}{|}\ Al_{III} + Ga(CH_3)_3 \longrightarrow \equiv Al\text{-}CH_3 + \equiv AlOGa(CH_3)_2$

Table 8-1

Densities of hydroxyl and Lewis acid and base sites on alumina.

| Dehydroxylation temperarture/ $^{0}C$ | # Lewis acid [a] sites/ 100 $Å^2$ | # Lewis base [b] sites/ 100 $Å^2$ | # surface OH [c] / 100 $Å^2$ | # $AlOGa(CH_3)_2$ [d] expected/ 100 $Å^2$ |
|---|---|---|---|---|
| 150 | 1.95 | 1.95 | 10.6 | 12.55 |
| 450 | 4.95 | 4.95 | 4.6 | 9.55 |
| 950 | 7.25 | 7.25 | - | 7.25 |

a,b,c - values from Knözinger and Ratnasamy ref. 99.

d - sum of b+c (see reactions 1 and 2).

then the relative quantities of the species $\equiv AlOGa(CH_3)_2$ and $\equiv Al\text{-}CH_3$ can be determined by their IR band intensities at 2963 and 2939cm$^{-1}$, respectively. From these data the ratio of hydroxyl sites to Lewis sites may be calculated and compared with that given by Knözinger.

In order to measure the band intensities as accurately as possible the following procedure was employed. The assumption was made that on a fully hydroxylated alumina (Sample A) there were no Lewis sites present for reaction with TMG and that the spectrum in Figure 8-2 for this sample in the region from 3100-2700cm$^{-1}$ represents the $-CH_3$ stretches for $-OAl(CH_3)_2$ only. The IR spectra of Samples B and C are expected, after reaction with TMG, to have $-CH_3$ stretches due to the species $\equiv Al\text{-}CH_3$ in the 3100-2700cm$^{-1}$ region, as well as those due to $\equiv AlOGa(CH_3)_2$. The IR peaks in the spectra of Samples B and C due to the species $\equiv AlOGa(CH_3)_2$ were removed by subtraction of the spectrum for this species from Sample A in the region 3100-2700cm$^{-1}$. Because the three samples were not necessarily of the same optical thickness, the spectrum of Sample A was scaled by different factors until the peak at 2963cm$^{-1}$ was just removed in the spectra of Samples B and C. The peaks assignable to $\equiv AlCH_3$ that remained after the subtractions for sample B and C were at 2939, 2900 and 2830cm$^{-1}$ and are shown in Figures 8-8a and 8-9a, respectively. The spectrum in Figure 8-8a was then subtracted from that in Figure 8-4 and this gave the "pure" spectrum of $AlOGa(CH_3)_2$ for sample B and this result is shown in Figure 8-8b. A similar subtraction was done for sample C and its result is shown in Figure 8-9b.

Sample C was almost completely dehydroxylated: therefore, the ratio of the intensities of the peaks at 2963cm$^{-1}$ and 2939cm$^{-1}$ in Figures 8-9a and 8-9b respectively should give the relative extinction coefficients of these bands for

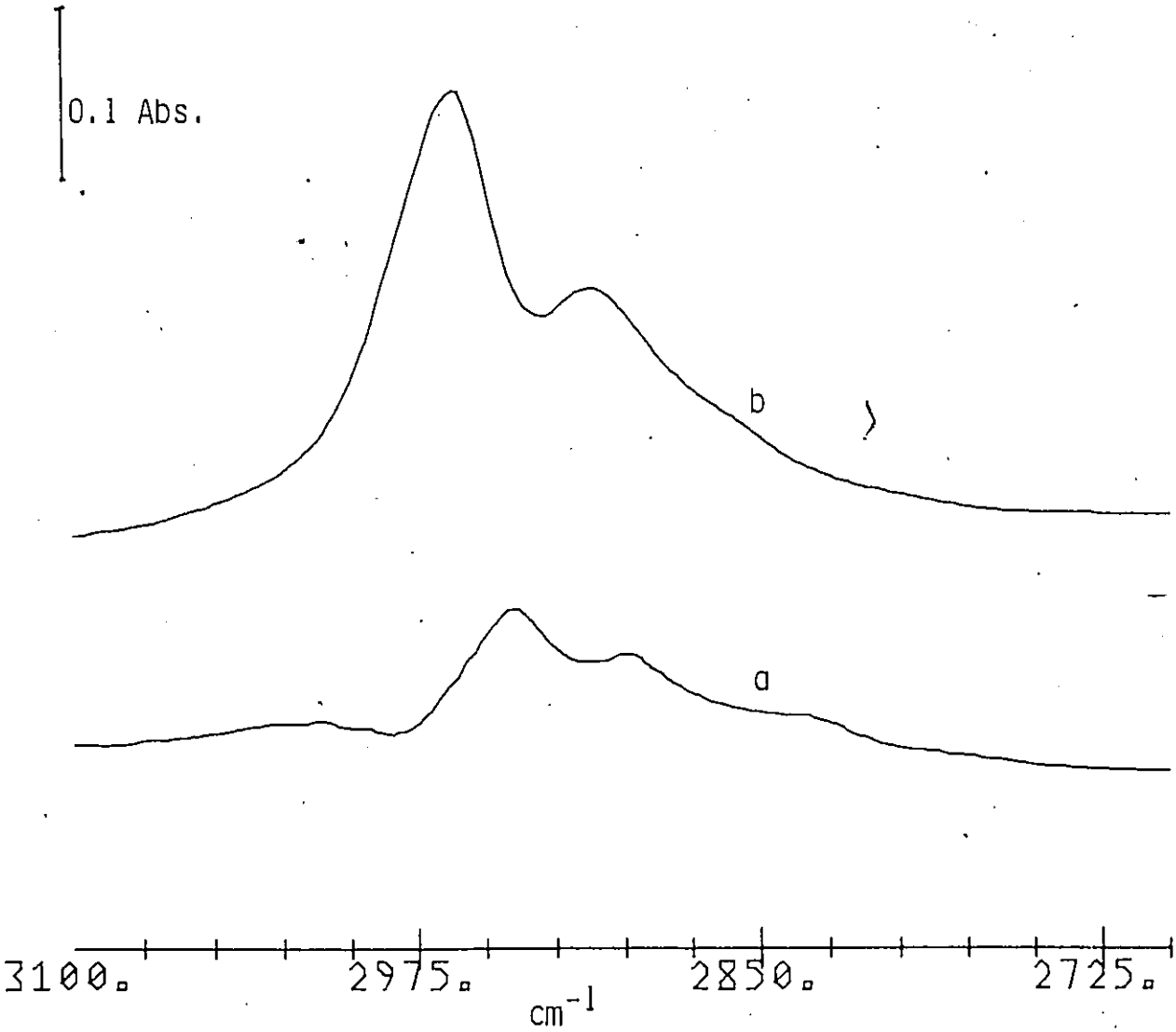


Figure 8-8
Difference spectra for the 450 and 150°C degassed aluminas in the CH stretching region
a) Figure 8-4 minus Figure 8-2
b) Figure 8-4 minus a)
See text for details.

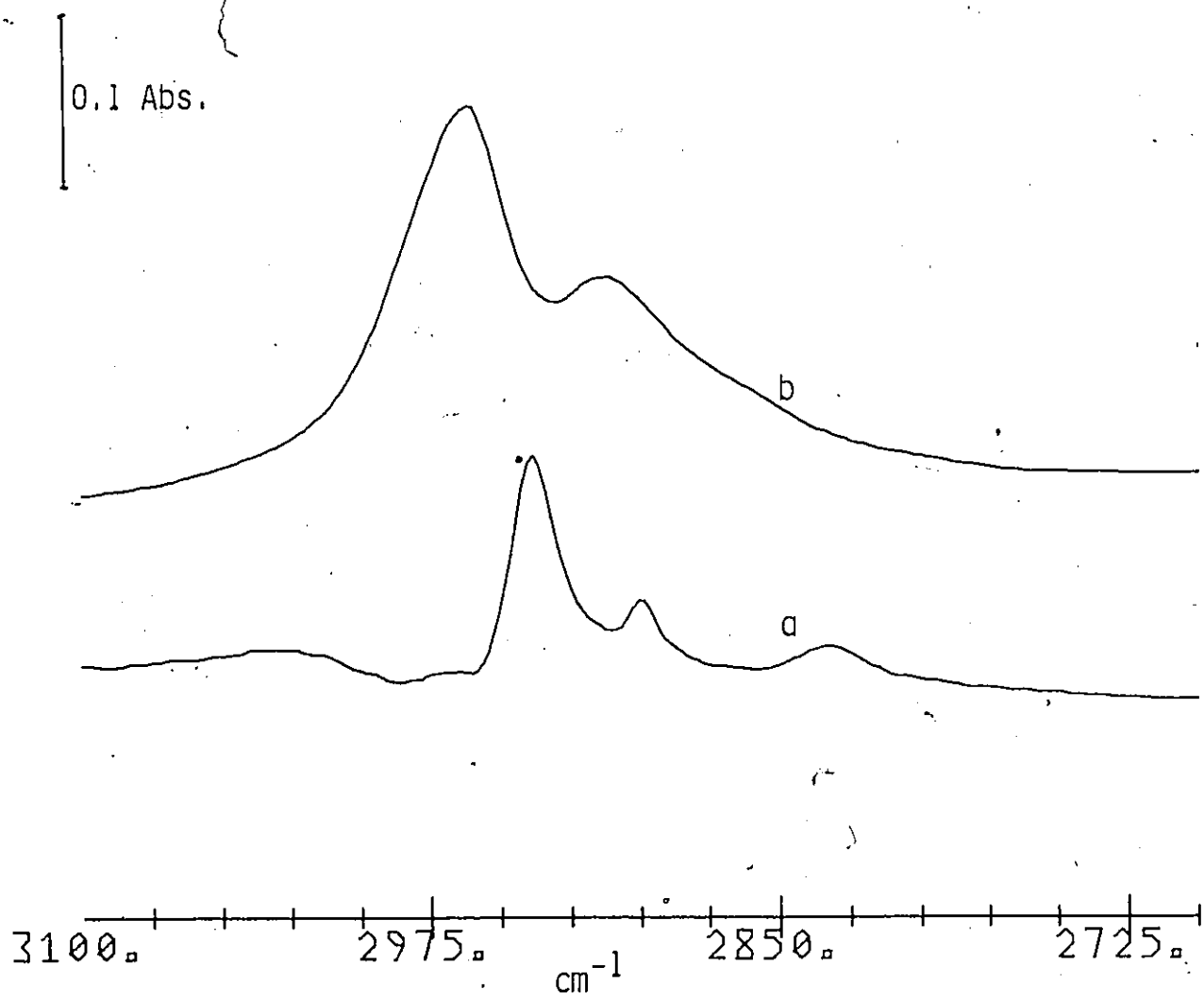


Figure 8-9
Difference spectra for the 950 and 150°C degassed aluminas in the CH stretching region
a) Figure 8-6 minus Figure 8-2
b) Figure 8-6 minus a)
See text for details.

Table 8-2

Determined intensities for the bands at 2963 and 2939 $cm^{-1}$ due to reactions 1 and 2 respectively.

| Absorbance | Sample B degassed at 450°C | Sample C degassed at 950°C |
|---|---|---|
| at 2939 $cm^{-1}$ (Al-Me) | 0.085 | 0.129 |
| at 2963 $cm^{-1}$ (Al-$OGaMe_2$) | 0.253 | 0.220 |
| at 2963 $cm^{-1}$ for reaction 1 | 0.109 | 0 |
| at 2963 $cm^{-1}$ for reaction 2 | 0.144 | 0.220 |

the species $\equiv AlCH_3$ and $\equiv AlOGa(CH_3)_2$ since they are formed at a ratio of 1:1 according to reaction (2) which was the only possible reaction for this sample. This relative extinction coefficient has a value of 1.70 and by applying this value to the spectra in Figures 8-8a and 8-8b the absorbances at 2963cm$^{-1}$ in Figure 8-8a due to $\equiv AlOGa(CH_3)_2$ formed by reactions (1) and (2) can be calculated. These results are summarized in Table 8-2.

The ratio of Lewis acid sites to hydroxyl sites for Sample B given by the data in Table 8-2 is 1.32(0.144/0.109=1.32), which is close to the value 1.08 given by the data in Table 8-1. The data given in Table 8-1 by Knözinger was based on calculations of the lattice site densities (surface Al and O) on the (111) face of $\gamma$-alumina and the loss of water during dehydroxylation at temperatures between 20 and 500°C. The choice of one crystal face or another as a model for high surface area aluminas, as has been previously discussed, is questionable. The choice of crystal face would change the ratios of Lewis sites to hydroxyl sites in Table 8-2.

The results presented here represent a direct chemical method to determine the relative amounts of Lewis sites to hydroxyl sites on any alumina. Two reference samples are required by this technique. One sample must be fully hydroxylated and must not contain any Lewis sites while the second sample must be completely dehydroxylated, containing only Lewis sites. This technique is fast, accurate and requires little sample preparation beyond degassing at the required temperatures. An infrared spectrometer with a computer for spectral subtraction is, however, required.

# CHAPTER 9

## A STUDY OF ZEOLITE ZSM-5 BY RAMAN SPECTROSCOPY

### Introduction

The family of compounds called zeolites, of which ZSM-5 is one member, are crystalline aluminosilicates made up of open frameworks of linked tetrahedra, $TO_4$ (T = Al, Si) whose overall negative charge is balanced by cations $M^{n+}$ which are exchangeable in aqueous solutions. The general formula for a zeolite is therefore $M^{n+}_{x/n}[(AlO_2)_x (SiO_2)_y] z\ H_2O$. The $z\ H_2O$ refers to the variable quantity of water which occupies the free space inside the zeolite framework, which may be more than 50% of the crystal volume. Depending upon the family of zeolite, this free space may consist of one, two or three- dimensional networks of interconnected cavities and channels of molecular dimensions, i.e., approximately 3-12A.

The family of zeolites presently consists of 37 naturally occurring minerals (some of which are extremely rare) and over 100 synthetic types including ZSM-5. Within each family of zeolites, particularly the synthetic ones, the Si/Al ratio may be continuously varied and the Si and Al atoms may be substituted in the synthesis by Be, Mg, B, Ga, Ge and P. The highest value of the Si/Al ratio is approximately 10,000/1 while the lowest value is 1/1 (in Zeolite-A). The reason for the latter is that Al-O-Al linkages, which would be present at a ratio less than 1/1, are unstable and not allowed by the so called Lowenstein rule.

The water which normally occupies the void space in the zeolite can be removed by heating and results in a porous material which can now accommodate

other molecules of suitable dimensions. The ability of zeolites to absorb different molecules and to undergo ion-exchange has long been recognized and exploited. The ion-exchange properties of zeolites are utilized commercially in e.g., the separation of radioactive strontium and cesium from nuclear wastes, water softening, in the treatment of brackish water, the recovery of precious metals (as complex cations) and the removal of ammonium from sewage. The sorptive capacity of zeolites is utilized in the separation of $N_2$ and $O_2$ in air and in the separation of hydrocarbon mixtures. By far the most important uses of zeolites, particularly those with high Si/Al ratios (which makes the zeolite hydrophobic but not organophobic) and with $H^+$ as the exchangeable cation, are as highly active and selective catalysts for the cracking (conversions of heavy hydrocarbons to lighter ones), hydrocracking (conversion of unsaturated and partially saturated hydrocarbons to more highly saturated ones) and the isomerization of hydrocarbons.

Although amorphous silica-alumina gels are also catalysts for the above hydrocarbon conversions, the performance of zeolites for these functions is much superior. The advantages of zeolites are that:

(1) they possess a high density of well defined catalytically active sites,

(2) they have good molecular sieving properties and,

(3) the electrostatic fields within the zeolitic framework are well defined and controllable. Point (2) above encompasses an effect called shape selectivity which in principle means that in a mixture of molecules exposed to the zeolite under given conditions only certain molecules, because of size and shape, will react and they will produce only products of certain size and shape. The factors determining shape selectivity are:

(1) The molecular sieving of reactants entering the zeolite channels

and migrating to active sites.

(2) The molecular sieving of product molecules migrating from active sites in the cavities (or channels).

(3) A restriction on the size of the transition state complex during the reaction inside a cavity or channel.

The zeolite ZSM-5 (Zeolite -Standard Oil Co. New York (SOCONY) - Mobil) has all the advantages of a zeolite catalyst mentioned above but, more importantly, it is a more silaceous zeolite than those previously produced. In addition, the pore size of ZSM-5 is about 6Å , which is midway between the sizes for other zeolites typified by zeolite A and Y, which have pore sizes of 4 and 8Å respectively. The higher Si/Al ratio results in greater thermal stability than other zeolites and this means that it can undergo many more regeneration cycles at high temperatures. While the higher Si/Al ratio produces fewer Brönsted acid sites per mole of zeolite these sites are more acidic so that reactions which could not have occured under the mildly acidic condition in other zeolites occur with ZSM-5.

The intermediate pore size of ZSM-5 with respect to those of zeolites A and Y allows a different selectivity in the sizes of reactant and product molecules, which fortuitously are in the range of the components of high octane gasoline. Thus, ZSM-5 is much used in the petroleum industry in the production of gasoline. ZSM-5 also has an added advantage over other zeolites that have been used in hydrocarbon conversion and this is called reverse molecular selectivity. During the hydrocarbon conversions in other zeolites, highly carboneceous products are deposited in the cavities and eventually block the active sites because the products are too big to migrate from the large cavities through the restrictive channels. In the case of ZSM-5, however, the size and shape of the cavities are

such that even the largest molecules formed in them can migrate, if only slowly, through the channels. This, therefore, avoids a build up of coke-like products which block the active sites and it also makes regeneration of the catalyst easier.

The channel system and the interconnected cavities in ZSM-5 are shown as reported by Kokotailo[214] in Figure 9-1. The straight channels have a nearly circular cross-section of 5.4 x 5.6 Å while the sinusoidal ones have an elliptical cross-section of 5.2 x 5.8 Å. A skeletal diagram of the framework of the ZSM-5 unit cell ($M^{n+}_{x/n}Al_xSi_{96-x}O_{192}$) viewed in the direction of the sinusoidal channels is shown in Figure 9-2a and for the straight ones in Figure 9-2b.

Several techniques have been used to study the structure of ZSM-5, and the adsorption and subsequent reactions of various molecules. One of the most valuable tools has been silicon-29 and aluminum-27 nuclear magnetic resonance spectroscopy[215-18]. From such studies important information has been obtained regarding the structure of ZSM-5, probable arrangements of Si and Al atoms in the framework as well as Si/Al ratios. Nuclear magnetic resonance (nmr) has also been used to study the adsorption of molecules with nmr active nuclei, e.g., $^{13}C$ and $^{1}H$[219-23]. Infrared studies of the adsorption of methanol, ethylene, and pyridine have been reported by several authors[224, 225]. The adsorption of methanol and ethylene is of particular importance in the conversion of methanol to gasoline using ZSM-5 catalysts[226, 227]. Chromatographic techniques have been used as well to study the product fractions in the methanol to gasoline conversion using ZSM-5[228]. Temperature programmed desorption and microcalorimetry of ammonia adsorbed on ZSM-5 with either $H^+$ or $Na^+$ as the exchange cation have been used to study the acidity of ZSM-5 and to compare its acid strength with

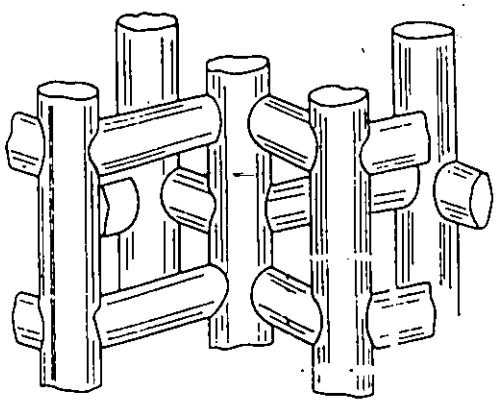

Figure 9-1
The channel system in ZSM-5.

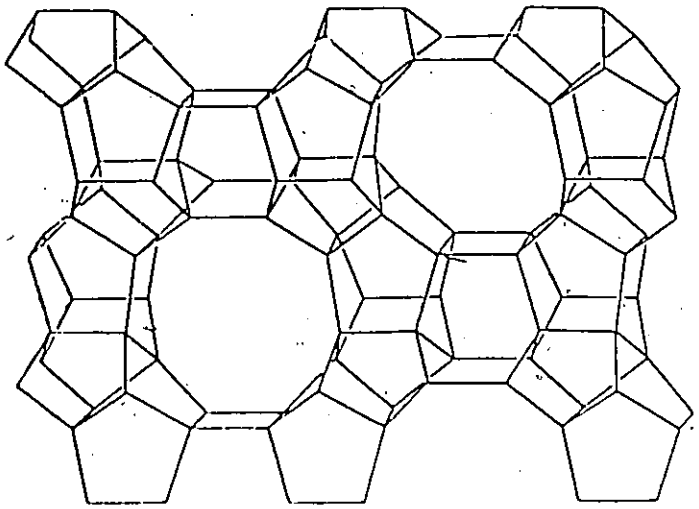

a

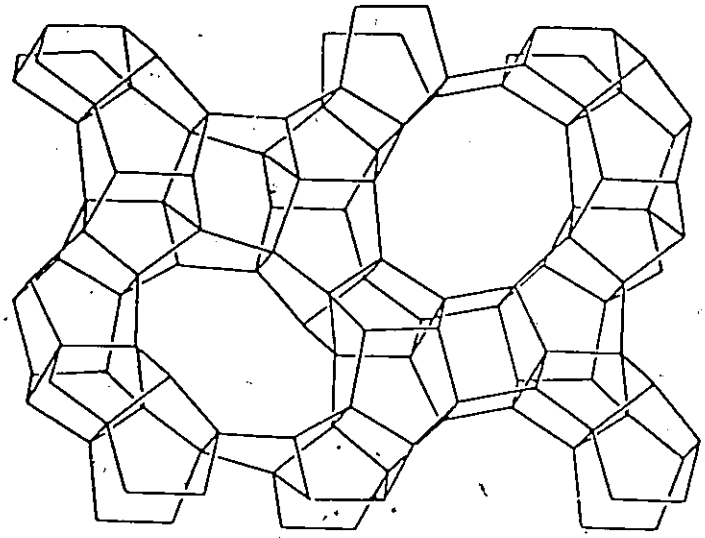

b

Figure 9-2
a) Skeletal diagram of the (010) face of the ZSM-5 unit cell. The 10-membered ring apertures with near circular cross-section (5.4 X 5.6 Å ) are at the entrance to the straight channel depicted in Figure 9-1.
b) A similar diagram for the (100) face showing elliptical apertures (5.2 X 5.8 Å ) at the entrance to the sinusoidal channels.

that of other zeolites[229]. A large portion of the reports in the chemical literature concerning ZSM-5 deal with either the methanol to gasoline conversion reaction or some other hydrocarbon conversion which is of great industrial importance, using one or more of the above techniques.

The aim of the present investigation was to attempt to use Raman spectroscopy to study the adsorption and reactions of molecules such as $CH_3OH$, $C_2H_4$, $H_2S$, $SO_2$ and $NO_2$ on ZSM-5. For reasons mentioned earlier, Raman spectroscopy is a potentially powerful technique for obtaining vibrational information about adsorbates on oxides. The present investigations were not successful but a few significant observations were made regarding the Raman spectrum of ZSM-5 which have not been reported in the literature. Also, these investigations, despite certain problems encountered, do show the potential for further investigation using Raman spectroscopy.

## Experimental

### Synthesis of ZSM-5

Eleven samples of ZSM-5 with Si/Al ratio ranging from 40.7 to 203.5 were synthesized. The procedure used was taken from the original Mobil patent[230] for ZSM-5 with some modifications. The ZSM-5 crystals were grown from a solution containing tetrapropylammonium hydroxide (TPA), sodium aluminate, water and Ludox silica ( a colloidal sol of sodium silicate containing approximately 30% wt. of $SiO_2$), which was heated in a teflon-lined stainless steel autoclave at 150°C for 5 days.

In a typical ZSM-5 synthesis the required Si/Al ratio was decided and then the ratios of $TPA/Na^+$, $H_2O/OH^-$ and $OH^-/SiO_2$ were calculated using an iterative computer program so that the optimum ratios listed in the above patent

was attained and so that the total volume of the reaction mixture was less than 300 mls (The Parr stainless steel, teflon-lined autoclave had a capacity of about 350 mls). The required volume of Ludox silica was placed in the teflon-lined autoclave and the required amount of sodium aluminate dissolved in the determined amount of water was added and the mixture stirred rapidly with a glass rod. The TPA was then rapidly added with stiring, along with a magnetic stir bar and the autoclave was sealed. Air was then evacuated from the autoclave until the pressure dropped to less than 1 torr under dynamic vacuum. This step was found to be necessary in order to prevent corrosion of the autoclave in oxygen during the reaction at 150°C. The autoclave was then placed upright on a magnetic stirring plate and surrounded by a tube furnace at 150°C.

After 5 days the autoclave was cooled under cold water, the vessel was opened and the teflon-liner containing the crystal and mother liquor was removed. The clear liquid phase was decanted and the final white crystals of ZSM-5 were placed in a Nalgene centrifuge bottle of 200 ml capacity. The crystals were repeatedly washed in 150 mls of triply distilled organic free water, and centrifuged at 3000 rpms for 10 minutes, until no hydroxide precipitated from the washings when a few drops of 0.1 M $AgNO_3$ were added. The product, which was brilliant white, was dried at 90°C for 4 hrs. Typical yields were 15-20g which corresponds to about 80% yield.

Ion - Exchanged ZSM-5

Ion exchanges using a ZSM-5 with a Si/Al ratio of 40.7 were undertaken. The procedures followed were those outlined by Jacobs and Von Ballmoos[231] and Chu and Dwyer[232]. The only exchanges undertaken were those with alkali metal ions and ammonium. The procedure involved the partial decomposition of the tetrapropyl

ion in a 3g. sample of the zeolite by heating at 400°C in air for 36 hrs during which time the sample colour changed from white to dark brown. This sample was then continuously stirred in 200mls of a 0.1N NaCl solution for 36 hrs at 25°C. The sample was then washed and centrifuged and the complete removal of chloride ions was tested for by adding a few drops of 0.1N $AgNO_3$ to the washings. This sample was then heated in air at 500°C for 15 hrs after which the sample was white and was now, according to Jacobs and Von Ballmoos, completely $Na^+$ exchanged ZSM-5. Six 0.5 g portions of the above sample were then added to O.1N solution of the chlorides of $NH_4^+$, $Li^+$, $Na^+$, $K^+$, $Rb^+$ and $Cs^+$ in polypropylene bottles and stirred continuously at 25°C for 3 days. The solutions were washed as above to remove the chlorides and then dried at 90°C for 14 hrs.

Measurements

The x-ray diffraction patterns of all the as synthesized zeolites were obtained using a Norelco 4273/0 x-ray difractometer emitting the CuKα line with a nickel filter and had a resolution of 0.01°2θ. A Siemens scanning electron microscope was used to obtain photographs of the crystals in some ZSM-5 samples. Raman spectra of the as synthesized zeolites were obtained from 100mg discs having a diameter of 1 cm. Raman spectra were recorded of the zeolites after calcination in air at temperatures of 500 to 920°C. For adsorption studies, the Raman cell previously described was used. The ZSM-5 used in these studies had a Si/Al ratio of 40.7 and was heated in 600 torr of oxygen at 480°C for 2 hrs prior to degassing at this temperature for 1 hr, cooled in oxygen and finally evacuated at 25°C.

Infrared spectra of the zeolites calcined at 500 to 920°C were recorded on a Perkin-Elmer 283 infrared spectrometer. The spectrum was recorded only in the 1500-200 $cm^{-1}$ region and this was accomplished by spreading a thin film of the sample on a CsBr infrared window.

Commercial analyses of the zeolites to determine Si/Al ratios were obtained. The silicon was determined gravimetrically as $SiO_2$ and the aluminum by x-ray fluorescence. The Si/Al ratios obtained were bulk values and would include any trace of non-crystalline silica or alumina. This determination might be considerably different from that determined by nmr mentioned earlier which yields Si/Al ratio of the crystalline ZSM-5 component only.

Results and Discussion

The lattice parameters found for the as synthesized, calcined and ion-exchanged ZSM-5 agreed well with those reported in the Mobil patent for this zeolite[230]. It is well known that the lattice parameters will vary with substitution of $Si^{4+}$ by $Al^{3+}$ in the lattice of ZSM-5[233] and also with the exchanged cations[220]. These effects were not studied in the present case because x-ray diffraction was used only to determine that crystalline ZSM-5 free from other crystalline impurities was produced and thus was only recorded at low angular resolution. A typical diffraction pattern obtained with ZSM-5 is shown in Figure 9-3.

The Raman spectra of the uncalcined and calcined ZSM-5 (Si/Al = 40.7) are shown in Figures 9-4 and 9-5. The surprising aspect of these Raman spectra was the complete absence of any background fluorescence which is known to be present in most zeolites and makes the recording of Raman spectra difficult[234, 234a]. Kuie-Jung Chao et al.[235] had reported the Raman spectrum of an uncalcined ZSM-5 just prior to the start of these studies and their spectrum shown in Figure 9-6 showed signs of background fluorescence and the resulting lower signal/noise ratio in the spectrum. Peuker et al.[236] has recently reported the Raman spectrum of uncalcined and calcined ZSM-5. Their reported

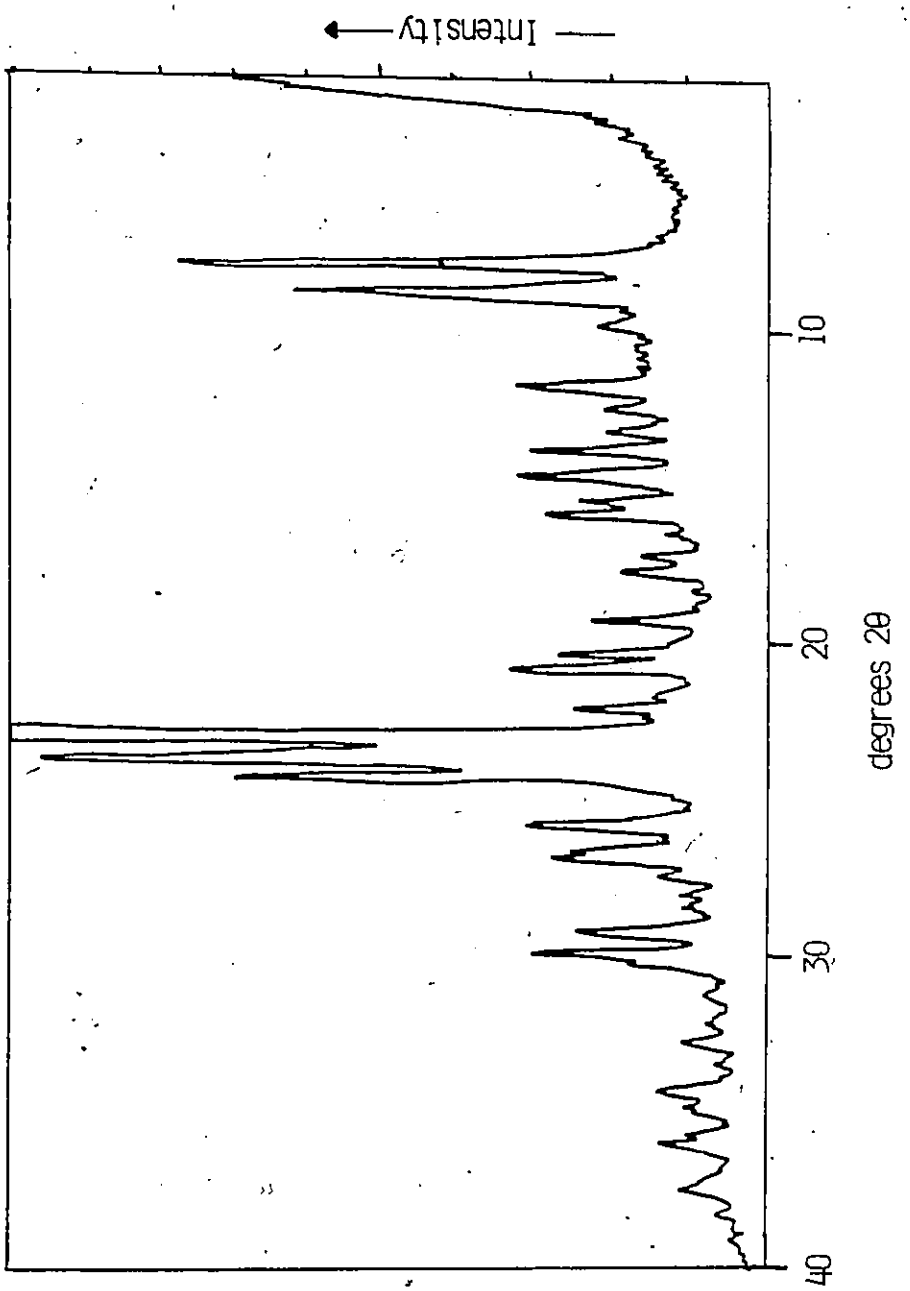


Figure 9-3
X-ray diffraction pattern typical of a synthesized ZSM-5.

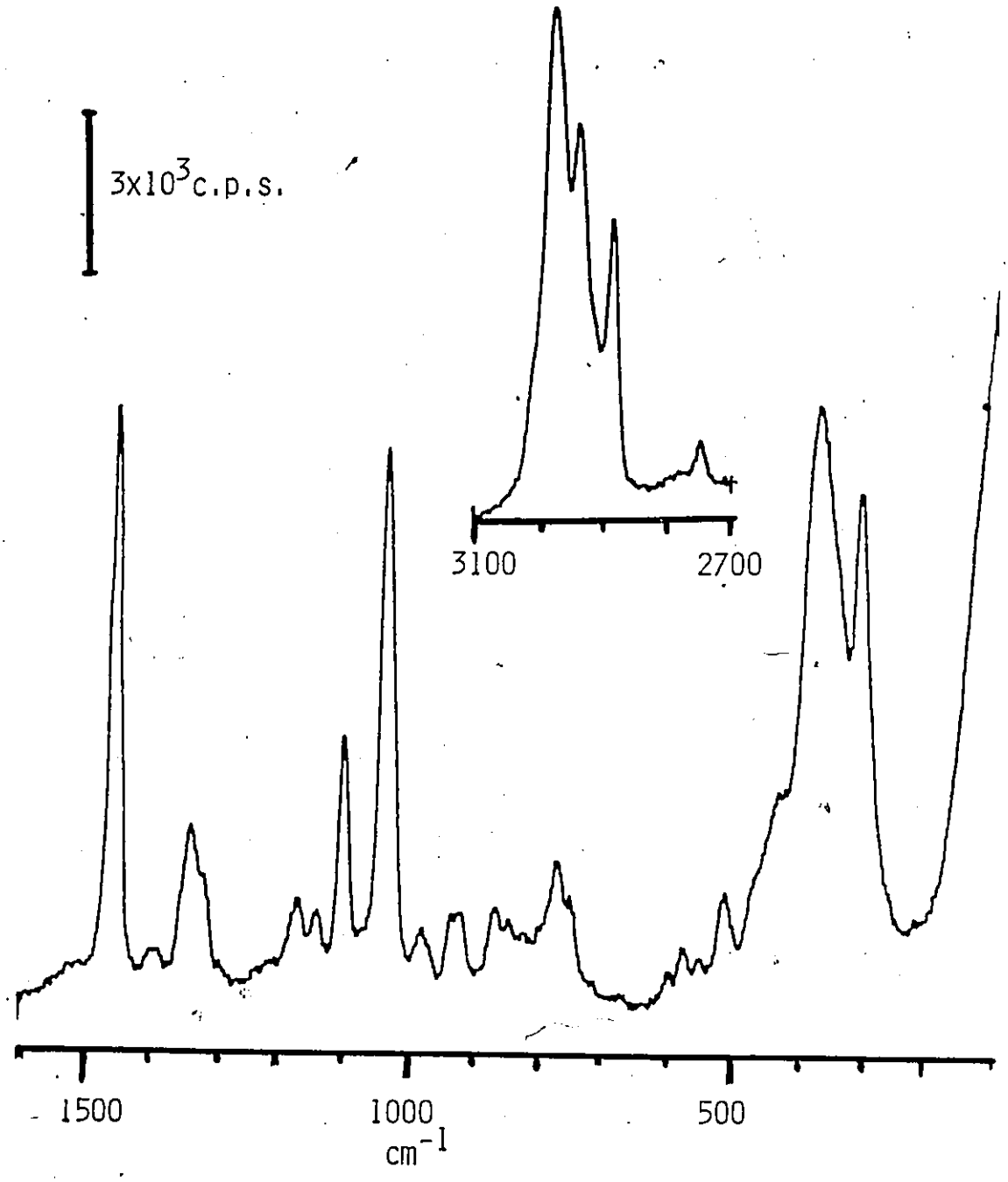


Figure 9-4
Raman spectrum of an as synthesized ZSM-5 having a Si/Al ratio of 40.7.

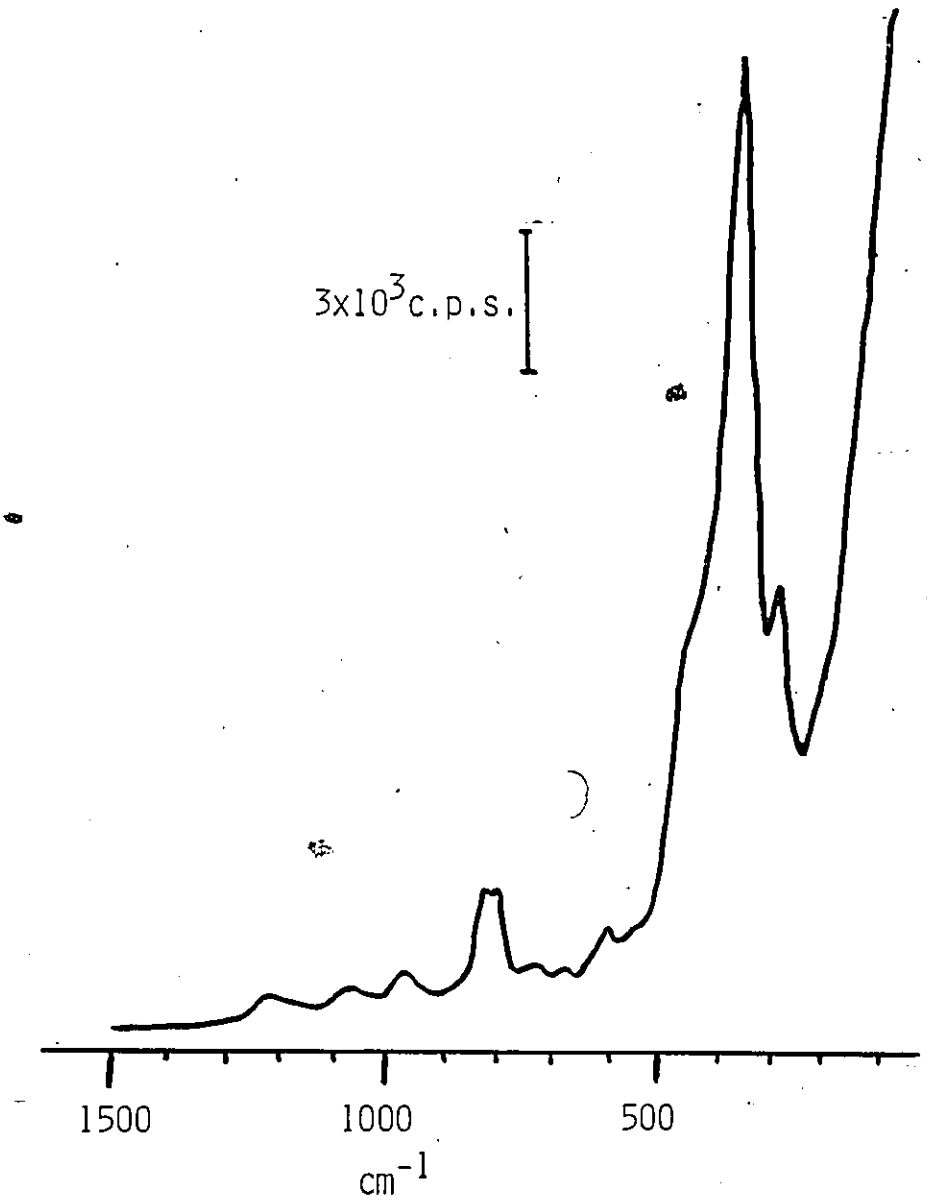


Figure 9-5
Raman spectrum of the ZSM-5 from Figure 9-4 after calcining at 500°C.

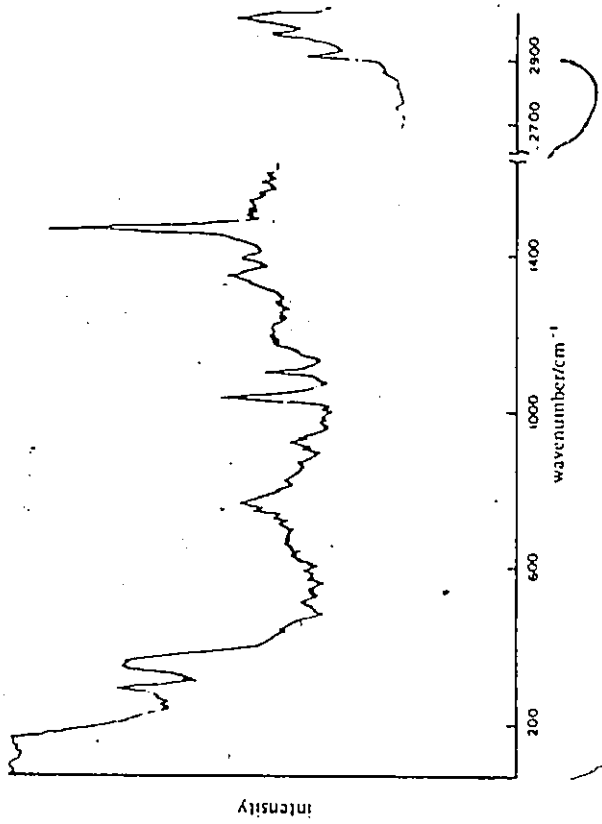


Figure 9-6.
Raman spectrum of a ZSM-5 sample reported by Kuie-Jung Chao et al. ref. 235.

spectra are of better signal to noise ratio than that of Chao but of lower quality than that obtained in these studies. The present studies also showed that there were no changes in the Raman spectrum due to ion-exchange of the calcined zeolites. There were also no spectral changes which could be correlated with a changing Si/Al ratio. The spectrum also did not change after calcination for 14 hrs at either 500°C or at 920°C. Although subtle changes in the unit cell parameters can be observed by x-ray diffraction techniques after calcination at various temperaturesit is apparent that Raman spectroscopy is not sensitive to the subtle changes in crystal structure and crystallinity.

The infrared spectrum of ZSM-5 in the 4000-200 $cm^{-1}$ region has been reported by several workers[231, 235-9]. Jacobs[231] has reported that in the OH stretching region infrared bands were observed at 3720 and 3600 $cm^{-1}$. The band at 3600 $cm^{-1}$ was assigned to framework hydroxyls while that at 3720$cm^{-1}$ was attributed to silanols on the external surface of the zeolite and to silica gel impurities. Jacobs notes that the larger the crystal size, i.e., the greater the ratio of internal surface area to external area, the smaller the intensity of the 3720 $cm^{-1}$ band compared to that at 3600 $cm^{-1}$, and samples with crystal sizes of 15-20 nm had only weak bands at 3720 $cm^{-1}$.

Scanning electron microscopy showed that the crystal sizes in the zeolites synthesized for the present studies were about 2 nm in diameter and showed no presence of colloidal impurities. The infrared spectrum of $H^+$ZSM-5 produced by degassing $NH_4^+$ exchanged ZSM-5 (Si/Al=40.7) at 400°C for 1 hr (1)did show bands at 3738 and 3614 $cm^{-1}$ as would be expected from the results of Van Ballmoos (Figure 9-7).

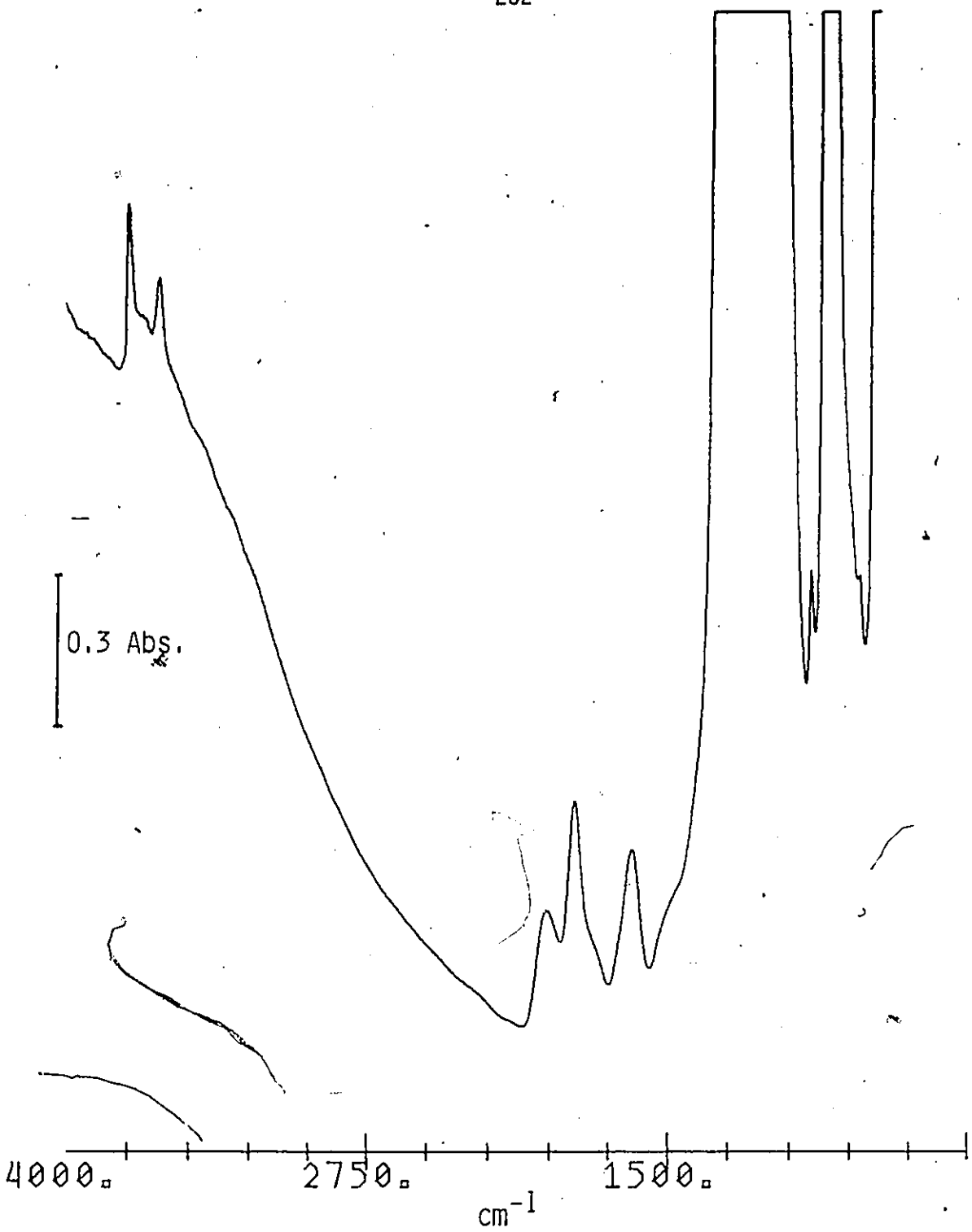


Figure 9-7
Infrared spectrum of a ZSM-5 with a Si/Al ratio of 40.7 after exchange with $NH_4Cl$ and evacuation at 500°C for 1 hr.

(1) 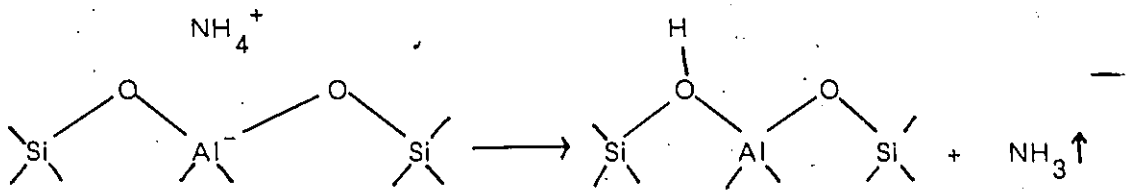

The infrared spectrum of ZSM-5 between 1500 - 200 $cm^{-1}$ is shown in Figure 9-8. Jacobs et al.[238] have assigned the bands in the spectrum to asymmetric, symmetric stretches and bending modes of $TO_4$ (T = Si or Al) in the double -5- rings which make up the ZSM-5 framework (Figure 9-2). The frequencies of these vibrations were found by Jacobs to be similar for zeolites of different structures which contain five-membered rings (e.g., ferrierite) but somewhat different from zeolites with double -4 or -6 -membered rings. The unit cell of ZSM-5 is centro-symmetric and a calculation of the number and symmetry of all the infrared and Raman active vibrational modes was done. The results are:

IR active modes: $108\Gamma^{Au} + 143\Gamma^{B1u} + 107\Gamma^{B2u} + 143\Gamma^{B3u}$

Raman active modes: $108\Gamma^{Ag} + 71\Gamma^{B1g} + 107\Gamma^{B2g} + 71\Gamma^{B3g}$

There are 501 infrared active vibrational modes and 357 Raman active ones. As expected, those modes which are Raman active are not infrared active and vice versa. The frequencies of all Raman and infrared bands are listed in Table 9-1. The table shows that there is at least one coincidence in the infrared and Raman bands, i.e. at 1230 $cm^{-1}$, but while this band is very strong in the IR it is extremely weak in the Raman spectrum. There are some near coincidences e.g. at 800/805 $cm^{-1}$ and 460/470 $cm^{-1}$, but the mutual exclusion of IR and Raman activity appears to be confirmed.

The adsorption of nitrogen dioxide on $H^+$-ZSM-5 was investigated to de-

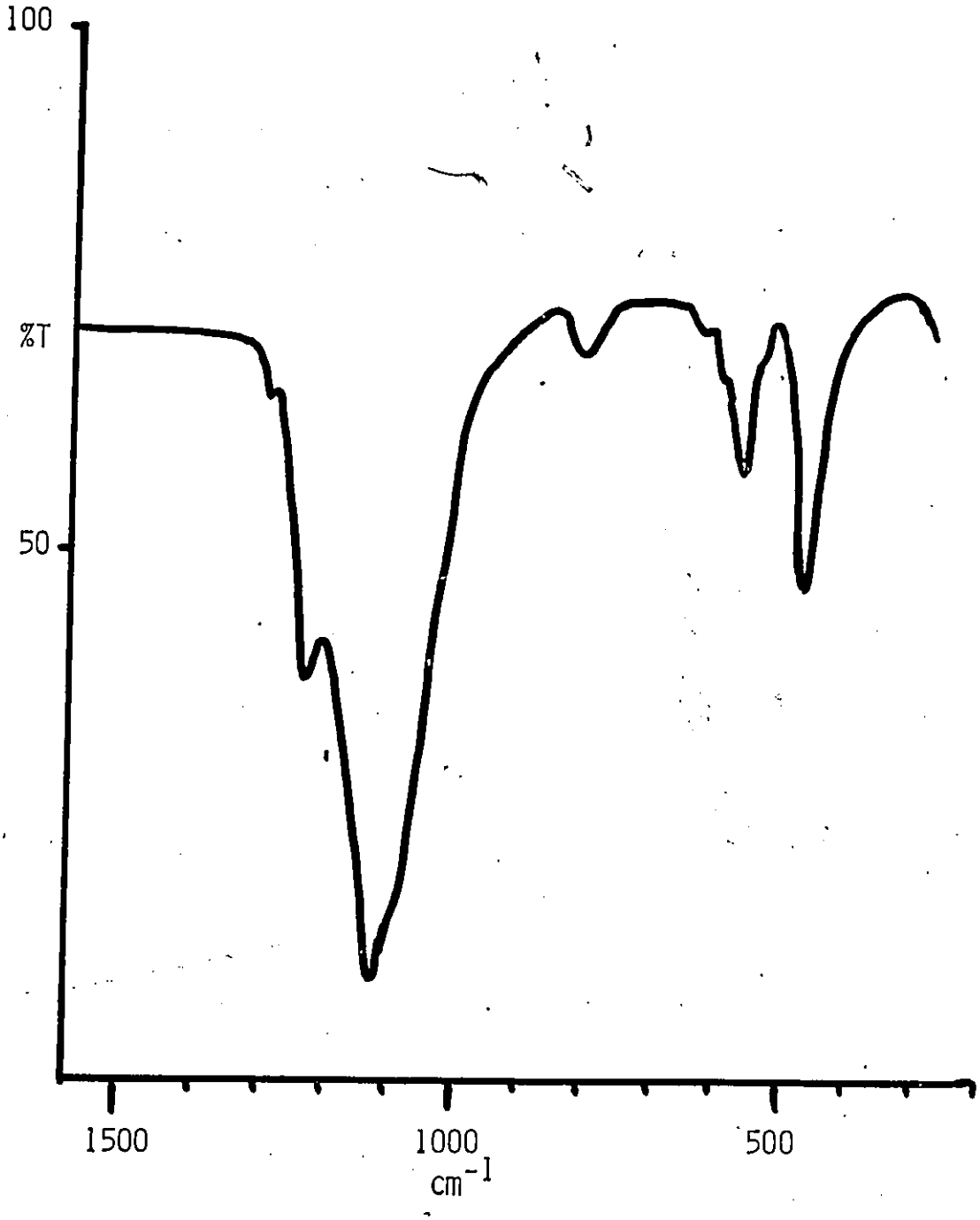


Figure 9-8
Infrared spectrum of a thin film of the ZSM-5 sample from Figure 9-5.

Table 9-1

Frequencies of infrared and Raman bands observed for a calcined ZSM-5(Si/Al=24).

| Infrared bands($cm^{-1}$) | Raman bands($cm^{-1}$) |
|---|---|
| 1230 | 1230 w |
| 1115 vs | 1090 w |
| 950 w | 980 w |
| 800 | 805,830 m |
| 620 w | - |
| 590 sh | - |
| 555 | - |
| 460 m | 470 |
| - | 440 |
| - | 380 vs |
| - | 295 |

vs- very strong
m - medium
w - weak
sh- shoulder

termine if unusual ionic oxides of nitrogen were produced as reported for other zeolites[240]. Upon the addition of 5 torr of $NO_2$ to $H^+$ - ZSM-5 (Si/Al=40.7), which had been degassed at 480°C for 1 hr, several bands due to physisorbed $NO_2$ appeared. These bands decreased slightly after evacuation for 1 minute at 25°C but could be completely removed by evacuation for 1 hr at 25°C, and their frequencies and relative intensities were very close to those reported for gaseous $NO_2$[241]. The observed frequencies for adsorbed $NO_2$ did not change if $Li^+$ or $Rb^+$ exchanged ZSM-5 was used. The physical adsorption by the sample of $NO_2$ could be clearly observed in the cell as the brown colour due to gaseous $NO_2$ became less pronounced while the ZSM-5 sample turned to an orange colour.

Ethylene and benzene are useful as probes of the electronic environment in zeolites[234]. The addition of ethylene or benzene to $H^+$-ZSM-5 resulted in the appearance of a large fluorescence background. With 2 torr of benzene in the cell a weak band at 993 $cm^{-1}$ could be observed but the fluorescence background was continuously increasing and no other bands could be observed. In the case of ethylene, very weak bands were just discernible at 1620 and 1340 $cm^{-1}$. The bands observed with benzene and ethylene are close to those of the free molecules and so these are probably due to physisorbed species. The fluorescence background observed was not reversible with the addition and evacuation of ethylene and benzene. The cause of this large fluorescence background is not known.

In view of the importance of the catalytic reactions of methanol on ZSM-5 this reaction was investigated by Raman spectroscopy. The addition of 5 torr of methanol to $H^+$-ZSM-5 resulted in the appearance of bands due to physisorbed methanol. No changes in the spectrum occured over a period of 1 hour and attempts to heat the sample in methanol resulted in the appearance of an intense fluorescence background.

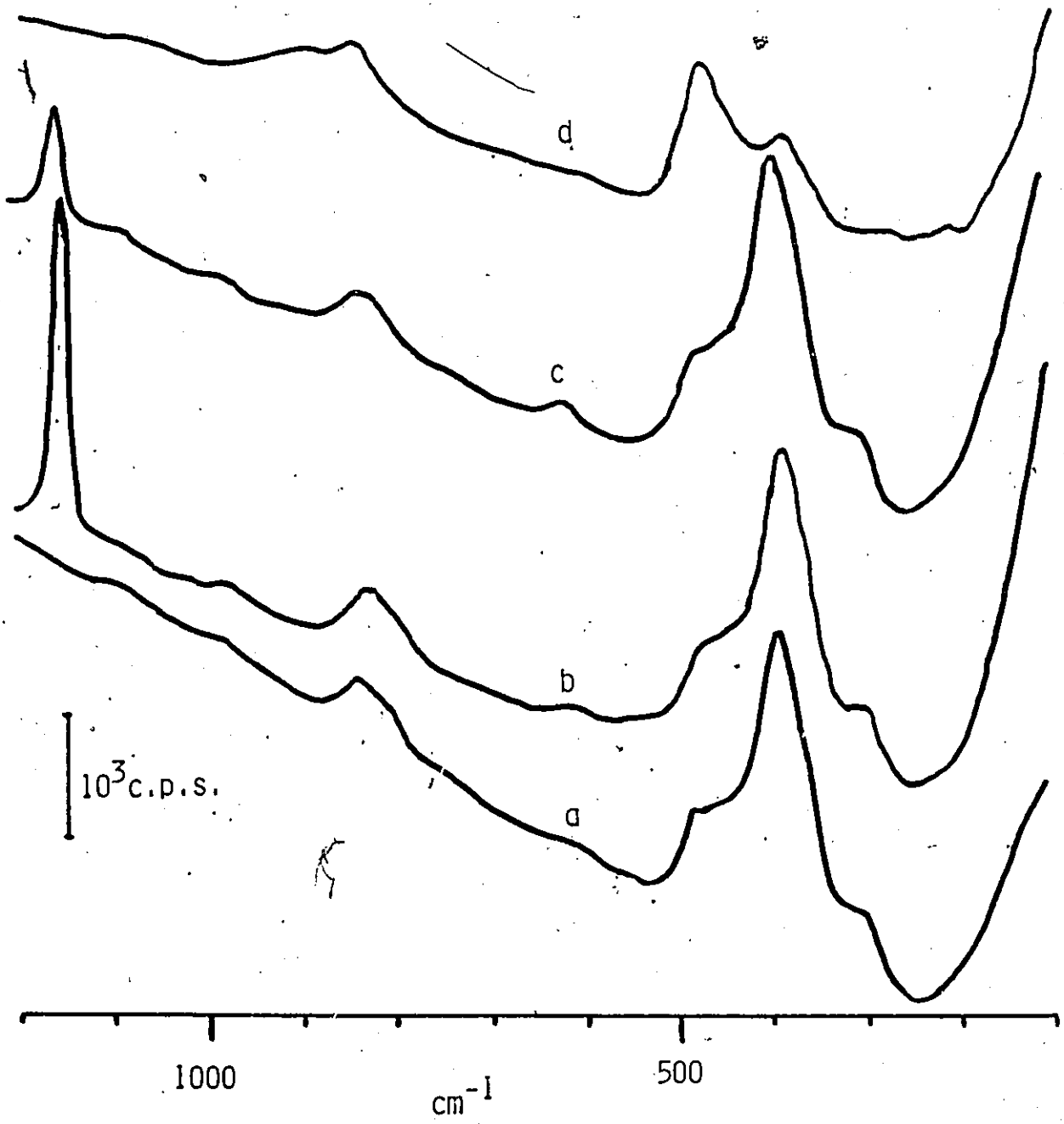


Figure 9-9
The Raman spectrum of the $NH_4^+$-ZSM-5 sample calcined at 500°C to produce $H^+$-ZSM-5
a) After degassing at 400°C for 1 hr.
b) Addition of 2 torr of $SO_2$ to a)
c) Evacuation of b) for 1 min.
d) Addition of 1 torr of $H_2S$ to c).

The Claus reaction (2) with a ZSM-5 catalyst was investigated.

(2) $2H_2S + SO_2 \longrightarrow 2H_2O + 3/nS_n$

Upon the addition of 2 torr of $SO_2$ to $H^+$ZSM-5 a strong Raman band was observed at 1150 $cm^{-1}$ which was assignable to the symmetric $SO_2$ stretch, and evacuation for 1 minute decreased the intensity of this band by a factor of 4 (Figures 9-9b and c respectively). The subsequent addition of 1 torr of $H_2S$ to the sample (Figure 9-9d) resulted in the disappearance of the band at 1150 $cm^{-1}$ and the appearance of a strong band at 480 $cm^{-1}$ with weaker ones at 220 and 150 $cm^{-1}$. A broad weak band was also observed at 900 $cm^{-1}$ and also around 300-400 $cm^{-1}$ but the latter was not very clear due to overlap with those for ZSM-5. The bands observed at 480, 220 and 150 $cm^{-1}$ are similar in frequency and of the same relative intensities as those due to sulphur. It therefore appears that the Claus reaction may occur on $H^+$ZSM-5. No attempts were made to study this reaction further for the effect of exchange cation and Si/Al ratio. Further study of this system appears quite feasible since there was negligible fluorescence background created during the reaction.

The results presented show that relatively fluorscencefree ZSM-5 can be synthesized for Raman spectroscopic studies of the adsorptions of catalytically important molecules. In all but one of the cases presented, adsorption and/or reaction of gases on ZSM-5 led to considerable background fluorescence and very little useful information could be obtained. The study involving $H_2S$ and $SO_2$ adsorption showed the potential for further study.

## REFERENCES


1. N.G. Yaroslavsky and A.N. Terenin, Dokl. Acad. Nauk. S.S.S.R., 66, 885 (1949).
2. L.N. Kurbatov and G.G. Neuimin, Dokl. Acad. Nauk. S.S.S.R., 68, 341 (1949).
3. M.L. Hair, "Infrared Spectroscopy in Surface Chemistry", Marcel Dekker Inc., New York, N.Y., (1967).
4. L.H. Little, "Infrared Spectra of Adsorbed Species", Acad. Press, London (1966).
5. A.V. Kiselev and V.I. Lygin, "Infrared Spectra of Surface Compounds", Wiley, New York, (1975).
6. A.E. Geissberger and P.J. Bray, J. Non-Crystalline Solids, 13, 251 (1973).
7. J.A. Hockey, Chem. Ind., 57 (1965).
8. L.R. Snyder and J.W. Ward, J. Phys. Chem., 70, 3941 (1966).
9. A.V. Kiselev, Y.S. Nikitin, R.S. Petrova, K.D. Shcherbakova and Y.I. Yashin, Anal. Chem., 36, 1526 (1964).
10. A.V. Kiselev, V.M. Lykyanovich, Yu. S. Nikitin, E.B. Organesyan and A.I. Arakhov, Kolloidn. Zh. 31, 388 (1969); ibid. 31, 525 (1969).
11. R.S. McDonald, J. Phys. Chem., 62,1168 (1958).
12. G.J. Young, J. Coll. Sci., 13, 67 (1958).
13. E. Koberstein and M. Voll, Z. Phys. Chem., 71, 275 (1970).
14. W.H. Zachariasen, J. Am. Chem. Soc., 54, 3841 (1932).
15. R.L. Mozzi and B.E. Warren, J. Appl. Crystallogr., 2, 164 (1969).
16. H.A. Benesi and A.C. Jones, J. Phys.Chem ., 63, 179 (1959).

17. J.B. Peri, J. Phys. Chem., 70, 2937 (1966).

18. G.A. Galkin, A.V. Kiselev and V.I. Lygin, Russ. J. Phys. Chem., 43, 1292 (1969).

19. J.J. Fripiat and J. Uttyerhoeven, J. Phys. Chem., 66, 800 (1962).

20. J.J. Fripiat, M. Gastuche and R. Brichard, J. Phys. Chem., 66, 805 (1962).

21. J. Demaraquay and J. Fraissard, React. Solids, Proc. Int. Symp., 8th 1976, 611-16. Plenum, New York, N.Y.

22.a) G. Ghiotti, E. Garrone, C. Morterra and F. Boccuzzi, J. Phys. Chem., 83, 2863 (1979).

b) F. Boccuzzi, S. Coluccia, G. Ghiotti, C. Morterra and A. Zecchina, J. Phys., Chem., 82, 1298 (1978).

23. J.A. Hockey and B.A. Pethica, Trans. Faraday Soc., 57, 2247 (1961).

24. V.M. Bermudez, J. Phys. Chem., 75, 3243 (1971).

25. A.V. Kiselev, V.A. Loknzsievskii and V.I. Lygin, Zh. Fiz. Chim., 49, 1796 (1975).

26. A.J. Tyler, F.H. Hambleton and J.A. Hockey, J. Catal., 13, 35, (1969).

27. K. Klier, J.H. Shen and A.C. Zettlemoyer, J. Coll. Int. Sci., 34, 3 (1970).

28.a) F.H. Hambleton, J.A. Hockey and J.A.G. Taylor, Trans. Faraday Soc., 62, 795 (1966).

b) idem. ibid., 62, 801 (1966).

29. A.J. van Roosmalen and J.C. Mol, J. Phys. Chem., 83, 2485 (1979).

30. B.A. Morrow and I.A. Cody, J. Phys. Chem., 79, 761 (1975).

31. B.A. Morrow and I.A. Cody, J. Phys. Chem., 80, 1995, 1998 (1976).

32. B.A. Morrow, I.A. Cody and L.S.M. Lee, J. Phys. Chem., 80, 2761 (1976).

33. G.A. Galkin, A.V. Kiselev and V.I. Lygin, Russ. J. Phys. Chem., 43, 1117, (1969).

34. S. Brunauer, P.H. Emmett and E. Teller, J. Amer. Chem. Soc., 60, 309 (1938).

35. G.A. Galkin, A.V. Kiselev and V.I. Lygin, Russ. J. Phys. Chem., 41, 386 (1967).

36. W. Lowen and E.C. Broge, J. Phys. Chem., 65, 16 (1961).

37. I. Shapiro and I.M. Kolthoff, J. Am. Chem. Soc., 72, 776 (1950).

38. J.H. Anderson and K.A. Wickersheim, Surf. Sci., 2, 252 (1964).

39. L.T. Zhuralev and A.V. Kiselev, Russ. J. Phys. Chem., 41, 386 (1967).

40. G.A. Galkin, A.V. Kiselev and V.I. Lygin, Russ. J. Phys. Chem., 41, 20 (1967).

41. idem. ibid., 42, 765 (1968).

42. A.V. Kiselev and Russ. J. Phys. Chem., 38, 1491 (1964); ibid., 41, 1338 (1967).

43. A.V. Volkov, A.V. Kiselev and V.I. Lygin, Russ. J. Phys. Chem., 48, 703 (1974).

44. P. Hobza, J. Sauer, C. Morgeneyer, J. Hurych and R. Zahradnik, J. Phys. Chem., 85, 4061 (1981).

45. P.R. Ryason and B.G. Russel, J. Phys. Chem., 79, 1276 (1975).

46. J.H. DeBoer and J.M. Vleeskens, Proc. Koninkl. Ned. Acad. Watenschap, B61, 2 (1958).

47. D.W. Sindorf and G.E. Maciel, J. Phys. Chem., 87, 5516 (1983).

48. M.P. McDaniel, J. Phys. Chem., 85, 532 (1981).

49. G. Berendsen and L. de Galan, J. Liq. Chromatogr. 1, 403 (1978).

50. A.M. Khalil, Surf. Technol., 14, 383 (1981).

51. B.A. Morrow, R.A. McFarlane and A. McFarlan, to be published.

42. J.B. Peri and A.L. Hensley Jr., J. Phys. Chem., 72, 2926 (1968).

53 C.G. Armistead, A.J. Tyler, F.H. Hambleton, S.A. Mitchell and J.A. Hockey, J. Phys. Chem., 73, 3947 (1969).

54. M.L. Hair and W. Hertl, J. Phys. Chem., 73, 2372 (1969).

55. F.H. van Cauwelaert, P.A. Jacobs and J.B. Utterhoeven, J. Phys. Chem., 76, 1434 (1972).

56. J.A. Hockey, J. Phys. Chem., 74, 2570 (1970).

57. B.A. Morrow and I.A. Cody, J. Phys. Chem., 77, 1465 (1973).

58. A.J. van Roosmalen and J.C. Mol, J. Phys. Chem., 82, 2748 (1978).

59. G.E. Maciel and D.W. Sindorf, J. Am. Chem. Soc. 102, 7607 (1980).

60. H.C. Marsmann, Z Naturforsch., B29, 495 (1974).

61. C.A. Fyfe, "Solid State NMR for Chemists", C.F.C. Press, Canada (1983).

62. J. Sauer and K. -P. Schroder, Z. Phys. Chemie, Leipzig 266, 379 (1985).

63. E. Borella, A. Zecchina and C. Morterra, J. Phys. Chem., 71, 2938 (1967).

64. G.A. Blomfield and L.H. Little, Can. J. Chem., 51, 1771 (1973).

65. B.A. Morrow and A. Devi, J. Chem. Soc.; Chem. Commun., 1237 (1971).

66. V.Y. Davydov, A.V. Kiselev and L.T. Zhuralev, Trans. Faraday Soc., 60, 2254 (1964).

67. P.G. Rouxhet, R. Touillaux, M. Mestdagh and J.J. Fripiat, Proc. Int. Clay Conf., Tokyo, 1, 109 (1969).

68. I.A. Cody, Ph.D. Thesis, University of Ottawa, 1975.

69. L.B. Magnussen, J. Phys. Chem., 74, 4221 (1970).

70. A.J. Tursi and E.R. Nixon, J. Chem. Phys., 52, 1521 (1970).

71. K. Klier, J.H. Shen and A.C. Zettlemayer, J. Phys. Chem., 77, 1458 (1973).

72. R.B. Laughlin and J.D. Joannopoulos, Phys. Rev. B 16, 2942 (1977).

73. P.H. Gaskell and D.W. Johnson, J. Non-Cryst. Solids, 20, 171 (1976).

74. G.E. Walrafen, J. Chem. Phys., 62, 297 (1975).

75. G.E. Walrafen and S.R. Samanta, J. Chem. Phys., 69, 493 (1978).

76. C.M. Hartwig, J. Chem. Phys., 66, 227 (1977).

77. C.A. Murray and T.J. Greytak, Phys. Rev. B, 20, 3368 (1979).

78. E.J. Heilweil, J.P. Casassa , R.R. Cavanagh and J.C. Stephenson, J. Chem. Phys. 82, 5216 (1985).

79. R.H. Stolen, J.T. Krause and C.R. Kurkjian, Discuss. Faraday Soc., 50, 103 (1970).

80. R.H. Stolen and G.E. Walrafen, J. Chem. Phys., 64, 2623 (1976).

81. F.L. Galeener, J.C. Mikkelsen, Jr. and N.M. Johnson, "The Physics of $SiO_2$ and Its Interfaces", Pergamon, New York (1978).

82. W.D. Compton and G.W. Arnold, Discuss. Faraday Soc., 31, 130 (1961).

83. E.J. Friebele, D.L. Griscom, M. Stapelbrock and R.A. Weeks, Phys. Rev. Lett. 42, 1346 (1979).

84. D.L. Griscom, Phys. Rev. B22, 4192 (1980).

85. J.B. Bates, R.W. Hendricks and L.B. Shaffer, J. Chem. Phys., 61, 4163 (1974).

86. F.L. Galeener, N.M. Johnson and R.H. Geils, "Proceedings of the International Topical Conference on the Physics of $SiO_2$ and Interfaces, Yorktown Heights, March 1978" Plenum, New York (1978).

87. R.B. Laughlin and J.D. Joannopoulos, Phys. Rev. B17, 4922 (1978).

88. R.B. Laughlin, J.D. Joannopoulos, C.A. Murray, K.J. Hartnett and T.J. Greytak, Phys. Rev. Lett. 40, 461 (1978).

89. J.C. Mikkelsen, Jr. and F.L. Galeener, J. Non-Cryst. Solids, 37, 71 (1980).

90. A.R. Silin, P.J. Bray and J.C. Mikkelsen, Jr., J. Non-Cryst. Solids, 64, 185 (1984).

91. C.G. Armistead and J.A. Hockey, Trans. Faraday Soc., 63, 2549 (1967).

92. R.J. Peglar, F.H. Hambleton and J.A. Hockey, J. Catal., 20, 309 (1971).

93. D.J.C. Yates, G.W. Dembinski, W.R. Kroll and J.J. Elliott, J. Phys. Chem., 73, 911 (1969).

94. J. Kunawicz, P. Jones and J.A. Hockey, Trans. Far. Soc., 67, 848 (1971).

95. M.J.D. Low, A.G. Severida and J. Chan, J. Catal., 69, 384 (1981).

96. M.L. Hair and W. Hertl, J. Phys. Chem., 77, 2070 (1973).

97. O.H. Ellestad and U. Blindheim, J. Mol. Catal., 33, 275 (1985).

98. C.L. Thomas, "Catalytic Processes and Proven Catalysts", Academic Press, New York (1970).

99. H. Knözinger and P. Ratnasamy, Catal. Rev., 17, 31 (1978).

100. H. Knözinger, Stud. Surf. Sci. Catal. 20, 111 (1985).

101. B.C. Lippens and J.H. de Boer, Acta Cryst., 17, 1312 (1964).

102. B.C. Lippens, Thesis, Delft, (1961).

103. A.J. Leonard, P.N. Semaille and J.J. Fripiat, Proc. Br. Ceram. Soc., 103 (1969).

104. C.S. John, N.C.M. Alma and G.R. Hays, Appl. Catal., 6, 341 (1983).

105. J.B. Peri, J. Phys. Chem., 69, 220 (1965).

106. J.B. Butt and L.T. Starzec, J. Catal., 32, 99 (1974).

107. J.E. Dabrowski, J. Butt and H. Bliss, J. Catal., 18, 297 (1970).

108. L.H. Jones, J. Chem. Phys., 22, 217 (1954).

109. G. Herzberg, "Spectra of Diatomic Molecules", Van Nostrand, New York (1950).

110. E. Borello, G. Della Gatta, B. Fubini, C. Morterra and G. Venturello, J. Catal., 35, 1 (1974).

111. J.B. Peri and R.B. Hannan, J. Phys. Chem., 64, 1526 (1960).

112. J.B. Peri, J. Phys. Chem., 69, 211 (1965).

113. H. Knözinger, Adv. Catal., 25, 184 (1976).

114. G. Della Gatt, B. Fubini, G. Ghiotti and C. Morterra, J. Catal., 43, 90 (1976).

115. P. Fink, Z. Chem., 7, 324 (1967).

116. V.I. Yakerson, L.I. Lafer, V.Y. Danyashevskii and A.M. Rubinshtein, Izv. Akad. Nauk. S.S.S.R., Ser. Khim., 19, (1969).

117. N.D. Parkyns, J. Chem. Soc. A, 410 (1969).

118. N.D. Parkyns, J. Phys. Chem., 75, 526 (1971).

119. H. Krientenbrink and H. Knozinger, Z. Phys. Chem. (Frankfurt) 102, 43 (1976).

120. H. Knozinger, H. Krientenbrink, H. -D. Muller and W. Schulz, Proc. 6th Int. Cong. Catal., London (1976).

121. B.A. Morrow and P. Ramamurthy, J. Phys. Chem. 77, 3052 (1973).

122. B.A. Morrow and A.H. Hardin, J. Phys. Chem., 83, 3135 (1979).

123. J. Chimielowiec and B.A. Morrow, J. Colloid Interface Sci., 94, 319 (1983).

124. J. Murray, M.J. Sharp and J.A. Hockey, J. Catal. 18, 52 (1970).

125. M.L. Hair, J. Colloid. Interface Sci. 60, 154 (1977).

126. J.B. Kinney and R.H. Staley, J. Phys. Chem., 87, 3735 (1983).

127. A.J. McFarlan, B.Sc. Thesis University of Ottawa (1986).

128. H. Kriegsmann and K. Licht, Z. Electrochem., 62, 1163 (1958).

129. K. Nakamoto, "Infrared Spectra of Inorganic and Coordination Compounds", Wiley, New York (1970).

130. B.A. Morrow, I.A. Cody and L.S.M. Lee, J. Phys. Chem., 79, 2405 (1975).

131. M. Hino and H. Sato, Bull. Chem. Soc. Jpn., 44, 33 (1971).

132. A.V. Kiselev and V.I. Lygin, Kolloidn. Zh., 21, 581 (1959).

133. G.D. Chukin and V.I. Malevich, Zh. Prikl. Spectrosk., 26, 294 (1977).

134. A.L. Smith and D.R. Anderson, Appl. Spectrosc., 38, 822 (1984).

135. J.B. Benziger, S.J. McGovern and B.S.H. Royce, A.C.S. Symp. Ser. 288, (Catal. Charact. Sci.), 449 (1985).

137. B.A. Morrow, J. Chem. Soc. Faraday 1, 70, 1527 (1974).

138. B.A. Morrow, L.W. Thomson and R.W. Wetmore, J. Catal 28, 332 (1973).

139. D. Kunath and D. Schulz, J. Colloid Interface Sci., 66, 379, (1978), and references therein.

140. A. Zecchina, G. Ghiotti, L. Ceruti and C. Morterra, J. Chim. Phys. 62, 1479 (1971).

141. W. Bruser, S. Schroder and K. Witke, Z. Anorg. Allg. Chem. 421, 89 (1976).

142. W.J. Lehmann, C.O. Wilson, Jr. and I. Shapiro, J. Chem. Phys., 28, 781 (1958).

143. S.L. Holt, Jr., "Inorganic Synthesis" vol 22, Wiley, New York (1983).

144. H.G. Weiss and I. Shapiro, J. Am. Chem. Soc., 75, 1221 (1953), ibid., 57, 219 (1953).

145. H.G. Weiss, I. Shapiro and J.A. Knight, J. Am. Chem. Soc., 81, 1823 (1959).

146. C. Naccache, J. Francoise-Rossetti and B. Imelik, Bull. Soc. Chim. Fr., 404 (1959).

147. C. Naccache and B. Imelik, C.R. Hebd. Seances Acad. Sci. 250, 2019 (1960), ibid., Bull. Soc. Chim. Fr., 553 (1961).

148. J.J. Fripiat and M. van Tongelen, J. Catal. 5, 158 (1965).

149. M.V. Mathieu and B. Imelik, J. Chim. Phys., 59, 1189 (1962).

150. M. Baverez and J. Bastick, Bull. Soc. Chim Fr., 3226 (1964).

151. A.I. Mashchenko, Kinet. Katal., 15, 903 (1974).

152. B.A. Morrow and L.E. Moran, J. Catal., 62, 294 (1980).

153. B.A. Morrow and R.A. McFarlane, Langmuir 2, 315 (1986).

154. S.K. Wason and R.F. Porter, J. Phys. Chem., 68, 1443 (1964).

155. F. Watari, Inorg. Chem., 21, 1442 (1982).

156. L.H. Jones, R.C. Taylor and R.T. Paine, J. Chem. Phys., 70, 749 (1979).

157. C.L. Cluff and R.C. Taylor, Nature, 182, 390 (1958).

158. R.C. Taylor and T.C. Bissel, J. Chem. Phys., 25, 780 (1956).

159. C.W. Heitch and J.G. Verkade, Inorg. Chem., 1, 863 (1962).

160. J.L. Duncan, D.C. McKean, I. Torto, G.D. and Nivellini, J. Mol. Spectrosc., 85, 16 (1981).

161. G.J. Lucovsky, Vac. Sci. Technol., 16, 1225 (1979).

162. C.M. Hartwig, J. Chem. Phys. 66, 227 (1977).

163. R.J. Brotherton and H. Steinberg, "Progress in Boron Chemistry" Vol. 3, Pergamon (Hungary) (1970).

164. R.C. Taylor, "Boron-Nitrogen Chemistry Advances in Chemistry Vol. 42 ACS, Washington (1964).

165. H.C. Brown and C.D. Pfaffenberger, J. Am. Soc., 89, 5475 (1967).

166. H.C. Brown and E. Negishi, J. Am. Chem. Soc., 94, 3567 (1972)., ibid., 95, 6757 (1973).

167. T. Matsuda, H. Kawashima and M. Ojima, Bull. Japan. Petrol. Inst. 18, 67 (1976).

168. T. Matsuda and H. Kawashima, J. Catal. 49, 141 (1977).

169. G.D. Parfitt, Progress in Surface Membrane Chemistry 11, 181 (1976).

170. H.G. Weiss and I. Shapiro, J. Am. Chem. Soc., 80, 3195 (1958), ibid., 79, 3294 (1957).

171. L.L. McDowell and M.E. Ryan, Int. J. Appl. Radiation and Isotopes, 17, 179 (1966).

172. A.R. Emery and R.C. Taylor, Spectrochim. Acta., 16, 1455 (1960).

173. H. Noth and R. Hartwimmer, Chem. Ber., 93, 2238 (1960).

174. H. Shirakawa and S. Ikeda, Polymer J., 4, 460 (1973).

175. H. Shirakawa, T. Ito and S. Ikeda, Polymer J., 2, 231 (1971).

176. A.K. Holliday, W. Reade, K.R. Seddon and I.A. Steer, J. Organometal. Chem., 67, 1 (1974).

177. D.J.C. Yates and P.J. Luccesi, J. Chem. Phys. 35, 243 (1961).

178. M.M. Bhasin, C. Curran and G.S. Joh, J. Phys. Chem., 74, 3973 (1970).

179. J. Heaviside, P.J. Hendra, P. Tsai and R.P. Cooney, J. Chem. Soc., Faraday Trans 1., 74, 2570 (1978).

180. R.M. Biefeld, J. Crystal Growth, 56, 382 (1982).

181. D.J. Schyler and M.A. Ring, J. Electrochem. Soc., 130, 413 (1977).

182. J. Nishizawa and P. Ramamurthy, J. Phys. Chem., 77, 3052 (1983).

183. H.M. Manasevit, F.M. Erdmann and W.I. Simpson, J. Electrochem. Soc., 118, 1864 (1971).

184. R. Tubis, B. Hamlett, R. Lester, C.G. Newman and M.A. Ring, Inorg. Chem., 18, 3275 (1979).

185a. T.A. Gilmore and J.J. Rooney, J. Chem. Soc. Chem. Comm., 219 (1975).

185b. E. Borello, A. Zecchina and C. Morterra, J. Phys. Chem., 71, 2938 (1967).

186. J.R. Hall, L.A. Woodward and E.A.V. Ebsworth, Spectrochim. Acta, 20, 1249 (1964).

187. J.R. Durig and K.K. Chatterjee, J. Raman Spectrosc., 11, 168 (1981).

188. S. Kvisle and E. Rytter, Spectrochim. Acta, 40A, 939 (1984).

189. J.R. Durig, C.B. Bradley and J.D. Odom, Inorg. Chem., 21, 1466 (1982).

190. J.D. Odom, K.K. Chatterjee and J.R. Durig, J. Mol. Struct., 72, 73 (1981).

191. C. Morterra and M.J.D. Low, Annal. N.Y. Acad. Sci., 229, 135 (1973).

192. E.P. Parry, J. Catal., 2, 371 (1963).

193. F.B. Carleton, H.A. Quinn and J.J. Rooney, J. Chem. Soc., Chem. Commun., 231 (1973).

194. F.B. Carleton, T.A. Gilmore and J.J. Rooney, Proc. Int. Congr. Catal., 6th 1976 (Pub. 197) England.

195. H.G. Karge, R. Tower, Z. Dudzik and Z.M. George, Proc. 7th Intern. Congr. Catal., Tokyo, 1980, 1, 643 (1981).

196a. H.G. Karge, I.C. Dalla Lana and S. Trevizan de Suarez, Yingzhen Zhang, Proc. 8th Intern, Congr. Catal., West Berlin, 3, 84 (1984).

196b. D.W. Scott, J.P. McCullough and F.H. Druse, J. Mol. Spec., 13, 313 (1964).

197. C.E. Sjogren and P. Klaeboe, Spectrochim. Acta., 40A, 457 (1984).

198. M.C. Drake and G.M. Rosenblatt, J. Chem. Phys., 65, 4067 (1976).

199. I.R. Beattie and J.R. Horder, J. Chem. Soc. Dalton Trans., 2655, (1969); ibid, 2433 (1970).

200. J. Roziere, M.T. Bories and A. Manteghetti, A. Potier, Can. J. Chem., 52, 3274 (1974).

201. O.T. Beachley and R.G. Simmons, Inorg. Chem. 19, 1021 (1980).

202. W.A. Senior and W.K. Thompson, Nature, 205, 170 (1965).

203. N. Gailer and E.K. Plyler, J. Chem. Phys. 24, 1139 (1956).

204. G. Picotin, J. Roziere, J. Potier and A. Potier, Advances in Molecular Relaxation Processes, 7, 177 (1975).

205a. M. Goldstein, Spectrochim. Acta., 22, 1389 (1966).

205b. P. Fink and I. Plotzki, Wiss. Z. Fredrich-Schiller-Univ., Jena, Math.-Naturwiss. Reighe 29, 809 (1980).

206. M. Guido and G. Gigli, J. Chem. Phys. 60, 721 (1974).

207. G. Wittig and H. Bille, Z. Naturforsch, 6B, 226 (1951).

208. G.E. Coates and R.N. Mukherjee, J. Chem. Soc., 229 (1963).

209. R. Ehrlich and A.R. Young, J. Inorg. Nucl. Chem., 28, 674 (1966).

210. T. Ehemann and K. Dehnicke, J. Organometallic Chem., 64, C33 (1974).

211. I. Kanesaka, Y. Hase and K. Kawai, Bull. Chem. Soc. Jpn. 45, 1595 (1972).

212. A.G. Maki and L.R. Blaine, J. Mol. Spectrosc., 12, 45 (1964).

213. B.A. Morrow and I.A. Cody, J. Chem. Soc. Faraday, Trans 1 71, 1021 (1975).

214. G.T. Kokotailo, S.L. Lawton, D.H. Lawson and W.M. Meir, Nature 272, 437 (1978).

215. J.B. Nagy, Z. Gabelica, E.G. Derouane and P.A. Jacobs, Chem. Lett., 2003 (1982).

216. G. Boxhoorn, A.G.T.G. Kortbeek, G.R. Hays and N.C.M. Alma, Zeolites 4, 15, (1984).

217. C.A. Fyfe, G.C. Gobbi, J. Klinowski, J.M. Thomas and S. Ramdas, Nature 296, 530 (1982).

218. A.P.M. Kentgens, K.F.M.G.J. Scholle and W.S. Veeman, J. Phys. Chem., 87, 4357 (1983).

219. E.G. Derouane, J.-P. Gilson and J.B. Nagy, Zeolites 2, 42 (1981).

220. J.P. van den Berg, J.P. Wolthuizen, A.D.H. Clague, G.R. Hays, R. Huis and J.H.C. van Hooff, J. Catal, 80, 130 (1983).

221. J.B. Nagy, E.G. Derouane, H.A. Resing and G.R. Miller, J. Phys. Chem. 87, 833 (1983).

222. K.F.M.G.J. Scholle, A.P.M. Kentgens, W.S. Veeman, P. Frenken and G.P.M. van der Velden, J. Phys. Chem., 88, 5 (1984).

223. K.F.M.G.J. Scholle, W.S. Veeman, J.G. Post and J.H.C. van Hooff, Zeolites 3, 214 (1983).

224. B. Kontnik, M. Gorska, J. Eysymontt and A. Salek, J. Mol. Struct., 80, 199 (1982).

225. N.-U. Topsoe, K. Pedersen and E.G. Derouane, J. Catal., 70, 41 (1981).

226. S.L. Meisel, J.P. McCullough, C.H. Lechthaler and P.B. Weiz, Chem. Technol., 6, 86 (1976).

227. E.G. Derouane and J.C. Vedrine, J. Mol. Catal. 8, 479 (1980).

228. N.Y. Chen and W.J. Reagan, J. Catal. 59, 123 (1979).

229. A. Auroux, J.C. Vedrine and P.C. Gravelle, Stud. Surf. Catal., 10, 227 (1982).

230. Robert J. Argauer and George Landolt (Mobil Oil Corp.) U.S. Patent 3, 702, 886.

231. P.A. Jacobs and R. von Ballmoos, J. Phys. Chem., 86, 3050 (1982).

232. P. Chu and F.G. Dwyer, A.C.S. Symposium Series Vol. 218 "Intrazeolite Chemistry", 59 (1983).

233. D.M. Bibby, L.P. Aldridge and N.B. Milestone, J. Catal., 72, 373 (1981).

234. B.A. Morrow, A.C.S. Symposium Series Vol. 137, "Vibrational Spectroscopies for Adsorbed Species", 119 (1980) and references therein.

234a. C.L. Angell, J. Phys. Chem., 77, 222 (1973).

235. K.-J. Chao, T.C. Tsai and M.-S. Chem, J. Chem., Faraday Trans. 1, 77, 547, (1981).

236. Von Ch. Peuker, W. Pilz, B. Fahlke, E. Loffler, J. Richter-Mendau and W. Schirmer, Z. phys. chemie, Leipzig 266, 74 (1984).

237. G.L. Woolery, L.B. Alemany, R.M. Dessau and A.W. Chester, Zeolites 6, 14 (1968).

238. P.A. Jacobs, H.K. Beyer and J. Valyon, Zeolites 1, 161 (1981).

239. L. Kubelkova, H. Hoser, A. Riva and F. Trifiro, Zeolites 3, 244 (1983).

240. R.P. Cooney and P. Tsai, J. Raman Spectrosc., 9, 33 (1980).

241. D.E. Tevault and L. Andrews, Spectrochim. Acta, 30A, 969 (1974).

242. D.S. Maciver, H.H. Tobin and R.T. Barth, J. Catal., 2, 458 (1963)